GOBIERNO DE ESPAÑA
MINISTERIO DE ECONOMÍA, INDUSTRIA Y COMPETITIVIDAD
AGENCIA ESTATAL DE INVESTIGACIÓN
IOCAG Instituto de Oceanografía y Cambio Global
QUIMA QUÍMICA MARINA ULPGC

ULPGC

Oxidation of Fe(II) in North Atlantic Ocean in the presence of organic compounds

Tesis Doctoral

Carolina Santana González

Noviembre 2018

UNIVERSIDAD DE LAS PALMAS DE GRAN CANARIA

# Tesis Doctoral

*Doctorado en Oceanografía y Cambio Global*

# Oxidation of Fe(II) in North Atlantic Ocean in the presence of organic compounds

Carolina Santana González

Las Palmas de Gran Canaria

Noviembre

2018

UNIVERSIDAD DE LAS PALMAS
DE GRAN CANARIA

**D. SANTIAGO HERNÁNDEZ LEÓN COORDINADOR DEL PROGRAMA DE DOCTORADO OCEANOGRAFÍA Y CAMBIO GLOBAL DE LA UNIVERSIDAD DE LAS PALMAS DE GRAN CANARIA,**

**INFORMA,**

Que la Comisión Académica del Programa de Doctorado, en su sesión de fecha 27 de Julio de dos mil dieciocho tomó el acuerdo de dar el consentimiento para su tramitación, a la tesis doctoral titulada "Oxidation of Fe(II) in North Atlantic Ocean in the presence of organic compounds" presentada por la doctoranda Dª Carolina Santana González y dirigida por los Doctores J. Magdalena Santana Casiano y Melchor González Dávila.

Asimismo, se acordó el informar favorablemente la solicitud para optar a la Mención Internacional del Título de Doctor, por cumplir los requisitos reglamentarios.

Y para que así conste, y a efectos de lo previsto en el Artº 11 del Reglamento de Estudios de Doctorado (BOULPGC 7/10/2016) de la Universidad de Las Palmas de Gran Canaria, firmo la presente en Las Palmas de Gran Canaria, a 27 de Julio de dos mil dieciocho.

UNIVERSIDAD DE LAS PALMAS DE GRAN CANARIA

**UNIVERSIDAD DE LAS PALMAS DE GRAN CANARIA**

**ESCUELA DE DOCTORADO**

*Programa de doctorado de Oceanografía y Cambio Global*

**Título de la Tesis**

# *Oxidation of Fe(II) in North Atlantic Ocean in the presence of organic compounds*

Tesis Doctoral presentada por Dª. Carolina Santana González

Dirigida por la Dra. Dª. J. Magdalena Santana Casiano

Codirigida por el Dr. D. Melchor González Dávila

La Directora, El Codirector, La Doctoranda,

Las Palmas de Gran Canaria, a 27 de Julio de 2018

UNIVERSIDAD DE LAS PALMAS
DE GRAN CANARIA

# Tesis Doctoral

*Doctorado en Oceanografía y Cambio Global*

# *Oxidation of Fe(II) in North Atlantic Ocean in the presence of organic compounds*

Carolina Santana González

Las Palmas de Gran Canaria

Noviembre

2018

The present PhD Thesis was carried out in the Universidad de Las Palmas de Gran Canaria, at the Instituto de Oceanografía y Cambio Global (IOCAG), in the QUIMA group, inside the IOCAG Doctoral Program in Oceanography and Global Change. The Thesis is entitled "Oxidation of Fe(II) in the North Atlantic waters in the presence of organic compounds". It is framed in the research projects: EACFe (CTM2014-52342-P) and ATOPFe (CTM2017-83476-P) projects by the Ministerio de Economía y Competitividad of the Spanish Government. Additionally, the work was made possible by the FPI grant with reference number BES-2015-071245 of the Ministerio de Economía y Competitividad of the Spanish Government associated to the EACFe (CTM2014-52342-P) project. The PhD was supervised by Dra. J. Magdalena Santana Casiano and Dr. Melchor González Dávila.

This PhD thesis is structured into a general introduction that explains the most relevant aspects of Fe(II) chemistry in the ocean and the need for studying the oxidation kinetics of Fe(II) in the ocean. The three chapters are composed by the articles: "Emissions of Fe(II) and its kinetic of oxidation at Tagoro submarine volcano, El Hierro" (Marine Chemistry, DOI: 10.1016/j.marchem.2017.02.001), "Fe(II) oxidation kinetics in the North Atlantic along the 59.5ºN during 2016" (Marine Chemistry, DOI: 10.1016/j.marchem.2018.05.002) and "Organic Matter effect on the Fe(II) oxidation kinetics in the Labrador Sea" (Chemical Geology, in review). Finally there is a general conclusion of the thesis.

In order to comply with the requirements established by the Universidad de Las Palmas de Gran Canaria for PhD Thesis (BOULPGC. Art. 10, 7 de Octubre de 2016), a summary in Spanish with a general introduction, objectives and conclusions is included.

Esta Tesis Doctoral ha sido financiada por el Ministerio de Economía y Competitividad del Gobierno de España en el año 2015 (BES-2015-071245) asociada al proyecto EACFe (CTM2014-52342-P), por ello quiero agradecer a esta institución la beca otorgada para el desarrollo de mi Tesis Doctoral.

La presente Tesis Doctoral la he realizado bajo la supervisión de los Doctores J. Magdalena Santana Casiano y Melchor González Dávila. A ellos quiero agradecer profundamente el apoyo, motivación, dedicación y orientación que me han dado desde el comienzo. Ellos me han enseñado valores que van más allá de la química-física como el ser autocrítica con el trabajo, el esfuerzo día a día por mejorar y lo valioso de hacer un buen trabajo aún cuando se está trabajando con adversidades; transmitiéndome en todo momento su entusiasmo por la ciencia.

Durante todo este tiempo ha sido muy importante el apoyo recibido por todos los compañeros del laboratorio que están o han pasado por el grupo QUIMA: la Dr. Norma, el Dr. Guillermo, Rayco, Anna, Vanessa, Dani, Verónica, Maite, Manu, Adrián e Idaira. A ellos quiero agradecer toda su ayuda y los buenas recuerdos que dejan de las vivencias en el laboratorio y las campañas de barco. Gracias a todos por enseñarme el valor del trabajo en equipo y lo importante de entender la condición humana, mostrándome siempre vuestra mejor sonrisa. Quiero agradecer especialmente a el Dr. Aridane González por su apoyo y motivación, ayudándome en todo momento, incluso desde la distancia.

La Tesis doctoral la he realizado en el laboratorio que tiene el grupo QUIMA en el Instituto de Oceanografía y Cambio Global. Durante estos tres años he compartido muchos momentos con los compañeros de otros grupos y personal de servicio, entre ellos quiero destacar a: Mine, Cory, Nau, Laia, Isa, María e Isabel León. Gracias por todos los momentos vividos, la ayuda brindada y el apoyo que me habéis dado.

Quiero agradecer a Judit y David por sus revisiones y comentarios del inglés, que han sido muy valiosos para poder enviar los trabajos. Al profesor Ángelo Santana del Pino por su ayuda con los cálculos estadísticos y al Dr. Christoph Vöelker por aceptarme para realizar una estancia en el Alfred-Wegener Institut (Alemania). Además quiero agradecer a CHARTER 100 GC por su financiación para la realización de la estancia.

Fuera del ámbito académico hay personas que siempre están presentes para mí y su apoyo ha sido un pilar básico para dedicarme a la ciencia. En primer lugar quiero agradecer profundamente a mis padres, Luis y Paqui, por vuestro amor y apoyo incondicional en todas mis decisiones, aunque algunas las sufran en silencio; por enseñarme que siempre hay que luchar por lo que se quiere y a ser honesta y libre. A mi hermana pequeña Coraima, que siempre está dispuesta a ayudarme, con la que comparto largas charlas de la vida y consejos. A mi tíos y primos que siempre son un apoyo, especialmente en una familia tan grande como la mía. En particular quiero agradecer a mi tía Fefa, por ser como una madre para mí y darme todo su cariño incondicional. A mis amigas de toda la vida por apoyarme y estar ahí para mí: Lore, Ilidia y Nereida. A mi profesor de primaria, Don Rafael, por inculcarnos el amor por la naturaleza y la curiosidad para entender el mundo. Quiero agradecer el cariño y apoyo incondicional de tres personas muy valiosas, que aunque ya no están con nosotros, siempre me transmitieron mucho amor, fuerza y valentía: mi abuela Carmen, mi tía Vitaliana y mi tío Antonio.

Finalmente he dejado unas palabras de enorme agradecimiento para mi novio Paco, gracias por comprenderme y ayudarme sin pedir nada a cambio, darme la libertad de poder ser yo misma en todos los momentos. Estar conmigo en los buenos y malos momentos e incluso cuando nos separaban más de 7000 km. Porque eres mi mayor apoyo en esta aventura y por ello esta Tesis en parte es tuya.

***"Science does not know about countries, because knowledge belongs to humanity and is the torch that illuminates the world. Science is the soul of the prosperity of nations and the source of all progress"***

–Louis Pasteur (1822-1895, France) chemist and bacteriologist, founder of microbiology and pioneer of modern medicine.

The Fe(II) oxidation kinetics has been studied in seawater of the North Atlantic Ocean. The spatial distribution of the samples affected the oxidation rate of Fe(II) due to the chemical characteristics of each water mass sampled. Faster Fe(II) oxidation rates were observed within the chlorophyll maximum, in surface and coastal samples than in deep waters related with the remineralization state of the organic matter.

In the volcanic area of the Tagoro submarine volcano, the emissions of Fe(II) was intermittent and inversely correlated with pH values. The Fe(II) oxidation rate constants in the different conditions were higher than those expected in oligotrophic seawater. These rates can be explained by the effect of the nutrient concentrations of the seawater samples, in particular silicates.

The studies of Fe(II) oxidation kinetics in natural conditions carried out in the Subarctic North Atlantic and in the Labrador Sea show that temperature, pH and salinity were the master variables controlling the Fe(II) oxidation kinetics. However the sources and characteristics of the organic matter present were important factors influencing the oxidation of Fe(II), displaying both positive and negative effects on the Fe(II) oxidation rate.

In this PhD Thesis, a general equation for the oxidation rate was obtained which allows computation of Fe(II) oxidation rate taking into account the effects of temperature, pH and salinity under natural conditions for the Subarctic North Atlantic and Labrador Sea. A novel approach was applied to the oxidation kinetics of Fe(II) in the Labrador Sea, which allowed to determine the average contribution of the organic matter over the inorganic effect.

# Chapter I.

## General Introduction

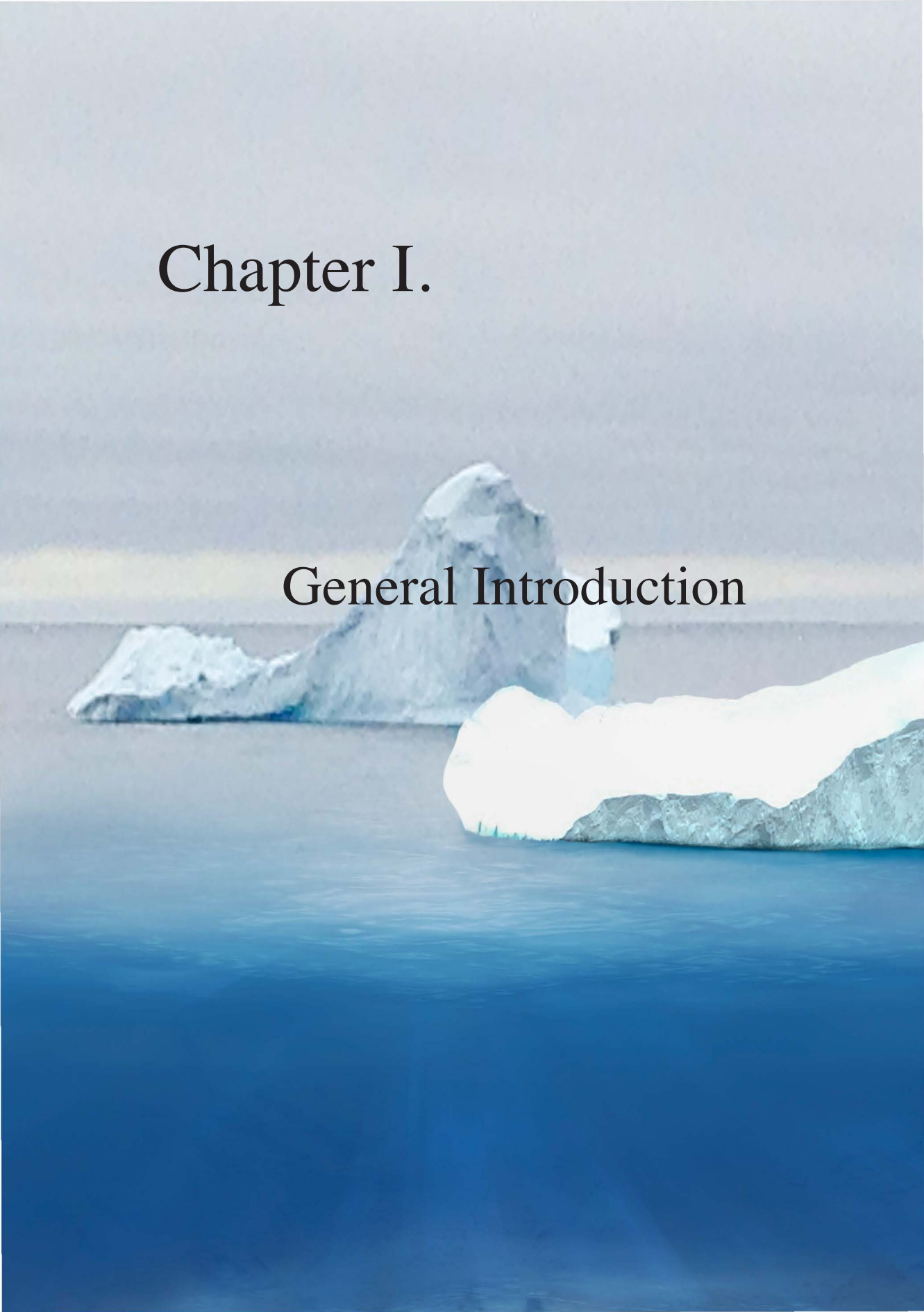

## *1.1. Iron in the oceans*

Iron (Fe) is the fourth most abundant element in the earth crust (McDonough and Sun, 1995). However, Fe concentrations in the open ocean are in trace amounts (< 1.0 nM) due to its low solubility in oxygenated waters (Millero, 1998).

The major seawater Fe sources are atmospheric dust deposition, riverine inputs including estuaries, shelf margin resuspension, hydrothermal inputs and subsurface waters enriched by upwelling (Abadie et al., 2017; Bowie et al., 1998; Ye et al., 2009). The major oceanic Fe cycle processes are represented by Tagliabue et al. (2017) (Fig. 1.1), including iron sources, biological uptake, degradation, adsorption, desorption, precipitation and dissolution processes.

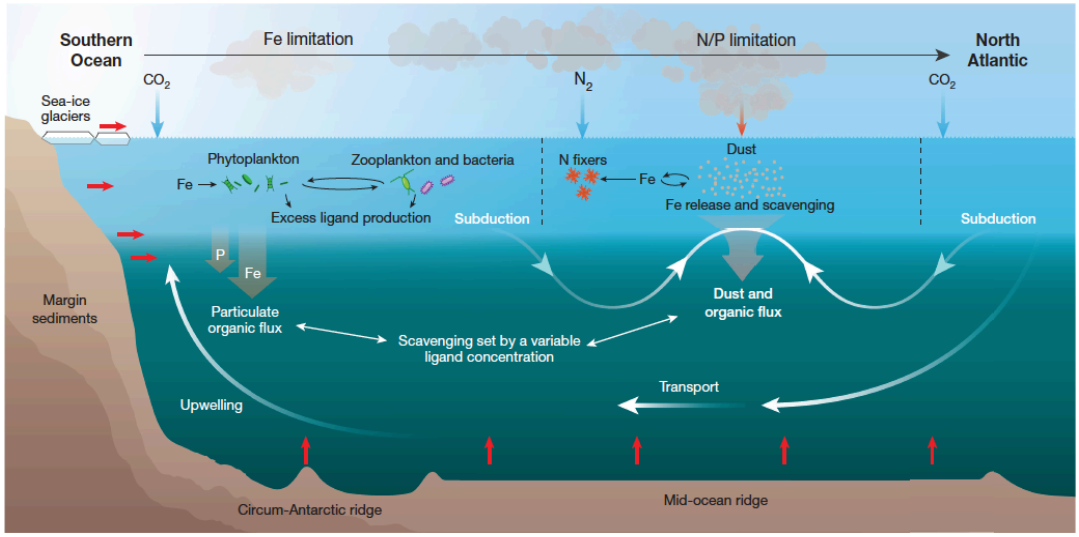


Figure 1.1. The Iron cycle in the ocean (obtained from Tagliabue et al. (2017))

Iron is an essential micronutrient for organisms (Martin et al., 1991), playing a key role in the biochemistry and physiology of oceanic phytoplankton (Sunda et al., 1991). It has an important role as a co-factor in cellular enzymes, related with photosynthesis, respiratory electron transport (Chereskin and Castelfranco, 1982), nitrate uptake (Van Leeuwe et al., 1997), nitrogen fixation (Williams, 1981) and detoxification of reactive oxygen species (Sunda and Huntsman, 1995). Therefore, iron has been recognized to be an important micronutrient in regulating the magnitude and dynamics of ocean

primary productivity (Martin et al., 1991).

### *1.2. Iron size fractionation*

Iron in seawater exists in a variety of chemical and physical forms, including dissolved organic complexes, colloidal and particulate bound forms (Ye et al., 2009). Iron is classified according the size fractionation classes as: particulate (pFe) (>0.2μm), dissolve (dFe) (<0.2μm), colloidal (cFe) (0.02-0.2μm) and soluble (sFe) (<0.02μm) size fractions (Ussher et al., 2010). The total dissolve iron (TdFe) is the unfiltered fraction and the total dissolvable (TDFe) fraction is the TdFe acidified to pH of 2 and analyzed after six months of sampling. The distributions of Fe have been studied in different oceans and seas, Atlantic, Pacific and Mediterranean among others and are included in the Table 1.1. The total dissolve Fe in the Atlantic Ocean is represented in Fig. 1.2.

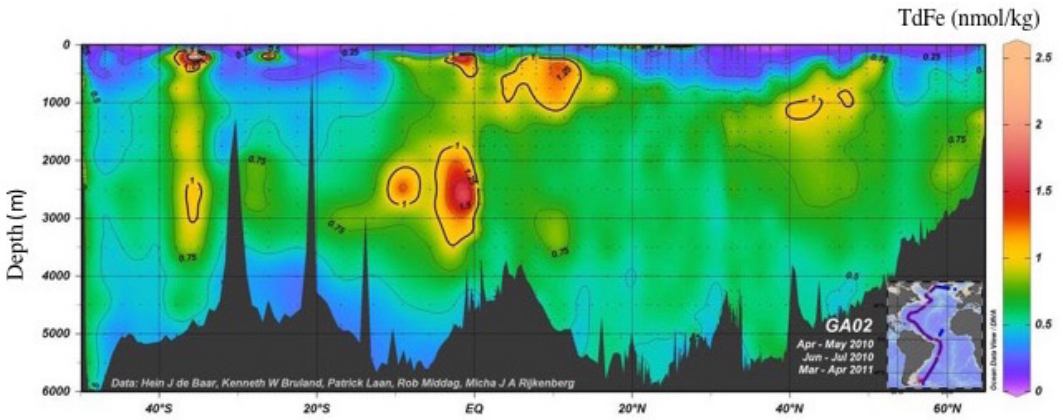


Fig. 1.2. Distributions of total dissolve Fe in the Atlantic Ocean (webpage: http://www.geotraces.org)

Table 1.1. Iron distribution in the oceans

| | | dFe nM | sFe nM | cFe nM | pFe nM | TDFe nM | Ref. |
|---|---|---|---|---|---|---|---|
| Atlantic Ocean | Surface | 0.23–0.34 | 0.21-0.4 | 0.1-0.3 | | 0.28-1.67 | (Bergquist and Boyle, 2006; Bergquist et al., 2007; Bowie et al., 2003; Bowie et al., 2006; Bowie et al., 1998; Bowie et al., 2004; Bowie et al., 2002; Boye et al., 2006; Buck et al., 2016; Cullen et al., 2006; Fitzsimmons and Boyle, 2014; Fitzsimmons et al., 2013; Laës et al., 2003; Laës et al., 2005; Mills et al., 2004; Mohamed et al., 2011; Powell et al., 1995; Saito et al., 2013; Ussher et al., 2010; Wu et al., 2001) |
| | 1000 m | 0.62–0.86 | | | | | |
| | 2000 m | 1.19–1.12 | | | | | |
| | >2500 m | 0.71-0.79 | | | | | |
| Pacific Ocean | Surface | <1 nM | 0.05-0.4 | 0-0.8 | | | (Chase et al., 2005; Coale, 1991; Hong and Kester, 1986; Mackey et al., 2002; Nishioka et al., 2001; Resing et al., 2015; Schmidt and Hutchins, 1999; Wu et al., 2001; Wu et al., 2011). |
| | > 100 m | 5-7 up to 800 * | | | | | |
| Indian Ocean | Surface | 0.15-0.3 nM | | | | | (Nishioka et al., 2013) |
| Southern Ocean | Surface nearshore | 5.3-12.6 | | | | | (Bowie et al., 2004; Bucciarelli et al., 2001; Chever et al., 2010; De Jong et al., 1998; Klunder et al., 2011; Tagliabue et al., 2012); |
| | Mid Layer depth | 0.04-0.42 | | | | Mid Layer depth 0.15-0.71 | |
| | Surface offshore | 0.1-0.3 | | | | | |
| | 2000-3000 | 0.6-0.7 | | | | | |
| | Deep water | 0.22-0.82 | | | | Deep water 0.39-1.75 | |
| Artic Ocean | | 0.13-2.08[a] | | | | 0.6-63.08[b] | (Campbell and Yeats, 1982; Crusius et al., 2017; Klunder et al., 2012; Thuróczy et al., 2011; Wehrmann et al., 2014) |
| Arabian Sea | | 0.5-2.4 | | | | | (Measures and Vink, 1999) |
| Mediterranean Sea | | 0.13-4.8 | | | 0.8 - 14.5 | 0.7 -7.0 | |

* Hydrothermal, upwelling or riverine.
(a) Which increase from 4 nM in surface to >10 nM nearshore.
(b) With extreme values of 1000 nM in nearshore.

## *1.3. Iron speciation in seawater*

Iron exists in two redox states, ferrous (Fe(II)) and ferric (Fe(III)). Each species exhibits different chemical characteristics. Iron(II) is very soluble, but is rapidly oxidized in the presence of oxygen. Fe(III) is the thermodynamically stable species in natural waters, but it can be reduced to Fe(II) under the influence of light (Miller et al., 1995) and microorganisms causing the formation of a significant steady state concentration of Fe(II) in surface waters (Laglera and van den Berg, 2007).

The concentration of dissolved Fe(II) (dFe(II)) in the open ocean is very low, between 0.02 and 2 nM, due to its fast oxidation rate under high oxygen concentrations (González-Davila et al., 2005; Santana-Casiano et al., 2005). In oxygen minimum zones, suboxic and anoxic waters, Fe concentrations can range from 300 to 3000 nM. In marine sediments interstitial waters, concentrations can reach about 300 μM while hydrothermal fluids can contain as much as 3 mM of dissolved iron (de Baar and de Jong, 2001). The presence of upwelling systems can increase Fe(II) concentration to 50 nM (Hong and Kester, 1986). In the NE Atlantic Ocean, Fe(II) ranged from less than 0.1 nM to 0.55 nM (Boye et al., 2006). Organic complexation, photochemical reactions and interactions with colloids and particle surfaces influence Fe speciation (Weber et al., 2005). The different inputs, chemical reactions, biological uptake and remineralization processes modify Fe concentrations, redox and aggregation state (Ye et al., 2009). These changes in the Fe speciation make Fe concentration difficult to measure and therefore the determination of Fe residence time in the sunlit surface ocean, where it can be used by phytoplankton, is complex. Furthermore, not all Fe forms in seawater are equally available for phytoplankton uptake (Hudson et al., 1990).

### *1.3.1. Iron inorganic speciation in seawater*

The interactions of Fe(II) and Fe(III) have been examined with the major and minor inorganic ligands found in natural waters ($Na^+$, $Mg^{2+}$, $Ca^{2+}$, $K^+$, $Sr^{2+}$, $Cl^-$, $SO_4^{2-}$, $HCO_3^-$, $Br^-$, $CO_3^{2-}$, $B(OH)_4^-$, $B(OH)_3$, $CO_2$, $OH^-$ and $HS^-$) using the specific interaction and ion pairing models (Millero et al., 1995). The first iron oxidation quantitative investigation in natural waters was published by (Stumm and Lee, 1961). This work was followed by further research with more detailed Fe(II) oxidation kinetic studies including all the inorganic speciation (González-Davila et al., 2005; Millero et al., 1987; Santana-Casiano et al., 2005) (Fig 1.3.). Those works quantified the role of ionic strength and media composition on Fe(II) oxidation by oxygen and hydrogen peroxide

over a range of temperature, pH, salinity, the presence of high nutrients concentrations and included the copper effect on the competition with Fe for the redox cycling.

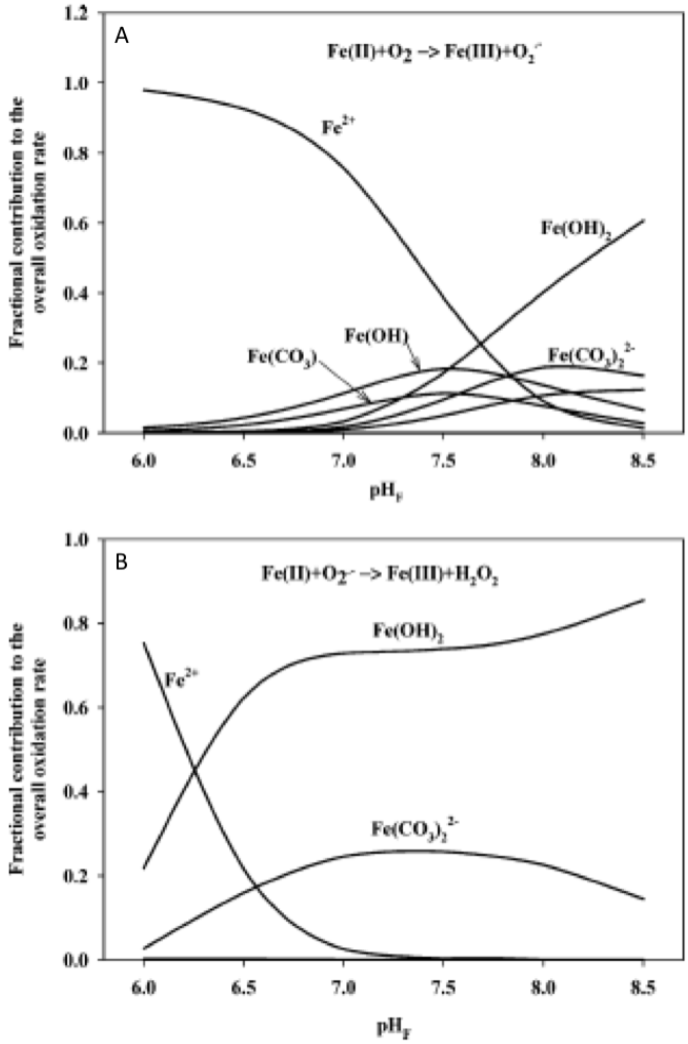


Fig 1.3. The different contributions of specific Fe(II) species in total Fe(II) oxidation: A) by oxygen and B) by oxygen and superoxide (Santana-Casiano et al., 2005).

### *1.3.2. Organic speciation of iron*

In the ocean 90-99.9% of dFe is formed by Fe(III) bound to organic ligands (Bruland, 2001). Organic complexation affects bioavailability and toxicity of metals (Sander and Koschinsky, 2011). Organic compounds can form complexes with Fe(II) and Fe(III) according to the solution pH and therefore, will have the ability to stabilize the inorganic Fe forms (Santana-Casiano et al., 2000). Four distinct classes of Fe-binding ligands, with different Fe complexing affinities, have been identified based on their absolute ligand strength, $\log k^{cond}_{FeL,Fe'}$ (Bundy et al., 2015) (Table 1.2.).

Table 1.2. Conditional stability constants for Fe-binding ligands in seawater, estuarine and coastal waters (obtained by Bundy et al. (2015)).

| Class of Fe-binding ligands | $\log k^{cond}_{FeL,Fe'}$ |
|---|---|
| $L_1$ | ≥12 |
| $L_2$ | 12-11 |
| $L_3$ | 11-10 |
| $L_4$ | <10 |

The stronger Fe binding ligand class ($L_1$) is found in the upper water column up-to 200 m depths. Weaker Fe binding ligand classes ($L_{2-4}$) are observed throughout the water column and in estuarine and coastal waters (Bundy et al., 2015). Stronger ligands found in seawater are associated to biological activities including the breakdown of sinking organic particulate matter (Santana-Casiano et al., 2000; Spokes et al., 2001); ligands produced by marine bacteria such as polysaccharides, porphyrins and siderophores (Ibisanmi et al., 2011) and/or terrestrial inputs (transported from rivers and continental shelves) (Macrellis et al., 2001). Siderophores are ligands which have different molecular structure as hidroxamates and catecholates (Wilhelm and Trick, 1994), mixed functional moieties as β-hydroxyaspartate/catecholate ligands with functional groups which include carboxylic acid, amines, thiols and hydroxyl groups (Reid et al., 1993). However, the composition of these ligands is still unknown, since almost any organic matter, can be suitable to generate metal-binding ligands (Hunter and Boyd, 2007).

Substances such as humic acids (HA) and fulvic acids (FA) (Laglera and van den Berg, 2009) which consist predominantly of polyphenols and benzoic/carboxylic acids originating from the decay of dead organisms (Buffle et al., 1990) have been studied. In the deep chlorophyll maximum, the excretion of ligand and/or regeneration of Fe through organic matter degradation, ingestion of particles and consequent dissolution and release of bioavailable Fe results in an enhancement of dFe concentrations (Bowie et al., 2002). The formation of complexes also affects the free Fe(II) oxidation rate (Santana-Casiano et al., 2000).

### *1.4. Solubility/precipitation*

The most stable thermodynamic form of Fe in seawater is Fe(III), however the inorganic chemistry of Fe(III) in seawater is controlled primarily by its hydrolysis (Turner and Hunter, 2001). Iron forms various hydrolyzed species in seawater through the sequential loss of protons from coordinated water molecules in the inner sphere at seawater pH. This process initially results in the formation of simple amorphous hydrous ferric oxyhydroxide which is converted over time to thermodynamically more stable solids including hematite, maghemite, goethite and lepidocrocite, such transformations result in a decrease in the solubility (Kuma et al., 1993). The hydrolysis is fast and shows that the precipitated solid is quite labile initially but rapidly becomes much less, with important implications for sequestration by organic ligands (Rich and Morel, 1990).

The Fe concentration in ocean waters is typically 0.1 to 0.8 nM, 100 fold higher than its solubility (Laglera and van den Berg, 2009). In seawater, the soluble Fe is inorganically controlled by temperature, pH (Liu and Millero, 2002), ionic strength (Liu and Millero, 1999) and aging time (Kuma et al., 1996). The effect on solubility due to changes in the pH has been attributed to a solid-state transformation of $Fe(OH)_3$ to FeOOH (Liu and Millero, 1999).

However, the presence of organic ligands in seawater changes the solubility of Fe(III), becoming the main Fe solubility control (Liu and Millero, 2002). The Fe(III) solubility differs from surface coastal waters to the open-ocean waters, attributed to higher organic ligand concentrations in coastal waters (Kuma et al., 1996). Iron cycling is ultimately limited in environmental and biological systems by the loss of $Fe(III)_{aq}$ through precipitation (Gunnars et al., 2002).

### *1.5. Changes in redox state of iron*

In surface water iron can be reduced by chemical or photochemical processes that allows measurable concentrations of Fe(II) (Bowie et al., 1998). Iron(II) is thermodynamically unstable and is rapidly oxidized to Fe(III) by $O_2$ and $H_2O_2$ following the Haber-Weiss process (Haber and Weiss, 1934) (Eqs. 1.1-1.4).

$$Fe(II) + O_2 \rightarrow Fe(III) + O_2^{\cdot -} \quad (1.1)$$

$$Fe(II) + O_2^{\cdot -} \xrightarrow{2H^+} Fe(III) + H_2O_2 \quad (1.2)$$

$$Fe(II) + H_2O_2 \rightarrow Fe(III) + OH^{\cdot} + OH^- \quad (1.3)$$

$$Fe(II) + OH^{\cdot} \rightarrow Fe(III) + OH^- \quad (1.4)$$

In addition, this mechanism can be completed by considering the reduction of Fe(III), the hydrolysis and formation of colloidal Fe(III), such as the competitive reaction between active oxygen species ($O_2^{\cdot -}$ and $H_2O_2$) with other species such as copper (Santana-Casiano et al., 2005) (Eqs. 1.5-1.8). The difference in the oxidation state affects to the speciation and the bioavailability of Fe (O'Sullivan et al., 1995).

$$Fe(III) + O_2^{\cdot -} \rightarrow Fe(II) + O_2 \quad (1.5)$$

$$Fe(III) + 3OH^- \rightarrow Fe(OH)_{2(s)} \quad (1.6)$$

$$Cu(II) + O_2^{\cdot -} \rightarrow Cu(I) + O_2 \quad (1.7)$$

$$Cu(I) + O_2^{\cdot -} \xrightarrow{2H^+} Cu(II) + H_2O_2 \quad (1.8)$$

### *1.6. Iron (II) oxidation kinetics*

The concentration of dissolved Fe(II) in the photic zone and in deep waters depends on the Fe(II) oxidation rate (González-Davila et al., 2005; Santana-Casiano et al., 2005). The oxidation rate of Fe(II) controls, in part, the steady-state concentration of Fe(II) and, as a consequence, the bioavailable Fe pool. At oxic–anoxic interfaces, the oxidation of Fe(II) by oxygen will produce a range of free radical oxidants and hydrogen peroxide (King, 1998). Essential to comprehending these complicated systems is a detailed mechanistic understanding of the electron transfer reactions involved in Fe(III).

The overall Fe(II) oxidation rate ($k_{app}$) can be explained in terms of the weighted sum of the oxidation rates of individual Fe(II) species, which react at different rates with oxygen (González-Davila et al., 2005; González-Dávila et al., 2006; Millero et al., 1987; Santana-Casiano et al., 2006; Santana-Casiano et al., 2005). The Fe(II) oxidation rate is expressed as an apparent oxidation rate, $k_{app}$ ($M^{-1}$ $min^{-1}$) taking into account the inorganic and organic speciation of Fe(II) (Eq 1.9).

$$k_{app} = k_{Fe^{2+}}\alpha_{Fe^{2+}} + k_{FeOH^+}\alpha_{FeOH^+} + k_{Fe(OH)_2}\alpha_{Fe(OH)_2} + k_{FeHCO_3^+}\alpha_{FeHCO_3^+} + k_{Fe(CO_3)}\alpha_{Fe(CO_3)} + k_{Fe(CO_3)_2^{2-}}\alpha_{Fe(CO_3)_2^{2-}} + k_{Fe(CO_3)OH^-}\alpha_{Fe(CO_3)OH^-} + k_{FeCl^+}\alpha_{FeCl^+} + k_{FeSO_4}\alpha_{FeSO_4} + k_{FeH_3SiO_4^+}\alpha_{FeH_3SiO_4^+} + \Sigma_i\, k_{L_i}\alpha_{FeL_i} \quad (1.9)$$

Iron(II) is thermodynamically unstable and is rapidly oxidized (seconds to minutes) by $O_2$ and $H_2O_2$ (González-Davila et al., 2005; Santana-Casiano et al., 2005) as a function of pH, ionic strength, temperature (Millero et al., 1987) and [$HCO3^-$] (Santana-Casiano et al., 2005). Moreover nutrients, specially silicate (González et al., 2010; Samperio-Ramos et al., 2016) and phosphate (Burns et al., 2011), Cu (González et al., 2016) and organic matter composition (Santana-Casiano et al., 2000) also control the oxidation process. At seawater pH, when $H_2O_2$ concentration is below 200 nM and [Fe(II)] is at nanomolar levels $O_2$ is the most important oxidant (Santana-Casiano et al., 2006).

Organic complexation formations often alter Fe(II) oxidation kinetics by either accelerating or retarding the oxidation rate, depending on the source and characteristics of the Fe-binding organic ligands (Emmenegger et al., 1998; Santana-Casiano et al., 2000; Theis and Singer, 1974). The effect of individual organic compounds on the oxidation kinetics of Fe(II) has been studied in laboratory experiments (Kuma et al., 1995; Santana-Casiano et al., 2010; Santana-Casiano et al., 2000). Some studies in open ocean have proposed the complexation of Fe(II) by organic ligands as an underlying mechanism to explain the changes in Fe(II) oxidation rates (Roy and Wells, 2011; Roy et al., 2008; Sarthou et al., 2011). It still remains unclear how the origin and molecular composition of dissolved organic matter influences the variation in Fe(II) oxidation in natural waters (Lee et al., 2016) and how the changes in composition of strong ligands across different nutrient regimes (Boiteau et al., 2016) could affect the Fe(II) oxidation rate and steady-state concentration (Daugherty et al., 2017). A significant fraction of these ligands are apparently bound within colloids (Boyd and Ellwood, 2010). The Fe-binding ligands present in seawater play a key role in keeping Fe, by prevention of formation of insoluble inorganic Fe complexes (Rijkenberg et al., 2008).

## *1.7. Behavior of Fe(II) inside a global change effect scenario*

Iron is a very reactive element in seawater. The concentration, distribution, speciation and the redox changes are mainly affected by the inputs, outputs, the redox reactions due to the seawater conditions and the possible different effects due to the organic matter complexation. The seawater characteristics in temperature, pH, salinity, oxygen, $H_2O_2$, [$HCO_3^-$], ionic strength, nutrients, metals concentrations and organic matter composition imply a change in the Fe behavior. According the main indications of Intergovernmental Panel on Climate Change (IPCC) (webpage: http://www.ipcc.ch) on the predicted ocean changes we introduced these possible effects on Fe(II) kinetics oxidation inside the forecast for the next century.

### *1.7.1. Temperature*

Temperature is one of the most important key factors controlling Fe(II) oxidation kinetics. An increase in temperature accelerates the Fe(II) oxidation rate (Millero et al., 1987; Santana-Casiano et al., 2005). The different IPCC scenarios show surface warming between about 1ºC (RCP2.6) to more than 3ºC in (RCP8.5). In the global ocean, the warming change between 0.5°C (RCP2.6) and 1.5°C (RCP8.5), with the effect affecting the first kilometer of the water column (Collins et al., 2013). The

patterns are further characterized by a slight cooling in parts of the northern mid and high latitudes below 1000 m depths and a pronounced heat uptake in the deep Southern Ocean by the end of the 21st century (Collins et al., 2013). The heat is transported within the ocean by its large-scale general circulation and by smaller-scale mixing processes. Those changes in transports lead to redistribution of existing heat content and can cause local cooling even though the global mean heat content rises (Banks and Gregory, 2006). Climate model projections reveal an increase of high latitude temperature and precipitation, both of these effects tend to make the high latitude surface waters lighter and hence increase their stability (Meehl et al., 2007).

### *1.7.2. Acidification*

The acidification term implies a decrease in the pH of the seawater. The pH is a key factors controlling Fe(II) oxidation kinetics. An increase in pH accelerates the Fe(II) oxidation rate (Millero et al., 1987; Santana-Casiano et al., 2005). The atmospheric $CO_2$ concentrations have increased from 280 μatm at pre-industrial times to about 400 μatm (Le Quéré et al., 2017) and are predicted to reach up to 1000 μatm by the end of this century (IPCC scenario RPC6.0) (Collins et al., 2013). About 30% of the released $CO_2$ is absorbed by the oceans (Sabine et al., 2004), affecting the carbonate system in the oceans and leading to a decrease in pH of about 0.3 units by the end of the current century (Ciais et al., 2014). Over the last three decades, DIC and $pCO_2$ content of surface waters has increased, pH and saturation states for $CaCO_3$ minerals have decreased and the capacity of the ocean to absorb $CO_2$ from the atmosphere has declined (Bates et al., 2014). The reduction in the ocean $CO_2$ system buffering capacity is a critical response with significant potential feedbacks (Riebesell et al., 2009). It is predicted to affect different biogeochemical and marine biological processes, potentially resulting in adverse effects not only on the species level but also on the community and ecosystem level (Riebesell et al., 2007).

The seawater pH affects phytoplankton physiology, including its exudates which can complex Fe, altering its solubility and cycling (Riebesell, 2004). The pH dependence of iron chelation and iron hydroxide precipitation may be responsible for maintaining elevated dFe in the high $CO_2$ environment (Kuma et al., 1996). A pH decrease may affect iron-ligand complex stabilities, resulting in altered photolability of Fe(III)-ligand complexes (Lewis et al., 1995). Reoxidation of Fe(II) to Fe(III) will possibly enhance the formation of Fe colloids, which may be reflected in the higher dFe concentrations in the high $CO_2$ treatments.

Ocean acidification may lead to enhanced Fe-bioavailability due to an increased fraction of dFe and elevated Fe(II) concentrations in coastal systems (Breitbarth et al., 2010).

### *1.7.3. Deoxygenation*

Oxygen is the main oxidant of Fe(II). Ocean warming and increased stratification of the upper ocean will lead to declines in dissolved $O_2$ (Keeling et al., 2010). Oxygen concentrations on continental margins are declining in many regions due to increased anthropogenic nutrient loadings (Rabalais et al., 2002). However the oxygen content of the ocean interior is determined by the influx of the gas across the air-sea surface and consumption due primarily to microbial respiration (Falkowski et al., 2011). Ocean models predict declines between 1 to 7% in the global ocean $O_2$ inventory over the next century (Keeling et al., 2010). Deoxygenation will be more important in oxygen minimum zones areas where $O_2$ levels are too low to support many macrofauna and profound changes in biogeochemical cycling occur (Keeling et al., 2010). Oxygen already appears to be declining in both the central North Pacific Ocean and tropical oceans (Falkowski et al., 2011; Keeling et al., 2010).

### *1.7.4. Salinity changes*

Salinity is another of the most important key factors controlling Fe(II) oxidation kinetics in seawater. An increase in salinity slows down the Fe(II) oxidation rate (Millero et al., 1987). The available 5$^{th}$ Phase of the Coupled Model Intercomparison Project (CMIP5) climate model projections suggest that high Sea Surface Salinity (SSS) subtropical regions, which are dominated by net evaporation, are typically getting more saline; while lower SSS regions at high latitudes are typically getting fresher (Durack and Wijffels, 2010).

## *1.8. Models of global ocean distribution of Fe*

Numerous global ocean Fe speciation and distribution models have been proposed in order to represent the oceans Fe biogeochemical cycle, which include the Global Change related variables.

These numerical models have been used to describe the Fe cycling between physical and chemical forms in the upper mixed layer (Weber et al., 2005), Fe speciation and biogeochemistry (Ye et al., 2009), more recently the Fe(II) oxidation rate (Tagliabue and Voelker, 2011), siderophores mediated Fe uptake (Völker and Wolf-Gladrow, 1999) and the uptake by phytoplankton cells (Völker and Wolf-Gladrow, 2000). These models consider the different inputs of Fe: dust, river, hydrothermal, sediments and have been improved including variables such as iron speciation and ligand concentration, chemical reactions, complexation and scavenging. Includes phytoplankton, zooplankton, particle size classes, limiting nutrients ($NO_3$, $PO_4$, DFe, $NH_4$, and $Si(OH)_4$), oxygen, dissolved inorganic carbon, dissolved organic carbon, alkalinity, calcite, and biogenic silica and the full carbon system is simulated (See Appendix D).

## *References*

Abadie, C., Lacan, F., Radic, A., Pradoux, C. and Poitrasson, F., 2017. Iron isotopes reveal distinct dissolved iron sources and pathways in the intermediate versus deep Southern Ocean. Proceedings of the National Academy of Sciences, 114(5): 858-863.

Banks, H.T. and Gregory, J.M., 2006. Mechanisms of ocean heat uptake in a coupled climate model and the implications for tracer based predictions of ocean heat uptake. Geophysical Research Letters, 33(7).

Bates, N. et al., 2014. A time-series view of changing ocean chemistry due to ocean uptake of anthropogenic $CO_2$ and ocean acidification. Oceanography, 27(1): 126-141.

Bergquist, B. and Boyle, E., 2006. Dissolved iron in the tropical and subtropical Atlantic Ocean. Global Biogeochemical Cycles, 20(1).

Bergquist, B., Wu, J. and Boyle, E., 2007. Variability in oceanic dissolved iron is dominated by the colloidal fraction. Geochimica et Cosmochimica Acta, 71(12): 2960-2974.

Boiteau, R.M. et al., 2016. Siderophore-based microbial adaptations to iron scarcity across the eastern Pacific Ocean. Proceedings of the National Academy of Sciences, 113(50): 14237-14242.

Bowie, A.R., Achterberg, E.P., Mantoura, R.F.C. and Worsfold, P.J., 1998. Determination of sub-nanomolar levels of iron in seawater using flow injection with chemiluminescence detection. Analytica Chimica Acta, 361(3): 189-200.

Bowie, A.R., Whitworth, D.J., Achterberg, E.P., Mantoura, R.F.C. and Worsfold, P.J., 2002. Biogeochemistry of Fe and other trace elements (Al, Co, Ni) in the upper Atlantic Ocean. Deep Sea Research Part I: Oceanographic Research Papers, 49(4): 605-636.

Bowie, A.R. et al., 2003. Shipboard analytical intercomparison of dissolved iron in surface waters

along a north–south transect of the Atlantic Ocean. Marine Chemistry, 84(1): 19-34.

Bowie, A.R., Sedwick, P.N. and Worsfold, P.J., 2004. Analytical intercomparison between flow injection chemiluminescence and flow injection spectrophotometry for the determination of picomolar concentrations of iron in seawater. Limnology and Oceanography: methods, 2(2): 42-54.

Bowie, A.R. et al., 2006. A community-wide intercomparison exercise for the determination of dissolved iron in seawater. Marine Chemistry, 98(1): 81-99.

Boyd, P. and Ellwood, M., 2010. The biogeochemical cycle of iron in the ocean. Nature Geoscience, 3(10): 675.

Boye, M. et al., 2006. The chemical speciation of iron in the north-east Atlantic Ocean. Deep Sea Research Part I: Oceanographic Research Papers, 53(4): 667-683.

Breitbarth, E. et al., 2010. Ocean acidification affects iron speciation during a coastal seawater mesocosm experiment. Biogeosciences (BG), 7(3): 1065-1073.

Bruland, K.W.R., E. L., 2001. Analytical methods for the determination of concentrations and speciation of iron. In: I.D.R.T.K.A.H. (Eds.) (Editor), The biogeochemistry of iron in sea water (IUPAC Series on Analytical and Physical Chemistry of Environmental Systems). John Wiley & Sons Ltd., pp. 255.

Bucciarelli, E., Blain, S. and Tréguer, P., 2001. Iron and manganese in the wake of the Kerguelen Islands (Southern Ocean). Marine Chemistry, 73(1): 21-36.

Buck, K.N., Gerringa, L.J.A. and Rijkenberg, M.J.A., 2016. An Intercomparison of Dissolved Iron Speciation at the Bermuda Atlantic Time-series Study (BATS) Site: Results from GEOTRACES Crossover Station A. Frontiers in Marine Science, 3(262).

Buffle, J., Altmann, R.S., Filella, M. and Tessier, A., 1990. Complexation by natural heterogeneous compounds: site occupation distribution functions, a normalized description of metal complexation. Geochimica et Cosmochimica Acta, 54(6): 1535-1553.

Bundy, R.M. et al., 2015. Iron-binding ligands and humic substances in the San Francisco Bay estuary and estuarine-influenced shelf regions of coastal California. Marine Chemistry, 173: 183-194.

Burns, J.M., Craig, P.S., Shaw, T.J. and Ferry, J.L., 2011. Short-Term Fe Cycling during Fe(II) Oxidation: Exploring Joint Oxidation and Precipitation with a Combinatorial System. Environmental Science & Technology, 45(7): 2663-2669.

Campbell, J. and Yeats, P., 1982. The distribution of manganese, iron, nickel, copper and cadmium in the waters of Baffin-Bay and the Canadian arctic archipelago. Oceanologica Acta, 5(2): 161-168.

Chase, Z. et al., 2005. Manganese and iron distributions off central California influenced by

upwelling and shelf width. Marine Chemistry, 95(3): 235-254.

Chereskin, B.M. and Castelfranco, P.A., 1982. Effects of iron and oxygen on chlorophyll biosynthesis II. Observations on the biosynthetic pathway in isolated etiochloroplasts. Plant physiology, 69(1): 112-116.

Chever, F. et al., 2010. Physical speciation of iron in the Atlantic sector of the Southern Ocean along a transect from the subtropical domain to the Weddell Sea Gyre. Journal of Geophysical Research: Oceans, 115(C10).

Ciais, P. et al., 2014. Carbon and other biogeochemical cycles, Climate change 2013: the physical science basis. Contribution of Working Group I to the Fifth Assessment Report of the Intergovernmental Panel on Climate Change. Cambridge University Press, pp. 465-570.

Coale, K.H., 1991. Effects of iron, manganese, copper, and zinc enrichments on productivity and biomass in the subarctic Pacific. Limnology and Oceanography, 36(8): 1851-1864.

Collins, M. et al., 2013. Long-term climate change: projections, commitments and irreversibility.

Crusius, J., Schroth, A.W., Resing, J.A., Cullen, J. and Campbell, R.W., 2017. Seasonal and spatial variability in northern Gulf of Alaska surface-water iron concentrations driven by shelf sediment resuspension, glacial meltwater, a Yakutat eddy, and dust. Global Biogeochemical Cycles: n/a-n/a.

Cullen, J.T., Bergquist, B.A. and Moffett, J.W., 2006. Thermodynamic characterization of the partitioning of iron between soluble and colloidal species in the Atlantic Ocean. Marine Chemistry, 98(2): 295-303.

Daugherty, E.E., Gilbert, B., Nico, P.S. and Borch, T., 2017. Complexation and Redox Buffering of Iron(II) by Dissolved Organic Matter. Environmental Science & Technology, 51(19): 11096-11104.

de Baar, H.J. and de Jong, J.T., 2001. Distributions, sources and sinks of iron in seawater. IUPAC series on analytical and physical chemistry of environmental systems, 7: 123-254.

De Jong, J. et al., 1998. Dissolved iron at subnanomolar levels in the Southern Ocean as determined by ship-board analysis. Analytica Chimica Acta, 377(2): 113-124.

Durack, P.J. and Wijffels, S.E., 2010. Fifty-year trends in global ocean salinities and their relationship to broad-scale warming. Journal of Climate, 23(16): 4342-4362.

Emmenegger, L., King, D.W., Sigg, L. and Sulzberger, B., 1998. Oxidation kinetics of Fe(II) in a eutrophic Swiss lake. Environmental science & technology, 32(19): 2990-2996.

Falkowski, P.G. et al., 2011. Ocean deoxygenation: past, present, and future. Eos, Transactions American Geophysical Union, 92(46): 409-410.

Fitzsimmons, J.N., Zhang, R. and Boyle, E.A., 2013. Dissolved iron in the tropical North Atlantic Ocean. Marine Chemistry, 154: 87-99.

Fitzsimmons, J.N. and Boyle, E.A., 2014. Both soluble and colloidal iron phases control dissolved iron variability in the tropical North Atlantic Ocean. Geochimica et Cosmochimica Acta, 125: 539-550.

González, A.G., Pérez-Almeida, N., Santana-Casiano, J.M., Millero, F.J. and González-Dávila, M., 2016. Redox interactions of Fe and Cu in seawater. Marine Chemistry, 179: 12-22.

González, A.G., Santana-Casiano, J.M., Pérez, N. and González-Dávila, M., 2010. Oxidation of Fe(II) in natural waters at high nutrient concentrations. Environmental science & technology, 44(21): 8095-8101.

González-Davila, M., Santana-Casiano, J.M. and Millero, F.J., 2005. Oxidation of iron(II) nanomolar with $H_2O_2$ in seawater. Geochimica et Cosmochimica Acta, 69(1): 83-93.

González-Dávila, M., Santana-Casiano, J.M. and Millero, F.J., 2006. Competition between $O_2$ and $H_2O_2$ in the oxidation of Fe (II) in natural waters. Journal of solution chemistry, 35(1): 95-111.

Gunnars, A., Blomqvist, S., Johansson, P. and Andersson, C., 2002. Formation of Fe(III) oxyhydroxide colloids in freshwater and brackish seawater, with incorporation of phosphate and calcium. Geochimica et Cosmochimica Acta, 66(5): 745-758.

Haber, F. and Weiss, J., 1934. The catalytic decomposition of hydrogen peroxide by iron salts. Proc. R. Soc. Lond. A, 147(861): 332-351.

Hong, H. and Kester, D.R., 1986. Redox state of iron in the offshore waters of Peru. Limnology and Oceanography, 31(3): 612-626.

Hudson, R.J., Morel, F.M. and Morel, F., 1990. Iron transport in marine phytoplankton: Kinetics of cellular and medium coordination reactions. Limnol. Oceanogr, 35(5): 1002-1020.

Hunter, K.A. and Boyd, P.W., 2007. Iron-binding ligands and their role in the ocean biogeochemistry of iron. Environmental Chemistry, 4(4): 221-232.

Ibisanmi, E., Sander, S.G., Boyd, P.W., Bowie, A.R. and Hunter, K.A., 2011. Vertical distributions of iron-(III) complexing ligands in the Southern Ocean. Deep Sea Research Part II: Topical Studies in Oceanography, 58(21-22): 2113-2125.

Keeling, R.F., Körtzinger, A. and Gruber, N., 2010. Ocean deoxygenation in a warming world. Marine Science, 2.

King, D.W., 1998. Role of carbonate speciation on the oxidation rate of Fe(II) in aquatic systems. Environmental science & technology, 32(19): 2997-3003.

Klunder, M., Laan, P., Middag, R., De Baar, H. and Van Ooijen, J., 2011. Dissolved iron in the Southern Ocean (Atlantic sector). Deep Sea Research Part II: Topical Studies in Oceanography, 58(25): 2678-2694.

Klunder, M.B. et al., 2012. Dissolved iron in the Arctic shelf seas and surface waters of the central Arctic Ocean: Impact of Arctic river water and ice-melt. Journal of Geophysical Research: Oceans, 117(C1).

Kuma, K., Nakabayashi, S. and Matsunaga, K., 1995. Photoreduction of Fe(III) by hydroxycarboxylic acids in seawater. Water Research, 29(6): 1559-1569.

Kuma, K., Nishioka, J. and Matsunaga, K., 1996. Controls on iron(III) hydroxide solubility in seawater: the influence of pH and natural organic chelators. Limnology and Oceanography, 41(3): 396-407.

Kuma, K., Suzuki, Y. and Matsunaga, K., 1993. Solubility and dissolution rate of colloidal γ-FeOOH in seawater. Water research, 27(4): 651-657.

Laës, A. et al., 2003. Deep dissolved iron profiles in the eastern North Atlantic in relation to water masses. Geophysical Research Letters, 30(17): n/a-n/a

Laës, A. et al., 2005. Impact of environmental factors on in situ determination of iron in seawater by flow injection analysis. Marine Chemistry, 97(3): 347-356.

Laglera, L.M. and van den Berg, C.M., 2009. Evidence for geochemical control of iron by humic substances in seawater. Limnology and Oceanography, 54(2): 610-619.

Laglera, L.M. and van den Berg, C.M.G., 2007. Wavelength Dependence of the Photochemical Reduction of Iron in Arctic Seawater. Environmental Science & Technology, 41(7): 2296-2302.

Le Quéré, C. et al., 2017. Global carbon budget 2017. Earth System Science Data Discussions: 1-79.

Lee, Y.P., Fujii, M., Terao, K., Kikuchi, T. and Yoshimura, C., 2016. Effect of dissolved organic matter on Fe(II) oxidation in natural and engineered waters. Water Research, 103: 160-169.

Lewis, B.L. et al., 1995. Voltammetric estimation of iron(III) thermodynamic stability constants for catecholate siderophores isolated from marine bacteria and cyanobacteria. Marine Chemistry, 50(1-4): 179-188.

Liu, X. and Millero, F.J., 1999. The solubility of iron hydroxide in sodium chloride solutions. Geochimica et Cosmochimica Acta, 63(19): 3487-3497.

Liu, X. and Millero, F.J., 2002. The solubility of iron in seawater. Marine Chemistry, 77(1): 43-54.

Mackey, D., O'Sullivan, J.O. and Watson, R., 2002. Iron in the western Pacific: a riverine or hydrothermal source for iron in the Equatorial Undercurrent? Deep Sea Research Part I: Oceanographic Research Papers, 49(5): 877-893.

Macrellis, H.M., Trick, C.G., Rue, E.L., Smith, G. and Bruland, K.W., 2001. Collection and detection of natural iron-binding ligands from seawater. Marine Chemistry, 76(3): 175-187.

Martin, J.H., Gordon, M. and Fitzwater, S.E., 1991. The case for iron. Limnology and Oceanography, 36(8): 1793-1802.

McDonough, W.F. and Sun, S.-S., 1995. The composition of the Earth. Chemical geology, 120(3-4): 223-253.

Meehl, G.A. et al., 2007. Global climate projections.

Measures, C. and Vink, S., 1999. Seasonal variations in the distribution of Fe and Al in the surface waters of the Arabian Sea. Deep Sea Research Part II: Topical Studies in Oceanography, 46(8): 1597-1622.

Miller, W.L., King, D.W., Lin, J. and Kester, D.R., 1995. Photochemical redox cycling of iron in coastal seawater. Marine Chemistry, 50(1): 63-77.

Millero, F.J., 1998. Solubility of Fe (III) in seawater. Earth and Planetary Science Letters, 154(1): 323-329.

Millero, F.J., Sotolongo, S. and Izaguirre, M., 1987. The oxidation kinetics of Fe (II) in seawater. Geochimica et Cosmochimica Acta, 51(4): 793-801.

Millero, F.J., Yao, W. and Aicher, J., 1995. The speciation of Fe (II) and Fe (III) in natural waters. Marine Chemistry, 50(1): 21-39.

Mills, M.M., Ridame, C., Davey, M., La Roche, J. and Geider, R.J., 2004. Iron and phosphorus co-limit nitrogen fixation in the eastern tropical North Atlantic. Nature, 429(6989): 292-294.

Mohamed, K.N., Steigenberger, S., Nielsdottir, M.C., Gledhill, M. and Achterberg, E.P., 2011. Dissolved iron(III) speciation in the high latitude North Atlantic Ocean. Deep Sea Research Part I: Oceanographic Research Papers, 58(11): 1049-1059.

Nishioka, J., Takeda, S., Wong, C. and Johnson, W., 2001. Size-fractionated iron concentrations in the northeast Pacific Ocean: distribution of soluble and small colloidal iron. Marine Chemistry, 74(2): 157-179.

Nishioka, J., Obata, H. and Tsumune, D., 2013. Evidence of an extensive spread of hydrothermal dissolved iron in the Indian Ocean. Earth and Planetary Science Letters, 361: 26-33.

O'Sullivan, D.W., Hanson, A.K. and Kester, D.R., 1995. Stopped flow luminol chemiluminescence determination of Fe (II) and reducible iron in seawater at subnanomolar levels. Marine Chemistry, 49(1): 65-77.

Powell, R.T., King, D.W. and Landing, W.M., 1995. Iron distributions in surface waters of the south Atlantic. Marine Chemistry, 50(1): 13-20.

Rabalais, N.N., Turner, R.E. and Wiseman Jr, W.J., 2002. Gulf of Mexico hypoxia, aka "The dead zone". Annual Review of ecology and Systematics, 33(1): 235-263.

Reid, R.T., Livet, D.H., Faulkner, D.J. and Butler, A., 1993. A siderophore from a marine bacterium with an exceptional ferric ion affinity constant. Nature, 366(6454): 455.

Resing, J.A. et al., 2015. Basin-scale transport of hydrothermal dissolved metals across the South Pacific Ocean. Nature, 523(7559): 200-203.

Rich, H.W. and Morel, F.M., 1990. Availability of well-defined iron colloids to the marine diatom Thalassiosira weissflogii. Limnology and Oceanography, 35(3): 652-662.

Riebesell, U., 2004. Effects of $CO_2$ Enrichment on Marine Phytoplankton. Journal of Oceanography, 60(4): 719-729.

Riebesell, U., Körtzinger, A. and Oschlies, A., 2009. Sensitivities of marine carbon fluxes to ocean change. Proceedings of the National Academy of Sciences, 106(49): 20602-20609.

Riebesell, U. et al., 2007. Enhanced biological carbon consumption in a high $CO_2$ ocean. Nature, 450(7169): 545.

Rijkenberg, M.J. et al., 2008. Changes in iron speciation following a Saharan dust event in the tropical North Atlantic Ocean. Marine Chemistry, 110(1): 56-67.

Sabine, C.L. et al., 2004. The oceanic sink for anthropogenic $CO_2$. science, 305(5682): 367-371.

Saito, M.A. et al., 2013. Slow-spreading submarine ridges in the South Atlantic as a significant oceanic iron source. Nature Geoscience, 6(9): 775-779.

Samperio-Ramos, G., Casiano, J.M.S. and Dávila, M.G., 2016. Effect of ocean warming and acidification on the Fe(II) oxidation rate in oligotrophic and eutrophic natural waters. Biogeochemistry, 128(1-2): 19-34.

Sander, S.G. and Koschinsky, A., 2011. Metal flux from hydrothermal vents increased by organic complexation. Nature Geoscience, 4(3): 145-150.

Santana-Casiano, J., Gonzalez-Davila, M. and Millero, F., 2006. The role of Fe(II) species on the oxidation of Fe(II) in natural waters in the presence of $O_2$ and $H_2O_2$. Marine chemistry, 99(1): 70-82.

Santana-Casiano, J.M., González-Dávila, M., González, A. and Millero, F., 2010. Fe(III) reduction in the presence of catechol in seawater. Aquatic geochemistry, 16(3): 467-482.

Santana-Casiano, J.M., González-Dávila, M. and Millero, F.J., 2005. Oxidation of nanomolar levels of Fe(II) with oxygen in natural waters. Environmental science & technology, 39(7): 2073-2079.

Santana-Casiano, J.M., González-Dávila, M., Rodrıguez, M.J. and Millero, F.J., 2000. The effect of organic compounds in the oxidation kinetics of Fe(II). Marine Chemistry, 70(1): 211-222.

Schmidt, M.A. and Hutchins, D.A., 1999. Size-fractionated biological iron and carbon uptake along

a coastal to offshore transect in the NE Pacific. Deep Sea Research Part II: Topical Studies in Oceanography, 46(11–12): 2487-2503.

Spokes, L., Jickells, T. and Jarvis, K., 2001. Atmospheric inputs of trace metals to the northeast Atlantic Ocean: the importance of southeasterly flow. Marine Chemistry, 76(4): 319-330.

Stumm, W. and Lee, G.F., 1961. Oxygenation of ferrous iron. Industrial & Engineering Chemistry, 53(2): 143-146.

Sunda, W.G. and Huntsman, S.A., 1995. Iron uptake and growth limitation in oceanic and coastal phytoplankton. Marine Chemistry, 50(1-4): 189-206.

Sunda, W.G., Swift, D.G. and Huntsman, S.A., 1991. Low iron requirement for growth in oceanic phytoplankton. Nature, 351(6321): 55.

Tagliabue, A. and Voelker, C., 2011. Towards accounting for dissolved iron speciation in global ocean models. Biogeosciences, 8(10): 3025.

Tagliabue, A. et al., 2012. A global compilation of dissolved iron measurements: focus on distributions and processes in the Southern Ocean. Biogeosciences, 9(6): 2333-2349.

Tagliabue, A. et al., 2017. The integral role of iron in ocean biogeochemistry. Nature, 543(7643): 51-59.

Theis, T.L. and Singer, P.C., 1974. Complexation of iron(II) by organic matter and its effect on iron(II) oxygenation. Environmental Science and Technology, 8(6): 569-573.

Thuróczy, C.E. et al., 2011. Distinct trends in the speciation of iron between the shallow shelf seas and the deep basins of the Arctic Ocean. Journal of Geophysical Research: Oceans, 116(C10).

Turner, D.R. and Hunter, K.A., 2001. The biogeochemistry of iron in seawater, 6. Wiley Chichester.

Ussher, S.J. et al., 2010. Distribution of size fractionated dissolved iron in the Canary Basin. Marine environmental research, 70(1): 46-55.

Van Leeuwe, M., Scharek, R., De Baar, H., De Jong, J. and Goeyens, L., 1997. Iron enrichment experiments in the Southern Ocean: physiological responses of plankton communities. Deep Sea Research Part II: Topical Studies in Oceanography, 44(1): 189-207.

Völker, C. and Wolf-Gladrow, D.A., 1999. Physical limits on iron uptake mediated by siderophores or surface reductases. Marine Chemistry, 65(3): 227-244.

Völker, C. and Wolf-Gladrow, D.A., 2000. Numerical models of iron uptake by phytoplankton cells. Journal of plant nutrition, 23(11-12): 1657-1665.

Weber, L., Völker, C., Schartau, M. and Wolf-Gladrow, D., 2005. Modeling the speciation and biogeochemistry of iron at the Bermuda Atlantic Time-series Study site. Global Biogeochemical

Cycles, 19(1).

Wehrmann, L.M. et al., 2014. Iron and manganese speciation and cycling in glacially influenced high-latitude fjord sediments (West Spitsbergen, Svalbard): Evidence for a benthic recycling-transport mechanism. Geochimica et Cosmochimica Acta, 141: 628-655.

Wilhelm, S.W. and Trick, C.G., 1994. Iron-limited growth of cyanobacteria: Multiple siderophore production is a common response. Limnology and Oceanography, 39(8): 1979-1984.

Williams, R.J.P., 1981. The Bakerian Lecture, 1981 Natural Selection of the Chemical elements. Proc. R. Soc. Lond. B, 213(1193): 361-397.

Wu, J., Boyle, E., Sunda, W. and Wen, L.-S., 2001. Soluble and colloidal iron in the oligotrophic North Atlantic and North Pacific. Science, 293(5531): 847-849.

Wu, J., Wells, M.L. and Rember, R., 2011. Dissolved iron anomaly in the deep tropical–subtropical Pacific: Evidence for long-range transport of hydrothermal iron. Geochimica et Cosmochimica Acta, 75(2): 460-468.

Ye, Y., Völker, C. and Wolf-Gladrow, D.A., 2009. A model of Fe speciation and biogeochemistry at the Tropical Eastern North Atlantic Time-Series Observatory site. Biogeosciences, 6(10): 2041-2061.

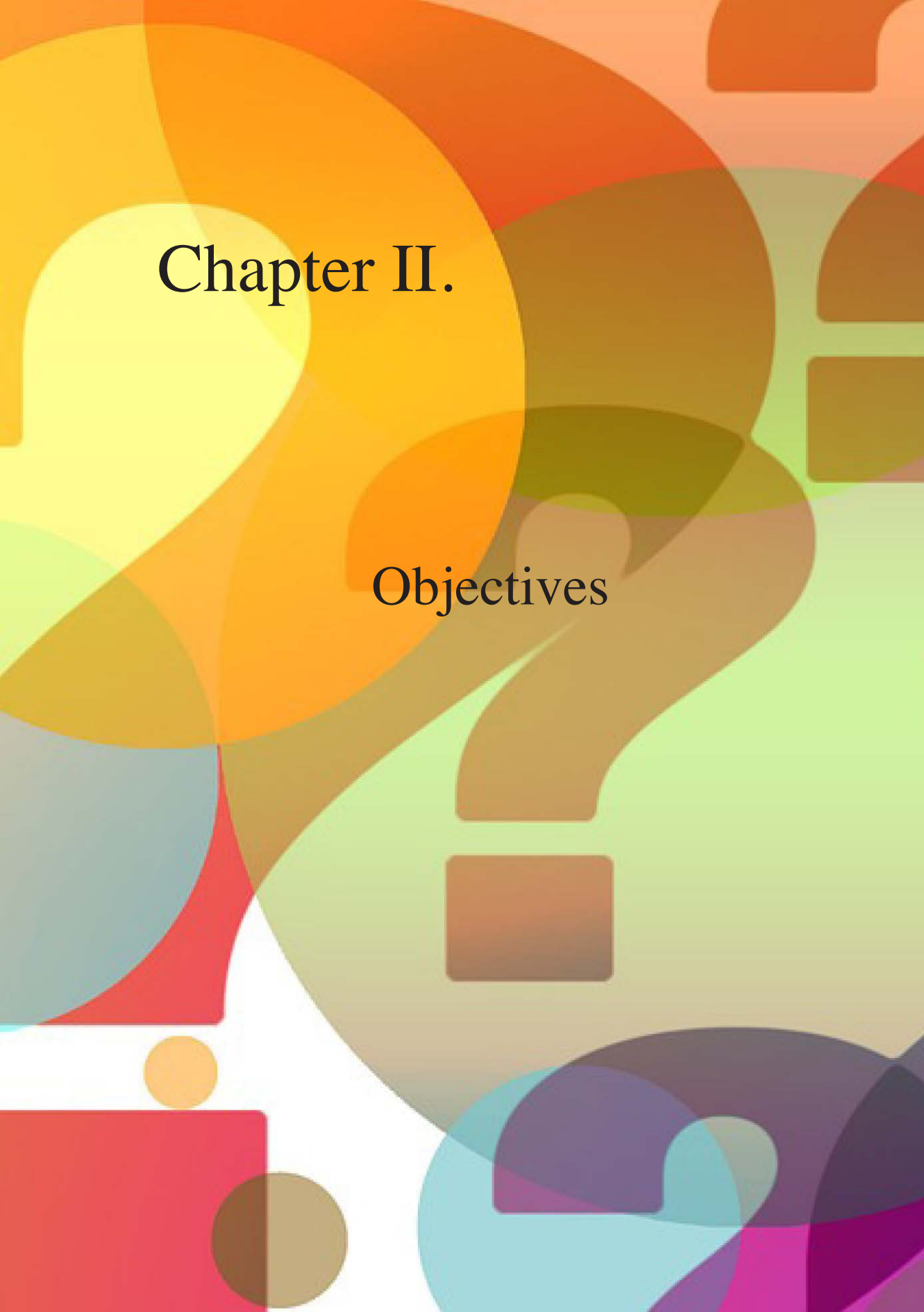

# Chapter II.

## Objectives

The general objective of this Thesis was to study the oxidation kinetics of Fe(II) in the area of the Tagoro submarine volcano (El Hierro, Canary Islands) and in the North Atlantic Ocean (Atlantic Subarctic and Labrador Sea), in order to understand the effect of the temperature, the pH, the salinity, the oxygen concentration and the organic matter in the control of the oxidation rate of this trace metal and to determinate the contribution of each variable to the oxidation rate process in natural conditions.

***Objectives for the Chapter III: "Emissions of Fe(II) and its kinetic of oxidation at Tagoro submarine volcano, El Hierro"***

1st Aim: To detect any variation in concentrations of TdFe(II) due to hydrothermal vent emissions in the post-eruptive phase of the submarine volcano Tagoro.

2nd Aim: To study the changes in the TdFe(II) concentration of the surrounding waters of the submarine volcano and the correlation of those changes with the pH.

3rd Aim: To study the temporal variability of TdFe(II) concentration over periods ranging from hours to days over the main and two secondary cones in the volcanic edifice of the Tagoro submarine volcano.

4th Aim: To study the oxidation kinetics of Fe(II) analyzing the effects of the seawater properties in the proximities of the volcano on the oxidation rate constants and $t_{1/2}$ (half-life time) of ferrous iron.

***Objectives for the Chapter IV: "Fe(II) oxidation kinetics in the North Atlantic along the 59.5ºN during 2016"***

1st Aim: To study the Fe(II) oxidation rate in different water masses present in the Subarctic North Atlantic Ocean, which is one of the most sensitive areas for ocean acidification, in order to know the time Fe(II) would be available in seawater.

2nd Aim: To study the variables which controll the Fe(II) oxidation rate in the ocean: temperature, pH, salinity and total organic carbon (TOC), under different temperature and pH conditions.

3rd Aim: To study the combined effects of the variables that control the Fe(II) oxidation kinetics in the ocean.

4th Aim: To understand the behavior of organic matter on the Fe(II) kinetics oxidation.

5th Aim: To understand the energy requirement for Fe(II) oxidation in surface and bottom waters.

6th Aim: To obtain an empirical equation for Fe(II) oxidation rate constants in the region considering the natural conditions of temperature, $pH_F$ and salinity for the area.

***Objectives for the Chapter V: "Organic Matter effect on the Fe(II) oxidation kinetics in the Labrador Sea"***

1st Aim: To study the Fe(II) oxidation rate in different water masses present in the Labrador Sea from coastal to open ocean and from surface to bottom waters.

2nd Aim: To study the variables that controll the Fe(II) oxidation rate in ocean: temperature, pH, salinity and total organic carbon (TOC), under different conditions.

3rd Aim: To study the combined effects of the variables that control the Fe(II) oxidation kinetics in the ocean.

4th Aim: To understand the behavior of organic matter on the Fe(II) kinetics oxidation.

5th Aim: understand the energy requirement for Fe(II) oxidation in surface, intermediate and bottom waters.

6th Aim: To obtain an empirical equation for Fe(II) oxidation rate constants in the Labrador Sea considering the natural conditions of temperature, $pH_F$ and salinity for

the area, which is also valid for the North Atlantic Ocean and can be incorporated into global Fe models.

7th Aim: To obtain a theoretical approach that considers the temperature and inorganic interactions on the oxidation kinetics to provide the organic ligand effects on the Fe(II) oxidation rate.

# Chapter III.

## Emissions of Fe(II) and its kinetics of oxidation at Tagoro Submarine volcano, El Hierro

Carolina Santana-González, J. Magdalena Santana-Casiano, Melchor González-Dávila, Eugenio Fraile-Nuez

Marine Chemistry 195 (2017) 129-137

## *Abstract*

The eruptive process that took place in October 2011 in the submarine volcano Tagoro off the Island of El Hierro and the subsequent degasification stage, five months later, have increased the concentration of TdFe(II) (Total dissolved iron(II)) in the waters nearest to the volcanic edifice. In order to detect any variation in concentrations of TdFe(II) due to hydrothermal emissions, three cruises were carried out two years after the eruptive process in October 2013, March 2014 and May 2015. The results from these cruises confirmed important positive anomalies in TdFe(II), which coincided with negatives anomalies in $pH_{F,is}$ (pH in free scale, at in situ conditions) located in the proximity of the main cone. Maximum values in TdFe(II) both at the surface, associated to chlorophyll a maximum, and at the sea bottom, were also observed, showing the important influence of organic complexation and particle re-suspension processes. Temporal variability studies were carried out over periods ranging from hours to days in the stations located over the main and two secondary cones in the volcanic edifice with positive anomalies in TdFe(II) concentrations and negative anomalies in $pH_{F,is}$ values. Observations showed an important variability in both $pH_{F,is}$ and TdFe(II) concentrations, which indicated the volcanic area was affected by a degasification process that remained in the volcano after the eruptive phase had ceased. Fe(II) oxidation kinetic studies were also undertaken in order to analyze the effects of the seawater properties in the proximities of the volcano on the oxidation rate constants and $t_{1/2}$ (half-life time) of ferrous iron. The increased TdFe(II) concentrations and the low associated $pH_{F,is}$ values acted as an important fertilization event in the seawater around the Tagoro volcano at the Island of El Hierro providing optimal conditions for the regeneration of the area.

## *3.1. Introduction*

Dissolved iron is the most bioavailable form assimilated by organisms (Brand, 1991; Hutchins et al., 1993). However, it is known that Fe(II) is thermodynamically unstable and is rapidly oxidized to Fe(III) in oxic waters (within seconds to minutes) (Kustka et al., 2005; Millero and Izaguirre, 1989; Santana-Casiano et al., 2005). Fe(III) has a very low solubility (Liu and Millero, 2002). The concentration of TdFe(II) dissolved in shallow and deep waters depends on the rate of oxidation of Fe(II) which is a function of both the $O_2$ and $H_2O_2$ concentration, pH, temperature, [$HCO_3^-$], ionic strength and nutrient concentration (González-Davila et al., 2005; González-Dávila et al., 2006; González et al., 2010; King and Farlow, 2000; Miller et al., 1995; Santana-Casiano et al., 2005; Shi et al., 2010). For this reason, the concentrations of dissolved Fe(II) in the open ocean are very low, with typical values in the 0.02 to 2 nmol $L^{-1}$ ranges. However, typical concentrations of dissolved iron in hydrothermal vents are 1–3 mmol $L^{-1}$, with extreme values of about 18.7 mmol $L^{-1}$ measured in the Juan de Fuca Ridge (de Baar and de Jong, 2001). In these areas, Fe(II) remains in solution over longer time periods due to pH and pε (reduction potential) conditions.

Hydrothermal vents require hydrothermal fluid circulation during tectonic or magmatic and volcanic activity, which provides fluid pathways in the fractured oceanic crust and heat sources (Mantas et al., 2011). The composition of the hydrothermal fluid, which migrates to the subsurface and finally discharges at the sea floor, depends on a number of critical parameters including temperature, pressure, phase separation and host rock composition (Sander and Koschinsky, 2011). Hydrothermal emissions of gases and particles are an important source of material of different size, texture and chemical composition, such as gases and metals, especially reduced iron (Santana-Casiano et al., 2013).

The hydrothermal vents affect the chemical composition of seawater (Resing et al., 2015; Tagliabue et al., 2010) and their diffuse fluxes regulate the magnitude of dissolved Fe in the plume to the deep ocean (Resing et al., 2015; Tagliabue et al., 2010; German et al., 2015). These vents could provide from 9% (Sander and Koschinsky, 2011) to 12–22% of the global deep-ocean dissolved Fe budget (Bennett et al., 2008). However, geographic variability in the production of Fe(III) particles in hydrothermal plumes is more dependent on chemical conditions in the ambient deep water than on compositional variations in the primary vent fluid. These variations may cause Fe(II) oxidation rates (Field and Sherrell, 2000) and residence time scales to vary greatly among the ocean basins which receive hydrothermal input (Nishioka et al., 2013). After

the hydrothermal emission, Fe(II) is oxidized under the presence of dissolved oxygen and precipitates into various mineral forms, mainly oxy-hydroxide (de Baar and de Jong, 2001) forming massive deposits of iron, but around 4% of the total emitted iron is stabilized against loss from solution due to complexation by dissolved organic ligands (Bennett et al., 2008; Resing et al., 2015), or by incorporation into inorganic or organic colloids which reside within the dissolved size fraction (Resing et al., 2015). Moreover, reduced species of Fe and S form an FeS colloidal complex, which remains suspended in the water and is modified as the pH changes (Luther et al., 2001). These nanoparticles can remain suspended in the deep sea for years with slower settling rates (Yücel et al., 2011), solubilizing and releasing the Fe(II). The complexation significantly increases metal content from hydrothermal systems, increasing trace-metal flux to the global ocean. The largest and most widespread Fe anomalies have been found in the Pacific, the Indian and the Atlantic basins (Tagliabue et al., 2010).

In 2011, Tagoro submarine volcano was formed 1.8 km south of the Island of El Hierro, the westernmost island of the Canary Archipelago. During the eruptive stage that was initiated on October 10 of 2011 and finished in March 2012, large amounts of gases and reduced chemical species were emitted (Fraile-Nuez et al., 2012). During these five first months, the carbonate system in the seawater was strongly affected and the pH decreased to 5.1 due to $CO_2$ emissions. Fe(II) and reduced sulfur concentrations increased to 50 μmol $L^{-1}$ and 200 μmol $L^{-1}$, respectively. The reaction between the reduced species of Fe(II) and S also contributed to the acidification of the system (Eq. 3.1) and the FeS formed contributed to stabilizing the Fe(II) (Santana-Casiano et al., 2013).

$$Fe(II) + H_2S \leftrightarrow FeS + 2H^+ \quad (3.1)$$

Just after the molten eruptive phase, changes in the characteristics of the gas and reduced species emissions also modified the carbonate system and decreased both pε and pH, which favor the presence of Fe(II). Emissions of $CO_2$ gas and carbonate alkalinity from the El Hierro submarine volcano accounted for 60% and 40%, respectively, of the pH change in local seawater (Santana-Casiano et al., 2016).

This work focuses on the study of the variation in the concentration of total dissolved Fe(II) and $pH_{F,is}$ in the seawater column due to hydrothermal emissions from the shallow submarine Tagoro volcano. The presence of shallow hydrothermal vents close to the coastal area in the post-eruptive phase of the submarine volcano (Santana-

Casiano et al., 2016) provided the opportunity to study the emission of total dissolved Fe(II), the changes in the pH of the surrounding waters and the correlation of those changes with the TdFe(II) concentration. The results obtained generated information about both the oxidation kinetics of Fe(II) and the effects of the natural Fe(II) fertilization process taking place in the area.

## *3.2. Material and methods*

### *3.2.1. Study location*

The study was conducted in the region of the Tagoro submarine volcano, south of the island of El Hierro (Canary Islands, Spain, at 27°37'07''N–017°59'28''W, Fig. 3.1A), during the oceanographic cruises of VULCANO in October 2013 and March 2014 and VULCANA in May 2015 on board the R/V Ángeles Alvariño. A grid of CTD stations around the El Hierro Island (Fig. 3.1B) and a high-resolution CTD study along the main cone of the volcano edifice (Fig. 3.1C) were carried out, with samples taken at different depths. A map of active hydrothermal vents location has been published (Santana-Casiano et al., 2016) generated following both pH and ORP (oxidation-reduction potential) anomalies in the Tagoro volcano.

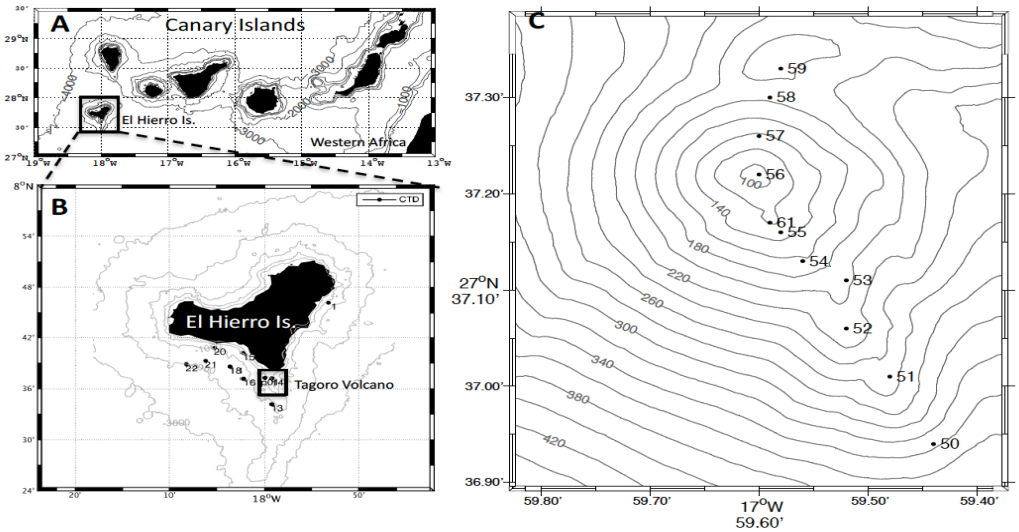


Fig. 3.1. A) General map of the Canary Archipelago. B) Island of El Hierro and reference stations sampled. C) Stations sampled in the high-resolution study.

### *3.2.2. Reagents*

#### *3.2.2.1. Iron stock*

An iron stock of 6.21 x $10^{-4}$ mol $L^{-1}$ was prepared using ammonium iron(II) sulfate hexahydrate (SIGMA-ALDRICH). HCl (HIPERPURPLUS, previously quartz distilled, Q-HCl) was added to the water to lower the pH to 2 and retard any oxidation. It was then stored in the dark until use. A diluted stock was prepared daily with a final concentration of 2.42 x $10^{-6}$ mol $L^{-1}$.

#### *3.2.2.2. Luminol*

The luminol was prepared using 0.2487 g of 5-amino-2,3-dihydro-1,4-phthalazinedione (FLUKA), 26.4976 g of $Na_2CO_3$ (SIGMA-ALDRICH) and 188.175 mL of $NH_3$ (PANREAC) (HIPERPUR-PLUS, previously distilled) in a total volume of 5 L of luminol reagent. The final pH was adjusted to 10.4 by adding 6 M Q-HCl. At this pH, luminescence is optimal (Bowie et al., 1998). The luminol solution was stored in the dark due to its light sensitivity. To ensure complete dilution, it was prepared a few days prior to use. The solution became more stable 24 h after preparation and for at least a month after (King et al., 1995).

#### *3.2.2.3. Carrier*

The carrier used was 0.7 M NaCl, to achieve an ionic strength similar to that of seawater in standards and samples. All the reagents were prepared with deionized ultrapure water (Milli-Q, 18.2 MΩ.$cm^{-1}$, Millipore). Milli-Q water was used as a cleaner between injections.

### *3.2.3. Sampling*

TdFe(II) and pH samples in the water column were collected using 10 L Niskin bottles mounted on a 24 position rosette frame fitted with a SeaBird SBE11 Plus CTD and with a SBE18 pH sensor. Acid pre-cleaned 50 mL polyethylene containers were

used and fitted with 45 mL of unfiltered sample. Prior to sampling, 10 µL of Q-HCl (6 M) was added to the containers in order to keep the seawater solution at pH 6. The samples were stored in the refrigerator at 4 °C until analysis to reduce the rate of Fe(II) oxidation. All the samples were always analyzed in a period of time lower than 3 h and no statistically significant differences were observed with samples that were analyzed immediately. The same methodology was followed for all the samples in this study. An intercomparison exercise was done at the initial stages of the cruise at four stations (50, 54, 59 and 61) where Go-Flo bottles with Kevlar cable and the Niskin bottles in the CTD rosette were used at the same depth (16 m) (Supplementary material, Table 3.1). Samples were also taken at 1 m from the bottom with the Go-Flo bottles. All the samples were transferred to a clean room on the ship for sampling and analysis.

Before use, all the material was rinsed three times with distilled water, three times with Milli-Q water and stored in 10% HCl solution for cleaning. When the material was going to be used, it was rinsed three times with distilled water and three times with Milli-Q water. After the analysis, the material was cleaned and re-stored in the HCl solution.

### *3.2.4. Measurements*

#### *3.2.4.1. Fe (II) concentration*

All the samples were analyzed on board. Before injection into the system, the samples were tempered at 20 °C. In order to determine the concentration of TdFe(II) in seawater the FeLume system (Waterville Analytical) was selected. The FIA-chemiluminescence technique uses luminol as the reagent (King et al., 1995). Dissolved, colloidal and labile phases of Fe(II) are determined and expressed as TdFe(II).

In the FIA system, four hoses are used and placed in a peristaltic pump (Rainin Dynamax 15.8 V), which connects them to the mixing chamber and to the detector. Subsequently, the pressure is regulated in the hoses while Milli-Q water passes through it. This allows the flow to be uniform and not in pulses. After adjusting the pressure in the hoses, the water-cleaning mode was enabled during 3 min. After this time, air was allowed to pass and then each hose was introduced into the corresponding receptacles: luminol, NaCl, Milli-Q water and sample. The software executed in the FeLume-chemiluminescence was provided by Waterville analytical (WA control V105, photo

counter control). An analysis time of 100 s was selected, to allow full recording of the peak signal. The peak area mode was selected in order to compute the signal. Three measurements for each sample were carried out and values were presented as average values. After a set of analyses, Milli-Q water was used to clean all hoses, and finally air was run to empty them.

### *3.2.4.2. Standards and calibration procedure*

Seawater used in the calibration procedure of the chemiluminescence signal was taken from a station unaffected by the volcano and aerated with a magnetic stirrer during 60 min in atmospheric contact. The solution was stirred at maximum speed for 1 h to oxygenate the sample at the selected temperature and pH. This time was sufficient to achieve complete oxidation of Fe(II) (Hansard and Landing, 2009; Santana-Casiano et al., 2004), and the matrix of the sample was maintained following the procedure carried out by Hansard and Landing (2009).

25 mL flasks, into which 10 μL of 6 mol $L^{-1}$ Q-HCl was added, were used in the standardization process. The required diluted iron stock was added to reach the final concentration and the flask was filled with seawater. The final pH in the flask was 6. A control with no addition of iron was prepared at each calibration step. Every day, three standards were performed to ensure that the initial calibration was maintained and small changes in the sensitivity were corrected. The calibration curves used were made in the concentration range 0.9 to 7.7 nmol $L^{-1}$ with correlation coefficients of $r^2 = 0.999$. The detection limit obtained was 0.09 nM (LD = 3x[STD], n = 4) and the quantification limit was 0.3 nM (LQ = 10x[STD], n = 4).

### *3.2.4.3. pH*

pH was measured in the whole water column using an SBE18 pH sensor that provides the values expressed in an NBS (National Bureau of Standards) scale. It uses a pressure-balanced glass-electrode Ag/AgCl-reference pH probe to provide in situ measurements at depths of up to 1200 m. The pH sensor was calibrated against precision buffer solutions of 4, 7, and 10 with ±0.02 pH units standard deviation.

Discrete samples were measured on the total scale at a constant temperature

of 25 °C ($pH_{T,25}$) by the UV–Vis spectrophotometric technique (Clayton and Byrne, 1993), using m-cresol purple as indicator (González-Dávila et al., 2003). The standard deviation for the measurements was ±0.002 and the accuracy of the system was 0.002.

In order to homogenize all $pH_{NBS}$ values provided by the sensor and to convert them to pH in total scale at in situ conditions, $pH_{T,is}$, a correlation equation was obtained. First, the measured $pH_{T,25}$ values were converted to in situ conditions using dissolved inorganic carbon data (data not shown) and the $CO_2$ Sys program (Lewis et al., 1998; Santana-Casiano and González-Dávila, 2011). Then, the converted pH values were correlated with those measured with the sensor. Due to changes in the pH sensor reading with deployments, the equation changed for each of them.

In the kinetic experiments, pH was measured on the free scale and Tris buffer was used (Millero, 1986). All the pH data in the text and in the figures, including kinetic and profile data are expressed in free scale.

*3.2.4.4. ORP*

The ORP sensor has a platinum working electrode and an Ag/AgCl reference electrode located in a single PEEK thermoplastic body. The sensor range was –500 to +500 mV, with output scaled to 0–5 V for an auxiliary analog channel on the CTD. The ORP sensor does not provide an absolute electric potential, however, the sensors respond instantaneously to the presence of reduced chemical species with a decrease in the measured potential. ORP data were expressed as a time derivative (dorp/dz), and anomalies were identified by negative values (Santana-Casiano et al., 2016).

*3.2.4.5. Kinetic studies*

The kinetic studies were carried out in a thermo-regulated cell connected to a thermostatic bath (PolyScience). For each study, the seawater was tempered to the chosen temperature. When the temperature was stable, the pH for the sample and for the Tris buffer was measured.

For the kinetics studies, 75 mL of seawater samples from two different depths

were used (341 m at station 50 and 5 m at tow-yo site_04). The initial concentration of added TdFe(II) was 4 nM. Fe(II) concentrations of 16 nM and 9.6 nM were also used for those kinetic studies where the oxidation rate was quick and the $t_{1/2}$ was lower than 1.7 min. All studies were done in the dark.

For each kinetic study, the seawater was placed in the glass cell and the magnetic stirrer was switched on for 1 h to attain the equilibrium oxygen concentration. When the solution was tempered and the pH stable at the desired value, the sample hose was introduced into the cell. After that, the iron stock was added and the stopwatch was started simultaneously at time 0 s.

The rates of oxidation of Fe(II) (Santana-Casiano et al., 2005) were expressed as an apparent oxidation rate, $k_{app}$ ($M^{-1}$ $min^{-1}$)

$$\frac{d[Fe(II)]}{dt} = -k_{app}[Fe(II)][O_2] \tag{3.2}$$

The brackets denote the total molar concentration. The oxygen concentration was calculated using the Benson and Krause (1984) equation. In aerate solutions, the Fe(II) kinetic studies followed a pseudofirst- order, $k'$ ($min^{-1}$)

$$\frac{d[Fe(II)]}{dt} = -k'[Fe(II)] \tag{3.3}$$

where: $k' = k_{app}[O_2]$

### *3.3. Results*

A high spatial resolution CTD study following the alignment of the main and secondary cones of the submarine volcano and several CTD yo-yo studies, at the stations close to the main cone, were carried out in all the cruises (Santana-Casiano et al., 2016). The changes in temperature and salinity due to the effect of the emissions as the CTD approached the active vents were not appreciable in this shallow-low temperature hydrothermal system. For that reason, chemical sensors were used. The variables measured for each station (temperature, salinity, pH, TdFe(II) and dorp/dz)

have been included in the Supplementary Table 3.2.

During the yo-yo studies, bottle samples were taken only when extreme anomalies were observed in the pH and/or ORP sensors in the downward CTD-rosette scanning. Nine hydrographical CTD stations around the whole island were used as reference stations (13, 14, 15, 16, 18, 20, 21, 22 and p_01) (Fig. 3.1B). $pH_{F,is}$ and TdFe(II) concentrations were analyzed in all the stations in order to quantify both the contribution of the hydrothermal vent to the pool of TdFe(II) and to determine whether the emission continued with time. Beyond the influence of the volcano, in the reference stations, typical vertical profiles of TdFe(II) and $pH_{F,is}$ were obtained. For the reference stations, TdFe(II) values below 0.1 nM were characteristic and the $pH_{F,is}$ changed from 8.10 in the surface water to 8.03 at 200 m depths. No significant differences were observed between TdFe(II) samples from Go-Flo and Niskin bottles in the selected stations where both bottles were used (Supplementary Table 3.1).

The vertical distribution of TdFe(II) concentration along the high resolution section across the volcano is shown in Fig. 3.2A. The sea surface waters presented low TdFe(II), with values of around 0.2 nM, except in stations 54 and 58 where concentrations of TdFe(II) reached 2.72 and 2.32 nM, respectively. Most of the stations, including the reference stations, showed a slight increase in iron concentration at 25 m, associated to the maximum of chlorophyll a in the section (not shown), with values from 0.2 to 0.9 nM. Moreover, all the stations sampled over the high resolution study presented an important increase in TdFe(II) from 50 m to the lowest measurable depth, with the exception of the southernmost and deepest station (50), which showed only a small increase of 0.2 nM. Values between 1.5 and 1.8 nM were measured at the bottom (160–200m) for stations 52, 53 and 54. The maximum anomaly in TdFe(II), 7.34 nM, was measured at 100 m in station 55, the station closest to the top of the volcano.

The vertical distribution of $pH_{F,is}$ at in situ conditions in the high-resolution study along the volcano is shown in Fig. 3.2B. At the sea surface, $pH_{F,is}$ was 8.160, except in stations 55, 56 and 58, which had values of 8.149, 8.152 and 8.145, respectively. All the stations presented a decrease in $pH_{F,is}$ values from 50 m to the bottom. However, values were 0.01 to 0.02 units lower than those observed at station 50. Minimum $pH_{F,is}$ values were recorded at station 55, with a pH of 7.96 at 100 m, 0.17 units lower than for station 50. This pH value increased as we moved away from station 55.

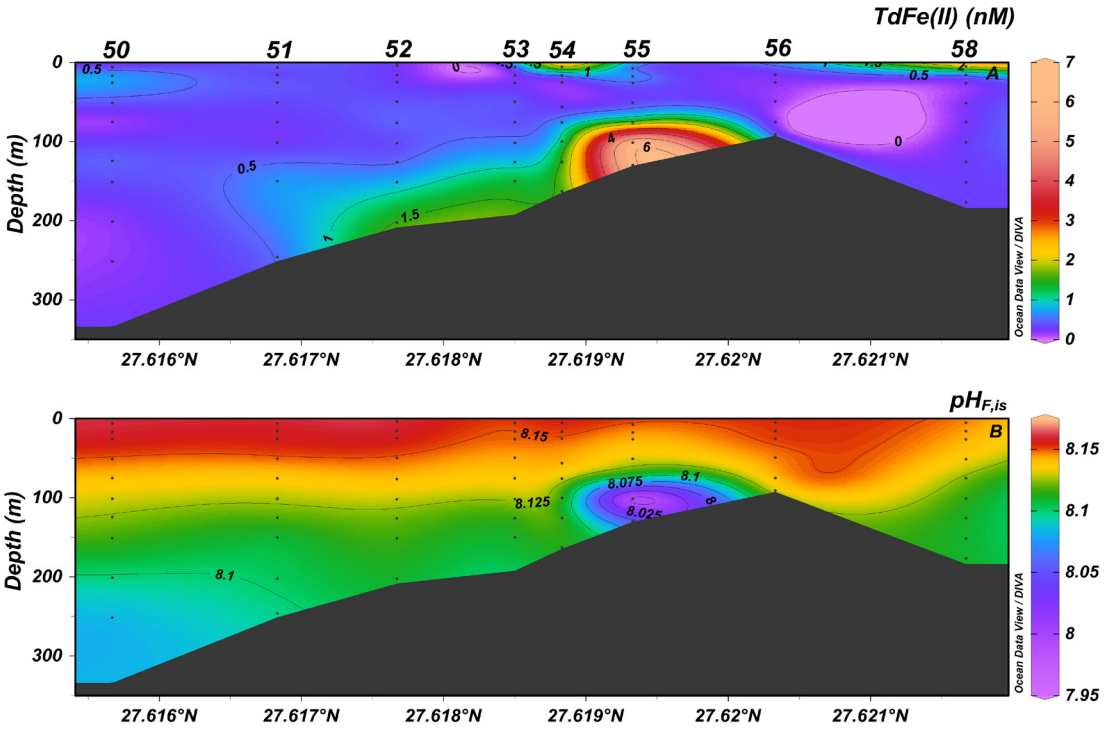


Fig. 3.2. A) TdFe(II) and B) pHF,is vertical distributions in the high-resolution study along the volcano transect in November 2013.

As can be observed in Fig. 3.2A and B, an important anomaly was observed in station 55 for both TdFe(II) and $pH_{F,is}$. In order to verify this anomaly, station 55 was measured 106 times from the surface to 1 m above the seabed during eight yo-yo CTD studies with 22, 45, 6, 9, 12, 5, 4 and 3 CTD casts, respectively. TdFe(II) was sampled at selected depths during casts 01, 68 and 83 on November 3 (13:00), 5 (21:00) and 7 (18:00), respectively. The TdFe(II) vertical profiles for stations 55, 55–68 and 55–83, are plotted in Fig. 3.3A. In all the studies, an important iron anomaly was observed at the same depth of 100 m. This anomaly reached values as high as 7.34 nM, 1.4 nM and 48.92 nM on November 3, 5 and 7, respectively. As can be seen in Fig. 3.3B, the vertical profiles of $pH_{F,is}$ for stations 55, 55–68 and 55–83 also show important $pH_{F,is}$ anomalies. Surface values ranged between 8.14 and 8.11, while at 100 m depths an important anomalous decrease in $pH_{F,is}$ was observed, reaching values of 7.96, 8.03 and 7.91 on November 3, 5 and 7, respectively.

In March 2014, a similar study was repeated and TdFe(II) and $pH_{F,is}$ were sampled along the high-resolution section. The sea surface waters presented TdFe(II) concentrations with values ranging between 0.1 and 1 nM. Similarly to the previous study, a slight enhanced iron concentration was observed at 25 m for some stations, associated to the maximum in chlorophyll a, and all the stations presented a slight increase of Fe(II) from 100 m to the bottom, with the highest anomaly values recorded at station 56, in the main crater, close to station 55. The $pH_{F,is}$ at in situ conditions also presented the highest values in the surface waters, 8.20, as in the previous studies, but in this case, 0.05 units higher than in November 2013, due to the seasonal variability of pH in the Canary region (Santana-Casiano and González-Dávila, 2011). All the stations presented a decrease in $pH_{F,is}$ from 50 m to the bottom. However, minimum $pH_{F,is}$ values were measured at station 56, along the whole profile, with a $pH_{F,is}$ value of 8.16 at the bottom.

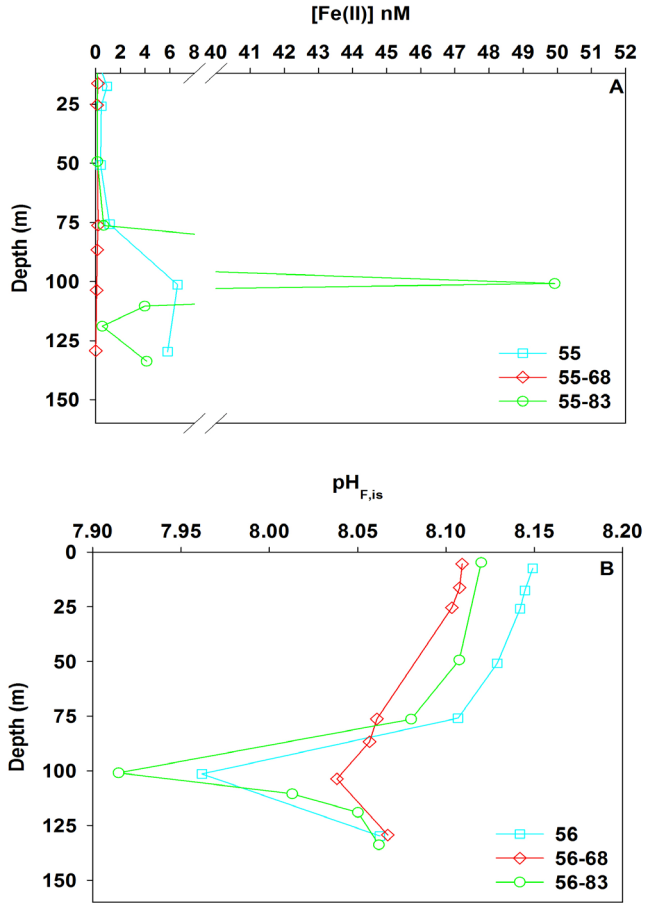


Fig. 3.3. A) TdFe(II) and B) $pH_{F,is}$ at station 55 on three different days during the same cruise. The stations 55, 55–68 and 55–83 were sampled on November 2013, 3, 5 and 7, respectively.

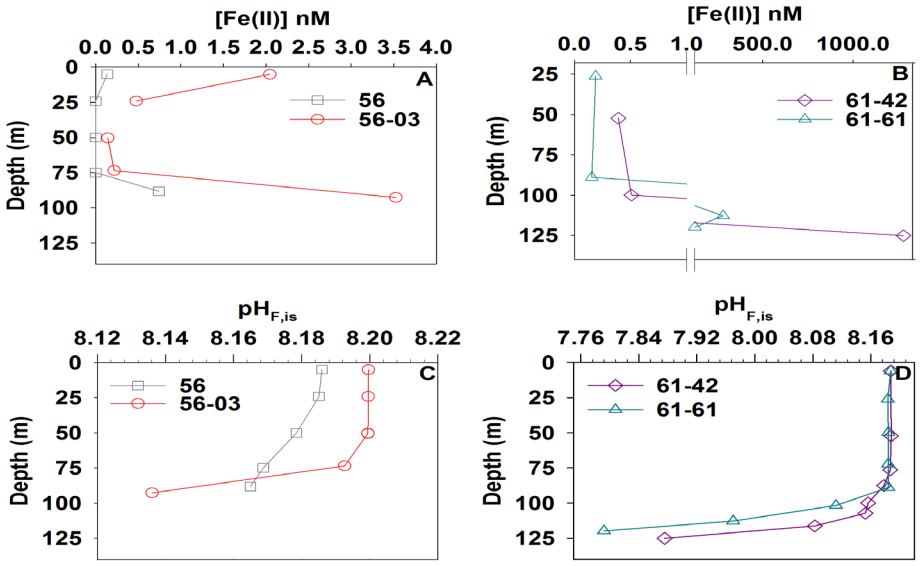


Fig. 3.4. A) Profiles of TdFe(II) at stations 56 and 56–03, on March 12 and 17 of 2014, respectively. B) Profiles of TdFe(II) at stations 61–42 and 61–61 on March 19. C) Profiles of $pH_{F,is}$ at stations 56 and 56–03 on March 12 and 17, respectively. D) Profiles of $pH_{F,is}$ at stations 61–42 and 61–61 on March 19.

During the March 2014 cruise, 7 tow-yos were done in an area chosen specifically to more precisely determine the extent of the $pH_{F,is}$ anomalies around the volcanic edifice (Santana-Casiano et al., 2016). On this occasion, two stations were selected to carry out the yo-yo CTD studies, stations 56 and 61. Fig. 3.4A and B show the anomalies in the vertical profile of TdFe(II) at stations 56 and 61. In station 56 this anomaly was located at all depths, especially at 90 m. The values were 0.13 nM and 2.04 nM at surface waters and 0.74 nM and 3.52 nM at 90 m, in stations 56 and 56–03, respectively. The time difference between the two samplings was five days. In station 61, the anomaly was more intense and located at around 120 m. The values of TdFe(II) in the bottom water were 1278.9 nM and 281 nM in stations 61–42 and 61–61, respectively. These stations were sampled within only four and a half hours of each other. $pH_{F,is}$ anomalies were also observed in stations 56 and 61, at the same depths (Fig. 3.4C and D). Changes of $pH_{F,is}$ between stations 56 and 56–03 were 0.01 in surface waters and 0.02 at 90 m, with a time difference of five days between the two samplings. The anomaly was observed all along the water column. In station 61, the anomaly was much more intense in the deeper waters, with changes of 0.08 units between casts.

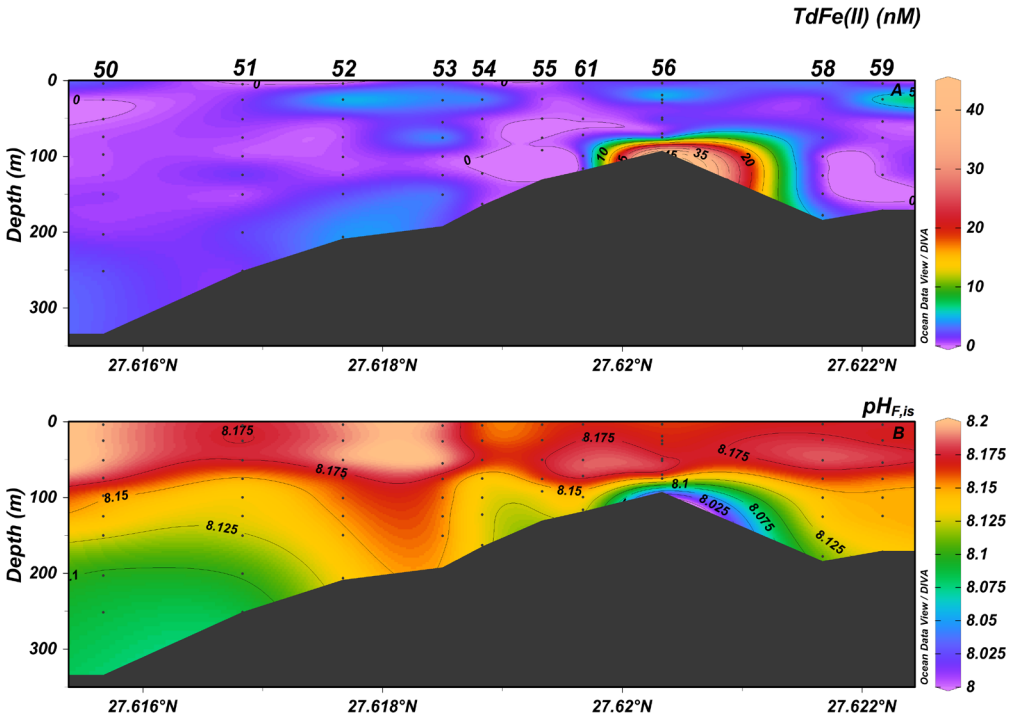


Fig. 3.5. Vertical distributions of A) TdFe(II) and B) $pH_{F,is}$ in the high resolution study along the volcano transect in May 2015.

One year later (Fig. 3.5A), the study was repeated and a similar pattern to that of the previous two cruises was found. Stations 56 and 58 presented TdFe(II) surface values that reached 3.06 and 3.24 nM, respectively. An enhanced iron concentration was observed at 25 m for almost all stations and a sharp increase in TdFe(II) was located at 97 m in station 56 with a value of 44.61 nM. With respect to the $pH_{F,is}$ (Fig. 3.5B), an important decrease to 8.00 was observed in station 56, representing a change of 0.15 units for this station. Sampling at station 56 was repeated two hours later and values of TdFe(II) of 5.53 nM and $pH_{F,is}$ of 8.08 were obtained at the same depth.

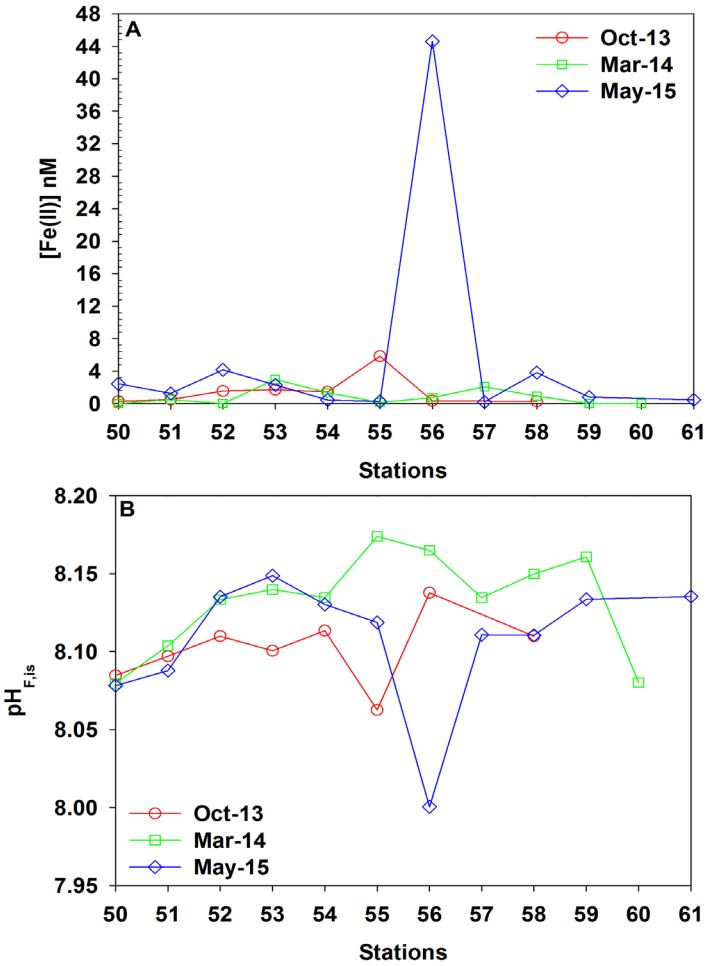


Fig. 3.6. A) TdFe(II) during October 2013, March 2014 and May 2015 at the bottom of the high-resolution section along the volcano transect. The main cone is located at station 56. B) $pH_{F,is}$ at the bottom of the high resolution section of the volcano transect.

Fig. 3.6A shows the concentrations of TdFe(II) at the bottom depth between 343 m (station 50) and 88 m (station 56), following the volcano shape. Two iron anomalies were detected during the October 2013 cruise: the first one between stations 52 and 53, where values of 1.59 nM and 1.77 nM were obtained, respectively, and the second at station 55, where a concentration of 6.44 nM was obtained. During the March 2014 cruise, two iron anomalies were again observed: the first one between stations 53–02 and 54, with values of 2.96 nM and 1.33nM, respectively, and the second one at station 57,

where a concentration of 2.06 nM was obtained. During May 2015, a very strong signal was located at station 56 of 44.61 nM and two weak signals were located at stations 52 and 58 with values of 4.16 and 3.80, respectively. Fig. 3.6B shows the results for $pH_{F,is}$. A trend opposite to that showed by the TdFe(II) (Fig. 3.6A) was observed. In the October 2013 cruise, a low $pH_{F,is}$ value was observed at station 55 (8.06), the lowest for the section. Moreover, a slight decrease in $pH_{F,is}$ was also measured in station 53 (value of 8.10, lower than those at the adjacent stations) and at stations 50, 51 and 58 which had values of 8.08, 8.09 and 8.10, respectively. However, in the March 2014 cruise, low $pH_{F,is}$ values were observed at stations 56 and 57 (8.16 and 8.13, respectively), and at station 54, with a value of 8.13. During the May 2015 cruise, a strong decrease in $pH_{F,is}$ was found in station 56,with a value of 8.00. This value represents 0.13 and 0.16 units less than the corresponding values at the same depths in October 2013 and March 2014, respectively. There were also two low values at stations 52 and 58, of 8.13 and 8.11, respectively.

The correlation coefficients between the changes in pH and those in TdFe(II) for each 2013, 2014 and 2015 cruise were 0.6, 0.5 and 0.6, respectively, indicating that the emitted fluids were rich in both carbonate species and TdFe(II). These coefficients also show that the correlation between changes in pH (due to the concentration of dissolved $CO_2$) and changes in TdFe(II) may vary because of other factors that control TdFe(II). The changes in the ORP sensor values (dorp/dz) were also correlated with the anomalies observed for TdFe(II). However, no significant correlation was found between dorp/dz and TdFe(II), indicating that other reduced species were affecting the change in the ORP signal.

Bearing in mind that the half-life time of Fe(II) in seawater depends principally on the oxygen concentration, the pH, and the composition of the medium, these waters offered a unique opportunity to study the kinetics of oxidation of Fe(II) in an area affected by hydrothermal conditions. For this purpose, several kinetic oxidation studies were carried out in order to gain insight on the behavior of Fe(II) in these conditions and the results were compared with data presented in the literature. Kinetics studies were done with two water samples: surface water with a salinity of 36.92 and deeper water with a salinity of 35.46. Each kinetic study was performed at different temperatures between 5 and 25 °C. Fig. 3.7 shows a linear dependence between the log $k_{app}$ ($M^{-1}$ $min^{-1}$) and the temperature (1000/T $K^{-1}$) for both salinities. The energy of activation obtained was 35.5 kJ $mol^{-1}$ and 72.1 kJ $mol^{-1}$ at surface and deeper water, respectively. It is important to note that these results obtained at different pH values and salinities providing two different energies of activation, indicate that the oxidation mechanism is not the same at the surface and close to the emission area, with Fe(II) oxidation

moreover affected by the $pH_{F,is}$ and salinity.

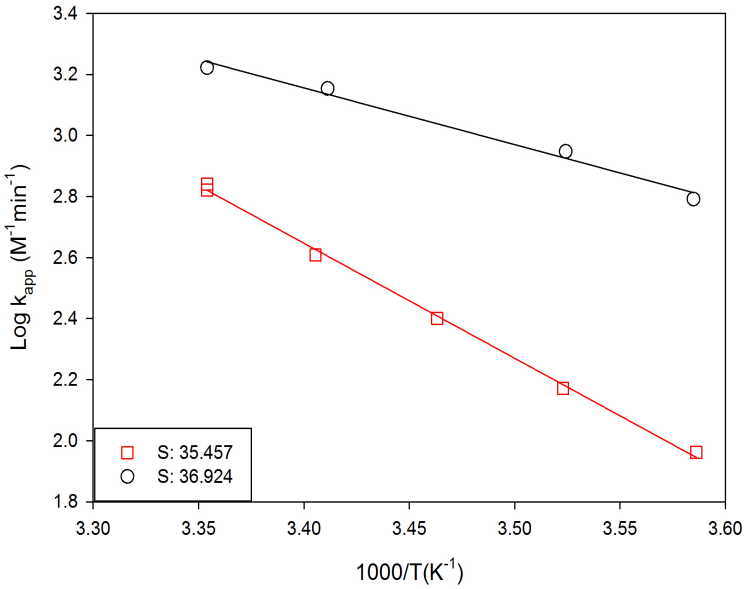


Fig. 3.7. Plot of log *k*app ($M^{-1}$ $min^{-1}$) and temperature (1000/K $T^{-1}$) for the kinetic studies.

Table 3.1. Measured and calculated Fe(II) oxidation rate constants at the different experimental conditions.

| Salinity | t (ºC) | $pH_F$ | $t_{1/2}$ (min) | log *k*' ($min^{-1}$) | Standard error | log $k_{app}$ ($M^{-1}$ $min^{-1}$) | log $k_{app}$ ($M^{-1}$ $min^{-1}$) (a) | log $k_{app}$ ($M^{-1}$ $min^{-1}$) (b) |
|---|---|---|---|---|---|---|---|---|
| 35.457 | 25 | 7.75 | 4.69 | 0.831 | 0.01 | 2.841 | 2.741 | 2.650 |
| | 25 | 7.75 | 4.91 | 0.850 | 0.01 | 2.821 | 2.741 | 2.650 |
| | 20.5 | 7.77 | 7.41 | 1.029 | 0.01 | 2.609 | 3.012 | 2.882 |
| | 15.6 | 7.82 | 10.93 | 1.198 | 0.01 | 2.400 | 2.331 | 2.221 |
| | 10.7 | 7.84 | 16.78 | 1.384 | 0.01 | 2.171 | 2.078 | 1.962 |
| | 5.7 | 7.94 | 24.32 | 1.545 | 0.01 | 1.962 | 1.908 | 1.776 |
| 36.924 | 25* | 8.13 | 1.61 | 0.365 | 0.01 | 3.222 | 3.176 | 3.077 |
| | 20** | 8.21 | 1.71 | 0.392 | 0.01 | 3.154 | 3.023 | 2.917 |
| | 10.6 | 8.26 | 2.25 | 0.511 | 0.01 | 2.948 | 2.587 | 2.473 |
| | 5.8 | 8.34 | 2.87 | 0.616 | 0.01 | 2.791 | 2.187 | 2.069 |

$[Fe(II)]_0$ = 4.026 nM, * 16.106 nM, ** 9.664 nM

The theoretical value of log $K_{app}$ ($M^{-1}$ $min^{-1}$) in seawater enriched with nutrients was calculated from (a) González et al. (2010) and (b) Samperio-Ramos et al. (2016).

The surface waters (5 m) had $pH_F$ values of 8.13 and slightly higher and the deeper water (343m) values of 7.75 and slightly higher at 25 °C. Values of $t_{1/2}$ (min), log *k'* ($min^{-1}$) and log $k_{app}$ ($M^{-1}$ $min^{-1}$) are shown as a function of temperature and $pH_F$ in Table 3.1. The oxidation of Fe(II) follows a pseudo-first-order behavior. The Fe(II) oxidation kinetic in surface waters with higher $pH_F$ had faster oxidation rates than those at deeper waters, where the $pH_F$ was lower.

### *3.4. Discussion*

The hydrothermal emissions around Tagoro submarine volcano off El Hierro island affect the pH of the surrounding waters as well as the TdFe(II) distribution in the water column. In the high resolution study along the volcanic edifice, positive anomalies in the vertical distribution of iron concentration were observed (Fig. 3.2A), located around 100 m depths, in station 55 in October 2013 and station 56 in March 2014 and May 2015. The iron concentration anomaly was also accompanied by an important anomaly in the $pH_{F,is}$ signal (Fig. 3.2B) (correlation coefficients of 0.6) at the same transect and at the same depth, with an opposite behavior. The low $pH_{F,is}$ values in the vertical distribution, along the full depth, are associated to $CO_2$ emissions from hydrothermal vents located in the volcano area. The three carbonate system variables measured in these cruises, with high values of total dissolved inorganic carbon and alkalinity (data not shown) together with the low values of pH, are completely consistent with the set of carbonic acidity constants of Mehrbach et al. (1973), refitted by Dickson and Millero (1987). These emissions also included important amounts of Fe(II) (Santana-Casiano et al., 2016, 2013). Low pH values help to maintain Fe(II) in solution for a longer period of time due to a decrease in its oxidation rate.

When a yo-yo sampling was carried out at station 55 (Fig. 3.3A and B), increases in the iron concentrations were also accompanied by a decrease in the $pH_{F,is}$ values for all the anomalies recorded. Both the decrease in the oxidation rate at low pH and the formation of complexed iron can help to maintain high concentrations of TdFe(II) in solution. The tow-yo sampling carried out across the volcano during the March 2014 cruise allowed us to more accurately determine the location of the sub-cones and emissions (Santana-Casiano et al., 2016). During the tow-yo sampling, important temporal anomalies were also detected in stations 56 and 61, indicating changes in the emitted fluid composition with time.

Although the $pH_{F,is}$ at the bottom of station 61, 61–61, was lower than that three and half hours before, 61–42, (Fig. 3.4B), the TdFe(II) concentration decreased. This behavior could be explained by considering changes in the emitted iron concentration and due to scavenging onto surfaces or the presence of less effective complexing substances. The high value obtained at the bottom depth of station 61–42 of 1278.9 nM was, however, three orders of magnitude lower than the range of values determined in other hydrothermal vents, of 1–3 mmol $L^{-1}$ (de Baar and de Jong, 2001).

Moreover, values recorded for all cruises at the bottom across the volcano transect showed TdFe(II) concentrations (Fig. 3.6A) were a mirror image of those for $pH_{F,is}$ (Fig. 3.6B). The relationship between low $pH_{F,is}$ and high TdFe(II) concentrations indicated that emissions of hydrothermal fluids rich in acid and iron were active in the area, particularly in the proximities of station 55, during October 2013, and station 56, in March 2014 and May 2015, which were affecting the $pH_{F,is}$ and TdFe(II) profiles and the surrounding sea bottom values. However, other factors such as organic complexation and scavenging could also be important.

The Fe(II) oxidation kinetic studies carried out during May 2015 in the surrounding waters affected by the volcanic emissions provided important results. Both surface (S= 36.92) and deep (341 m, S = 35.46) seawater followed a pseudo-first-order Fe(II) kinetic. For each value of salinity, oxidation became faster as the temperature increased. Moreover, the oxidation of Fe(II) was faster in surface waters with salinity of 36.92 and $pH_{F,is}$ over 8.12 than in deeper seawater (at 341 m) with salinity of 35.46 and $pH_{F,is}$ over 7.75 at the same temperature.

In order to compare the log $k_{app}$ with other previous data obtained at high nutrient concentrations, the experimental conditions of these studies (pH, T and S) were included in the empirical equation of González et al. (2010) and Samperio-Ramos et al. (2016), valid at high nutrient water concentration (Table 3.1). The log $k_{app}$ ($M^{-1}$ $min^{-1}$) obtained at both salinities presented values very close to those obtained by González et al. (2010) and Samperio-Ramos et al. (2016). These values are faster than those expected in natural oligotrophic seawater with low concentrations of macronutrients (Santana-Casiano et al., 2005). In deeper water, with salinity 35.46, 25 °C and $pH_F$ 7.75, log $k_{app}$ ($M^{-1}$ $min^{-1}$) was 2.841, a similar value to the theoretical value of 2.741 reported in González et al. (2010) and 2.650 in Samperio-Ramos et al. (2016). At 5.7 °C and $pH_F$ 7.94, log $k_{app}$ ($M^{-1}$ $min^{-1}$) was 1.962. This value is closer to the 1.908 reported in González et al. (2010) than the 1.776 reported in Samperio- Ramos et al. (2016). However, at 20.5 °C and $pH_F$ 7.77, the log $k_{app}$ ($M^{-1}$ $min^{-1}$) was 2.609, a value

closer to the 2.882 reported in Samperio-Ramos et al. (2016) than the 3.012 value in González et al. (2010). In surface water, with salinity 36.92, the rate was faster than in the deeper waters at the same temperature. This difference can be explained by considering the dependence of the Fe(II) oxidation rate on pH and on the different nutrient concentrations (data not shown) of the seawater samples and those in the model. Log $k_{app}$ presented values that were closer to those obtained in González et al. (2010) for 25 °C and 20 °C. However, at colder temperatures than 10.6 °C the log $k_{app}$ presented higher values than the theoretical ones (when temperature increases $pH_F$ decreases due to the temperature effect and a gradual increase in log $k_{app}$ values should be observed).

Kinetic studies carried out in the volcanic area showed Fe(II) oxidation rates were faster than those expected in natural oligotrophic seawater. In general, the values were more in line with those at high nutrient concentration. González et al. (2010) and Samperio-Ramos et al. (2016) demonstrated that the effect of high nutrient seawater, particularly related to higher silicate concentration, increases the Fe(II) oxidation rate. During the eruptive phase, important inputs of silicate in the area were measured (Santana-Casiano et al., 2013). The differences in log $k_{app}$ between the three studies are probably due to different nutrient contents, metal interactions and the effect of nutrient content and type of organic matter. The emission of iron and nutrients (Santana-Casiano et al., 2013) also increases the rate of phytoplankton production (Fitzwater et al., 1996; Martin et al., 1994) which induces changes in organic iron complexation and Fe(II) oxidation rates favored at the low pH values in the area (Breitbarth et al., 2010). Iron-ligand complexes have been found in the seawater hydrothermal plumes rising above the vents (Bennett et al., 2008; Statham et al., 2005), which will affect metal concentration in hydrothermal fluids (Sander and Koschinsky, 2011) and change the reactivity of the Fe species, preventing precipitation of Fe and scavenging onto particulate phases (Bennett et al., 2008). Authors such as Breitbarth et al. (2010) observed that ocean acidification may lead to enhanced Fe-bioavailability due to an increased fraction of dFe and elevated Fe(II) concentrations in coastal systems. Moreover, seawater pH affects phytoplankton physiology (Fu et al., 2008), and thus indirect effects via phytoplankton exudates that complex iron may also alter the biological influence on iron solubility and cycling (Breitbarth et al., 2010). In our study, sub-maxima values of Fe(II) were always associated to the depth of the chlorophyll maximum, where organic excreted ligands could play the aforementioned roles. The anomalies observed at the bottom areas in $pH_{F,is}$ and TdFe(II) during the three cruises confirmed the emission of gases and reduced compounds in the volcano region, especially in the sub-cone located at station 55 in October 2013, at stations 56 and 61 in March 2014, and at station 56 in May 2015. The emission of hydrothermal fluids, rich in $CO_2$ and in reduced iron forms (among other emitted metals which have not been considered), whose concentrations can change

with time as was observed in the yo-yo studies, affects the surrounding volcanic area and contributes to an increase in the TdFe(II) that can enhance the biological activity as a result of this natural fertilization event.

### *3.5. Conclusions*

The studies carried out during the three cruises in the area of the Tagoro submarine volcano off El Hierro island, showed important positive TdFe(II) anomalies, which were inversely correlated with negative anomalies in $pH_{F,is}$. These studies allowed investigation of the temporal evolution of the total dissolved Fe(II) concentrations in the area and an analysis of the natural Fe(II) fertilization process.

It was observed that emissions of TdFe(II) continue in the area four years after cessation of the molten eruptive phase. The magnitude of TdFe(II) was not the same in all the sampling periods, with high variability over a short time scale, and was also inversely related to pH. This may be due to changes in the mixing process along the shape of the volcano or changes in the amount of emitted fluids in the hydrothermal vents that mixed with the surrounded oxygenated waters. The kinetic studies in the volcanic area showed Fe(II) oxidation rates were higher than those expected in oligotrophic seawater. The increase in the Fe(II) oxidation rate can be explained by the higher amount of macronutrients, in particular silicates, in these waters.

This study has showed that the increased TdFe(II) concentrations due to the hydrothermal emissions may be acting as an important fertilization event in the seawater around the Tagoro submarine volcano near the island of El Hierro, providing optimal conditions for the regeneration of the area.

**Acknowledgements**

This work was supported by the Ministerio de Economía y Competitividad of the Spanish Government, through the ECOFEMA (CTM2010-19517), EACFe (CTM2014-52342-P) and VULCANO (CTM2012-36317) projects and by the Spanish Institute of Oceanography through the VULCANA (2015–2017) project. This work was completed while C.S-G was a Ph.D. student in the IOCAG Doctoral Program in Oceanography and Global Change. Special thanks go to J. González-Santana and Stephen Henry Burns for

their kind revision of the English and their comments.

## *References*

Bennett, S.A., et al., 2008. The distribution and stabilisation of dissolved Fe in deep-sea hydrothermal plumes. Earth Planet. Sci. Lett. 270 (3), 157–167.

Benson, B.B., Krause, D., 1984. The concentration and isotopic fractionation of oxygen dissolved in freshwater and seawater in equilibrium with the atmosphere. Limnol. Oceanogr. 29 (3), 620–632.

Bowie, A.R., Achterberg, E.P., Mantoura, R.F.C.,Worsfold, P.J., 1998. Determination of subnanomolar levels of iron in seawater using flow injection with chemiluminescence detection. Anal. Chim. Acta 361 (3), 189–200.

Brand, L.E., 1991. Minimum iron requirements of marine phytoplankton and the implications for the biogeochemical control of new production. Limnol. Oceanogr. 36 (8), 1756–1771.

Breitbarth, E., et al., 2010. Ocean acidification affects iron speciation during a coastal seawater mesocosm experiment. Biogeosciences 7 (3), 1065–1073.

Clayton, T.D., Byrne, R.H., 1993. Spectrophotometric seawater pH measurements: total hydrogen ion concentration scale calibration of m-cresol purple and at-sea results. Deep-Sea Res. I Oceanogr. Res. Pap. 40 (10), 2115–2129.

de Baar, H.J.W., de Jong, J.T.M., 2001. Distributions, sources and sinks of iron in seawater. In: Turner, D.R., Hunter, K.A. (Eds.), The Biogeochemistry of Iron in Sea Water. John Wiley & Sons Ltd, p. 123.

Dickson, A., Millero, F.J., 1987. A comparison of the equilibrium constants for the dissociation of carbonic acid in seawater media. Deep Sea Res. Part A 34 (10), 1733–1743.

Field, M.P., Sherrell, R.M., 2000. Dissolved and particulate Fe in a hydrothermal plume at 9°45′N, East Pacific rise: slow Fe(II) oxidation kinetics in Pacific plumes. Geochim.Cosmochim. Acta 64 (4), 619–628.

Fitzwater, S.E., Coale, K.H., Gordon, R.M., Johnson, K.S., Ondrusek, M.E., 1996. Iron deficiency and phytoplankton growth in the equatorial Pacific. Deep-Sea Res. II Top. Stud. Oceanogr. 43 (4), 995–1015.

Fraile-Nuez, E., et al., 2012. The submarine volcano eruption at the island of El Hierro: physical-chemical perturbation and biological response. Sci. Rep. 2, 1–6.

Fu, F.-X., et al., 2008. Interactions between changing $pCO_2$, $N_2$ fixation, and Fe limitation in the marine unicellular cyanobacterium Crocosphaera. Limnol. Oceanogr. 53 (6), 2472–2484.

German, C., et al., 2015. Hydrothermal Fe cycling and deep ocean organic carbon scavenging: model-based evidence for significant POC supply to seafloor sediments. Earth Planet. Sci. Lett. 419, 143–153.

González, A.G., Santana-Casiano, J.M., Pérez, N., González-Dávila,M., 2010. Oxidation of Fe(II) in natural waters at high nutrient concentrations. Environ. Sci. Technol. 44 (21), 8095–8101.

González-Dávila, M., Santana-Casiano, J.M., Rueda, M.J., Llinás, O., González-Dávila, E.F., 2003. Seasonal and interannual variability of sea-surface carbon dioxide species at the European station for time series in the ocean at the Canary Islands (ESTOC) between 1996 and 2000. Glob. Biogeochem. Cycles 17 (3), 1–5.

González-Davila, M., Santana-Casiano, J.M., Millero, F.J., 2005. Oxidation of iron(II) nanomolar with $H_2O_2$ in seawater. Geochim. Cosmochim. Acta 69 (1), 83–93.

González-Dávila, M., Santana-Casiano, J.M., Millero, F.J., 2006. Competition between $O_2$ and $H_2O_2$ in the oxidation of Fe(II) in natural waters. J. Solut. Chem. 35 (1), 95–111.

Hansard, S.P., Landing, W.M., 2009. Determination of iron(II) in acidified seawater samples by luminol chemiluminescence. Limnol. Oceanogr. Methods 7 (3), 222–234.

Hutchins, D.A., DiTullio, G.R., Burland, K.W., 1993. Iron and regenerated production: evidence for biological iron recycling in two marine environments. Limnol. Oceanogr. 38 (6), 1242–1255.

King, D., Farlow, R., 2000. Role of carbonate speciation on the oxidation of Fe(II) by $H_2O_2$. Mar. Chem. 70 (1), 201–209.

King, D.W., Lounsbury, H.A.,Millero, F.J., 1995. Rates and mechanism of Fe(II) oxidation at nanomolar total iron concentrations. Environ. Sci. Technol. 29 (3), 818–824.

Kustka, A.B., Shaked, Y., Milligan, A.J., King, D.W., Morel, F.M., 2005. Extracellular production of superoxide by marine diatoms: contrasting effects on iron redox chemistry and bioavailability. Limnol. Oceanogr. 50 (4), 1172–1180.

Lewis, E., Wallace, D., Allison, L.J., 1998. Program Developed for $CO_2$ System Calculations. Carbon Dioxide Information Analysis Center, Managed by Lockheed Martin Energy Research Corporation for the US Department of Energy Tennessee.

Liu, X., Millero, F.J., 2002. The solubility of iron in seawater. Mar. Chem. 77 (1), 43–54.

Luther, G.W., et al., 2001. Chemical speciation drives hydrothermal vent ecology. Nature 410 (6830), 813–816.

Mantas, V.M., Pereira, A.,Morais, P.V., 2011. Plumes of discolored water of volcanic origin and possible implications for algal communities. The case of the home reef eruption of 2006 (Tonga, Southwest Pacific Ocean). Remote Sens. Environ. 115 (6), 1341–1352.

Martin, J.H., et al., 1994. Testing the iron hypothesis in ecosystems of the equatorial Pacific Ocean. Nature 371, 123.

Mehrbach, C.C.C.H., Hawley, J.E., Pytkowicx, R.M., 1973. Measurement of the apparent dissociation constants of carbonic acid in seawater at atmospheric pressure. Limnol. Oceanogr. 18 (6), 10.

Miller, W.L., King, D.W., Lin, J., Kester, D.R., 1995. Photochemical redox cycling of iron in coastal seawater. Mar. Chem. 50 (1), 63–77.

Millero, F.J., 1986. The pH of estuarine waters. Limnol. Oceanogr. 31 (4), 839–847.

Millero, F.J., Izaguirre, M., 1989. Effect of ionic strength and ionic interactions on the oxidation of Fe (II). J. Solut. Chem. 18 (6), 585–599.

Nishioka, J., Obata, H., Tsumune, D., 2013. Evidence of an extensive spread of hydrothermal dissolved iron in the Indian Ocean. Earth Planet. Sci. Lett. 361, 26–33.

Resing, J.A., et al., 2015. Basin-scale transport of hydrothermal dissolvedmetals across the South Pacific Ocean. Nature 523 (7559), 200–203.

Samperio-Ramos, G., Santana Casiano, J.M., González Dávila, M., 2016. Effect of ocean warming and acidification on the Fe(II) oxidation rate in oligotrophic and eutrophic natural waters. Biogeochemistry 128 (1), 19–34.

Sander, S.G., Koschinsky, A., 2011. Metal flux from hydrothermal vents increased by organic complexation. Nat. Geosci. 4 (3), 145–150.

Santana-Casiano, J., González-Dávila, M., 2011. pH decrease and effects on the chemistry of seawater. In: Duarte, P., Santana-Casiano, J.M. (Eds.), Oceans and the Atmospheric Carbon Content. Springer Netherlands, pp. 95–114.

Santana-Casiano, J.M., González-Dávila, M., Millero, F.J., 2004. The oxidation of Fe (II) in NaCl–$HCO_3^-$ and seawater solutions in the presence of phthalate and salicylate ions: a kinetic model. Mar. Chem. 85 (1), 27–40.

Santana-Casiano, J.M., González-Dávila, M.,Millero, F.J., 2005. Oxidation of nanomolar levels of Fe(II) with oxygen in natural waters. Environ. Sci. Technology 39 (7), 2073–2079.

Santana-Casiano, J.M., et al., 2013. The natural ocean acidification and fertilization event caused by the submarine eruption of El Hierro. Sci. Rep. 3, 1–8.

Santana-Casiano, J., et al., 2016. Significant discharge of $CO_2$ from hydrothermalism associated with the submarine volcano of El Hierro Island. Sci. Rep. 6.

Shi, D., Xu, Y., Hopkinson, B.M., Morel, F.M., 2010. Effect of ocean acidification on iron availability to marine phytoplankton. Science 327 (5966), 676–679.

Statham, P., German, C., Connelly, D., 2005. Iron(II) distribution and oxidation kinetics in hydrothermal plumes at the Kairei and Edmond vent sites, Indian Ocean. Earth Planet. Sci. Lett. 236 (3), 588–596.

Tagliabue, A., et al., 2010. Hydrothermal contribution to the oceanic dissolved iron inventory. Nat. Geosci. 3 (4), 252–256.

Yücel, M., Gartman, A., Chan, C.S., Luther, G.W., 2011. Hydrothermal vents as a kinetically stable source of iron-sulphide-bearing nanoparticles to the ocean. Nat. Geosci. 4 (6), 367–371.

Supplementary Table 3.1. Intercomparison exercise between Go-flo and Niskin bottles. Differences among studies were non statistically significative. Data presented in supplementary Table 3.2 are all determined with Niskin bottles.

| Sampling bottle | Bottom depth (m) | St | [TdFe(II)] nM |
|---|---|---|---|
| Go-Flo | 1 | 50 | 1.79 ± 0.09 |
| | | 54 | 1.55 ± 0.08 |
| | | 59 | 1.47 ± 0.07 |
| | | 61 | 0.75 ± 0.04 |
| | 16 | 50 | 1.31 ± 0.07 |
| | | 54 | 1.30 ± 0.06 |
| | | 59 | 1.48 ± 0.07 |
| | | 61 | 0.38 ± 0.02 |
| Niskin | 16 | 50 | 1.36 ± 0.07 |
| | | 54 | 1.35 ± 0.07 |
| | | 59 | 1.49 ± 0.07 |
| | | 61 | 0.43 ± 0.02 |

Supplementary Table 3.2. Experimental values determined for the three cruises. Standard deviation (std) for triplicate measurements are also included.

| Station | Depth (db) | Salinity | T (ºC) | $pH_{F, is}$ | std | [Fe(II)] nM | std |
|---|---|---|---|---|---|---|---|
| **OCTOBER --2013** | | | | | | | |
| 13 | 1050.50 | 35.32 | 7.75 | 7.913 | 0.001 | 0.51 | 0.03 |
| Lat: 27.5700 | 801.28 | 35.32 | 8.70 | 7.906 | 0.002 | 0.24 | 0.01 |
| Long: -17.9869 | 601.00 | 35.55 | 11.14 | 7.943 | 0.003 | 0.27 | 0.01 |
| | 299.20 | 36.06 | 14.76 | 8.042 | 0.001 | 0.57 | 0.03 |
| | 200.72 | 36.39 | 16.65 | 8.085 | 0.002 | 0.52 | 0.03 |
| | 100.26 | 36.74 | 19.39 | 8.121 | 0.001 | 1.97 | 0.10 |
| | 50.58 | 36.95 | 22.96 | 8.151 | 0.002 | 0.93 | 0.05 |
| | 26.55 | 36.97 | 23.53 | 8.155 | 0.002 | 0.60 | 0.03 |
| | 5.53 | 36.97 | 23.54 | 8.157 | 0.001 | 0.61 | 0.03 |
| 14 | 208.47 | 36.32 | 16.22 | 8.105 | 0.001 | 0.67 | 0.03 |
| Lat: 27.6201 | 153.28 | 36.44 | 16.93 | 8.108 | 0.002 | 0.83 | 0.04 |
| Long: -17.9868 | 100.87 | 36.64 | 18.30 | 8.121 | 0.001 | 0.56 | 0.03 |
| | 52.21 | 36.97 | 22.84 | 8.154 | 0.001 | 0.33 | 0.02 |
| | 27.47 | 36.98 | 22.97 | 8.166 | 0.002 | 0.44 | 0.02 |
| | 5.52 | 36.97 | 23.53 | 8.169 | 0.001 | 0.78 | 0.04 |
| 15 | 461.72 | 35.87 | 13.60 | | | 0.14 | 0.01 |
| Lat: 27.6696 | 301.88 | 36.17 | 15.36 | | | 0.40 | 0.02 |
| Long: -18.0367 | 201.33 | 36.45 | 17.01 | | | 0.14 | 0.01 |
| | 101.24 | 36.74 | 19.04 | | | 0.22 | 0.01 |
| | 27.85 | 36.97 | 23.41 | | | 0.57 | 0.03 |
| | 5.05 | 36.98 | 23.63 | | | 0.25 | 0.01 |
| 16 | 1395.57 | 35.30 | 6.35 | | | < D.L. | |
| Lat: 27.6198 | 1201.55 | 35.34 | 7.21 | | | 0.15 | 0.01 |
| Long: -18.0364 | 1001.81 | 35.30 | 7.95 | | | 0.12 | 0.01 |
| | 801.80 | 35.39 | 9.47 | | | 0.16 | 0.01 |
| | 602.17 | 35.60 | 11.59 | | | 3.19 | 0.16 |
| | 301.65 | 36.09 | 14.97 | | | 0.15 | 0.01 |
| | 202.60 | 36.35 | 16.39 | | | 0.62 | 0.03 |
| | 102.11 | 36.78 | 19.54 | | | 0.18 | 0.01 |
| | 27.12 | 36.98 | 23.57 | | | 0.23 | 0.01 |
| | 5.18 | 36.98 | 23.65 | | | 0.48 | 0.02 |
| 18 | 1501.57 | 35.27 | 6.00 | | | 0.11 | 0.01 |
| Lat: 27.6433 | 1201.38 | 35.34 | 7.28 | | | 0.10 | 0.00 |
| Long: -18.0594 | 1101.85 | 35.32 | 7.54 | | | 0.11 | 0.01 |
| | 1001.24 | 35.28 | 7.81 | | | < D.L. | |
| | 801.39 | 35.36 | 9.21 | | | 0.11 | 0.01 |
| | 600.31 | 35.57 | 11.24 | | | < D.L. | |
| | 302.11 | 36.14 | 15.25 | | | < D.L. | |
| | 201.41 | 36.46 | 16.99 | | | < D.L. | |
| | 101.39 | 36.70 | 18.88 | | | < D.L. | |
| | 26.16 | 36.98 | 23.55 | | | < D.L. | |
| | 5.33 | 36.98 | 23.57 | | | < D.L. | |
| 20 | 905.59 | 35.31 | 8.37 | | | 0.33 | 0.02 |
| Lat: 27.6804 | 801.54 | 35.34 | 8.91 | | | 0.63 | 0.03 |
| Long: -18.0869 | 702.22 | 35.45 | 10.07 | | | 0.47 | 0.02 |
| | 601.40 | 35.56 | 11.17 | | | 0.45 | 0.02 |
| | 301.56 | 36.06 | 14.75 | | | 0.53 | 0.03 |
| | 201.77 | 36.41 | 16.75 | | | 0.91 | 0.05 |

| | | | | | | | |
|---|---|---|---|---|---|---|---|
| | 126.77 | 36.69 | 18.43 | | | 0.40 | 0.02 |
| | 102.29 | 36.75 | 19.05 | | | 0.65 | 0.03 |
| | 26.93 | 36.99 | 23.63 | | | 0.70 | 0.04 |
| | 5.75 | 36.99 | 23.66 | | | 1.52 | 0.08 |
| 21 | 1726.39 | 35.18 | 5.09 | | | 0.96 | 0.05 |
| Lat: 27.6547 | 1501.27 | 35.26 | 5.89 | | | 0.32 | 0.02 |
| Long: -18.1024 | 1199.32 | 35.34 | 7.33 | | | 0.32 | 0.02 |
| | 1000.82 | 35.29 | 7.76 | | | 0.40 | 0.02 |
| | 801.50 | 35.34 | 8.98 | | | 0.51 | 0.03 |
| | 601.92 | 35.54 | 11.04 | | | 0.33 | 0.02 |
| | 301.51 | 36.05 | 14.69 | | | 0.35 | 0.02 |
| | 202.11 | 36.40 | 16.66 | | | 0.36 | 0.02 |
| | 126.28 | 36.67 | 18.29 | | | 0.39 | 0.02 |
| | 102.10 | 36.75 | 18.96 | | | 0.35 | 0.02 |
| | 27.67 | 36.98 | 23.73 | | | 0.83 | 0.04 |
| | 17.45 | 36.98 | 23.75 | | | 1.03 | 0.05 |
| 22 | 2022.94 | 35.10 | 4.30 | | | 0.15 | 0.01 |
| Lat: 27.6481 | 1751.12 | 35.17 | 4.92 | | | 0.66 | 0.03 |
| Long: -18.1370 | 1501.52 | 35.25 | 5.83 | | | 0.19 | 0.01 |
| | 1201.25 | 35.34 | 7.02 | | | 0.25 | 0.01 |
| | 1101.12 | 35.33 | 7.45 | | | 0.94 | 0.05 |
| | 1001.56 | 35.30 | 7.72 | | | 0.23 | 0.01 |
| | 801.45 | 35.33 | 8.84 | | | 0.44 | 0.02 |
| | 600.99 | 35.56 | 11.16 | | | 0.29 | 0.01 |
| | 299.48 | 36.12 | 15.11 | | | 2.81 | 0.14 |
| | 200.78 | 36.41 | 16.71 | | | 0.14 | 0.01 |
| | 125.44 | 36.68 | 18.37 | | | 0.20 | 0.01 |
| | 100.34 | 36.78 | 19.20 | | | 0.21 | 0.01 |
| | 26.24 | 36.97 | 23.71 | | | 0.50 | 0.03 |
| | 4.74 | 36.97 | 23.82 | | | 0.41 | 0.02 |
| 50 | 334.58 | 35.99 | 14.34 | 8.085 | 0.001 | 0.28 | 0.01 |
| Lat: 27.6156 | 251.61 | 36.12 | 15.06 | 8.084 | 0.002 | 0.17 | 0.01 |
| Long: -17.9906 | 200.92 | 36.33 | 16.31 | 8.099 | 0.003 | 0.16 | 0.01 |
| | 151.11 | 36.55 | 17.63 | 8.117 | 0.001 | 0.36 | 0.02 |
| | 124.31 | 36.59 | 17.89 | 8.124 | 0.002 | 0.49 | 0.02 |
| | 101.38 | 36.67 | 18.66 | 8.130 | 0.001 | <D.L. | 0.00 |
| | 75.24 | 36.74 | 19.30 | 8.140 | 0.002 | 0.11 | 0.01 |
| | 51.12 | 36.98 | 22.88 | 8.149 | 0.002 | 0.40 | 0.02 |
| | 25.69 | 36.97 | 22.93 | 8.157 | 0.001 | 0.68 | 0.03 |
| | 16.75 | 36.97 | 23.11 | 8.159 | 0.001 | 0.82 | 0.04 |
| | 6.06 | 36.97 | 23.24 | 8.160 | 0.002 | 0.28 | 0.01 |
| 51 | 246.17 | 36.23 | 15.71 | 8.097 | 0.003 | 0.49 | 0.02 |
| Lat: 27.6168 | 202.32 | 36.37 | 16.54 | 8.103 | 0.001 | <D.L. | 0.00 |
| Long: -17.9913 | 150.06 | 36.50 | 17.35 | 8.107 | 0.002 | 0.73 | 0.04 |
| | 101.26 | 36.65 | 18.41 | 8.127 | 0.001 | 0.22 | 0.01 |
| | 75.66 | 36.75 | 19.51 | 8.137 | 0.002 | 0.29 | 0.01 |
| | 50.58 | 36.96 | 22.69 | 8.149 | 0.002 | 0.34 | 0.02 |
| | 25.70 | 36.98 | 22.91 | 8.156 | 0.001 | 0.46 | 0.02 |
| | 15.80 | 36.98 | 23.36 | 8.157 | 0.001 | 0.27 | 0.01 |
| | 6.44 | 36.99 | 23.53 | 8.159 | 0.002 | 0.43 | 0.02 |
| 52 | 202.29 | 36.34 | 16.37 | 8.110 | 0.003 | 1.56 | 0.08 |

| | | | | | | | |
|---|---|---|---|---|---|---|---|
| Lat: 27.6177 | 151.22 | 36.55 | 17.66 | 8.117 | 0.001 | 0.79 | 0.04 |
| Long:-17.9920 | 126.06 | 36.59 | 17.99 | 8.121 | 0.002 | 0.45 | 0.02 |
| | 101.88 | 36.65 | 18.43 | 8.129 | 0.001 | 0.35 | 0.02 |
| | 76.36 | 36.79 | 19.89 | 8.141 | 0.002 | 0.50 | 0.03 |
| | 49.63 | 36.97 | 22.71 | 8.149 | 0.002 | 0.41 | 0.02 |
| | 24.60 | 36.96 | 23.09 | 8.157 | 0.001 | 0.26 | 0.01 |
| | 15.77 | 36.99 | 23.53 | 8.158 | 0.001 | 0.27 | 0.01 |
| | 3.92 | 36.99 | 23.53 | 8.160 | 0.002 | 0.27 | 0.01 |
| 53 | 196.63 | 36.37 | 16.53 | 8.101 | 0.003 | 1.72 | 0.09 |
| Lat: 27.6185 | 149.85 | 36.62 | 18.17 | 8.110 | 0.001 | 1.49 | 0.07 |
| Long:-17.9920 | 125.86 | 36.65 | 18.45 | 8.112 | 0.002 | 0.87 | 0.04 |
| | 101.61 | 36.71 | 19.03 | 8.124 | 0.001 | 0.69 | 0.03 |
| | 75.53 | 36.82 | 20.34 | 8.135 | 0.002 | 0.41 | 0.02 |
| | 49.71 | 36.96 | 22.63 | 8.142 | 0.002 | 0.46 | 0.02 |
| | 25.90 | 36.96 | 23.12 | 8.149 | 0.001 | 0.37 | 0.02 |
| | 16.56 | 36.98 | 23.38 | 8.149 | 0.001 | 0.17 | 0.01 |
| | 5.71 | 36.97 | 23.54 | 8.151 | 0.001 | 0.22 | 0.01 |
| 54 | 162.71 | 36.60 | 18.05 | 8.113 | 0.001 | 1.45 | 0.07 |
| cast:11 | 125.73 | 36.65 | 18.44 | 8.122 | 0.002 | 1.28 | 0.06 |
| | 100.17 | 36.69 | 18.70 | 8.126 | 0.003 | 0.75 | 0.04 |
| | 75.81 | 36.75 | 19.49 | 8.133 | 0.001 | 0.70 | 0.03 |
| | 56.23 | 36.91 | 21.90 | 8.143 | 0.002 | 0.27 | 0.01 |
| | 25.53 | 36.96 | 23.04 | 8.150 | 0.001 | 0.17 | 0.01 |
| | 16.64 | 36.98 | 23.36 | 8.152 | 0.002 | 0.16 | 0.01 |
| | 5.56 | 36.99 | 23.55 | 8.155 | 0.002 | 2.55 | 0.13 |
| 55 | 129.71 | 36.69 | 18.74 | 8.063 | 0.001 | 5.83 | 0.29 |
| Lat: 27.6193 | 101.37 | 36.71 | 19.09 | 7.962 | 0.001 | 6.63 | 0.33 |
| Long:-17.9930 | 75.85 | 36.79 | 19.88 | 8.107 | 0.002 | 1.12 | 0.06 |
| | 50.80 | 36.95 | 22.42 | 8.129 | 0.003 | 0.40 | 0.02 |
| | 25.90 | 36.97 | 23.02 | 8.142 | 0.001 | 0.46 | 0.02 |
| | 17.51 | 36.98 | 23.27 | 8.145 | 0.002 | 0.92 | 0.05 |
| | 7.43 | 36.99 | 23.52 | 8.149 | 0.001 | 0.21 | 0.01 |
| 55 | 129.28 | 36.53 | 17.61 | 8.067 | 0.001 | <D.L. | 0.00 |
| cast: 68 | 103.66 | 36.64 | 18.47 | 8.038 | 0.002 | <D.L. | 0.00 |
| | 86.64 | 36.69 | 18.88 | 8.057 | 0.003 | 0.14 | 0.01 |
| | 76.26 | 36.71 | 19.04 | 8.061 | 0.001 | 0.19 | 0.01 |
| | 52.08 | 36.81 | 20.33 | 8.095 | 0.002 | <D.L. | 0.00 |
| | 25.38 | 36.94 | 22.81 | 8.103 | 0.001 | 0.13 | 0.01 |
| | 16.29 | 36.94 | 23.03 | 8.108 | 0.002 | 0.18 | 0.01 |
| | 5.38 | 36.97 | 23.17 | 8.109 | 0.002 | 0.09 | 0.00 |
| 55 | 133.73 | 36.62 | 18.29 | 8.062 | 0.001 | 4.13 | 0.21 |
| cast: 83 | 118.92 | 36.64 | 18.52 | 8.050 | 0.001 | 0.54 | 0.03 |
| | 110.44 | 36.69 | 18.99 | 8.013 | 0.002 | 3.97 | 0.20 |
| | 100.87 | 36.68 | 18.99 | 7.915 | 0.003 | 49.92 | 2.50 |
| | 76.34 | 36.76 | 20.00 | 8.080 | 0.001 | 0.65 | 0.03 |
| | 49.31 | 36.86 | 21.42 | 8.108 | 0.002 | 0.15 | 0.01 |
| | 4.78 | 36.89 | 23.18 | 8.120 | 0.001 | 0.14 | 0.01 |
| 56 | 90.87 | 36.75 | 90.87 | 8.138 | 0.001 | 0.35 | 0.02 |
| cast:2 | 90.91 | 36.74 | 90.91 | 8.128 | 0.002 | 0.20 | 0.01 |
| | 75.07 | 36.81 | 75.07 | 8.142 | 0.003 | 0.17 | 0.01 |
| | 49.21 | 36.96 | 49.21 | 8.146 | 0.001 | 0.20 | 0.01 |

| | | | | | | | |
|---|---|---|---|---|---|---|---|
| | 25.37 | 36.97 | 25.37 | 8.152 | 0.002 | 0.22 | 0.01 |
| | 15.75 | 36.98 | 15.75 | 8.152 | 0.001 | 0.21 | 0.01 |
| 58 | 176.71 | 36.54 | 17.60 | 8.110 | 0.001 | 0.28 | 0.01 |
| Lat: 27.6217 | 151.46 | 36.58 | 17.91 | 8.109 | 0.002 | 0.30 | 0.01 |
| Long:-17.9932 | 125.75 | 36.61 | 18.07 | 8.111 | 0.003 | 0.27 | 0.01 |
| | 101.19 | 36.63 | 18.30 | 8.114 | 0.001 | 0.32 | 0.02 |
| | 75.36 | 36.77 | 19.87 | 8.122 | 0.002 | 0.23 | 0.01 |
| | 51.16 | 36.88 | 21.63 | 8.135 | 0.001 | 0.26 | 0.01 |
| | 26.29 | 36.96 | 22.97 | 8.142 | 0.002 | 0.29 | 0.01 |
| | 16.07 | 36.97 | 23.09 | 8.144 | 0.002 | 0.26 | 0.01 |
| | 5.27 | 36.99 | 23.45 | 8.146 | 0.001 | 2.20 | 0.11 |
| | | | **MARCH --2014** | | | | |
| 13 | 1044.26 | 35.35 | 7.92 | 8.206 | 0.001 | < D.L. | |
| Lat: 27.5700 | 900.75 | 35.39 | 8.89 | 8.205 | 0.002 | < D.L. | |
| Long: -17.9869 | 700.79 | 35.46 | 10.16 | 8.212 | 0.001 | < D.L. | |
| | 500.31 | 35.66 | 11.98 | 8.261 | 0.001 | 0.17 | 0.01 |
| | 249.84 | 36.10 | 15.11 | 8.333 | 0.002 | < D.L. | |
| | 126.39 | 36.62 | 17.88 | 8.383 | 0.001 | < D.L. | |
| | 76.08 | 36.91 | 19.02 | 8.418 | 0.001 | 0.17 | 0.01 |
| | 25.63 | 36.91 | 19.02 | 8.414 | 0.002 | 0.15 | 0.01 |
| | 5.11 | 36.91 | 19.03 | 8.411 | 0.001 | 0.33 | 0.02 |
| 14 | 211.97 | 36.09 | 14.90 | 8.303 | 0.001 | 0.42 | 0.02 |
| Lat: 27.6201 | 147.60 | 36.38 | 16.59 | 8.335 | 0.002 | 3.03 | 0.15 |
| Long: -17.9868 | 125.54 | 36.53 | 17.34 | 8.348 | 0.001 | 2.00 | 0.10 |
| | 102.27 | 36.77 | 18.45 | 8.379 | 0.001 | 0.76 | 0.04 |
| | 74.83 | 36.83 | 18.70 | 8.390 | 0.002 | 0.18 | 0.01 |
| | 52.13 | 36.86 | 18.80 | 8.391 | 0.001 | 0.35 | 0.02 |
| | 25.11 | 36.86 | 18.83 | 8.390 | 0.001 | 0.13 | 0.01 |
| | 4.68 | 36.86 | 18.82 | 8.390 | 0.002 | 0.30 | 0.02 |
| 15 | 467.18 | 35.72 | 12.44 | 8.276 | 0.001 | < D.L. | |
| Lat: 27.6696 | 301.30 | 35.93 | 13.97 | 8.313 | 0.001 | < D.L. | |
| Long: -18.0367 | 200.22 | 36.18 | 15.46 | 8.341 | 0.002 | < D.L. | |
| | 101.63 | 36.79 | 18.54 | 8.406 | 0.001 | < D.L. | |
| | 24.74 | 36.81 | 18.72 | 8.423 | 0.001 | 0.41 | 0.02 |
| | 6.67 | 36.82 | 18.90 | 8.421 | 0.002 | 0.13 | 0.01 |
| 16 | 1198.98 | 35.35 | 7.14 | 8.240 | 0.001 | 0.52 | 0.03 |
| Lat: 27.6198 | 1000.41 | 35.35 | 7.94 | 8.227 | 0.001 | 0.94 | 0.05 |
| Long: -18.0364 | 800.73 | 35.40 | 9.17 | 8.222 | 0.002 | 0.22 | 0.01 |
| | 600.63 | 35.57 | 11.08 | 8.257 | 0.001 | 0.46 | 0.02 |
| | 300.65 | 36.00 | 14.37 | 8.333 | 0.001 | 0.33 | 0.02 |
| | 200.51 | 36.26 | 15.96 | 8.359 | 0.002 | < D.L. | |
| | 98.52 | 36.82 | 18.66 | 8.419 | 0.001 | < D.L. | |
| | 23.49 | 36.88 | 18.93 | 8.433 | 0.001 | < D.L. | |
| | 4.29 | 36.89 | 19.26 | 8.426 | 0.002 | 0.56 | 0.03 |
| 18 | 1199.79 | 35.34 | 7.17 | 8.229 | 0.001 | < D.L. | |
| Lat: 27.6433 | 1100.69 | 35.35 | 7.50 | 8.226 | 0.001 | 0.75 | 0.04 |
| Long: -18.0594 | 1000.59 | 35.33 | 7.93 | 8.213 | 0.002 | < D.L. | |
| | 799.97 | 35.38 | 9.10 | 8.209 | 0.001 | 1.30 | 0.06 |
| | 601.12 | 35.56 | 11.02 | 8.249 | 0.001 | < D.L. | |
| | 299.78 | 35.92 | 13.90 | 8.316 | 0.002 | < D.L. | |
| | 200.94 | 36.25 | 15.95 | 8.353 | 0.001 | 0.92 | 0.05 |

| | | | | | | | |
|---|---|---|---|---|---|---|---|
| | 101.24 | 36.83 | 18.69 | 8.421 | 0.001 | 0.17 | 0.01 |
| 20 | 909.39 | 35.37 | 8.96 | 8.191 | 0.002 | 0.61 | 0.03 |
| Lat: 27.6804 | 801.86 | 35.39 | 9.31 | 8.197 | 0.001 | < D.L. | |
| Long: -18.0869 | 500.87 | 35.63 | 11.75 | 8.252 | 0.001 | < D.L. | |
| | 250.66 | 36.17 | 15.51 | 8.336 | 0.002 | < D.L. | |
| | 151.61 | 36.44 | 17.00 | 8.362 | 0.001 | 0.67 | 0.03 |
| | 124.89 | 36.65 | 17.96 | 8.387 | 0.001 | 0.28 | 0.01 |
| | 44.14 | 36.82 | 18.68 | 8.411 | 0.002 | 0.23 | 0.01 |
| | 25.63 | 36.83 | 18.73 | 8.417 | 0.001 | 1.17 | 0.06 |
| | 6.96 | 36.85 | 18.91 | 8.419 | 0.001 | 0.24 | 0.01 |
| 21 | 1199.50 | 35.36 | 7.20 | 8.211 | 0.002 | 0.36 | 0.02 |
| Lat: 27.6547 | 998.15 | 35.36 | 7.94 | 8.201 | 0.001 | 0.51 | 0.03 |
| Long: -18.1024 | 798.61 | 35.40 | 9.33 | 8.192 | 0.001 | < D.L. | |
| | 601.99 | 35.56 | 10.99 | 8.232 | 0.002 | < D.L. | |
| | 300.70 | 35.94 | 14.02 | 8.305 | 0.001 | < D.L. | |
| | 200.84 | 36.16 | 15.45 | 8.331 | 0.001 | 0.80 | 0.04 |
| | 126.09 | 36.59 | 17.69 | 8.374 | 0.002 | 0.17 | 0.01 |
| | 100.54 | 36.78 | 18.50 | 8.407 | 0.001 | 1.08 | 0.05 |
| | 25.17 | 36.84 | 18.76 | 8.419 | 0.001 | 1.48 | 0.07 |
| | 5.33 | 36.84 | 18.87 | 8.415 | 0.002 | 0.21 | 0.01 |
| 22 | 1199.92 | 35.36 | 7.24 | 8.222 | 0.001 | 1.01 | 0.05 |
| Lat: 27.6481 | 1101.30 | 35.34 | 7.52 | 8.216 | 0.001 | 0.93 | 0.05 |
| Long: -18.1370 | 1000.82 | 35.35 | 7.94 | 8.211 | 0.002 | 0.52 | 0.03 |
| | 599.75 | 35.54 | 10.94 | 8.234 | 0.001 | < D.L. | |
| | 300.42 | 36.03 | 14.68 | 8.325 | 0.001 | 0.57 | 0.03 |
| | 200.41 | 36.41 | 16.88 | 8.358 | 0.002 | 1.19 | 0.06 |
| | 126.01 | 36.85 | 18.78 | 8.412 | 0.001 | 0.23 | 0.01 |
| | 101.75 | 36.86 | 18.80 | 8.412 | 0.001 | 0.15 | 0.01 |
| | 25.15 | 36.90 | 19.04 | 8.420 | 0.002 | 0.27 | 0.01 |
| | 4.84 | 36.91 | 19.19 | 8.417 | 0.001 | 1.40 | 0.07 |
| 50 | 343.57 | 35.97 | 14.16 | 8.080 | 0.001 | <D.L. | |
| Lat: 27.6156 | 250.76 | 36.12 | 15.14 | 8.101 | 0.002 | <D.L. | |
| Long: -17.9906 | 200.86 | 36.47 | 17.11 | 8.133 | 0.003 | <D.L. | |
| | 150.88 | 36.59 | 17.73 | 8.150 | 0.001 | <D.L. | |
| | 125.82 | 36.67 | 18.06 | 8.155 | 0.002 | <D.L. | |
| | 100.65 | 36.70 | 18.18 | 8.163 | 0.001 | 0.33 | 0.02 |
| | 74.63 | 36.78 | 18.52 | 8.170 | 0.002 | <D.L. | |
| | 51.55 | 36.81 | 18.66 | 8.176 | 0.002 | <D.L. | |
| | 25.36 | 36.86 | 18.98 | 8.182 | 0.001 | 0.47 | 0.02 |
| | 5.41 | 36.86 | 18.98 | 8.183 | 0.001 | 0.50 | 0.03 |
| 51 | 247.27 | 36.20 | 15.56 | 8.104 | 0.003 | 0.50 | 0.02 |
| Lat: 27.6168 | 201.19 | 36.42 | 16.80 | 8.136 | 0.001 | 0.70 | 0.03 |
| Long: -17.9913 | 150.45 | 36.49 | 17.16 | 8.142 | 0.002 | 0.48 | 0.02 |
| | 125.81 | 36.66 | 17.99 | 8.160 | 0.001 | 0.44 | 0.02 |
| | 101.05 | 36.77 | 18.47 | 8.172 | 0.002 | 0.46 | 0.02 |
| | 72.67 | 36.84 | 18.80 | 8.179 | 0.002 | 0.20 | 0.01 |
| | 50.68 | 36.86 | 18.98 | 8.181 | 0.001 | 0.42 | 0.02 |
| | 25.05 | 36.87 | 18.99 | 8.182 | 0.001 | 0.65 | 0.03 |
| | 4.79 | 36.87 | 18.99 | 8.182 | 0.002 | 0.34 | 0.02 |
| 52 | 205.42 | 36.45 | 16.97 | 8.133 | 0.003 | <D.L. | |
| Lat: 27.6177 | 151.80 | 36.58 | 17.59 | 8.148 | 0.001 | 0.62 | 0.03 |

| | | | | | | | |
|---|---|---|---|---|---|---|---|
| Long:-17.9920 | 124.89 | 36.72 | 18.29 | 8.171 | 0.002 | 0.39 | 0.02 |
| | 101.24 | 36.80 | 18.61 | 8.179 | 0.001 | 0.62 | 0.03 |
| | 76.13 | 36.87 | 18.99 | 8.183 | 0.002 | < L.D. | |
| | 50.02 | 36.87 | 19.00 | 8.184 | 0.002 | 0.77 | 0.04 |
| | 24.51 | 36.87 | 18.99 | 8.186 | 0.001 | 0.60 | 0.03 |
| | 5.38 | 36.87 | 19.00 | 8.189 | 0.001 | 1.06 | 0.05 |
| 53 | 184.89 | 36.52 | 17.30 | 8.140 | 0.003 | 2.97 | 0.15 |
| Lat: 27.6185 | 151.09 | 36.56 | 17.52 | 8.150 | 0.001 | <D.L. | |
| Long:-17.9920 | 125.14 | 36.77 | 18.52 | 8.176 | 0.002 | 0.32 | 0.02 |
| | 101.28 | 36.80 | 18.62 | 8.179 | 0.001 | 0.63 | 0.03 |
| | 75.83 | 36.86 | 18.93 | 8.186 | 0.002 | 0.69 | 0.03 |
| | 50.64 | 36.87 | 18.99 | 8.187 | 0.002 | 0.54 | 0.03 |
| | 26.46 | 36.87 | 18.99 | 8.190 | 0.001 | 0.69 | 0.03 |
| | 2.23 | 36.87 | 19.03 | 8.194 | 0.001 | 0.76 | 0.04 |
| 54 | 167.77 | 36.42 | 16.81 | 8.135 | 0.003 | 1.34 | 0.07 |
| Lat: 27.6188 | 123.62 | 36.65 | 17.94 | 8.163 | 0.001 | 0.56 | 0.03 |
| long: -17.9927 | 99.66 | 36.72 | 18.28 | 8.170 | 0.002 | 0.10 | 0.01 |
| | 75.17 | 36.79 | 18.59 | 8.183 | 0.001 | <D.L. | |
| | 49.21 | 36.88 | 18.99 | 8.193 | 0.002 | 0.15 | 0.01 |
| | 24.09 | 36.88 | 19.00 | 8.193 | 0.002 | 0.14 | 0.01 |
| | 5.40 | 36.88 | 19.03 | 8.195 | 0.001 | 0.18 | 0.01 |
| 55 | 133.03 | 36.68 | 18.07 | 8.174 | 0.002 | 0.15 | 0.01 |
| cast:2 | 101.45 | 36.80 | 18.63 | 8.183 | 0.002 | <D.L. | |
| | 72.62 | 36.87 | 18.97 | 8.194 | 0.001 | 0.11 | 0.01 |
| | 50.43 | 36.88 | 18.98 | 8.195 | 0.001 | <D.L. | |
| | 24.64 | 36.88 | 19.01 | 8.195 | 0.002 | 0.12 | 0.01 |
| | 4.73 | 36.88 | 19.03 | 8.198 | 0.003 | 0.48 | 0.02 |
| 56 | 88.27 | 36.76 | 18.40 | 8.165 | 0.001 | 0.74 | 0.04 |
| Lat: 27.6203 | 74.95 | 36.77 | 18.45 | 8.169 | 0.002 | <D.L. | |
| long: -17.9933 | 50.02 | 36.83 | 18.68 | 8.178 | 0.003 | <D.L. | |
| | 24.08 | 36.84 | 18.76 | 8.185 | 0.001 | <D.L. | |
| | 4.86 | 36.84 | 18.76 | 8.186 | 0.002 | 0.14 | 0.01 |
| 56 | 92.67 | 36.68 | 18.09 | 8.136 | 0.001 | 3.53 | 0.18 |
| cast:3 | 73.52 | 36.84 | 18.82 | 8.193 | 0.002 | 0.22 | 0.01 |
| | 50.34 | 36.88 | 18.98 | 8.199 | 0.002 | 0.14 | 0.01 |
| | 24.04 | 36.88 | 19.01 | 8.200 | 0.001 | 0.48 | 0.02 |
| | 5.03 | 36.88 | 19.02 | 8.200 | 0.001 | 2.05 | 0.10 |
| 57 | 146.14 | 36.46 | 17.07 | 8.135 | 0.002 | 2.07 | 0.10 |
| Lat: 27.6211 | 100.58 | 36.81 | 18.65 | 8.190 | 0.003 | 0.13 | 0.01 |
| long: -17.9934 | 75.70 | 36.85 | 18.81 | 8.193 | 0.001 | <D.L. | |
| | 52.39 | 36.87 | 18.96 | 8.195 | 0.002 | <D.L. | |
| | 25.58 | 36.88 | 19.06 | 8.196 | 0.001 | 0.41 | 0.02 |
| 58 | 183.73 | 36.52 | 17.32 | 8.150 | 0.002 | 0.91 | 0.05 |
| Lat: 27.6217 | 150.35 | 36.53 | 17.39 | 8.155 | 0.002 | 0.71 | 0.04 |
| Long:-17.9932 | 124.52 | 36.58 | 17.62 | 8.162 | 0.001 | 0.19 | 0.01 |
| | 101.40 | 36.56 | 17.53 | 8.160 | 0.001 | 0.19 | 0.01 |
| | 81.13 | 36.69 | 18.15 | 8.172 | 0.002 | 0.32 | 0.02 |
| | 61.42 | 36.83 | 18.72 | 8.199 | 0.003 | <D.L. | |
| | 24.89 | 36.88 | 19.00 | 8.201 | 0.001 | 0.60 | 0.03 |
| | 5.27 | 36.88 | 19.04 | 8.201 | 0.002 | 0.19 | 0.01 |
| 59 | 166.17 | 36.58 | 17.62 | 8.161 | 0.002 | <D.L. | |

| | | | | | | | |
|---|---|---|---|---|---|---|---|
| Lat: 27.6222 | 149.17 | 36.63 | 17.87 | 8.168 | 0.002 | <D.L. | |
| long: -17.9930 | 124.31 | 36.58 | 17.63 | 8.163 | 0.001 | <D.L. | |
| | 99.87 | 36.79 | 18.59 | 8.192 | 0.001 | <D.L. | |
| | 74.71 | 36.85 | 18.81 | 8.196 | 0.002 | <D.L. | |
| | 50.60 | 36.88 | 18.97 | 8.201 | 0.003 | <D.L. | |
| | 24.73 | 36.88 | 19.03 | 8.200 | 0.001 | 0.18 | 0.01 |
| 60 | 360.34 | 35.90 | 13.72 | 8.080 | 0.002 | <D.L. | |
| Lat: 27.6199 | 300.85 | 36.15 | 15.35 | 8.117 | 0.001 | <D.L. | |
| long: -17.9990 | 249.10 | 36.19 | 15.53 | 8.121 | 0.002 | <D.L. | |
| | 200.65 | 36.42 | 16.87 | 8.135 | 0.002 | <D.L. | |
| | 150.38 | 36.60 | 17.70 | 8.163 | 0.001 | 0.43 | 0.02 |
| | 125.71 | 36.76 | 18.43 | 8.180 | 0.001 | 0.66 | 0.03 |
| | 101.24 | 36.76 | 18.44 | 8.181 | 0.002 | 0.21 | 0.01 |
| | 76.24 | 36.86 | 18.90 | 8.195 | 0.003 | 0.12 | 0.01 |
| | 51.29 | 36.88 | 19.02 | 8.195 | 0.001 | 0.19 | 0.01 |
| | 26.26 | 36.88 | 19.06 | 8.194 | 0.002 | 0.19 | 0.01 |
| | 5.34 | 36.88 | 19.07 | 8.194 | 0.001 | 0.98 | 0.05 |
| 61 | 125.09 | 36.40 | 16.98 | 7.875 | 0.001 | 1278.90 | 63.95 |
| cast:42 | 116.32 | 36.38 | 16.67 | 8.083 | 0.002 | 17.32 | 0.87 |
| | 107.27 | 36.60 | 17.90 | 8.152 | 0.003 | 2.23 | 0.11 |
| | 99.96 | 36.62 | 17.95 | 8.156 | 0.001 | 0.51 | 0.03 |
| | 52.25 | 36.85 | 18.87 | 8.188 | 0.002 | 0.39 | 0.02 |
| 61 | 119.84 | 36.58 | 17.88 | 7.792 | 0.001 | 124.78 | 6.24 |
| cast:61 | 112.79 | 36.57 | 17.82 | 7.970 | 0.002 | 281.05 | 14.05 |
| | 101.69 | 36.69 | 18.15 | 8.112 | 0.002 | 2.79 | 0.14 |
| | 88.92 | 36.77 | 18.49 | 8.184 | 0.001 | 0.16 | 0.01 |
| | 26.15 | 36.84 | 18.81 | 8.183 | 0.001 | 0.19 | 0.01 |
| **MAY --2015** | | | | | | | |
| 1 | 1318.71 | 35.29 | 6.35 | 7.940 | 0.001 | 0.74 | 0.04 |
| Lat: 27.7051 | 1200.08 | 35.31 | 6.95 | 7.927 | 0.002 | 2.59 | 0.13 |
| Long: -17.9246 | 1100.30 | 35.30 | 7.31 | 7.918 | 0.001 | 0.51 | 0.03 |
| | 1001.78 | 35.29 | 7.61 | 7.909 | 0.001 | 2.58 | 0.13 |
| | 900.99 | 35.28 | 7.90 | 7.900 | 0.002 | 1.20 | 0.06 |
| | 801.38 | 35.27 | 8.33 | 7.891 | 0.001 | 0.54 | 0.03 |
| | 601.23 | 35.46 | 10.54 | 7.925 | 0.001 | 0.76 | 0.04 |
| | 501.89 | 35.62 | 11.74 | 7.968 | 0.002 | 1.12 | 0.06 |
| | 301.24 | 35.96 | 14.14 | 8.053 | 0.001 | 1.90 | 0.09 |
| | 250.72 | 36.06 | 14.80 | 8.069 | 0.002 | 0.75 | 0.04 |
| | 202.90 | 36.29 | 15.98 | 8.099 | 0.001 | 1.11 | 0.06 |
| | 149.62 | 36.51 | 17.07 | 8.128 | 0.001 | 0.64 | 0.03 |
| | 124.61 | 36.61 | 17.47 | 8.139 | 0.002 | 0.43 | 0.02 |
| | 102.62 | 36.64 | 17.60 | 8.144 | 0.001 | 1.48 | 0.07 |
| | 74.68 | 36.72 | 17.97 | 8.155 | 0.001 | 0.96 | 0.05 |
| | 50.58 | 36.72 | 18.13 | 8.152 | 0.002 | 1.13 | 0.06 |
| | 25.18 | 36.90 | 20.78 | 8.173 | 0.001 | 1.28 | 0.06 |
| | 4.82 | 36.90 | 20.79 | 8.177 | 0.002 | 1.97 | 0.10 |
| 50 | 341.08 | 35.89 | 13.67 | 8.078 | 0.001 | 2.45 | 0.12 |
| Lat: 27.6156 | 251.56 | 35.97 | 14.22 | 8.088 | 0.002 | 2.33 | 0.12 |
| Long: -17.9906 | 202.77 | 36.04 | 14.63 | 8.096 | 0.003 | 0.92 | 0.05 |
| | 149.97 | 36.34 | 16.26 | 8.128 | 0.001 | 0.84 | 0.04 |
| | 124.68 | 36.46 | 16.76 | 8.145 | 0.002 | 0.45 | 0.02 |

| | | | | | | | |
|---|---|---|---|---|---|---|---|
| | 97.54 | 36.58 | 17.51 | 8.150 | 0.001 | 0.43 | 0.02 |
| | 74.33 | 36.77 | 18.35 | 8.183 | 0.002 | 0.44 | 0.02 |
| | 51.05 | 36.83 | 19.01 | 8.196 | 0.002 | < D.L. | |
| | 24.98 | 36.91 | 20.91 | 8.196 | 0.001 | < D.L. | |
| | 4.02 | 36.92 | 21.09 | 8.197 | 0.001 | 2.10 | 0.10 |
| 51 | 251.21 | 36.12 | 15.09 | 8.088 | 0.003 | 1.26 | 0.06 |
| Lat: 27.6168 | 200.51 | 36.29 | 15.99 | 8.102 | 0.001 | 2.09 | 0.10 |
| Long: -17.9913 | 150.38 | 36.50 | 16.99 | 8.124 | 0.002 | 0.30 | 0.02 |
| | 124.36 | 36.57 | 17.37 | 8.132 | 0.001 | 1.68 | 0.08 |
| | 99.88 | 36.61 | 17.57 | 8.134 | 0.002 | 0.33 | 0.02 |
| | 75.30 | 36.72 | 18.16 | 8.146 | 0.002 | 0.59 | 0.03 |
| | 51.06 | 36.83 | 19.11 | 8.177 | 0.001 | 1.07 | 0.05 |
| | 25.41 | 36.91 | 21.03 | 8.173 | 0.001 | 1.08 | 0.05 |
| | 4.94 | 36.92 | 21.13 | 8.176 | 0.002 | < D.L. | |
| 52 | 206.31 | 36.43 | 16.69 | 8.135 | 0.003 | 4.17 | 0.21 |
| Lat: 27.6177 | 149.60 | 36.52 | 17.10 | 8.147 | 0.001 | 2.18 | 0.11 |
| Long:-17.9920 | 124.36 | 36.58 | 17.37 | 8.152 | 0.002 | 0.53 | 0.03 |
| | 100.72 | 36.62 | 17.52 | 8.159 | 0.001 | 0.45 | 0.02 |
| | 74.49 | 36.70 | 18.03 | 8.165 | 0.002 | 0.37 | 0.02 |
| | 50.74 | 36.83 | 19.37 | 8.196 | 0.002 | 0.78 | 0.04 |
| | 25.13 | 36.91 | 20.98 | 8.189 | 0.001 | 5.06 | 0.25 |
| | 3.94 | 36.92 | 21.11 | 8.192 | 0.001 | < D.L. | |
| 53 | 194.58 | 36.50 | 16.98 | 8.149 | 0.003 | 2.29 | 0.11 |
| Lat: 27.6185 | 150.69 | 36.54 | 17.17 | 8.154 | 0.001 | 3.28 | 0.16 |
| Long:-17.9920 | 124.69 | 36.59 | 17.42 | 8.155 | 0.002 | 0.80 | 0.04 |
| | 100.18 | 36.65 | 17.79 | 8.159 | 0.001 | 0.34 | 0.02 |
| | 75.44 | 36.74 | 18.33 | 8.165 | 0.002 | 4.02 | 0.20 |
| | 55.14 | 36.83 | 19.42 | 8.199 | 0.002 | 1.53 | 0.08 |
| | 25.89 | 36.91 | 21.14 | 8.189 | 0.001 | 3.54 | 0.18 |
| | 5.12 | 36.92 | 21.19 | 8.191 | 0.001 | 2.10 | 0.11 |
| 54 | 162.83 | 36.58 | 17.40 | 8.130 | 0.003 | 0.44 | 0.02 |
| Lat: 27.6188 | 122.44 | 36.60 | 17.50 | 8.129 | 0.001 | 0.11 | 0.01 |
| long: -17.9927 | 100.17 | 36.63 | 17.69 | 8.133 | 0.002 | < D.L. | |
| | 74.86 | 36.68 | 17.99 | 8.134 | 0.001 | 0.39 | 0.02 |
| | 50.49 | 36.84 | 19.87 | 8.169 | 0.002 | 0.61 | 0.03 |
| | 24.95 | 36.90 | 20.89 | 8.160 | 0.002 | 3.79 | 0.19 |
| | 4.85 | 36.90 | 21.06 | 8.158 | 0.001 | 0.70 | 0.04 |
| 55 | 132.57 | 36.58 | 17.44 | 8.119 | 0.001 | 0.27 | 0.01 |
| Lat: 27.6193 | 92.00 | 36.65 | 17.83 | 8.133 | 0.001 | 0.10 | 0.01 |
| Long:-17.9930 | 75.40 | 36.76 | 18.43 | 8.166 | 0.002 | < D.L. | |
| | 50.27 | 36.82 | 19.37 | 8.174 | 0.003 | < D.L. | |
| | 24.58 | 36.88 | 20.69 | 8.165 | 0.001 | 0.40 | 0.02 |
| | 4.05 | 36.90 | 21.07 | 8.163 | 0.002 | 0.22 | 0.01 |
| 56 | 96.82 | 36.63 | 17.68 | 8.000 | 0.001 | 44.61 | 2.23 |
| Lat: 27.6203 | 69.78 | 36.80 | 19.03 | 8.171 | 0.002 | 2.05 | 0.10 |
| long: -17.9933 | 48.95 | 36.88 | 20.74 | 8.170 | 0.003 | 1.32 | 0.07 |
| | 29.58 | 36.89 | 20.84 | 8.168 | 0.001 | 1.52 | 0.08 |
| | 19.07 | 36.89 | 20.85 | 8.168 | 0.002 | 4.98 | 0.25 |
| | 3.36 | 36.89 | 21.15 | 8.164 | 0.001 | 3.07 | 0.15 |
| 56 | 92.74 | 36.44 | 16.74 | 8.085 | 0.002 | 5.54 | 0.28 |
| cast:2 | 92.66 | 36.45 | 16.74 | 8.086 | 0.002 | 6.14 | 0.31 |

| | | | | | | | |
|---|---|---|---|---|---|---|---|
| | 83.45 | 36.66 | 17.72 | 8.140 | 0.001 | 17.00 | 0.85 |
| | 74.66 | 36.71 | 18.06 | 8.154 | 0.001 | 0.58 | 0.03 |
| | 65.50 | 36.77 | 18.83 | 8.173 | 0.002 | 0.79 | 0.04 |
| | 54.97 | 36.81 | 19.27 | 8.174 | 0.003 | 10.85 | 0.54 |
| | 25.17 | 36.88 | 20.96 | 8.162 | 0.001 | 1.63 | 0.08 |
| | 4.32 | 36.90 | 21.25 | 8.159 | 0.002 | 3.33 | 0.17 |
| 57 | 115.98 | 36.36 | 16.36 | 8.111 | 0.001 | 0.21 | 0.01 |
| Lat: 27.6211 | 74.89 | 36.72 | 18.10 | 8.160 | 0.002 | 1.52 | 0.08 |
| long: -17.9934 | 51.68 | 36.81 | 19.49 | 8.182 | 0.003 | 2.42 | 0.12 |
| | 25.04 | 36.88 | 20.86 | 8.169 | 0.001 | 4.69 | 0.23 |
| | 3.50 | 36.90 | 21.33 | 8.164 | 0.002 | < D.L. | |
| 58 | 177.72 | 36.18 | 15.48 | 8.111 | 0.001 | 3.81 | 0.19 |
| Lat: 27.6217 | 149.18 | 36.32 | 16.21 | 8.127 | 0.002 | 0.79 | 0.04 |
| Long:-17.9932 | 125.43 | 36.47 | 16.88 | 8.139 | 0.002 | 0.30 | 0.02 |
| | 100.06 | 36.54 | 17.25 | 8.142 | 0.001 | < D.L. | |
| | 75.35 | 36.69 | 17.91 | 8.163 | 0.001 | 2.18 | 0.11 |
| | 50.97 | 36.83 | 19.46 | 8.186 | 0.002 | 1.09 | 0.05 |
| | 24.26 | 36.87 | 20.62 | 8.177 | 0.003 | 1.10 | 0.06 |
| | 3.31 | 36.89 | 21.30 | 8.172 | 0.001 | 3.24 | 0.16 |
| 59 | 171.73 | 36.44 | 16.77 | 8.134 | 0.001 | 0.81 | 0.04 |
| Lat: 27.6222 | 124.42 | 36.58 | 17.43 | 8.147 | 0.002 | 0.36 | 0.02 |
| long: -17.9930 | 100.18 | 36.60 | 17.55 | 8.147 | 0.002 | 0.50 | 0.03 |
| | 75.62 | 36.78 | 18.51 | 8.156 | 0.001 | 0.52 | 0.03 |
| | 54.01 | 36.83 | 20.20 | 8.180 | 0.001 | 0.37 | 0.02 |
| | 24.91 | 36.93 | 21.38 | 8.171 | 0.002 | 5.97 | 0.30 |
| | 3.97 | 36.92 | 21.49 | 8.174 | 0.003 | 1.02 | 0.05 |
| 61 | 116.34 | 36.56 | 17.28 | 8.135 | 0.001 | 0.47 | 0.02 |
| Lat: 27.6196 | 99.42 | 36.57 | 17.44 | 8.138 | 0.002 | 1.05 | 0.05 |
| Long: -17.9931 | 71.70 | 36.76 | 18.60 | 8.182 | 0.002 | 0.74 | 0.04 |
| | 50.67 | 36.83 | 19.44 | 8.183 | 0.001 | 0.17 | 0.01 |
| | 24.09 | 36.89 | 20.61 | 8.176 | 0.001 | 0.70 | 0.04 |
| | 3.63 | 36.90 | 21.05 | 8.168 | 0.002 | 1.60 | 0.08 |
| p01_3 | 361.78 | 35.83 | 13.33 | 8.041 | 0.001 | 0.97 | 0.05 |
| Lat: 27.6208 | 343.77 | 35.86 | 13.48 | 8.046 | 0.002 | 0.20 | 0.01 |
| Long: -17.9996 | 316.65 | 35.94 | 14.00 | 8.058 | 0.001 | 0.31 | 0.02 |
| | 298.40 | 36.00 | 14.40 | 8.063 | 0.002 | 0.35 | 0.02 |
| | 200.71 | 36.38 | 16.47 | 8.107 | 0.002 | 0.70 | 0.04 |
| | 99.47 | 36.68 | 17.93 | 8.145 | 0.001 | 0.35 | 0.02 |
| | 4.67 | 36.94 | 21.67 | 8.162 | 0.001 | 2.09 | 0.10 |

Values of $pH_{F,is}$ were obtained with the pH sensor in NBS scale and then converted to pH in situ at free scale. In October 2013, there was not pH reading from the sensor for stations 15-22.

# MARINE CHEMISTRY

**ISSN: 0304-4203**

ELSEVIER SCIENCE BV
PO BOX 211,1000 AE AMSTERDAM,NETHERLANDS
**NETHERLANDS**

**Go to Journal Table of Contents** **Go to Ulrich's**

**Titles**
ISO: Mar. Chem.
JCR Abbrev: MAR CHEM

**Categories**
CHEMISTRY, MULTIDISCIPLINARY - SCIE;
OCEANOGRAPHY - SCIE;

**Languages**
Multi-Language

10 Issues/Year;

## Key Indicators

| Year | Total Cites Graph | Journal Impact Factor Graph | Impact Factor Without Journal Self Cites Graph | 5 Year Impact Factor Graph | Immediacy Index Graph | Citable Items Graph | Cited Half-Life Graph | Citing Half-Life Graph | Eigenfacto Score Graph | Article Influence Score Graph | % Articles in Citable Items Graph | Normalizec Eigenfacto Graph | Average JIF Percentile Graph |
|---|---|---|---|---|---|---|---|---|---|---|---|---|---|
| 2017 | 9,014 | 3.337 | 3.011 | 3.416 | 0.417 | 84 | >10.0 | >10.0 | 0.00… | 1.167 | 100.00 | 0.92… | 79.087 |
| 2016 | 8,308 | 2.457 | 2.329 | 2.912 | 0.425 | 73 | >10.0 | >10.0 | 0.00… | 1.011 | 100.00 | 0.84… | 67.860 |
| 2015 | 9,112 | 3.412 | 2.675 | 3.853 | 1.093 | 182 | >10.0 | >10.0 | 0.00… | 1.182 | 98.90 | 0.84… | 81.022 |
| 2014 | 8,354 | 2.735 | 2.470 | 3.636 | 0.588 | 85 | >10.0 | >10.0 | 0.00… | 1.296 | 98.82 | 0.93… | 77.905 |
| 2013 | 8,111 | 3.200 | 2.841 | 3.850 | 0.619 | 97 | >10.0 | >10.0 | 0.01… | 1.518 | 100.00 | 1.16… | 81.485 |
| 2012 | 6,872 | 3.000 | 2.806 | 3.315 | 0.466 | 58 | >10.0 | >10.0 | 0.01… | 1.370 | 100.00 | Not … | 80.603 |
| 2011 | 6,836 | 3.074 | 2.771 | 3.551 | 0.540 | 87 | >10.0 | >10.0 | 0.01… | 1.434 | 100.00 | Not … | 83.362 |
| 2010 | 6,316 | 2.751 | 2.470 | 3.276 | 0.809 | 89 | >10.0 | 10.0 | 0.01… | 1.225 | 97.75 | Not … | 82.584 |
| 2009 | 6,299 | 2.726 | 2.474 | 3.503 | 0.397 | 73 | 10.0 | >10.0 | 0.01… | 1.267 | 98.63 | Not … | 83.304 |
| 2008 | 5,830 | 2.977 | 2.588 | 3.554 | 0.795 | 112 | 9.3 | 9.9 | 0.01… | 1.361 | 97.32 | Not … | 84.280 |
| 2007 | 5,919 | 3.085 | 2.685 | 3.789 | 0.565 | 147 | 9.6 | 9.7 | 0.01… | 1.435 | 99.32 | Not … | 87.711 |
| 2006 | 4,956 | 2.663 | 2.322 | Not … | 0.958 | 118 | 9.5 | >10.0 | Not … | Not … | 98.31 | Not … | 84.627 |
| 2005 | 4,375 | 2.103 | 1.943 | Not … | 0.476 | 82 | 9.1 | 9.7 | Not … | Not … | 93.90 | Not … | 82.448 |
| 2004 | 4,178 | 2.508 | 1.960 | Not … | 0.413 | 126 | 8.7 | 8.6 | Not … | Not … | 98.41 | Not … | 86.732 |
| 2003 | 4,085 | 2.555 | 2.335 | Not … | 0.290 | 69 | 8.5 | 8.4 | Not … | Not … | 100.00 | Not … | 86.992 |
| 2002 | 3,665 | 2.179 | 1.983 | Not … | 0.407 | 59 | 8.3 | 9.7 | Not … | Not … | 100.00 | Not … | 83.040 |

**Source Data**

- **Rank**
- **Cited Journal Data**
- **Citing Journal Data**
- **Box Plot**
- **Journal Relationships**

## Journal Source Data

| | Citable Items | | | Other (O) | Percentage (C/(C + O)) |
|---|---|---|---|---|---|
| | Articles | Reviews | Combined (C) | | |
| **Number in JCR Year 2017…** | 84 | 0 | **84** | 3 | 96% |
| **Number of References (B)** | 5,388 | 0 | 5,388 | 1 | 99% |
| **Ratio (B/A)** | 64.1 | 0.0 | 64.1 | 0.3 | |

*InCites Journal Citation Reports dataset updated Jun 06, 2018*

## JCR Impact Factor

| JCR Year | CHEMISTRY, MULTIDISCIPLINARY | | | OCEANOGRAPHY | | |
|---|---|---|---|---|---|---|
| | Rank | Quartile | JIF Percentile | Rank | Quartile | JIF Percentile |
| 2017 | 60/171 | Q2 | 65.205 | 5/64 | Q1 | 92.969 |
| 2016 | 69/166 | Q2 | 58.735 | 15/63 | Q1 | 76.984 |
| 2015 | 45/163 | Q2 | 72.699 | 7/61 | Q1 | 89.344 |
| 2014 | 48/157 | Q2 | 69.745 | 9/61 | Q1 | 86.066 |
| 2013 | 39/148 | Q2 | 73.986 | 7/59 | Q1 | 88.983 |
| 2012 | 43/152 | Q2 | 72.039 | 7/60 | Q1 | 89.167 |
| 2011 | 40/154 | Q2 | 74.351 | 5/59 | Q1 | 92.373 |
| 2010 | 38/147 | Q2 | 74.490 | 6/59 | Q1 | 90.678 |
| 2009 | 36/140 | Q2 | 74.643 | 5/56 | Q1 | 91.964 |
| 2008 | 29/127 | Q1 | 77.559 | 5/50 | Q1 | 91.000 |
| 2007 | 23/128 | Q1 | 82.422 | 4/50 | Q1 | 93.000 |
| 2006 | 27/124 | Q1 | 78.629 | 5/48 | Q1 | 90.625 |
| 2005 | 24/125 | Q1 | 81.200 | 8/46 | Q1 | 83.696 |
| 2004 | 23/125 | Q1 | 82.000 | 4/41 | Q1 | 91.463 |
| 2003 | 22/123 | Q1 | 82.520 | 4/41 | Q1 | 91.463 |
| 2002 | 22/119 | Q1 | 81.933 | 7/41 | Q1 | 84.146 |

## ESI Total Citations

| JCR Year | GEOSCIENCES |
|---|---|
| 2017 | 67/416-Q1 |
| 2016 | 65/417-Q1 |
| 2015 | 48/408-Q1 |
| 2014 | 47/393-Q1 |
| 2013 | 40/388-Q1 |

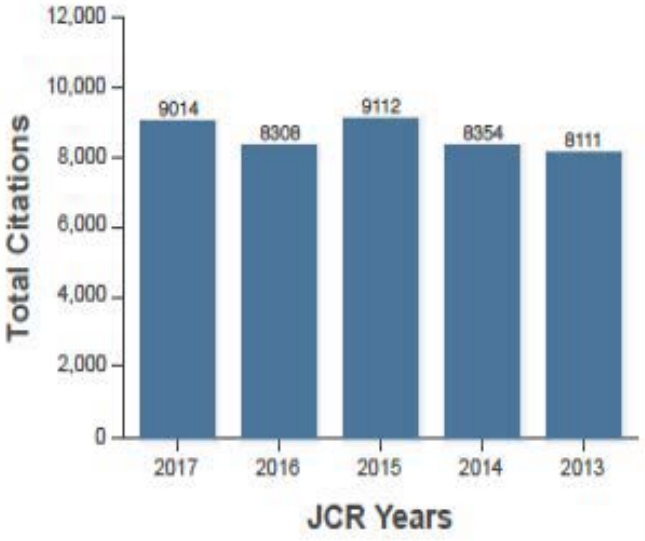

Marine Chemistry 195 (2017) 129–137

Contents lists available at ScienceDirect

Marine Chemistry

journal homepage: www.elsevier.com/locate/marchem

# Emissions of Fe(II) and its kinetic of oxidation at Tagoro submarine volcano, El Hierro

Carolina Santana-González [a], J. Magdalena Santana-Casiano [a,*], Melchor González-Dávila [a], Eugenio Fraile-Nuez [b]

[a] Instituto de Oceanografía y Cambio Global, IOCAG, Universidad de Las Palmas de Gran Canaria, Las Palmas de Gran Canaria, Spain
[b] Instituto Español de Oceanografía (IEO), Centro Oceanográfico de Canarias, Santa Cruz de Tenerife, Spain

ARTICLE INFO

*Article history:*
Received 11 October 2016
Received in revised form 22 December 2016
Accepted 1 February 2017
Available online 3 February 2017

*Keywords:*
Fe(II)
Oxidation
Acidification
Submarine volcano

ABSTRACT

The eruptive process that took place in October 2011 in the submarine volcano Tagoro off the Island of El Hierro and the subsequent degasification stage, five months later, have increased the concentration of TdFe(II) (Total dissolved iron(II)) in the waters nearest to the volcanic edifice. In order to detect any variation in concentrations of TdFe(II) due to hydrothermal emissions, three cruises were carried out two years after the eruptive process in October 2013, March 2014 and May 2015. The results from these cruises confirmed important positive anomalies in TdFe(II), which coincided with negatives anomalies in $pH_{F,is}$ (pH in free scale, at *in situ* conditions) located in the proximity of the main cone. Maximum values in TdFe(II) both at the surface, associated to chlorophyll *a* maximum, and at the sea bottom, were also observed, showing the important influence of organic complexation and particle re-suspension processes. Temporal variability studies were carried out over periods ranging from hours to days in the stations located over the main and two secondary cones in the volcanic edifice with positive anomalies in TdFe(II) concentrations and negative anomalies in $pH_{F,is}$ values. Observations showed an important variability in both $pH_{F,is}$ and TdFe(II) concentrations, which indicated the volcanic area was affected by a degasification process that remained in the volcano after the eruptive phase had ceased. Fe(II) oxidation kinetic studies were also undertaken in order to analyze the effects of the seawater properties in the proximities of the volcano on the oxidation rate constants and $t_{1/2}$ (half-life time) of ferrous iron. The increased TdFe(II) concentrations and the low associated $pH_{F,is}$ values acted as an important fertilization event in the seawater around the Tagoro volcano at the Island of El Hierro providing optimal conditions for the regeneration of the area.



## 1. Introduction

Dissolved iron is the most bioavailable form assimilated by organisms (Brand, 1991; Hutchins et al., 1993). However, it is known that Fe(II) is thermodynamically unstable and is rapidly oxidized to Fe(III) in oxic waters (within seconds to minutes) (Kustka et al., 2005; Millero and Izaguirre, 1989; Santana-Casiano et al., 2005). Fe(III) has a very low solubility (Liu and Millero, 2002). The concentration of TdFe(II) dissolved in shallow and deep waters depends on the rate of oxidation of Fe(II) which is a function of both the $O_2$ and $H_2O_2$ concentration, pH, temperature, $[HCO_3^-]$, ionic strength and nutrient concentration (González-Davila et al., 2005; González-Dávila et al., 2006; González et al., 2010; King and Farlow, 2000; Miller et al., 1995; Santana-Casiano et al., 2005; Shi et al., 2010). For this reason, the concentrations of dissolved Fe(II) in the open ocean are very low, with typical values in the 0.02 to 2 nmol $L^{-1}$ ranges. However, typical concentrations of dissolved iron in hydrothermal vents are 1–3 mmol $L^{-1}$, with extreme values of about 18.7 mmol $L^{-1}$ measured in the Juan de Fuca Ridge (de Baar and de Jong, 2001). In these areas, Fe(II) remains in solution over longer time periods due to pH and pε (reduction potential) conditions.

Hydrothermal vents require hydrothermal fluid circulation during tectonic or magmatic and volcanic activity, which provides fluid pathways in the fractured oceanic crust and heat sources (Mantas et al., 2011). The composition of the hydrothermal fluid, which migrates to the subsurface and finally discharges at the sea floor, depends on a number of critical parameters including temperature, pressure, phase separation and host rock composition (Sander and Koschinsky, 2011). Hydrothermal emissions of gases and particles are an important source of material of different size, texture and chemical composition, such as gases and metals, especially reduced iron (Santana-Casiano et al., 2013).

The hydrothermal vents affect the chemical composition of seawater (Resing et al., 2015; Tagliabue et al., 2010) and their diffuse fluxes regulate the magnitude of dissolved Fe in the plume to the deep ocean (Resing et al., 2015; Tagliabue et al., 2010; German et al., 2015). These

* Corresponding author.
*E-mail address:* magdalena.santana@ulpgc.es (J.M. Santana-Casiano).

http://dx.doi.org/10.1016/j.marchem.2017.02.001
0304-4203/

# Chapter IV.

## Oxidation kinetics of Fe(II) along 59.5ºN in the North Atlantic in 2016

Carolina Santana-González, J. Magdalena Santana-Casiano, Melchor González-Dávila, Angelo Santana-del Pino, S. Gladyshev, A. Sokov

Marine Chemistry 203 (2018) 64-77

## *Abstract*

The Fe(II) oxidation rate was studied in different water masses present in the Subartic North Atlantic ocean along the 59.5ºN transatlantic section. Temperature, pH, salinity and total organic carbon (TOC) in natural conditions, fixed temperature conditions and both fixed temperature and pH conditions, were considered in order to understand the combined effects of the variables that control the Fe(II) oxidation kinetics in the ocean. The study shows that in natural conditions, temperature was the master variable which controled 75% of the pseudo-first order kinetics rate (*k'*). This value rose to 90% when $pH_F$ (free scale) and salinity were also considered. At a fixed temperature, 72% of *k'* was controlled by pH and at both fixed temperature and pH, salinity controled 62% of the Fe(II) oxidation rate. Sources and characteristics of TOC are important factors influencing the oxidation of Fe(II). The organic matter had both positive and negative effects on Fe(II) oxidation. In surface and coastal waters, TOC accelerated *k'*, decreasing the Fe(II) half-life time ($t_{1/2}$). In Subpolar Mode Water, Labrador Sea Water (for the Irminger Basin) and Denmark Straight Overflow Water, TOC slowed down *k'*, increasing Fe(II) $t_{1/2}$. This shifting behaviour where TOC affects Fe(II) oxidation depending on its marine or terrestrial origin, depth and remineralization stage proves that TOC cannot be used as a variable in an equation describing *k'*. The temperature dependence study indicated that the energy requirement for Fe(II) oxidation in surface waters was 32% lower than the required for bottom waters at both pH 7.7 and 8.0. This variability confirmed the importance of the organic matter composition of the selected samples. The Fe(II) oxidation rate constants in the region can be obtained from an empirical equation considering the natural conditions of temperature, $pH_F$ and salinity for the area, producing an error of estimation of 0.0072 $min^{-1}$. This equation should be incorporated in global Fe models.

## *4.1. Introduction*

Oceanic Fe distribution has been extensively studied in the Atlantic Ocean (Bergquist and Boyle, 2006; Bergquist et al., 2007; Bowie et al., 2003; Bowie et al., 2006; Bowie et al., 1998; Bowie et al., 2004; Bowie et al., 2002; Boye et al., 2006; Buck et al., 2016; Cullen et al., 2006; Fitzsimmons and Boyle, 2014; Fitzsimmons et al., 2013; Laës et al., 2005; Mills et al., 2004; Mohamed et al., 2011; Powell et al., 1995; Saito et al., 2013; Ussher et al., 2010; Wu et al., 2001), the Pacific Ocean (Chase et al., 2005; Coale, 1991; Hong and Kester, 1986; Mackey et al., 2002; Nishioka et al., 2001; Resing et al., 2015; Roy et al., 2008; Schmidt and Hutchins, 1999; Wu et al., 2001; Wu et al., 2011), the Indian Ocean (Nishioka et al., 2013; Statham et al., 2005), the Southern Ocean (Bowie et al., 2004; Bucciarelli et al., 2001; Chever et al., 2010; De Jong et al., 1998; Klunder et al., 2011; Tagliabue et al., 2012), the Arctic Ocean (Campbell and Yeats, 1982; Crusius et al., 2017; Klunder et al., 2012; Thuróczy et al., 2011; Wehrmann et al., 2014), the Arabian Sea (Measures and Vink, 1999) and the Mediterranean Sea (Sarthou and Jeandel, 2001).

In the past, global ocean Fe distribution models have been proposed (Tagliabue et al., 2014; Tagliabue et al., 2010; Tagliabue et al., 2017). However, there is a lack of knowledge in the processes that control the behaviour of the different iron species and the transference between them. Iron(III) is the thermodynamically stable form of iron in seawater (Millero and Izaguirre, 1989), but significant concentrations of Fe(II) can also be found in the ocean. This aspect is very important because Fe(II) is more bioavailable for marine phytoplankton than Fe(III) (Morel et al., 2008; Shaked et al., 2005; Shaked and Lis, 2012). The bioavailability of Fe in aquatic environments is strongly affected by redox reactions which cycle Fe between Fe(II) and Fe(III) oxidation states and by complexation with organic ligands (Daugherty et al., 2017). The concentration of Fe(II) in the photic zone and in deep waters depends on the rate of oxidation of Fe(II). Iron(II) is oxidized in a period of seconds to minutes by $O_2$ and $H_2O_2$, temperature, [$HCO_3^-$], and ionic strength with the rate dependent on pH (González-Davila et al., 2005, 2006; King and Farlow, 2000; Kustka et al., 2005; Miller et al., 1995; Santana-Casiano et al., 2004; 2005, 2010; Shi, 2012 ; Trapp and Millero, 2007). At the pH of seawater, $O_2$ is the most important oxidant when $H_2O_2$ concentration is below 200 nM and [Fe(II)] is at nanomolar levels (Santana-Casiano et al., 2006).

The complexation of iron by organic ligands often alters the Fe(II) oxidation kinetics by either accelerating or retarding the oxidation rate, depending on the source and characteristics of the Fe-binding organic ligands (Emmenegger et al., 1998;

González et al., 2014; Pham and Waite, 2008; Rose and Waite, 2002, 2003; Roy and Wells, 2011; Santana-Casiano et al., 2000, 2004; Theis and Singer, 1974). Roy et al. (2008) proposed the complexation of Fe(II) by organic ligands as an underlying mechanism to explain the decrease in Fe(II) oxidation rates in the Western Subarctic Pacific. A similar behaviour was found by Bowie et al. (2002) in several stations in the Atlantic Ocean. The effect of individual organic compounds on the oxidation kinetics of Fe(II) in seawater showed that EGTA (Ethylene-bis(oxyethylenenitrilo)tetraacetic acid) inhibits and EDTA (Ethylenediaminetetraacetic acid) accelerates Fe(II) oxidation, while negligible effects were observed with alanine and glutamic acids (Santana-Casiano et al., 2000). Cysteine accelerated the effective rate of the reaction by complexing Fe(II) while catechol regenerated Fe(II) in the pH range 7.0–8.2, demonstrating that catechol can quantitatively reduce Fe(III) in natural waters in a pH-dependent process (Santana-Casiano et al. 2010). Kuma et al. (1995) studied Fe(II) oxidation in the presence of hydroxycarboxylic acids in seawater from Funka Bay (Japan), showing that glucaric, glucaric acid-1,4-1actone and citric acids accelerated the Fe(II) oxidation rate while glucuronic, glycolic, gluconic, lactic, tartaric, glyceric and malic acids retarded it.

In the Eastern Subarctic Pacific, Roy and Wells (2011) showed that Fe(III)-complexing ligands were found in both surface and deep waters, and higher Fe(II) oxidation rates were measured only near the chlorophyll maximum, suggesting that the chemical nature and perhaps origin of natural Fe(III)-complexing organic ligands differ between surface and deep waters. In laboratory cultures of diatoms (*P. tricornutum*), Santana-Casiano et al. (2014) reported that the presence of excreted organic compounds decreased the rate of oxidation of Fe(II) in the solution, while the same behaviour was also found for phenolic compounds such as catechin and sinapic acid. The exudates of *P. tricornutum,* both decrease the Fe(II) oxidation rate and reduce Fe(III) to Fe(II). Lee et al. (2016) demonstrated that Fe(II) oxidation is enhanced in the presence of humic-type dissolved organic matter (DOM) with a high aliphatic content. Hay and Myneni (2007) also showed that carboxyl groups clustered on aliphatic structures, including succinic and malonic acids and humic substances (which also provide multidentate coordination sites for divalent metals) likely play dominant roles in the oxidation properties of natural organic matter (Leenheer et al., 1998; Manceau and Matynia, 2010). Lee et al. (2017) showed the importance of hydrophobic and allochthonous DOM in accelerating Fe(II) oxidation in freshwater systems in the Shizugawa Bay watershed. The Fe(II) oxidation rates observed were slower compared to organic ligand-free seawater and freshwater at fixed pH, however carbonate concentrations were not fixed. This work also demonstrated Fe(II) oxidation was retarded in the presence of cellular exudates of *Chaetoceros radicans* and *Microcystis aeruginosa*. However, it still remains unclear how the origin and molecular composition of DOM influence the variation in Fe(II) oxidation in natural waters (Lee et al., 2016), and how the changes in composition of

strong ligands across different nutrient regimes (Boiteau et al., 2016), could affect the Fe(II) oxidation rate and steady-state concentration (Daugherty et al., 2017).

This work studies the Fe(II) oxidation kinetics rate in the Subarctic Atlantic Ocean, one of the most sensitive areas for ocean acidification (García-Ibáñez et al., 2016). The study was carried out in the Rockall Trough, the Iceland basin and the Irminger basin, along the 59.5º N transatlantic section. The Fe(II) oxidation kinetics was studied in different water masses found in the water column along the transect. The studies were performed considering temperature (T), salinity (S) and $pH_F$ under *in situ* conditions and also T and pH under fixed conditions. The amount of total dissolved organic carbon (TOC) present in the samples was also considered. The Fe(II) oxidation rate allows us to know the half-life of Fe(II) in seawater that would be available for uptake by organisms, taking into account the role of organic compounds in the biogeochemical cycle of the Fe(II)-Fe(III) system in seawater which is affected by ocean acidification and global warming. This study aimed to understand how the combined effects of variables such as T, pH, S and TOC affected the Fe(II) oxidation rate and to what extent. The effects of spatial distribution (depth and longitude) were also considered. This study provides new insights into the Fe(II) oxidation kinetics in different water masses. Furthermore, it describes the effect of different physicochemical conditions on the Fe(II) oxidation process for both surface and bottom waters.

## *4.2. Methods*

### *4.2.1. Study location and water mass characteristics*

The study was carried out on cruise 51 of the Russian oceanographic vessel Akademik Ioffe which took place from June 8 to July 11 2016. The samples were collected from northern Scotland to the southern tip of Greenland along the 59.5ºN transatlantic section in the Rockall Trough, Iceland Basin and Irminger Sea (Fig. 4.1).

The Rockall Trough, Iceland Basin and Irminger Sea, in the North Atlantic, are characterized by warm and saline surface waters as well as cold and less saline intermediate and deep waters (García-Ibáñez et al., 2016). The water masses located in these basins are defined by their potential density ($\sigma_\theta$) limits: Subpolar Model Water (SPMW, $27.3 < \sigma_\theta < 27.6$), Labrador Sea Water (LSW, $27.6 < \sigma_\theta < 27.80$), Iceland-Scotland Overflow Water (ISOW, $27.80 < \sigma_\theta < 27.88$) and Denmark Strait Overflow

Water (DSOW, $\sigma_\theta$ > 27.88) (García-Ibáñez et al., 2016; Gladyshev et al., 2017; Sarafanov et al., 2009).

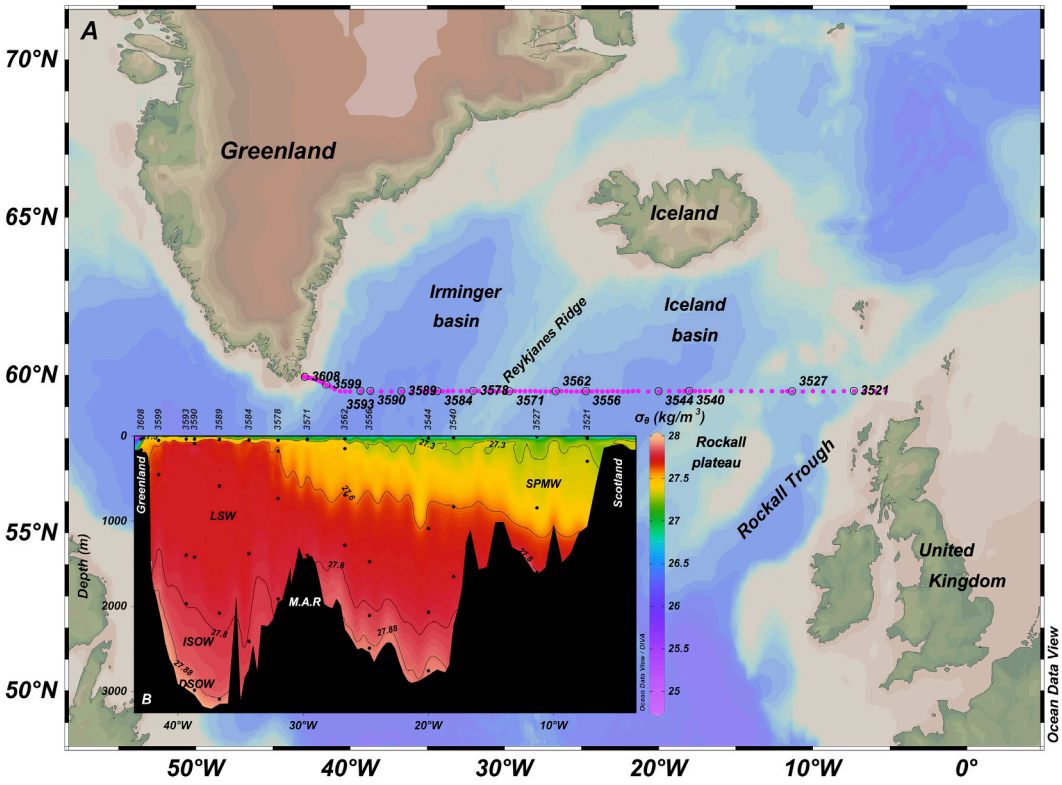


Fig. 4.1A) The North Atlantic Transept location; and B) The longitudinal distribution of the stations where dots represent sample depth and the $\sigma_\theta$ (kg/m$^3$) lines indicate the potential density limits between seawater masses in the area of study.

### *4.2.2. Reagents*

**Iron stock**. An iron stock of 6.21 x $10^{-4}$ mol $L^{-1}$ was prepared using ammonium iron(II) sulphate hexahydrate (Sigma-Aldrich). 0.01 mol $L^{-1}$ HCl (Hiperpur-Plus - Panreac, Barcelona, Spain) was added to water samples to lower the pH to 2 and slow down any oxidation. The solution was stored in the dark until use. A diluted stock was prepared daily with a final concentration of 2.42 x $10^{-6}$ mol $L^{-1}$.

**Luminol.** 5 L of luminol reagent was prepared using 2.71 x $10^{-4}$ mol $L^{-1}$ of 5-amino-2,3-dihydro-1,4-phthalazinedione (Sigma), 4.93 x $10^{-2}$ mol $L^{-1}$ of $Na_2CO_3$ (Sigma-Aldrich) and 0.4 mol $L^{-1}$ of 25% $NH_3$ (Panreac) previously distilled. The final pH was adjusted to 10.4 by adding 0.06 mol $L^{-1}$ Q-HCl. At this pH, luminescence is optimal (Bowie et al., 1998). The luminol solution was stored in the dark due to its light sensitivity. To ensure complete dilution, it was prepared a few days prior to use. The solution became more stable 24 hours after preparation and remains usable for a month (King et al., 1995).

**HCl**. 0.01 M HCl (Hiperpur-Plus) was used to set the pH in the kinetic experiments.

**$NH_3$**. 4.28 x $10^{-2}$ mol $L^{-1}$ of 20% $NH_3$ (Hiperpur-Plus) was prepared in Milli-Q to increase the pH in the water samples for the kinetic experiments.

**Ammonium acetate buffer**. 0.04 mol $L^{-1}$ ammonium acetate was prepared at pH 5.5 using acetic acid (glacial) to set the pH.

The reaction vessel and the tubing for the peristaltic pump were rinsed three times with distilled water, three times with Milli-Q water and stored in 10% HCl solution. Immediately prior to use, it was re-rinsed three times with distilled water and three times with Milli-Q water. After the analysis, the material was cleaned and re-stored in the HCl solution.

### *4.2.3. Sampling*

Water column samples were collected using 12 L Niskin bottles mounted on a 24-position rosette frame fitted with a SeaBird SBE11 Plus CTD.

Acid pre-cleaned polyethylene containers were used to collect the unfiltered samples. 15 mL low density polyethylene (LDPE, Nalgene) containers were used for the samples of total dissolved Fe(II) (TdFe(II)). To keep the seawater solution at pH 6 and avoid any oxidation of Fe(II) until the analysis, 10 μL of 2 M HCl was added to the containers prior to sampling. TdFe(II) was analysed on the sampling day. 250 mL LDPE (Nalgene) containers were used for the kinetic studies with zero air headspace

when sampling. TOC samples were collected in 50 mL polyethylene bottles and frozen until land-based laboratory analysis. All samples were kept in the dark until analysis.

#### *4.2.3.1. TdFe(II) samples*

The TdFe(II) unfiltered and acidified samples at pH of 6 and measured before 2 h were analysed on board. The concentration of TdFe(II) in seawater was determined using a FeLume system (Waterville Analytical). The Flow Injection Analysis by chemiluminescence (FIA-CL) technique uses luminol as the reagent (King et al., 1995). In the FIA system, four tygon tubes are placed in a peristaltic pump (Rainin Dynamax 15.8 V) which transfers the sample and reagents to the mixing chamber and to the detector. The tubing pressure is manipulated to allow a uniform flow. After adjusting the pressure in the tubing, the water-cleaning mode was enabled during 3 min. After this time, air was allowed to pass and then each line was introduced into the corresponding bottle: luminol, NaCl, Milli-Q water and sample. The software executed in the FeLume-chemiluminescence was provided by Waterville Analytical (WA control V105, photo counter control). An analysis time of 100 s was selected to allow full recording of the peak signal. The peak area mode was selected in order to compute the signal. Triplicate measurements were carried out for each sample and the results was obtained from the average. After each set of analyses, Milli-Q water was used to clean all the lines and finally air was run to empty them.

#### *4.2.3.2. Standards and calibration procedure*

The standard addition method was used to determinate TdFe(II) concentration at 15ºC, adding 3 standards to each sample. The required diluted iron stock was added after the sampling.

#### *4.2.3.3. Kinetic studies*

For the kinetic studies, the samples were measured directly using a connection between the sample and the buffer just before the introduction into the detector. The samples (1 mL $min^{-1}$ flux), ammonium acetate buffer (0.125 mL $min^{-1}$ flux) and luminol (1 mL $min^{-1}$ flux) were introduced into the detector with a peristaltic pump. This modification provided a continuous registration of the measure.

The kinetic studies were carried out in a thermo-regulated cell connected to a thermostatic bath (Julabo) with a control to 0.01ºC. For each study, the seawater sample was tempered to the desired temperature (in situ and 15ºC) as soon as they were sampled. When the temperature was stable, the $pH_F$ for the sample and Tris buffer was measured. For each kinetic study, 50 mL of seawater sampled without any headspace from different seawater masses and depths were used. The initial concentration of added Fe(II) was 0.97 nM and all studies were performed in the dark. The seawater was placed in the thermostated cell and the magnetic stirrer was switched on for 1 h to attain the equilibrium oxygen concentration. When the solution stabilized at the desired T and pH, the sample line was introduced into the cell. After that, the iron stock was added and a stopwatch was started.

The Fe(II) oxidation rate (Santana-Casiano et al., 2005) was expressed as an apparent oxidation rate, $k_{app}$ ($M^{-1}\,min^{-1}$)

$$\frac{d[Fe(II)]}{dt} = -k_{app}[Fe(II)][O_2] \tag{4.1}$$

The brackets denote the total molar concentration. The oxygen concentration was calculated using the Benson and Krause (1984) equation. In aerate solutions, the Fe(II) kinetic studies follow a pseudo-first-order, $k'$ ($min^{-1}$)

$$\frac{d[Fe(II)]}{dt} = -k'[Fe(II)] \tag{4.2}$$

where: $k' = k_{app}[O_2]$ (4.3)

and half-life time is $t_{1/2}$ (min)

$$t_{1/2} = \frac{\ln 2}{k'} \tag{4.4}$$

In the presence of organic ligands (L), the organic complexed ferrous iron can be oxidized to the corresponding ferric complex and the organic complexed ferric ion can be transformed into the ferrous one, modifying the generation of redox reactive species that acts together with the different $H_2O_2$ content already present in the water sample

(Santana-Casiano et al., 2004). An averaged vertical profile of $H_2O_2$ in the ocean with a typical exponential decrease in the upper 50–100 m from 50 to 25 nM and with $H_2O_2$ concentrations below the euphotic zone lower than 10 nM was assumed (Heller et al., 2013; Heller et al., 2016; Steigenberger and Croot, 2008). The presence of organic ligands and $H_2O_2$ could affect the observed linear behaviour.

#### *4.2.3.4. TOC samples*

TOC was measured with a continuous flow analyser (TOC-V, Shimadzu), previously calibrated with hydrogen phthalate standard (Sigma-Aldrich) (Arístegui, 2014). 10 mL of sample was acidified with 10 µL 85% $H_3PO_4$ and sparked with $CO_2$-free oxygen for at least 10 min to remove inorganic carbon. The sample was then passed into the quartz combustion tube packed with Pt gauze (Aldrich), 7% Pt on alumina catalyst. The Pt gauze and Pt beads were heated to 800ºC in the upper zone while the remaining packing material was heated to 600ºC in the lower zone. The resulting $CO_2$ flowed through two water traps and a final copper halide trap before detection with a $CO_2$ analyser (Hansell, 2001).

#### *4.2.3.5. Statistical analysis*

For the statistical analysis, the free R studio software (Team, 2016) was used. A correlation study between six independent variables (T, $pH_F$, S, TOC, depth and longitude) was performed to avoid any correlated independent variables effects. A principal component analysis was performed to study the combined effect of independent variables on the measured $t_{1/2}$ for the three sets of conditions considered in the present study. Two components were selected for the principal components analysis; the first component (PC1) was a combination of T, $pH_F$, TOC and depth and the second (PC2) a combination of TOC, S and longitude. The criteria to select two PC was that cumulative proportion and the proportion of variance could explain more than 70% of the variability. After the principal components study, a generalized additive model (GAM) (Hastie and Tibshirani, 1990) was used to determine the best fit between $t_{1/2}$ and each variable with empirical distribution functions which define the degree of the polynomial.

## *4.3. Results*

### *4.3.1. Oxidation kinetics of Fe(II)*

Iron(II) oxidation rate is independent of the initial Fe(II) concentration (Millero et al., 1987). Nevertheless, the oxidation rate can be affected when Fe(II) concentrations are low and when the $H_2O_2$ concentration change in the water column. The TdFe(II) concentration present in all the water samples used for the kinetic studies were measured and considered (see Table 4.1). The initial Fe(II) in the samples was the initially present plus the added Fe(II).

Table 4.1. TdFe(II) concentrations in the seawater used for the kinetics studies

| Basin | Depth (m) | TdFe(II) nM | std | n | |
|---|---|---|---|---|---|
| Rockall Trough | 0-200 | 0.43 | 0.01 | 2 | |
| | 200-1000 | 0.55 | 0.01 | 1 | |
| | 1000-2000 | 0.34 | 0.01 | 1 | |
| | 844 (11.33ºW) | 2.11 | 0.01 | 1 | * |
| Iceland | 0-200 | 0.89 | 0.18 | 5 | |
| | 200-1000 | 0.88 | 0.08 | 2 | |
| | 1000-2000 | 0.71 | 0.17 | 5 | |
| | 2000-bottom | 0.37 | 0.03 | 2 | |
| | 2758 (20.001ºW) | 0.53 | 0.01 | 1 | * |
| | 2495 (24.711ºW) | 0.84 | 0.01 | 1 | * |
| Irminger | 0-200 | 1.41 | 0.28 | 6 | |
| | 37 (42.927ºW) | 0.04 | 0.01 | 1 | * |
| | 37 (38.666ºW) | 0.65 | 0.01 | 1 | * |
| | 51 (41.535ºW) | 0.72 | 0.01 | 1 | * |
| | 178 (32ºW) | 0.45 | 0.01 | 1 | * |
| | 200-1000 | 0.5 | 0.04 | 3 | |
| | 1000-2000 | 0.46 | 0.17 | 4 | |
| | 1382 (34.329ºW) | 1.82 | 0.01 | 1 | * |
| | 2000-bottom | 0.5 | 0.12 | 3 | |
| | 2413 (34.329ºW) | 2.6 | 0.01 | 1 | * |
| | 2918 (39.332ºW) | 0.95 | 0.01 | 1 | * |

* Exclusions

In order to prove if the rate was affected by the initial Fe(II) concentration, different Fe(II) concentrations were added: 0.48, 0.97, 2.42 and 4.83 nM to a 3119 m deep sample (S = 34.986; 59.49558ºN, 37.99138ºW) at 25ºC and pH =8.0 (n=3). They showed similar *k'* ($min^{-1}$) values for the different Fe(II) additions (Table 4.2). These results agree with Roy and Wells (2011) for samples below the euphotic zone in the ocean indicating that $H_2O_2$ was low and in steady state in our samples. If $H_2O_2$ produced any changes in the oxidation rate, it did it at a level inside the experimental error. These results were assumed valid for all samples in our study.

Table 4.2. Oxidation rates at different Fe(II) initial concentration

| $[Fe(II)]_0$ nM | $k'$ ($min^{-1}$) | ln $k'$ ($min^{-1}$) | $t_{1/2}$ (min) |
|---|---|---|---|
| 0.48 | 0.147 ±0.007 | -1.918 ±0.044 | 4.72 ±0.21 |
| 0.97 | 0.148 ±0.001 | -1.913 ±0.009 | 4.69 ±0.04 |
| 2.42 | 0.156 ±0.005 | -1.857 ±0.029 | 4.44 ±0.13 |
| 4.83 | 0.153 ±0.003 | -1.879 ±0.020 | 4.54 ±0.09 |

The Fe(II) kinetic studies were carried out under three different sets of conditions: i) *in situ* conditions of temperature and $pH_F$, ii) fixed conditions of temperature (15ºC) and iii) fixed conditions of both temperature (15ºC) and $pH_F$ (8). A pseudo-first order kinetic reaction for the Fe(II) oxidation at nM levels for samples saturated with $O_2$ was observed in all samples before the $t_{1/2}$. This behavior indicated that both the organic matter present in the sample and changes in the $H_2O_2$ levels in the water column do not affect (or are compensated by) the observed pseudo-first order distribution. The pseudo-first order rate constant, *k'*, was calculated using Eq. 4.2 for the different samples selected to cover all the water masses found in the three basins. For the natural conditions study, representative Fe(II) decay curves are depicted in Fig. 4.2A together with the plot of log [TdFe(II)] versus time in Fig 4.2B. The $t_{1/2}$ was calculated using Eq. 4.4. The *k'* was correlated with the experimental conditions used. A description of *k'* is given in sections 4.3.1.1 to 4.3.1.3.

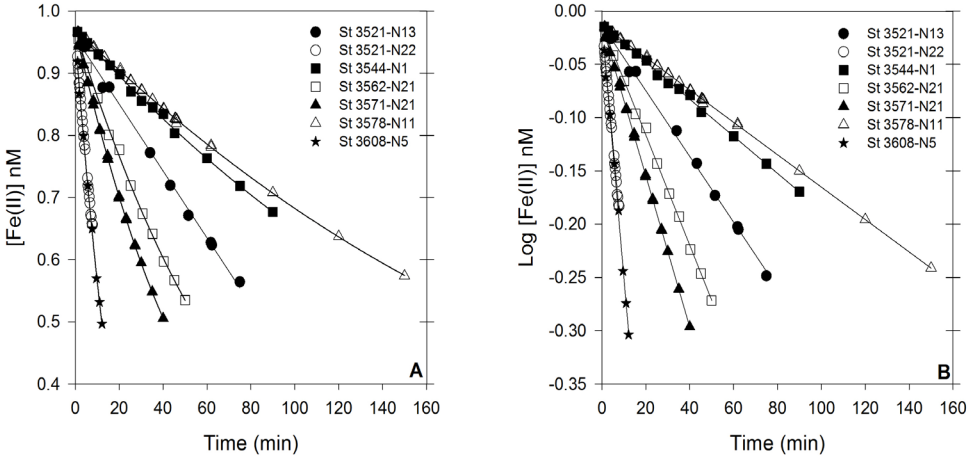


Fig. 4.2A) Fe(II) decay curves for the natural conditions in representative samples; B) Plot of Log [TdFe(II)] versus time.

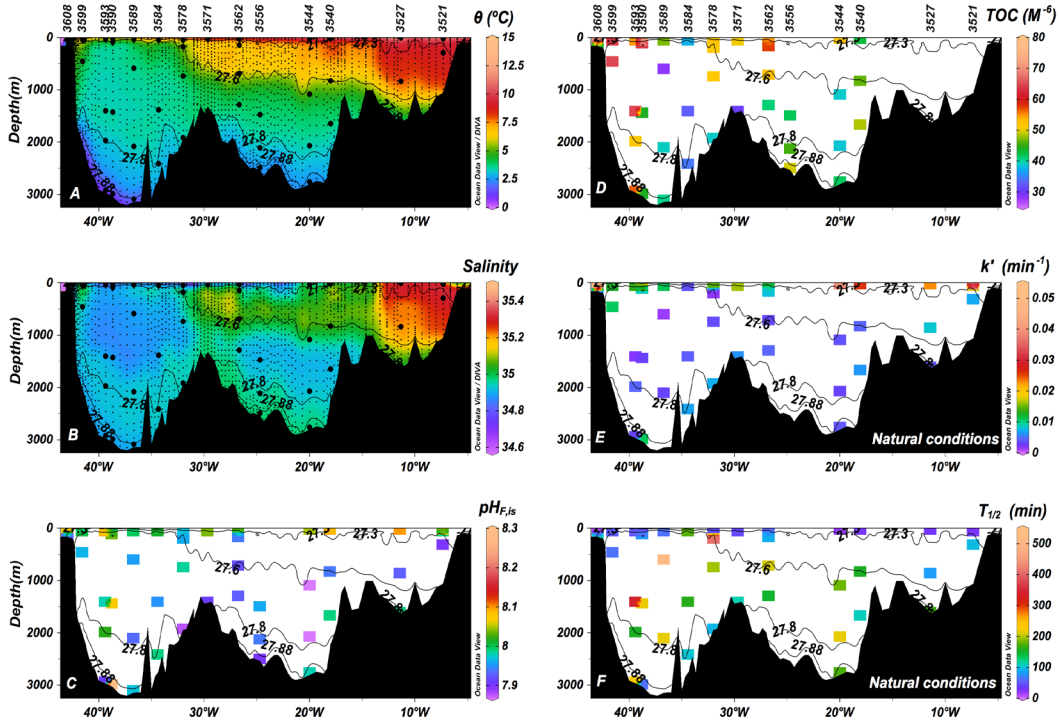


Fig. 4.3A) Potential temperature; B) Salinity; C) $pH_F$ in natural conditions; D) Total Organic Carbon; E) *k'* ($min^{-1}$) of Fe(II) oxidation in natural conditions; and F) Half-life time ($t_{1/2}$) of Fe(II) in the longitudinal section.

*4.3.1.1. Recreating in situ conditions*

For each water sample, the oxidation kinetics studies were carried out considering $pH_F$ and temperature under *in situ* conditions. The bath temperature was fixed at the same value than that indicated in the CTD for each sample. Temperature equilibrium was reached before the addition of Fe(II). Values computed using carbonate system variables (total alkalinity and total dissolved inorganic carbon) at *in situ* conditions of temperature and salinity were always inside 0.01 pH units (González-Dávila et al., unpublished data). Oxygen was not depleted in any initial seawater sample (Gladyshev et al., unpublished data). To keep a constant oxygen concentration along the kinetic study, the samples were aerated for 1 h prior to the study. The *k'* and $t_{1/2}$ values are represented in Table 4.3 and Fig. 4.3, together with the values of T, $pH_F$, S, TOC, depth and longitude. For each water mass, *k'* is represented in Fig. 4.3E. From the measured *k'* values, $t_{1/2}$ was calculated using Eq. 4.4. The statistical analysis was applied considering all water masses and basins in the studied transatlantic section.

The results of the statistical analysis for the dependence of *k'* on the physicochemical variables revealed that the main variable that explained 75% of the variation in *k'* (also in $t_{1/2}$) was T. When T and $pH_F$ were considered, this value remained at around 75%, and when S was also incorporated the dependency increases to 90%. However, when TOC was combined with S and $pH_F$ only 75% of *k'* observed was explained (Table 4.4). This implied that TOC effects on *k'* were strongly dependent on the water mass. Individual correlations between *k'* and TOC were analysed for each seawater mass and basin, obtaining the ratio *k'*:TOC ($min^{-1}/\mu M$ TOC). The ratio was negative for surface samples with a value of -1.17 ($r^2$=0.995, n=4) (excluding samples with TOC concentrations of 52.69 and 70.62 μM in Table 4.3) and for the LSW in the Iceland basin with -1.09 ($r^2$=0.689, n=5) (excluding samples with TOC concentrations of 48.51 and 38.53 μM TOC in Table 4.3). The ratio was positive in the SPMW with a value of +3.57 ($r^2$=0.778, n=7) and for the LSW in the Irminger basin with +2.83 ($r^2$=0.903, n=5) for samples west of the Irminger current.

When spatial distribution (potential density, depth and longitude) was considered with the physicochemical variables, 74% of the observed *k'* was explained after recreating *in situ* conditions for all water masses and basins The Fe(II) oxidation rate increased as T, $pH_F$ and TOC increased but slowed down with increases in S, depth and longitude (ºE).

The *k'* value was highly dependent on T, the main variable that controls the redox process. Surface water masses and the SPMW (Fig. 4.3) had the warmest and saltiest values, decreasing in an east-to-west direction. This was also observed in the $pH_F$ variable, with a $pH_F$ value of 8.10 in Rockall Trough, which decreased to 8.00 in the Greenland coast. The surface waters (including the SPMW) also presented the highest *k'* values (> 0.03 $min^{-1}$), with the lowest also found in the Greenland coast (0.013 $min^{-1}$). Below the SPMW, the intermediate water is formed by LSW. The potential temperature of these waters ranged from 3ºC to 6ºC and decreased with depth. The $pH_F$ values for intermediate waters ranged from 7.95-8.00 in the transatlantic section considered in this study, except for the Iceland basin with slightly lower $pH_F$ values of 7.92-7.96. Intermediate waters presented lower *k'* values than surface waters, ranging from 0.010 $min^{-1}$ to below 0.004 $min^{-1}$. In addition, low *k'* values of 0.001 $min^{-1}$ were found in the Irminger basin (588 m, 36.669ºW), which presented a $pH_F$ of 7.96 and the lowest salinity values (34.87±0.01). It was observed that most of the lowest *k'* areas presented low TOC concentrations, especially in the LSW in the Irminger Basin, with values as low as 28.31 µM. Exceptions were found closer to the Greenland coast, where TOC values ranged from 50 µM to 65.29 µM and *k'* was 0.012 $min^{-1}$, higher than the corresponding values of the surrounding water. The deep water masses are the densest waters and are composed of ISOW and DSOW that feed the Atlantic meridional overturning circulation (AMOC). They were the coldest waters in the section (Fig. 4.3), with temperatures below 2.5ºC, and high salinity values (>34.8). These samples presented low *k'* values of 0.005±0.002 $min^{-1}$.

Table 4.3. Fe(II) kinetics oxidation studies

| Basin | Seawater Mass | Salinity | TOC (μM) | Depth (m) | Longitude (ºW) | T (ºC) | $pH_F$ | $k'$ ($min^{-1}$) | Log $k_{app}$ ($M^{-1}$ $min^{-1}$) | $t_{1/2}$ (min) | $k'$ ($min^{-1}$) a | $k'$ ($min^{-1}$) b | $k'$ ($min^{-1}$) c | $k'$ ($min^{-1}$) d |
|---|---|---|---|---|---|---|---|---|---|---|---|---|---|---|
| Natural conditions | | | | | | | | | | | | | | |
| Rockall Trough | Surface | 35.31 | no data | 10 | 7.33 | 11.2 | 8.09 | 0.051 ± 4E-03 | 2.28 ± 4E-02 | 13.54 ± 0.13 | 0.043 | 0.038 | 0.029 | 0.050 |
| | | 35.32 | no data | 30 | 7.333 | 10.8 | 7.99 | 0.017 ± 1E-03 | 1.80 ± 4E-02 | 39.61 ± 0.38 | 0.026 | 0.033 | 0.019 | 0.037 |
| | | 35.31 | no data | 8 | 11.335 | 12.4 | 8.1 | 0.023 ± 2E-03 | 1.94 ± 4E-02 | 29.88 ± 0.28 | 0.054 | 0.043 | 0.034 | 0.059 |
| | SPMW | 35.3 | no data | 298 | 7.333 | 9.1 | 7.9 | 0.007 ± 5E-04 | 1.39 ± 4E-02 | 97.63 ± 0.93 | 0.014 | 0.025 | 0.012 | 0.024 |
| | | 35.22 | no data | 844 | 11.335 | 8.3 | 7.93 | 0.008 ± 6E-04 | 1.44 ± 4E-02 | 82.52 ± 0.79 | 0.014 | 0.024 | 0.012 | 0.024 |
| | ISOW | 35.31 | no data | 1607 | 11.335 | 3.7 | 7.99 | 0.004 ± 3E-04 | 1.10 ± 4E-02 | 169.06 ± 1.61 | 0.009 | 0.018 | 0.009 | 0.016 |
| Iceland | Surface | 34.97 | 42.91 | 19 | 18 | 10.1 | 8.09 | 0.026 ± 2E-03 | 1.97 ± 4E-02 | 26.56 ± 0.25 | 0.037 | 0.035 | 0.026 | 0.045 |
| | | 34.96 | 52.69 | 26 | 20.001 | 10.4 | 8.05 | 0.040 ± 3E-03 | 2.16 ± 4E-02 | 17.29 ± 0.16 | 0.032 | 0.034 | 0.023 | 0.041 |
| | | 34.91 | 54.97 | 34 | 26.664 | 8.1 | 8.03 | 0.012 ± 8E-04 | 1.62 ± 4E-02 | 58.25 ± 0.56 | 0.021 | 0.027 | 0.017 | 0.030 |
| | | 34.97 | 50.62 | 40 | 29.656 | 8.5 | 8.04 | 0.016 ± 1E-03 | 1.75 ± 4E-02 | 42.52 ± 0.41 | 0.023 | 0.029 | 0.018 | 0.032 |
| | SPMW | 35.01 | 57.74 | 147 | 26.664 | 6.5 | 7.94 | 0.008 ± 6E-04 | 1.43 ± 4E-02 | 91.2 ± 0.87 | 0.011 | 0.021 | 0.010 | 0.020 |
| | LSW | 35.05 | 46.49 | 830 | 18 | 5.9 | 7.94 | 0.005 ± 4E-04 | 1.22 ± 4E-02 | 154.03 ± 1.47 | 0.010 | 0.020 | 0.009 | 0.018 |
| | | 34.92 | 48.51 | 1651 | 18 | 3.8 | 7.99 | 0.006 ± 4E-04 | 1.27 ± 4E-02 | 108.3 ± 1.03 | 0.009 | 0.018 | 0.009 | 0.017 |
| | | 34.96 | 39.04 | 1086 | 20.001 | 4.7 | 7.86 | 0.004 ± 3E-04 | 1.11 ± 4E-02 | 182.41 ± 1.74 | 0.006 | 0.016 | 0.006 | 0.013 |
| | | 34.93 | 38.53 | 2069 | 20.001 | 3.6 | 7.85 | 0.003 ± 2E-04 | 0.97 ± 4E-02 | 216.61 ± 2.06 | 0.005 | 0.015 | 0.005 | 0.011 |
| | | 35.04 | 52.78 | 692 | 26.664 | 5.7 | 7.92 | 0.003 ± 2E-04 | 0.99 ± 4E-02 | 210.04 ± 2.00 | 0.009 | 0.019 | 0.009 | 0.017 |
| | | 34.92 | 41.945 | 1284 | 26.664 | 3.9 | 7.93 | 0.005 ± 4E-04 | 1.20 ± 4E-02 | 150 ± 1.43 | 0.007 | 0.017 | 0.007 | 0.014 |
| | | 34.98 | 30.5 | 1403 | 29.656 | 4 | 7.91 | 0.006 ± 4E-04 | 1.28 ± 4E-02 | 111.8 ± 1.07 | 0.007 | 0.016 | 0.007 | 0.014 |
| | DSOW | 34.98 | 41.7 | 2758 | 20.001 | 2.6 | 7.98 | 0.004 ± 3E-04 | 1.09 ± 4E-02 | 173 ± 1.65 | 0.007 | 0.016 | 0.007 | 0.014 |
| Irminger | Surface | 33.01 | 70.62 | 37 | 42.927 | 2 | 8.07 | 0.055 ± 4E-03 | 2.21 ± 4E-02 | 12.7 ± 0.12 | 0.010 | 0.017 | 0.010 | 0.017 |
| | | 34.9 | 52.95 | 50 | 32 | 7.4 | 7.97 | 0.015 ± 1E-03 | 1.71 ± 4E-02 | 47.8 ± 0.46 | 0.014 | 0.024 | 0.012 | 0.024 |
| | SPMW | 34.94 | 37.36 | 49 | 34.329 | 5.7 | 8.01 | 0.004 ± 3E-04 | 1.12 ± 4E-02 | 177.73 ± 1.69 | 0.013 | 0.022 | 0.012 | 0.022 |
| | | 34.93 | 47.23 | 39 | 36.669 | 5.8 | 8 | 0.011 ± 8E-04 | 1.56 ± 4E-02 | 63.59 ± 0.61 | 0.013 | 0.021 | 0.012 | 0.021 |
| | | 34.82 | 75.19 | 37 | 38.666 | 6.6 | 7.99 | 0.019 ± 1E-03 | 1.80 ± 4E-02 | 35.55 ± 0.34 | 0.014 | 0.023 | 0.012 | 0.023 |
| | | 34.82 | 55.09 | 38 | 39.339 | 6.3 | 8.09 | 0.013 ± 9E-04 | 1.63 ± 4E-02 | 51.73 ± 0.49 | 0.020 | 0.025 | 0.017 | 0.029 |
| | | 34.96 | 63.99 | 51 | 41.535 | 6.4 | 8 | 0.013 ± 9E-04 | 1.64 ± 4E-02 | 54.15 ± 0.52 | 0.014 | 0.023 | 0.012 | 0.023 |
| | | 34.66 | 43.32 | 164 | 42.927 | 4.2 | 7.93 | 0.006 ± 4E-04 | 1.28 ± 4E-02 | 110.02 ± 1.05 | 0.007 | 0.017 | 0.008 | 0.015 |

| | | | | | | | | | | | | | | |
|---|---|---|---|---|---|---|---|---|---|---|---|---|---|---|
| | LSW | 34.94 | 51.77 | 178 | 32 | 5 | 7.96 | 0.002 ± 1E-04 | 0.81 ± 4E-02 | 407.73 ± 3.89 | 0.009 | 0.019 | 0.009 | 0.018 |
| | | 34.9 | 51.49 | 737 | 32 | 3.8 | 7.98 | 0.004 ± 3E-04 | 1.10 ± 4E-02 | 198.04 ± 1.89 | 0.008 | 0.018 | 0.009 | 0.016 |
| | | 34.94 | 39 | 1916 | 32 | 3.3 | 7.88 | 0.007 ± 5E-04 | 1.34 ± 4E-02 | 94.95 ± 0.90 | 0.005 | 0.015 | 0.006 | 0.012 |
| | | 34.88 | 32.99 | 1382 | 34.329 | 3.5 | 7.95 | 0.004 ± 3E-04 | 1.09 ± 4E-02 | 161.2 ± 1.54 | 0.007 | 0.017 | 0.007 | 0.014 |
| | | 34.89 | 28.31 | 588 | 36.669 | 3.7 | 7.96 | 0.001 ± 7E-05 | 0.49 ± 4E-02 | 533.19 ± 5.08 | 0.008 | 0.017 | 0.008 | 0.015 |
| | | 34.93 | 39.38 | 2081 | 36.669 | 3.5 | 7.93 | 0.003 ± 2E-04 | 0.97 ± 4E-02 | 216.61 ± 2.06 | 0.007 | 0.016 | 0.007 | 0.014 |
| | | 34.9 | 64.22 | 91 | 38.666 | 4 | 8.04 | 0.009 ± 6E-04 | 1.45 ± 4E-02 | 79.67 ± 0.76 | 0.011 | 0.019 | 0.011 | 0.019 |
| | | 34.91 | 44.1 | 1424 | 38.666 | 3.6 | 8.07 | 0.003 ± 2E-04 | 0.97 ± 4E-02 | 216.61 ± 2.06 | 0.012 | 0.019 | 0.012 | 0.020 |
| | | 34.88 | 64.82 | 1401 | 39.332 | 3.5 | 7.98 | 0.002 ± 1E-04 | 0.79 ± 4E-02 | 346.57 ± 3.30 | 0.008 | 0.017 | 0.008 | 0.016 |
| | | 34.92 | 52.07 | 1972 | 39.332 | 3.3 | 8.02 | 0.005 ± 4E-04 | 1.19 ± 4E-02 | 154.03 ± 1.47 | 0.009 | 0.018 | 0.009 | 0.017 |
| | | 34.94 | 65.29 | 456 | 41.535 | 4.3 | 7.97 | 0.011 ± 8E-04 | 1.54 ± 4E-02 | 64.18 ± 0.61 | 0.009 | 0.018 | 0.009 | 0.017 |
| | ISOW | 34.94 | 39 | 1916 | 32 | 3.4 | 7.88 | 0.007 ± 5E-04 | 1.34 ± 4E-02 | 94.95 ± 0.90 | 0.005 | 0.015 | 0.006 | 0.012 |
| | | 34.94 | 34.46 | 2413 | 34.329 | 3.2 | 7.99 | 0.007 ± 5E-04 | 1.33 ± 4E-02 | 101.93 ± 0.97 | 0.008 | 0.017 | 0.008 | 0.015 |
| | | 34.9 | 44.14 | 2986 | 38.666 | 1.3 | 8.32 | 0.011 ± 8E-04 | 1.51 ± 4E-02 | 64.18 ± 0.61 | 0.027 | 0.021 | 0.027 | 0.034 |
| | | 34.9 | 56.77 | 2918 | 39.332 | 1.2 | 7.91 | 0.003 ± 2E-04 | 0.94 ± 4E-02 | 213 ± 2.03 | 0.004 | 0.013 | 0.005 | 0.010 |
| | | | | | | | Fix at 15℃ | | | | | | | |
| Rockall Trough | Surface | 35.31 | no data | 10 | 7.33 | 15 | 8.08 | 0.208 ± 1E-02 | 2.92 ± 4E-02 | 3.33 ± 0.03 | 0.073 | 0.052 | 0.042 | 0.074 |
| | | 35.32 | no data | 30 | 7.333 | 15 | 7.92 | 0.009 ± 6E-04 | 1.56 ± 4E-02 | 79.67 ± 0.76 | 0.037 | 0.043 | 0.023 | 0.048 |
| | | 35.31 | no data | 8 | 11.335 | 15 | 8.09 | 0.045 ± 3E-03 | 2.26 ± 4E-02 | 15.54 ± 0.15 | 0.076 | 0.053 | 0.044 | 0.077 |
| | SPMW | 35.3 | no data | 298 | 7.333 | 15 | 8.03 | 0.090 ± 6E-03 | 2.56 ± 4E-02 | 7.73 ± 0.07 | 0.059 | 0.049 | 0.035 | 0.065 |
| | | 35.22 | no data | 844 | 11.335 | 15 | 7.88 | 0.017 ± 1E-03 | 1.83 ± 4E-02 | 40.53 ± 0.39 | 0.032 | 0.040 | 0.021 | 0.044 |
| | ISOW | 35.31 | no data | 1607 | 11.335 | 15 | 7.98 | 0.005 ± 4E-04 | 1.30 ± 4E-02 | 133.3 ± 1.27 | 0.048 | 0.046 | 0.029 | 0.057 |
| Iceland | Surface | 34.97 | 42.91 | 19 | 18 | 15 | 8.04 | 0.016 ± 1E-03 | 1.81 ± 4E-02 | 43.59 ± 0.41 | 0.062 | 0.050 | 0.036 | 0.067 |
| | | 34.96 | 52.69 | 26 | 20.001 | 15 | 8.04 | 0.057 ± 4E-03 | 2.36 ± 4E-02 | 12.14 ± 0.12 | 0.062 | 0.050 | 0.036 | 0.067 |
| | | 34.91 | 54.97 | 34 | 26.664 | 15 | 7.94 | 0.030 ± 2E-03 | 2.08 ± 4E-02 | 22.95 ± 0.22 | 0.041 | 0.044 | 0.025 | 0.051 |
| | | 34.97 | 50.62 | 40 | 29.656 | 15 | 7.87 | 0.025 ± 2E-03 | 2.00 ± 4E-02 | 28.18 ± 0.27 | 0.031 | 0.040 | 0.020 | 0.043 |
| | SPMW | 35.01 | 57.74 | 147 | 26.664 | 15 | 7.86 | 0.007 ± 5E-04 | 1.45 ± 4E-02 | 99.02 ± 0.94 | 0.029 | 0.039 | 0.019 | 0.042 |
| | LSW | 35.05 | 46.49 | 830 | 18 | 15 | 7.88 | 0.014 ± 1E-03 | 1.75 ± 4E-02 | 51.34 ± 0.49 | 0.032 | 0.040 | 0.021 | 0.044 |
| | | 34.92 | 48.51 | 1651 | 18 | 15 | 7.81 | 0.011 ± 8E-04 | 1.64 ± 4E-02 | 64.18 ± 0.61 | 0.024 | 0.037 | 0.017 | 0.037 |
| | | 34.96 | 39.04 | 1086 | 20.001 | 15 | 7.91 | 0.012 ± 8E-04 | 1.68 ± 4E-02 | 58.74 ± 0.56 | 0.036 | 0.042 | 0.023 | 0.047 |

| | | | | | | | | | | | | | | |
|---|---|---|---|---|---|---|---|---|---|---|---|---|---|---|
| | | 34.92 | 42.12 | 1476 | 24.711 | 15 | 7.89 | 0.006 ± 4E-04 | 1.38 ± 4E-02 | 106.64 ± 1.01 | 0.033 | 0.041 | 0.021 | 0.045 |
| | | 35.04 | 52.78 | 692 | 26.664 | 15 | 7.85 | 0.018 ± 1E-03 | 1.86 ± 4E-02 | 37.88 ± 0.36 | 0.028 | 0.039 | 0.019 | 0.041 |
| | | 34.92 | 41.945 | 1284 | 26.664 | 15 | 7.91 | 0.017 ± 1E-03 | 1.83 ± 4E-02 | 40.07 ± 0.38 | 0.036 | 0.042 | 0.023 | 0.047 |
| | | 34.98 | 30.5 | 1403 | 29.656 | 15 | 7.86 | 0.012 ± 8E-04 | 1.68 ± 4E-02 | 59.24 ± 0.56 | 0.029 | 0.039 | 0.019 | 0.042 |
| | ISOW | 34.96 | 45.77 | 2109 | 24.711 | 15 | 7.89 | 0.007 ± 5E-04 | 1.45 ± 4E-02 | 105.02 ± 1.00 | 0.033 | 0.041 | 0.021 | 0.045 |
| | DSOW | 34.98 | 41.7 | 2758 | 20.001 | 15 | 7.96 | 0.014 ± 1E-03 | 1.75 ± 4E-02 | 50.5 ± 0.48 | 0.044 | 0.045 | 0.027 | 0.054 |
| | | 34.98 | 49.54 | 2495 | 24.711 | 15 | 7.89 | 0.006 ± 4E-04 | 1.38 ± 4E-02 | 119.51 ± 1.14 | 0.033 | 0.041 | 0.021 | 0.045 |
| Irminger | Surface | 33.01 | 70.62 | 37 | 42.927 | 15 | 7.95 | 0.077 ± 5E-03 | 2.48 ± 4E-02 | 9.05 ± 0.09 | 0.044 | 0.045 | 0.027 | 0.053 |
| | | 34.9 | 52.95 | 50 | 32 | 15 | 7.92 | 0.044 ± 3E-03 | 2.24 ± 4E-02 | 15.83 ± 0.15 | 0.037 | 0.043 | 0.024 | 0.048 |
| | SPMW | 34.94 | 37.36 | 49 | 34.329 | 15 | 7.93 | 0.022 ± 2E-03 | 1.94 ± 4E-02 | 31.22 ± 0.30 | 0.039 | 0.043 | 0.024 | 0.050 |
| | | 34.93 | 47.23 | 39 | 36.669 | 15 | 7.94 | 0.035 ± 2E-03 | 2.14 ± 4E-02 | 19.58 ± 0.19 | 0.041 | 0.044 | 0.025 | 0.051 |
| | | 34.82 | 75.19 | 37 | 38.666 | 15 | 7.94 | 0.042 ± 3E-03 | 2.22 ± 4E-02 | 16.43 ± 0.16 | 0.041 | 0.044 | 0.025 | 0.051 |
| | | 34.82 | 55.09 | 38 | 39.339 | 15 | 7.87 | 0.011 ± 8E-04 | 1.64 ± 4E-02 | 64.78 ± 0.62 | 0.031 | 0.040 | 0.020 | 0.043 |
| | | 34.96 | 63.99 | 51 | 41.535 | 15 | 7.92 | 0.032 ± 2E-03 | 2.11 ± 4E-02 | 21.94 ± 0.21 | 0.037 | 0.043 | 0.024 | 0.048 |
| | | 34.66 | 43.32 | 164 | 42.927 | 15 | 7.79 | 0.016 ± 1E-03 | 1.80 ± 4E-02 | 43.05 ± 0.41 | 0.023 | 0.036 | 0.016 | 0.036 |
| | LSW | 34.94 | 51.77 | 178 | 32 | 15 | 7.89 | 0.017 ± 1E-03 | 1.83 ± 4E-02 | 40.77 ± 0.39 | 0.033 | 0.041 | 0.021 | 0.045 |
| | | 34.9 | 51.49 | 737 | 32 | 15 | 7.84 | 0.009 ± 6E-04 | 1.56 ± 4E-02 | 73.74 ± 0.70 | 0.027 | 0.038 | 0.018 | 0.040 |
| | | 34.94 | 39 | 1916 | 32 | 15 | 7.85 | 0.012 ± 8E-04 | 1.68 ± 4E-02 | 56.35 ± 0.54 | 0.028 | 0.039 | 0.019 | 0.041 |
| | | 34.88 | 32.99 | 1382 | 34.329 | 15 | 7.87 | 0.008 ± 6E-04 | 1.50 ± 4E-02 | 84.57 ± 0.80 | 0.031 | 0.040 | 0.020 | 0.043 |
| | | 34.89 | 28.31 | 588 | 36.669 | 15 | 7.93 | 0.026 ± 2E-03 | 2.02 ± 4E-02 | 27.18 ± 0.26 | 0.039 | 0.043 | 0.025 | 0.050 |
| | | 34.93 | 39.38 | 2081 | 36.669 | 15 | 7.9 | 0.013 ± 9E-04 | 1.71 ± 4E-02 | 52.12 ± 0.50 | 0.035 | 0.042 | 0.022 | 0.046 |
| | | 34.9 | 64.22 | 91 | 38.666 | 15 | 7.83 | 0.015 ± 1E-03 | 1.78 ± 4E-02 | 44.72 ± 0.42 | 0.026 | 0.038 | 0.018 | 0.039 |
| | | 34.91 | 44.1 | 1424 | 38.666 | 15 | 7.88 | 0.011 ± 8E-04 | 1.64 ± 4E-02 | 64.78 ± 0.62 | 0.032 | 0.040 | 0.021 | 0.044 |
| | | 34.88 | 64.82 | 1401 | 39.332 | 15 | 7.91 | 0.005 ± 4E-04 | 1.30 ± 4E-02 | 126.03 ± 1.20 | 0.036 | 0.042 | 0.023 | 0.047 |
| | | 34.92 | 52.07 | 1972 | 39.332 | 15 | 7.87 | 0.012 ± 8E-04 | 1.68 ± 4E-02 | 59.24 ± 0.56 | 0.031 | 0.040 | 0.020 | 0.043 |
| | | 34.94 | 65.29 | 456 | 41.535 | 15 | 7.88 | 0.008 ± 6E-04 | 1.50 ± 4E-02 | 83.51 ± 0.79 | 0.032 | 0.040 | 0.021 | 0.044 |
| | ISOW | 34.94 | 39 | 1916 | 32 | 15 | 7.85 | 0.012 ± 9E-04 | 1.69 ± 4E-02 | 56.35 ± 0.54 | 0.028 | 0.039 | 0.019 | 0.041 |
| | | 34.94 | 34.46 | 2413 | 34.329 | 15 | 7.87 | 0.011 ± 8E-04 | 1.64 ± 4E-02 | 61.89 ± 0.59 | 0.031 | 0.040 | 0.020 | 0.043 |
| | DSOW | 34.9 | 40.37 | 3090 | 36.669 | 15 | 7.88 | 0.014 ± 1E-03 | 1.75 ± 4E-02 | 48.14 ± 0.46 | 0.032 | 0.040 | 0.021 | 0.044 |
| | | 34.9 | 44.14 | 2986 | 38.666 | 15 | 7.88 | 0.018 ± 1E-03 | 1.86 ± 4E-02 | 38.94 ± 0.37 | 0.032 | 0.040 | 0.021 | 0.044 |
| | | 34.9 | 56.77 | 2918 | 39.332 | 15 | 7.89 | 0.018 ± 1E-03 | 1.86 ± 4E-02 | 39.16 ± 0.37 | 0.033 | 0.041 | 0.021 | 0.045 |

| | | | | | Fiix at 15ºC, $pH_F$=8 | | | | | | | | | | | | | | | | |
|---|---|---|---|---|---|---|---|---|---|---|---|---|---|---|---|---|---|---|---|---|---|
| Rockall Trough | Surface | 35.31 | no data | 10 | 7.33 | 15 | 8.00 | 0.082 | ± | 6E-03 | 2.52 | ± | 4E-02 | 8.43 | ± | 0.07 | 0.052 | 0.047 | 0.031 | 0.060 |
| | | 35.32 | no data | 30 | 7.333 | 15 | 8.00 | 0.011 | ± | 8E-04 | 1.64 | ± | 4E-02 | 60.8 | ± | 0.53 | 0.052 | 0.047 | 0.031 | 0.060 |
| | | 35.31 | no data | 8 | 11.335 | 15 | 8.00 | 0.026 | ± | 2E-03 | 2.02 | ± | 4E-02 | 26.16 | ± | 0.23 | 0.052 | 0.047 | 0.031 | 0.060 |
| | SPMW | 35.3 | no data | 298 | 7.333 | 15 | 8.00 | 0.067 | ± | 5E-03 | 2.43 | ± | 4E-02 | 10.35 | ± | 0.09 | 0.052 | 0.047 | 0.031 | 0.060 |
| | | 35.22 | no data | 844 | 11.335 | 15 | 8.00 | 0.021 | ± | 1E-03 | 1.92 | ± | 4E-02 | 33.49 | ± | 0.29 | 0.052 | 0.047 | 0.031 | 0.060 |
| | ISOW | 35.31 | no data | 1607 | 11.335 | 15 | 8.00 | 0.006 | ± | 4E-04 | 1.38 | ± | 4E-02 | 113.03 | ± | 0.98 | 0.052 | 0.047 | 0.031 | 0.060 |
| Iceland | Surface | 34.97 | 42.91 | 19 | 18 | 15 | 8.00 | 0.051 | ± | 4E-03 | 2.31 | ± | 4E-02 | 13.49 | ± | 0.12 | 0.052 | 0.047 | 0.031 | 0.060 |
| | | 34.96 | 52.69 | 26 | 20.001 | 15 | 8.00 | 0.047 | ± | 3E-03 | 2.27 | ± | 4E-02 | 14.82 | ± | 0.13 | 0.052 | 0.047 | 0.031 | 0.060 |
| | | 34.91 | 54.97 | 34 | 26.664 | 15 | 8.00 | 0.031 | ± | 2E-03 | 2.09 | ± | 4E-02 | 22.22 | ± | 0.19 | 0.052 | 0.047 | 0.031 | 0.060 |
| | | 34.97 | 50.62 | 40 | 29.656 | 15 | 8.00 | 0.027 | ± | 2E-03 | 2.03 | ± | 4E-02 | 25.39 | ± | 0.22 | 0.052 | 0.047 | 0.031 | 0.060 |
| | SPMW | 35.01 | 57.74 | 147 | 26.664 | 15 | 8.00 | 0.017 | ± | 1E-03 | 1.83 | ± | 4E-02 | 40.53 | ± | 0.35 | 0.052 | 0.047 | 0.031 | 0.060 |
| | LSW | 35.05 | 46.49 | 830 | 18 | 15 | 8.00 | 0.020 | ± | 1E-03 | 1.90 | ± | 4E-02 | 34.31 | ± | 0.30 | 0.052 | 0.047 | 0.031 | 0.060 |
| | | 34.92 | 48.51 | 1651 | 18 | 15 | 8.00 | 0.017 | ± | 1E-03 | 1.83 | ± | 4E-02 | 41.26 | ± | 0.36 | 0.052 | 0.047 | 0.031 | 0.060 |
| | | 34.96 | 39.04 | 1086 | 20.001 | 15 | 8.00 | 0.017 | ± | 1E-03 | 1.83 | ± | 4E-02 | 40.01 | ± | 0.35 | 0.052 | 0.047 | 0.031 | 0.060 |
| | | 34.93 | 38.53 | 2069 | 20.001 | 15 | 8.00 | 0.014 | ± | 1E-03 | 1.75 | ± | 4E-02 | 49.87 | ± | 0.43 | 0.052 | 0.047 | 0.031 | 0.060 |
| | | 34.92 | 42.12 | 1476 | 24.711 | 15 | 8.00 | 0.012 | ± | 8E-04 | 1.68 | ± | 4E-02 | 57.76 | ± | 0.50 | 0.052 | 0.047 | 0.031 | 0.060 |
| | | 35.04 | 52.78 | 692 | 26.664 | 15 | 8.00 | 0.018 | ± | 1E-03 | 1.86 | ± | 4E-02 | 37.67 | ± | 0.33 | 0.052 | 0.047 | 0.031 | 0.060 |
| | | 34.92 | 41.945 | 1284 | 26.664 | 15 | 8.00 | 0.033 | ± | 2E-03 | 2.12 | ± | 4E-02 | 21.26 | ± | 0.18 | 0.052 | 0.047 | 0.031 | 0.060 |
| | | 34.98 | 30.5 | 1403 | 29.656 | 15 | 8.00 | 0.020 | ± | 1E-03 | 1.90 | ± | 4E-02 | 33.98 | ± | 0.30 | 0.052 | 0.047 | 0.031 | 0.060 |
| | ISOW | 34.96 | 45.77 | 2109 | 24.711 | 15 | 8.00 | 0.011 | ± | 8E-04 | 1.64 | ± | 4E-02 | 61.34 | ± | 0.53 | 0.052 | 0.047 | 0.031 | 0.060 |
| | DSOW | 34.98 | 41.7 | 2758 | 20.001 | 15 | 8.00 | 0.016 | ± | 1E-03 | 1.81 | ± | 4E-02 | 44.43 | ± | 0.39 | 0.052 | 0.047 | 0.031 | 0.060 |
| | | 34.98 | 49.54 | 2495 | 24.711 | 15 | 8.00 | 0.011 | ± | 8E-04 | 1.64 | ± | 4E-02 | 61.89 | ± | 0.54 | 0.052 | 0.047 | 0.031 | 0.060 |
| Irminger | Surface | 33.01 | 70.62 | 37 | 42.927 | 15 | 8.00 | 0.111 | ± | 8E-03 | 2.64 | ± | 4E-02 | 6.23 | ± | 0.05 | 0.054 | 0.048 | 0.033 | 0.060 |
| | SPMW | 34.94 | 37.36 | 49 | 34.329 | 15 | 8.00 | 0.028 | ± | 2E-03 | 2.05 | ± | 4E-02 | 24.58 | ± | 0.21 | 0.052 | 0.047 | 0.031 | 0.060 |
| | | 34.93 | 47.23 | 39 | 36.669 | 15 | 8.00 | 0.047 | ± | 3E-03 | 2.27 | ± | 4E-02 | 14.87 | ± | 0.13 | 0.052 | 0.047 | 0.031 | 0.060 |
| | | 34.82 | 75.19 | 37 | 38.666 | 15 | 8.00 | 0.060 | ± | 4E-03 | 2.38 | ± | 4E-02 | 11.59 | ± | 0.10 | 0.052 | 0.047 | 0.031 | 0.060 |
| | | 34.82 | 55.09 | 38 | 39.339 | 15 | 8.00 | 0.021 | ± | 1E-03 | 1.92 | ± | 4E-02 | 32.24 | ± | 0.28 | 0.052 | 0.047 | 0.031 | 0.060 |
| | | 34.96 | 63.99 | 51 | 41.535 | 15 | 8.00 | 0.062 | ± | 4E-03 | 2.39 | ± | 4E-02 | 11.16 | ± | 0.10 | 0.052 | 0.047 | 0.031 | 0.060 |
| | | 34.66 | 43.32 | 164 | 42.927 | 15 | 8.00 | 0.074 | ± | 5E-03 | 2.47 | ± | 4E-02 | 9.32 | ± | 0.08 | 0.052 | 0.047 | 0.031 | 0.060 |

| | | | | | | | | | | | | | |
|---|---|---|---|---|---|---|---|---|---|---|---|---|---|
| | 34.9 | 51.49 | 737 | 32 | 15 | 8.00 | 0.018 ± 1E-03 | 1.86 ± 4E-02 | 37.67 ± 0.33 | 0.052 | 0.047 | 0.031 | 0.060 |
| | 34.94 | 39 | 1916 | 32 | 15 | 8.00 | 0.031 ± 2E-03 | 2.09 ± 4E-02 | 22.15 ± 0.19 | 0.052 | 0.047 | 0.031 | 0.060 |
| | 34.88 | 32.99 | 1382 | 34.329 | 15 | 8.00 | 0.016 ± 1E-03 | 1.80 ± 4E-02 | 42.27 ± 0.37 | 0.052 | 0.047 | 0.031 | 0.060 |
| | 34.89 | 28.31 | 588 | 36.669 | 15 | 8.00 | 0.037 ± 3E-03 | 2.17 ± 4E-02 | 18.63 ± 0.16 | 0.052 | 0.047 | 0.031 | 0.060 |
| | 34.93 | 39.38 | 2081 | 36.669 | 15 | 8.00 | 0.030 ± 2E-03 | 2.08 ± 4E-02 | 23.42 ± 0.20 | 0.052 | 0.047 | 0.031 | 0.060 |
| | 34.9 | 64.22 | 91 | 38.666 | 15 | 8.00 | 0.071 ± 5E-03 | 2.45 ± 4E-02 | 9.83 ± 0.09 | 0.052 | 0.047 | 0.031 | 0.060 |
| | 34.91 | 44.1 | 1424 | 38.666 | 15 | 8.00 | 0.035 ± 2E-03 | 2.14 ± 4E-02 | 19.8 ± 0.17 | 0.052 | 0.047 | 0.031 | 0.060 |
| | 34.88 | 64.82 | 1401 | 39.332 | 15 | 8.00 | 0.014 ± 1E-03 | 1.75 ± 4E-02 | 49.51 ± 0.43 | 0.052 | 0.047 | 0.031 | 0.060 |
| | 34.92 | 52.07 | 1972 | 39.332 | 15 | 8.00 | 0.021 ± 1E-03 | 1.92 ± 4E-02 | 32.54 ± 0.28 | 0.052 | 0.047 | 0.031 | 0.060 |
| | 34.94 | 65.29 | 456 | 41.535 | 15 | 8.00 | 0.013 ± 9E-04 | 1.71 ± 4E-02 | 52.12 ± 0.45 | 0.052 | 0.047 | 0.031 | 0.060 |
| ISOW | 34.94 | 39 | 1916 | 32 | 15 | 8.00 | 0.031 ± 2E-03 | 2.10 ± 4E-02 | 22.15 ± 0.19 | 0.052 | 0.047 | 0.031 | 0.060 |
| | 34.94 | 34.46 | 2413 | 34.329 | 15 | 8.00 | 0.021 ± 1E-03 | 1.92 ± 4E-02 | 33.32 ± 0.29 | 0.052 | 0.047 | 0.031 | 0.060 |
| DSOW | 34.9 | 40.37 | 3090 | 36.669 | 15 | 8.00 | 0.016 ± 1E-03 | 1.80 ± 4E-02 | 42.79 ± 0.37 | 0.052 | 0.047 | 0.031 | 0.060 |
| | 34.9 | 44.14 | 2986 | 38.666 | 15 | 8.00 | 0.028 ± 2E-03 | 2.05 ± 4E-02 | 25.11 ± 0.22 | 0.052 | 0.047 | 0.031 | 0.060 |
| | 34.9 | 56.77 | 2918 | 39.332 | 15 | 8.00 | 0.133 ± 9E-03 | 2.72 ± 4E-02 | 5.22 ± 0.05 | 0.052 | 0.047 | 0.031 | 0.060 |

*4.3.1.2 Fixed temperature conditions*

Iron(II) oxidation rates are dependent on temperature (Santana-Casiano et al., 2005). Kinetics studies were carried out at a fixed temperature of 15ºC and at the resulting $pH_F$. The *k'* data were plotted in Fig. 4.4B and the corresponding values for *k'*, $t_{1/2}$ and $pH_F$ are shown in Table 4.3.

$pH_F$ values are also temperature dependant, and the effects have to be considered. Deep waters, normally at 1-3ºC, presented the highest changes in pH, while surface waters with initial temperatures of around 13ºC showed the lowest changes. Temperature gradients in surface waters had an important effect on the $pH_F$ values, with T decreasing east to west.

Notable differences in the Fe(II) oxidation rate and $t_{1/2}$ were observed (also at in situ conditions) for surface waters and SPMW (Fig. 4.4B), as these waters had the highest temperature differences within the same water mass. These waters had both the highest $pH_F$ values and $pH_F$ range, from 8.03 to 8.09, with a *k'* value of 0.089 $min^{-1}$ obtained at station 3521. The highest *k'* values were obtained from the Rockall Trough (0.208 $min^{-1}$ at 10 m) to the central branch of the NAC, the Subarctic front in the Iceland basin (0.057 $min^{-1}$ at 26 m). The pseudo-first order kinetics rate values fell below 0.04 $min^{-1}$ as seawater samples approached the Greenland coast. An exception was found over the Greenland plate, at 37 m depth, where a sample with a low $pH_F$ of 7.96 gave a *k'* value of 0.077 $min^{-1}$, the reason behind this phenomenon could be that these waters were polar overflow waters from the Greenland coastal current (Våge et al., 2011).

For intermediate waters, the Fe(II) oxidation rate displayed a much lower variation compared to those at the surface waters, ranging from 0.010 to 0.015 $min^{-1}$ for most of the section (Fig. 4.4B). Some exceptions were observed in the western part of the section, where high $pH_F$ values of 7.93 (compared to 7.88 at a nearby station) were accompanied by high *k'* values in LSW of 0.035 $min^{-1}$ (compared to nearby stations with a relatively constant value of 0.009±0.001 $min^{-1}$). The differences were related to the strong gradient in depth of those water masses between the east and west, which affected the initial temperature of the samples. Deep waters had an initial small T range. After being fixed at 15ºC, the *k'* values changed in a very narrow range (0.012±0.002 $min^{-1}$) (Fig. 4.4B).

A statistical analysis for the 15ºC fixed samples (pH was allowed to vary) was carried out for all three basins and water masses. In this case, the dependence of *k'* was evaluated on $pH_F$, which is the master variable that controls *k'*. $pH_F$ was able to explain 72% of *k'* measured values. When $pH_F$ and salinity were considered, they explained 82% of *k'* and when TOC was also included only 66% of *k'* was explained. Iron(II) oxidation rate increases with higher TOC and pH, but slowed down as S increases. When the physicochemical variables were considered together with the spatial distribution, only 69% of *k'* could be explained. The Fe(II) oxidation rate decreased as depth increased and in an east-to-west direction (Table 4.4).

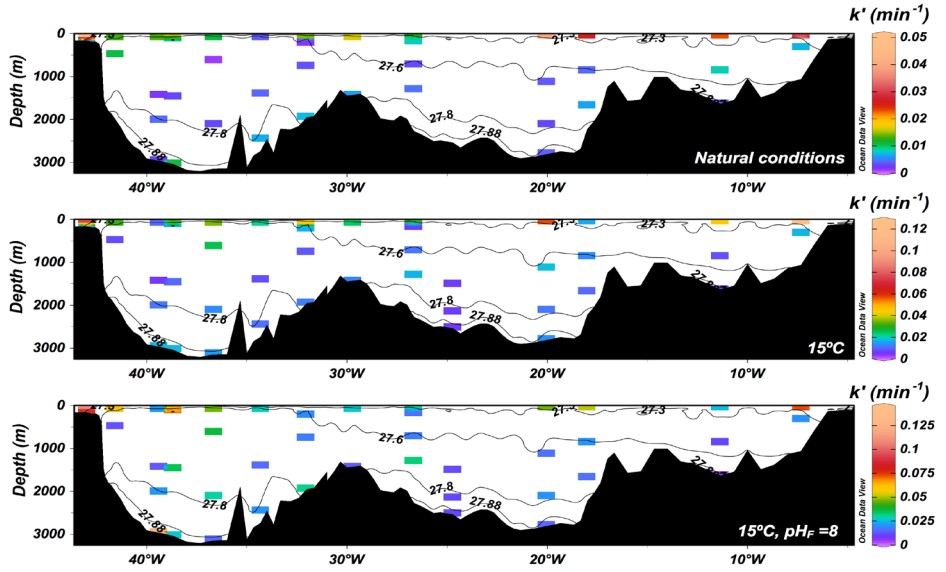


Fig. 4.4A) pseudo-first order constant *k'* ($min^{-1}$) in natural conditions; B) *k'* ($min^{-1}$) at a fixed temperature of 15ºC; and C) *k'* ($min^{-1}$) at a fixed temperature of 15ºC and fixed $pH_F$ of 8.

Table 4.4. Principal Components Analysis

| Conditions | | Components: | | | | |
|---|---|---|---|---|---|---|
| In situ conditions | Component | T | T+pH | T+pH+S | T+pH+S+TOC | T+pH+S+TOC * |
| | Standard deviation | 107.0610 | 107.0610 | 107.0610 | 110.6008 | 107.6954 |
| | Proportion of Variance | 0.9996 | 0.9996 | 0.9996 | 0.9912 | 0.0126 |
| | Cumulative Proportion | 0.749 | 0.752 | 0.899 | 0.749 | 0.740 |
| 15ºC | Component | pH | pH+S | pH+S+TOC | pH+S+TOC * | |
| | Standard deviation | 31.55153 | 31.55153 | 28.42381 | 26.47547 | |
| | Proportion of Variance | 0.99998 | 0.99998 | 0.88420 | 0.00069 | |
| | Cumulative Proportion | 0.717 | 0.815 | 0.662 | 0.687 | |
| 15ºC and $pH_F$=8 | Component | S | S+TOC | S+TOC * | | |
| | Standard deviation | 19.69602 | 10.1525761 | 14.42049 | | |
| | Proportion of Variance | 0.99996 | 0.3050516 | 0.000206506 | | |
| | Cumulative Proportion | 0.622 | 0.753 | 0.749 | | |

* Include the spatial distribution variables: longitude, depth and potential density

*4.3.1.3. Fixed temperature and $pH_F$ conditions*

The Fe(II) oxidation kinetics rate is both temperature and pH dependent (González-Davila et al., 2005; Santana-Casiano et al., 2005). Kinetics studies were performed at a fixed $pH_F$ of 8 and a constant temperature of 15ºC (Fig. 4.4C). Data for *k'* and $t_{1/2}$ are presented in Table 4.3.

Under the fixed T and $pH_F$ conditions, the S and the fraction of the TOC affecting the oxidation rate should account for the observed changes. Surface waters and SPMW presented higher *k'* (Fig. 4.4C) than deeper waters (Fig. 4.5). In surface waters, the *k'* values obtained were higher than 0.07 $min^{-1}$ while values for SPMW were between 0.020 to 0.060 $min^{-1}$. The highest rates in surface waters were accompanied by the highest TOC concentrations (60.08±17.17 μM).

Intermediate waters presented more homogeneous *k'* (with rates lower than 0.030 $min^{-1}$ (Fig. 4.4C)) and $t_{1/2}$ (Fig. 4.5) values. The Irminger basin presented higher *k'* values than the Iceland basin (in the order of 0.01 $min^{-1}$). Similarly, the Irminger basin's rates were 0.02 $min^{-1}$ higher than in the Rockall Trough (Fig. 4.4C). These differences may be due to the S gradient between basins, which decreased in an east-to-west direction (from 35.1 in the Rockall Trough to 34.9 in the Iceland basin and 34.8 in the Irminger basin (Fig. 4.3B)).

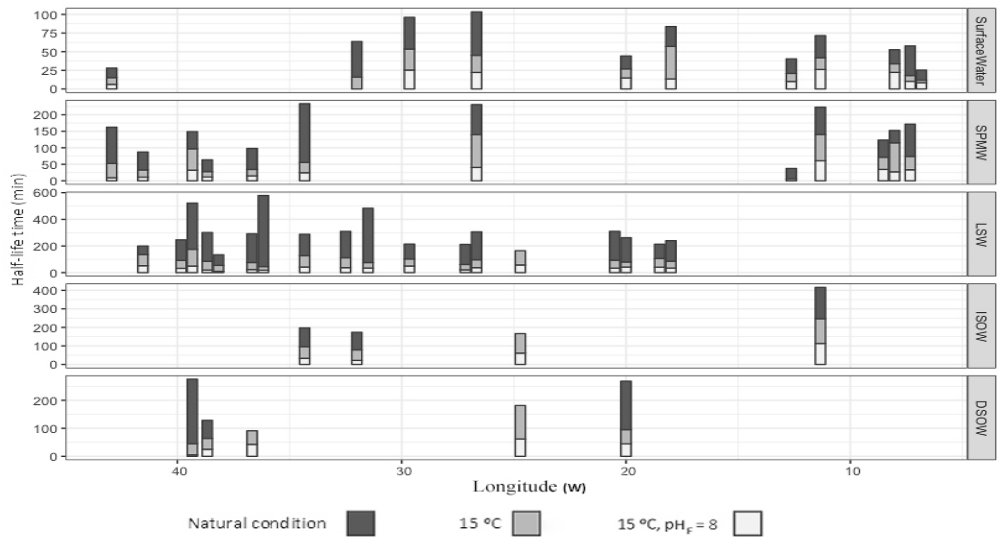


Fig. 4.5) Staked bar chart of half-life time in the study section separated by water mass and the condition studied.

Deep waters showed homogeneous *k'* values lower than 0.028 $min^{-1}$ (Fig. 4.4C). An east-to-west increase in *k'* was observed, with mean values of 0.006 $min^{-1}$ in the Rockall Trough, 0.013 $min^{-1}$ in the Iceland basin and 0.022 $min^{-1}$ in the Irminger basin. This increase could be due to changes in S, in accordance with S decreasing in an east-to-west direction (Fig. 4.3B), but also due to the different water masses present in each basin. A particularly high *k'* value of 0.133 $min^{-1}$ was observed at 2918 m (39.332ºW) in the DSOW in the Irminger basin close to Greenland, where high TOC concentrations were also found (56.77 μM). A linear correlation was observed between *k'* values and TOC in these three samples (+0.007 $min^{-1}$/μM, $r^2$=0.983).

In these studies, the dependence of *k'* on S was evaluated. Salinity explained 62% of *k'*, which increased to 75% when TOC was also considered (Table 4.4). The Fe(II) oxidation rate increased as TOC values rose, but slowed down as salinity increased. An exception was found with a positive *k'*:TOC ratio in the DSOW of +0.0075 $min^{-1}$/μM ($r^2$=0.984, n=4), excluding the sample with 49.54 μM TOC (Table 4.3). The consideration of the spatial distribution did not provide any improvements in the fitting values (75% of *k'* was explained). Iron(II) oxidation rate slowed down with depth and in an west-to east direction.

### *4.3.2. Temperature dependence study*

Temperature was the main controlling factor for the kinetic process. To follow the temperature effect, two water samples from different depths were selected. A bottom seawater sample (3119 m depth) and a surface seawater sample (53 m depth). The bottom seawater sample was collected in the Irminger Basin at 37.991ºW, 59.496ºN in the DSOW water mass with a salinity of 34.896. The surface seawater sample was collected at 32.832ºW, 59.501ºN in the SPMW water mass with a salinity of 34.909. The kinetic studies for each sample were performed at two fixed $pH_F$ values of 7.7 and 8.0, and at temperatures of 2, 5, 7.5, 10, 12.5 and 15ºC (Fig. 4.6).

The results were used to compute the energy of activation (Ea) for the oxidation reaction using the Arrhenius equation (Eqs. 4.5-4.6).

$$k = Ae^{\frac{-Ea}{RT}} \quad (4.5)$$

and: $Lnk = LnA - \frac{Ea}{RT}$ (4.6)

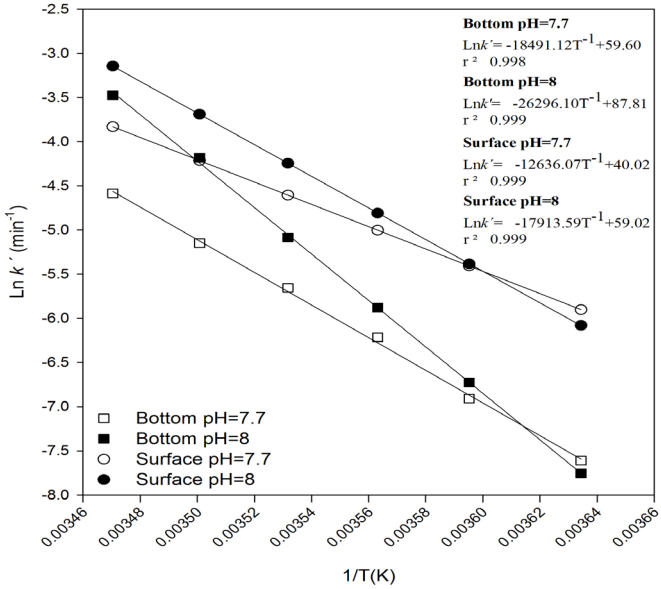


Fig. 4.6) Plot of ln *k'* ($min^{-1}$) and temperature (1/K $T^{-1}$) for the kinetics studies in surface and bottom water at $pH_F$ 7.7 and 8.0.

This study provides new knowledge about whether the oxidation process of Fe(II) in the surface water differs from that for the bottom water. For the bottom seawater sample, the Ea increased from 153.73 kJ $mol^{-1}$ at $pH_F$ 7.7 to 218.62 kJ $mol^{-1}$ at $pH_F$ 8.0. The Ea increased from 105.05 kJ $mol^{-1}$ at $pH_F$ 7.7 to 149.21 kJ $mol^{-1}$ at $pH_F$ 8.0 for the surface sample. These results suggest that the mechanism controlling Fe(II) oxidation in surface seawater involves different chemical species to those in bottom. Iron(II) removal is favoured in the surface water, with an energy requirement that is 32% lower at both pH values than the energy requirement for the bottom water. In the Fe(II) kinetic studies pH 7.7-7.8 is a critical pH range, where an inflection point in the Fe(II) species contribution to the kinetic process has been observed (Santana-Casiano et al., 2006). When pH is lower than 7.7-7.8 the $Fe^{2+}$ species predominate, while when the pH is higher than 7.7-7.8 the $Fe(OH)_2$ is the most important species controlling the Fe(II) oxidation rate (Santana-Casiano et al., 2006). When $pH_F$ was fixed, differences between both samples indicated that organic matter composition also controls the

oxidation mechanism. The most recent and less remineralized organic matter at the surface behaves as the one requiring less energy but, in general, accelerating the process, while the deepest and more remineralized organic ligands (both more refractory and single ligands) decreased the oxidation rate but demand more energetic requirements.

### *4.3.3. Empirical equation*

The Fe(II) oxidation kinetics studies conducted under natural conditions enabled the generation of an empirical equation (Eq. 4.7) for the estimation of *k'* as a function of T (ºC), $pH_F$ and S for the Northern North Atlantic seawater, with $r^2$=0.79 ($p<0.0001$) and a standard error of estimate of 0.0072 $min^{-1}$. TOC was not considered in this fitting procedure because it can both increase and decrease the oxidation rate. Values of *k'* measured and calculated from the empirical equation are represented in Fig. 4.7.

$$k^{'}\ (min^{-1}) = 0.6930 - 0.0004T + 0.0003T^2 + 0.0389pH_F - 0.0287Sal \qquad (4.7)$$

Eq. 4.7 offers a fast method to obtain the Fe(II) oxidation rate in the Northern North Atlantic inside any water mass from surface to deep waters. More studies are planned to validate the equation in other regions and seasons.

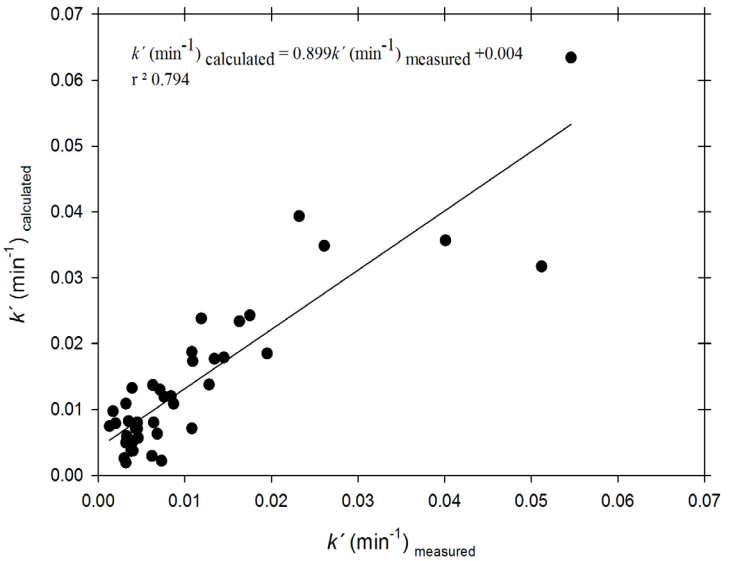


Fig. 4.7) Plot of *k'* ($min^{-1}$) measured in natural conditions and *k'* ($min^{-1}$) calculated for the empirical equation.

### *4.4. Discussion*

Current oceanic Fe biogeochemical cycles are still lacking in Fe(II) oxidation kinetic relationships and equations. Using the Fe(II) oxidation kinetics rate constant, *k'*, it was possible to determine the $t_{1/2}$ for Fe(II) in different water masses in the Subarctic North Atlantic. For this area, *k'* was evaluated for the main variables that control the Fe(II) oxidation rate: T, $pH_F$ and S. The organic matter effect (measured as TOC) on the oxidation rate of Fe(II) was also considered. The TdFe(II) samples were unfiltered and acidified to pH 6. As such, the concentrations observed in this study seem high in comparison to filtered samples obtained in the Atlantic Ocean (< 0.2 nM) (Sedwick et al., 2015).

Temperature was the master variable controlling 75% of the Fe(II) oxidation kinetics. At a fixed T, pH controlled 72% of the Fe(II) oxidation kinetics. In all cases, the principal component statistical analysis indicated that *k'* increased as T and $pH_F$ increased, but decreased with S, as it has been reported in previous laboratory studies (Millero and Izaguirre, 1989; Millero et al., 1987; Santana-Casiano et al., 2005).

Organic matter played an important role in controlling the Fe(II) oxidation, as reported by Lee et al. (2016) and Craig et al. (2009). However, when correlation analyses were performed in this study, both positive and negative effects on the rate constant were observed. This behaviour clearly indicates that organic matter characteristics could be an important factor influencing the oxidation of Fe(II). The kinetics studies were carried out in the dark to avoid photo-reduction processes and under oxygen saturated conditions. However, Fe(III) reduction could have also occur in some cases due to organic matter presence in the sample. Even if all these processes took place in the solution, a pseudo-first order oxidation dependence was always followed, at least until $t_{1/2}$. This indicates that the dissolved organic carbon (DOC) ligands, which affect the oxidation kinetics as shown in the T dependence studies, are controlled by the oxygen in the solution. Evidence shows that the measured effects are caused by ligands that can accelerate or slow down Fe(II) oxidation kinetics. The lack of effects in the Fe(II) oxidation kinetics could be due to a balance of the acceleration and slow down caused by ligands or due to difficulties in the measurement under the oxygen control conditions.

The study area in the Subarctic North Atlantic included coastal and surface and bottom oceanic waters. Different mixes of marine and terrestrial origin organic

matter were present in these waters. Moreover, water masses at different depths with differences in ventilation/remineralization affecting the organic matter composition, even with the same TOC content, were considered. The differences between the various effects could explain why the Fe(II) oxidation rate is sometimes accelerated or slowed down by TOC and why TOC cannot be included in the Eq. (4.7). As a general trend in the Subarctic North Atlantic area, TOC accelerated *k'*. However, some exceptions were found where TOC slowed down *k'*, indicating a different effect of TOC on the Fe(II) oxidation kinetics rate. The pseudo-first order kinetics rate was strongly affected in surface waters and in waters below the mixed layer when the same T and $pH_F$ were considered along with only small changes in S. In the SPMW and DSOW of the Iceland and Irminger basins and also in the LSW of the Irminger basin TOC slowed down *k'*. High fluvial fluxes of terrigenous organic matter combined with a highly stratified surface layer produce a DOC-enriched surface Arctic Ocean (Dittmar and Kattner, 2003). The stratification favours the slow accumulation of organic matter resistant to biological degradation (Bhatia et al., 2013; Hansell et al., 2009). These surface waters accumulate a more biologically resistant fraction of TOC (Hansell and Carlson, 1998), which remains as biologically semi-labile DOC (Carlson, 2002; Hansell, 2002).

The highest variations in *k'* values were observed in surface samples. Roy and Wells (2011) reported similar results. They observed a faster Fe(II) oxidation rate within the chlorophyll maximum and in surface seawater, where strong Fe(III)-complexing organic ligands were more abundant than in deep waters. They concluded that differences in the chemical nature and origin of natural Fe(III)- and Fe(II)-complexing organic ligands between surface and deep waters could explain their findings. This same process could affect the oxidation kinetics of Fe(II) in surface waters. The organic matter located in the surface and bottom seawater does not have the same degree of remineralization. In deep waters the organic matter is more degraded and therefore the type of ligands is different which could affect the oxidation rate in a different way.

Spatial distribution affects *k'* due to the chemical characteristics of each water mass. This is further influenced by water mass changes along the transect. Seawater transformation that takes place along the path of the North Atlantic Current (NAC) (Brambilla and Talley, 2008) makes the Iceland basin warmer and saltier than the Irminger basin. Importantly, the mixing of SPMW, which flows around the Reykjanes Ridge, in conjunction with air-sea heat loss, results in a colder and fresher SPMW layer in the Irminger basin (García-Ibáñez et al., 2016). In addition, the LSW layer changes its properties due to mixing with the surrounding waters during its journey from the formation regions (Bersch et al., 1999; García-Ibáñez, 2015; Pickart et al., 2003). The ISOW layer comes from the Iceland-Scotland sill and flows southwards into the Iceland

basin, where it mixes with the older North Atlantic Deep Water (NADW). It then crosses the Reykjanes Ridge through the Charlie-Gibbs Fracture Zone where it mixes with the LSW and DSOW, becoming fresher. At the bottom of the Irminger basin, the DSOW becomes the coldest, densest and freshest layer of the section (García-Ibáñez et al., 2016). Samples in this study close to the Scotland plate and also in the Greenland plate present faster Fe(II) oxidation rates than in the open ocean. The rate of oxidation was affected by water mass characteristics, with different trend behaviour when the samples were located in the limit zones between water masses or had Mid-Atlantic Ridge influences. Even considering these differences in the physical properties, the empirical equation (4.7) was able to fix the observed values to an extent of the 79% with a standard error of estimate of 0.0072 $min^{-1}$.

The interaction of Fe(II) with organic matter of both different origin and chemical characteristics produces a variety of interactions between Fe(II) with the multiple organic ligands present in the solution that generate different Fe(II)-L and Fe(III)-L species. This is in accordance with the observations made in a study of the complexation and redox buffering of Fe(II) by DOM (Daugherty et al., 2017). The Ea is an indicator of the mechanism that controls Fe(II) oxidation in seawater and signals the minimum energy required to carry out the chemical oxidation process (Arrhenius, 1889). For the Subarctic North Atlantic, surface samples presented lower Ea than bottom waters at both pH 7.7 and 8.0. The results show that different species must be involved in the two cases, with the surface waters having a 32% lower Ea requirement for Fe(II) oxidation than the bottom waters. The organic matter in the surface water is fresher and less remineralized than the one located deeper, and the interaction with both Fe(II) and Fe(III) could act on the oxidation mechanism accounting for the observed changes. Moreover, the differences in pH in the two studies also affect organic speciation and also the species complexation (Santana-Casiano et al., 2006). More studies are being carried out in this and other oceanic regions, including coastal, upwelling and temperate oceans in order to accounting for the different processes and to obtain a more general equation valid under all conditions.

### *4.5. Conclusions*

The Fe(II) oxidation kinetics studies carried out in 2016 in the Subarctic North Atlantic along the 59.5ºN section in the Rockall Trough and the Iceland and Irminger Basins show that T, pH and S were the master variables controlling the Fe(II) oxidation kinetics under natural conditions. The sources and characteristics of the organic matter present were important factors influencing the oxidation of Fe(II), displaying both

positive and negative effects on the Fe(II) oxidation rate. Spatial distribution affected *k'* due to the chemical characteristics of each water mass and their modification as the water mass moved from basin to basin and from the surface to the deep ocean. Surface waters required lower energy for Fe(II) oxidation than bottom waters indicating that the species involved in the Fe(II) oxidation kinetic must be different. In this work, a general equation was obtained which allows computation of *k'* taking into account the effect of T, pH and S under natural conditions. It is valid for the Subarctic North Atlantic, and can be incorporated into global Fe models. TOC cannot be used as a key variable in natural environment oxidation studies due to its heterogenity and the lack of specificity in the composition of the organic matter of this non-distinctive variable.

**Acknowledgements**

This work was supported by the Ministerio de Economía y Competitividad of the Spanish Government, through the EACFe (CTM2014-52342-P) project. CS-G was funded by the Spanish Grant BES-2015-071245. This work was completed while CS-G was a PhD student in the IOCAG Doctoral Program in Oceanography and Global Change. Special thanks go to David González-Santana for his comments and english revision, to Coraima Santana González for editing the figures and to the crew and captain of Akademik Ioffe. SG and AS were supported by RFBR grant No. 15-05-02250 and by RSF grant No. 14-17-00697.

## *References*

Arístegui, J.D., Carlos M.; Reche, Isabel; Gómez-Pinchetti, Juan L., 2014. Krill Excretion Boosts Microbial Activity in the Southern Ocean. PLOS ONE, 9(2).

Arrhenius, S., 1889. Über die Dissociationswärme und den Einfluss der Temperatur auf den Dissociationsgrad der Elektrolyte. Zeitschrift für physikalische Chemie, 4(1): 96-116.

Benson, B.B. and Krause, D., 1984. The concentration and isotopic fractionation of oxygen dissolved in freshwater and seawater in equilibrium with the atmosphere. Limnology and oceanography, 29(3): 620-632.

Bergquist, B. and Boyle, E., 2006. Dissolved iron in the tropical and subtropical Atlantic Ocean. Global Biogeochemical Cycles, 20(1).

Bergquist, B., Wu, J. and Boyle, E., 2007. Variability in oceanic dissolved iron is dominated by the colloidal fraction. Geochimica et Cosmochimica Acta, 71(12): 2960-2974.

Bersch, M., Meincke, J. and Sy, A., 1999. Interannual thermohaline changes in the northern North Atlantic 1991–1996. Deep Sea Research Part II: Topical Studies in Oceanography, 46(1): 55-75.

Bhatia, M.P. et al., 2013. Greenland meltwater as a significant and potentially bioavailable source of iron to the ocean. Nature Geoscience, 6(4): 274-278.

Boiteau, R.M. et al., 2016. Siderophore-based microbial adaptations to iron scarcity across the eastern Pacific Ocean. Proceedings of the National Academy of Sciences, 113(50): 14237-14242.

Bowie, A.R. et al., 2003. Shipboard analytical intercomparison of dissolved iron in surface waters along a north–south transect of the Atlantic Ocean. Marine Chemistry, 84(1): 19-34.

Bowie, A.R. et al., 2006. A community-wide intercomparison exercise for the determination of dissolved iron in seawater. Marine Chemistry, 98(1): 81-99.

Bowie, A.R., Achterberg, E.P., Mantoura, R.F.C. and Worsfold, P.J., 1998. Determination of sub-nanomolar levels of iron in seawater using flow injection with chemiluminescence detection. Analytica Chimica Acta, 361(3): 189-200.

Bowie, A.R., Sedwick, P.N. and Worsfold, P.J., 2004. Analytical intercomparison between flow injection-chemiluminescence and flow injection-spectrophotometry for the determination of picomolar concentrations of iron in seawater. Limnology and Oceanography: methods, 2(2): 42-54.

Bowie, A.R., Whitworth, D.J., Achterberg, E.P., Mantoura, R.F.C. and Worsfold, P.J., 2002. Biogeochemistry of Fe and other trace elements (Al, Co, Ni) in the upper Atlantic Ocean. Deep Sea Research Part I: Oceanographic Research Papers, 49(4): 605-636.

Boye, M. et al., 2006. The chemical speciation of iron in the north-east Atlantic Ocean. Deep Sea Research Part I: Oceanographic Research Papers, 53(4): 667-683.

Brambilla, E. and Talley, L.D., 2008. Subpolar Mode Water in the northeastern Atlantic: 1. Averaged properties and mean circulation. Journal of Geophysical Research: Oceans, 113(C4).

Bucciarelli, E., Blain, S. and Tréguer, P., 2001. Iron and manganese in the wake of the Kerguelen Islands (Southern Ocean). Marine Chemistry, 73(1): 21-36.

Buck, K.N., Gerringa, L.J.A. and Rijkenberg, M.J.A., 2016. An Intercomparison of Dissolved Iron Speciation at the Bermuda Atlantic Time-series Study (BATS) Site: Results from GEOTRACES Crossover Station A. Frontiers in Marine Science, 3(262).

Campbell, J. and Yeats, P., 1982. The distribution of manganese, iron, nickel, copper and cadmium in the waters of Baffin-Bay and the Canadian arctic archipelago. Oceanologica Acta, 5(2): 161-168.

Carlson, C.A., 2002. Production and removal processes. Biogeochemistry of marine dissolved organic matter: 91-151.

Chase, Z. et al., 2005. Manganese and iron distributions off central California influenced by upwelling and shelf width. Marine Chemistry, 95(3): 235-254.

Chever, F. et al., 2010. Physical speciation of iron in the Atlantic sector of the Southern Ocean along a transect from the subtropical domain to the Weddell Sea Gyre. Journal of Geophysical Research: Oceans, 115(C10).

Coale, K.H., 1991. Effects of iron, manganese, copper, and zinc enrichments on productivity and biomass in the subarctic Pacific. Limnology and Oceanography, 36(8): 1851-1864.

Craig, P.S., Shaw, T.J., Miller, P.L., Pellechia, P.J. and Ferry, J.L., 2009. Use of Multiparametric Techniques To Quantify the Effects of Naturally Occurring Ligands on the Kinetics of Fe(II) Oxidation. Environmental Science & Technology, 43(2): 337-342.

Crusius, J., Schroth, A.W., Resing, J.A., Cullen, J. and Campbell, R.W., 2017. Seasonal and spatial variability in northern Gulf of Alaska surface-water iron concentrations driven by shelf sediment resuspension, glacial meltwater, a Yakutat eddy, and dust. Global Biogeochemical Cycles: n/a-n/a.

Cullen, J.T., Bergquist, B.A. and Moffett, J.W., 2006. Thermodynamic characterization of the partitioning of iron between soluble and colloidal species in the Atlantic Ocean. Marine Chemistry, 98(2): 295-303.

Daugherty, E.E., Gilbert, B., Nico, P.S. and Borch, T., 2017. Complexation and Redox Buffering of Iron(II) by Dissolved Organic Matter. Environmental Science & Technology, 51(19): 11096-11104.

De Jong, J. et al., 1998. Dissolved iron at subnanomolar levels in the Southern Ocean as determined by ship-board analysis. Analytica Chimica Acta, 377(2): 113-124.

Dittmar, T. and Kattner, G., 2003. The biogeochemistry of the river and shelf ecosystem of the Arctic Ocean: a review. Marine Chemistry, 83(3): 103-120.

Emmenegger, L., King, D.W., Sigg, L. and Sulzberger, B., 1998. Oxidation kinetics of Fe(II) in a eutrophic Swiss lake. Environmental science & technology, 32(19): 2990-2996.

Fitzsimmons, J.N. and Boyle, E.A., 2014. Both soluble and colloidal iron phases control dissolved iron variability in the tropical North Atlantic Ocean. Geochimica et Cosmochimica Acta, 125: 539-550.

Fitzsimmons, J.N., Zhang, R. and Boyle, E.A., 2013. Dissolved iron in the tropical North Atlantic Ocean. Marine Chemistry, 154: 87-99.

García-Ibáñez, M.I., 2015. Acidification and transports of water masses and $CO_2$ in the North Atlantic.

García-Ibáñez, M.I., Carracedo, L.I., Ríos, A.F. and Pérez, F.F., 2016. Ocean acidification in the subpolar North Atlantic: rates and mechanisms controlling pH changes. Biogeosciences, 13(12): 3701.

Gladyshev, S., Gladyshev, V., Gulev, S. and Sokov, A., 2017. Subpolar mode water classes in the northeast Atlantic: Interannual and long-term variability, Doklady Earth Sciences. Springer, pp. 1203-1206.

González, A.G. et al., 2014. Iron adsorption onto soil and aquatic bacteria: XAS structural study. Chemical Geology, 372: 32-45.

González-Davila, M., Santana-Casiano, J.M. and Millero, F.J., 2005. Oxidation of iron(II) nanomolar with $H_2O_2$ in seawater. Geochimica et Cosmochimica Acta, 69(1): 83-93.

González-Dávila, M., Santana-Casiano, J.M. and Millero, F.J., 2006. Competition between $O_2$ and $H_2O_2$ in the oxidation of Fe(II) in natural waters. Journal of solution chemistry, 35(1): 95-111.

Hansell, D., 2002. DOC in the global ocean carbon cycle. Biogeochemistry of marine dissolved organic matter: 685-715.

Hansell, D.A. and Carlson, C.A., 1998. Net community production of dissolved organic carbon. Global Biogeochemical Cycles, 12(3): 443-453.

Hansell, D.A., Carlson, C.A., Repeta, D.J. and Schlitzer, R., 2009. Dissolved organic matter in the ocean: A controversy stimulates new insights.

Hansell, D.A., Carlson, Craig A., 2001. Biogeochemistry of total organic carbon and nitrogen in the Sargasso Sea: control by convective overturn. Deep Sea Research Part II: Topical Studies in Oceanography, 48(8-9): 18.

Hastie, T.J. and Tibshirani, R.J., 1990. Generalized additive models, volume 43 of Monographs on Statistics and Applied Probability. Chapman & Hall, London.

Hay, M.B. and Myneni, S.C.B., 2007. Structural environments of carboxyl groups in natural organic molecules from terrestrial systems. Part 1: Infrared spectroscopy. Geochimica et Cosmochimica Acta, 71(14): 3518-3532.

Heller, M.I., Gaiero, D.M. and Croot, P.L., 2013. Basin scale survey of marine humic fluorescence in the Atlantic: Relationship to iron solubility and $H_2O_2$. Global Biogeochemical Cycles, 27(1): 88-100.

Heller, M.I., Wuttig, K. and Croot, P.L., 2016. Identifying the sources and sinks of CDOM/FDOM across the Mauritanian Shelf and their potential role in the decomposition of superoxide($O_2^-$). Frontiers in Marine Science, 3: 132.

Hong, H. and Kester, D.R., 1986. Redox state of iron in the offshore waters of Peru. Limnology and Oceanography, 31(3): 612-626.

King, D. and Farlow, R., 2000. Role of carbonate speciation on the oxidation of Fe(II) by $H_2O_2$. Marine Chemistry, 70(1): 201-209.

King, D.W., Lounsbury, H.A. and Millero, F.J., 1995. Rates and mechanism of Fe(II) oxidation at

nanomolar total iron concentrations. Environmental science & technology, 29(3): 818-824.

Klunder, M., Laan, P., Middag, R., De Baar, H. and Van Ooijen, J., 2011. Dissolved iron in the Southern Ocean (Atlantic sector). Deep Sea Research Part II: Topical Studies in Oceanography, 58(25): 2678-2694.

Klunder, M.B. et al., 2012. Dissolved iron in the Arctic shelf seas and surface waters of the central Arctic Ocean: Impact of Arctic river water and ice-melt. Journal of Geophysical Research: Oceans, 117(C1).

Kuma, K., Nakabayashi, S. and Matsunaga, K., 1995. Photoreduction of Fe(III) by hydroxycarboxylic acids in seawater. Water Research, 29(6): 1559-1569.

Kustka, A.B., Shaked, Y., Milligan, A.J., King, D.W. and Morel, F.M., 2005. Extracellular production of superoxide by marine diatoms: Contrasting effects on iron redox chemistry and bioavailability. Limnology and Oceanography, 50(4): 1172-1180.

Laës, A. et al., 2005. Impact of environmental factors on in situ determination of iron in seawater by flow injection analysis. Marine Chemistry, 97(3): 347-356.

Lee, Y.P. et al., 2017. Importance of allochthonous and autochthonous dissolved organic matter in Fe(II) oxidation: A case study in Shizugawa Bay watershed, Japan. Chemosphere.

Lee, Y.P., Fujii, M., Terao, K., Kikuchi, T. and Yoshimura, C., 2016. Effect of dissolved organic matter on Fe(II) oxidation in natural and engineered waters. Water Research, 103: 160-169.

Leenheer, J.A., Brown, G.K., MacCarthy, P. and Cabaniss, S.E., 1998. Models of Metal Binding Structures in Fulvic Acid from the Suwannee River, Georgia. Environmental Science & Technology, 32(16): 2410-2416.

Mackey, D., O'Sullivan, J.O. and Watson, R., 2002. Iron in the western Pacific: a riverine or hydrothermal source for iron in the Equatorial Undercurrent? Deep Sea Research Part I: Oceanographic Research Papers, 49(5): 877-893.

Manceau, A. and Matynia, A., 2010. The nature of Cu bonding to natural organic matter. Geochimica et Cosmochimica Acta, 74(9): 2556-2580.

Measures, C. and Vink, S., 1999. Seasonal variations in the distribution of Fe and Al in the surface waters of the Arabian Sea. Deep Sea Research Part II: Topical Studies in Oceanography, 46(8): 1597-1622.

Miller, W.L., King, D.W., Lin, J. and Kester, D.R., 1995. Photochemical redox cycling of iron in coastal seawater. Marine Chemistry, 50(1): 63-77.

Millero, F.J. and Izaguirre, M., 1989. Effect of ionic strength and ionic interactions on the oxidation of Fe(II). Journal of Solution Chemistry, 18(6): 585-599.

Millero, F.J., Sotolongo, S. and Izaguirre, M., 1987. The oxidation kinetics of Fe(II) in seawater. Geochimica et Cosmochimica Acta, 51(4): 793-801.

Mills, M.M., Ridame, C., Davey, M., La Roche, J. and Geider, R.J., 2004. Iron and phosphorus co-limit nitrogen fixation in the eastern tropical North Atlantic. Nature, 429(6989): 292-294.

Mohamed, K.N., Steigenberger, S., Nielsdottir, M.C., Gledhill, M. and Achterberg, E.P., 2011. Dissolved iron(III) speciation in the high latitude North Atlantic Ocean. Deep Sea Research Part I: Oceanographic Research Papers, 58(11): 1049-1059.

Morel, F.M., Kustka, A. and Shaked, Y., 2008. The role of unchelated Fe in the iron nutrition of phytoplankton. Limnology and Oceanography, 53(1): 400-404.

Nishioka, J., Obata, H. and Tsumune, D., 2013. Evidence of an extensive spread of hydrothermal dissolved iron in the Indian Ocean. Earth and Planetary Science Letters, 361: 26-33.

Nishioka, J., Takeda, S., Wong, C. and Johnson, W., 2001. Size-fractionated iron concentrations in the northeast Pacific Ocean: distribution of soluble and small colloidal iron. Marine Chemistry, 74(2): 157-179.

Pham, A.N. and Waite, T.D., 2008. Oxygenation of Fe(II) in natural waters revisited: Kinetic modeling approaches, rate constant estimation and the importance of various reaction pathways. Geochimica et Cosmochimica Acta, 72(15): 3616-3630.

Pickart, R.S., Spall, M.A., Ribergaard, M.H., Moore, G.W.K. and Milliff, R.F., 2003. Deep convection in the Irminger Sea forced by the Greenland tip jet. Nature, 424(6945): 152-156.

Powell, R.T., King, D.W. and Landing, W.M., 1995. Iron distributions in surface waters of the south Atlantic. Marine Chemistry, 50(1): 13-20.

Resing, J.A. et al., 2015. Basin-scale transport of hydrothermal dissolved metals across the South Pacific Ocean. Nature, 523(7559): 200-203.

Rose, A.L. and Waite, T.D., 2002. Kinetic Model for Fe(II) Oxidation in Seawater in the Absence and Presence of Natural Organic Matter. Environmental Science & Technology, 36(3): 433-444.

Rose, A.L. and Waite, T.D., 2003. Kinetics of iron complexation by dissolved natural organic matter in coastal waters. Marine Chemistry, 84(1–2): 85-103.

Roy, E.G. and Wells, M.L., 2011. Evidence for regulation of Fe(II) oxidation by organic complexing ligands in the Eastern Subarctic Pacific. Marine Chemistry, 127(1): 115-122.

Roy, E.G., Wells, M.L. and King, D.W., 2008. Persistence of iron(II) in surface waters of the western subarctic Pacific. Limnology and Oceanography, 53(1): 89-98.

Saito, M.A. et al., 2013. Slow-spreading submarine ridges in the South Atlantic as a significant oceanic iron source. Nature Geoscience, 6(9): 775-779.

Santana-Casiano, J. et al., 2014. Characterization of phenolic exudates from Phaeodactylum tricornutum and their effects on the chemistry of Fe(II)–Fe(III). Marine chemistry, 158: 10-16.

Santana-Casiano, J., Gonzalez-Davila, M. and Millero, F., 2006. The role of Fe(II) species on the oxidation of Fe(II) in natural waters in the presence of $O_2$ and $H_2O_2$. Marine chemistry, 99(1): 70-82.

Santana-Casiano, J.M., González-Dávila, M., González, A. and Millero, F., 2010. Fe(III) reduction in the presence of catechol in seawater. Aquatic geochemistry, 16(3): 467-482.

Santana-Casiano, J.M., González-Dávila, M. and Millero, F.J., 2004. The oxidation of Fe(II) in NaCl–$HCO_3^-$ and seawater solutions in the presence of phthalate and salicylate ions: a kinetic model. Marine chemistry, 85(1): 27-40.

Santana-Casiano, J.M., González-Dávila, M. and Millero, F.J., 2005. Oxidation of nanomolar levels of Fe(II) with oxygen in natural waters. Environmental science & technology, 39(7): 2073-2079.

Santana-Casiano, J.M., González-Dávila, M., Rodrıguez, M.J. and Millero, F.J., 2000. The effect of organic compounds in the oxidation kinetics of Fe(II). Marine Chemistry, 70(1): 211-222.

Sarafanov, A., Falina, A., Mercier, H., Lherminier, P. and Sokov, A., 2009. Recent changes in the Greenland–Scotland overflow-derived water transport inferred from hydrographic observations in the southern Irminger Sea. Geophysical Research Letters, 36(13).

Sarthou, G. and Jeandel, C., 2001. Seasonal variations of iron concentrations in the Ligurian Sea and iron budget in the Western Mediterranean Sea. Marine Chemistry, 74(2): 115-129.

Schmidt, M.A. and Hutchins, D.A., 1999. Size-fractionated biological iron and carbon uptake along a coastal to offshore transect in the NE Pacific. Deep Sea Research Part II: Topical Studies in Oceanography, 46(11–12): 2487-2503.

Shaked, Y., Kustka, A.B. and Morel, F.M., 2005. A general kinetic model for iron acquisition by eukaryotic phytoplankton. Limnol. Oceanogr, 50(3): 872-882.

Shaked, Y. and Lis, H., 2012. Disassembling Iron Availability to Phytoplankton. Frontiers in Microbiology, 3: 123.

Shi, D.K., Sven A.; Kim, Ja-Myung; Morel, François M. M., 2012 Ocean acidification slows nitrogen fixation and growth in the dominant diazotroph Trichodesmium under low-iron conditions. Proceedings of the National Academy of Sciences 109 (45): 6.

Statham, P., German, C. and Connelly, D., 2005. Iron(II) distribution and oxidation kinetics in hydrothermal plumes at the Kairei and Edmond vent sites, Indian Ocean. Earth and Planetary Science Letters, 236(3): 588-596.

Steigenberger, S. and Croot, P.L., 2008. Identifying the processes controlling the distribution of $H_2O_2$ in surface waters along a meridional transect in the eastern Atlantic. Geophysical Research

Letters, 35(3).

Tagliabue, A., Aumont, O. and Bopp, L., 2014. The impact of different external sources of iron on the global carbon cycle. Geophysical Research Letters, 41(3): 920-926.

Tagliabue, A. et al., 2010. Hydrothermal contribution to the oceanic dissolved iron inventory. Nature Geoscience, 3(4): 252-256.

Tagliabue, A. et al., 2017. The integral role of iron in ocean biogeochemistry. Nature, 543(7643): 51-59.

Tagliabue, A. et al., 2012. A global compilation of dissolved iron measurements: focus on distributions and processes in the Southern Ocean. Biogeosciences, 9(6): 2333-2349.

Team, R.C., 2016. R: A language and envirnment for statistical computing. R Foundation for Statistical Computing, Viena, Austria.

Theis, T.L. and Singer, P.C., 1974. Complexation of iron(II) by organic matter and its effect on iron(II) oxygenation. Environmental Science and Technology, 8(6): 569-573.

Thuróczy, C.E. et al., 2011. Distinct trends in the speciation of iron between the shallow shelf seas and the deep basins of the Arctic Ocean. Journal of Geophysical Research: Oceans, 116(C10).

Trapp, J.M. and Millero, F.J., 2007. The oxidation of iron(II) with oxygen in NaCl brines. Journal of Solution Chemistry, 36(11-12): 1479-1493.

Ussher, S.J. et al., 2010. Distribution of size fractionated dissolved iron in the Canary Basin. Marine environmental research, 70(1): 46-55.

Våge, K. et al., 2011. The Irminger Gyre: Circulation, convection, and interannual variability. Deep Sea Research Part I: Oceanographic Research Papers, 58(5): 590-614.

Voelker, B.M. and Sedlak, D.L., 1995. Iron reduction by photoproduced superoxide in seawater. Marine Chemistry, 50(1): 93-102.

Wehrmann, L.M. et al., 2014. Iron and manganese speciation and cycling in glacially influenced high-latitude fjord sediments (West Spitsbergen, Svalbard): Evidence for a benthic recycling-transport mechanism. Geochimica et Cosmochimica Acta, 141: 628-655.

Wu, J., Boyle, E., Sunda, W. and Wen, L.-S., 2001. Soluble and colloidal iron in the oligotrophic North Atlantic and North Pacific. Science, 293(5531): 847-849.

Wu, J., Wells, M.L. and Rember, R., 2011. Dissolved iron anomaly in the deep tropical–subtropical Pacific: Evidence for long-range transport of hydrothermal iron. Geochimica et Cosmochimica Acta, 75(2): 460-468.

# MARINE CHEMISTRY

**ISSN: 0304-4203**

ELSEVIER SCIENCE BV
PO BOX 211,1000 AE AMSTERDAM,NETHERLANDS
**NETHERLANDS**

Go to Journal Table of Contents  Go to Ulrich's

**Titles**
ISO: Mar. Chem.
JCR Abbrev: MAR CHEM

**Categories**
CHEMISTRY, MULTIDISCIPLINARY - SCIE;
OCEANOGRAPHY - SCIE;

**Languages**
Multi-Language

10 Issues/Year;

## Key Indicators

| Year | Total Cites Graph | Journal Impact Factor Graph | Impact Factor Without Journal Self Cites Graph | 5 Year Impact Factor Graph | Immediacy Index Graph | Citable Items Graph | Cited Half-Life Graph | Citing Half-Life Graph | Eigenfacto Score Graph | Article Influence Score Graph | % Articles in Citable Items Graph | Normalizec Eigenfacto Graph | Average JIF Percentile Graph |
|---|---|---|---|---|---|---|---|---|---|---|---|---|---|
| 2017 | 9,014 | 3.337 | 3.011 | 3.416 | 0.417 | 84 | >10.0 | >10.0 | 0.00… | 1.167 | 100.00 | 0.92… | 79.087 |
| 2016 | 8,308 | 2.457 | 2.329 | 2.912 | 0.425 | 73 | >10.0 | >10.0 | 0.00… | 1.011 | 100.00 | 0.84… | 67.860 |
| 2015 | 9,112 | 3.412 | 2.675 | 3.853 | 1.093 | 182 | >10.0 | >10.0 | 0.00… | 1.182 | 98.90 | 0.84… | 81.022 |
| 2014 | 8,354 | 2.735 | 2.470 | 3.636 | 0.588 | 85 | >10.0 | >10.0 | 0.00… | 1.296 | 98.82 | 0.93… | 77.905 |
| 2013 | 8,111 | 3.200 | 2.841 | 3.850 | 0.619 | 97 | >10.0 | >10.0 | 0.01… | 1.518 | 100.00 | 1.16… | 81.485 |
| 2012 | 6,872 | 3.000 | 2.806 | 3.315 | 0.466 | 58 | >10.0 | >10.0 | 0.01… | 1.370 | 100.00 | Not … | 80.603 |
| 2011 | 6,836 | 3.074 | 2.771 | 3.551 | 0.540 | 87 | >10.0 | >10.0 | 0.01… | 1.434 | 100.00 | Not … | 83.362 |
| 2010 | 6,316 | 2.751 | 2.470 | 3.276 | 0.809 | 89 | >10.0 | 10.0 | 0.01… | 1.225 | 97.75 | Not … | 82.584 |
| 2009 | 6,299 | 2.726 | 2.474 | 3.503 | 0.397 | 73 | 10.0 | >10.0 | 0.01… | 1.267 | 98.63 | Not … | 83.304 |
| 2008 | 5,830 | 2.977 | 2.588 | 3.554 | 0.795 | 112 | 9.3 | 9.9 | 0.01… | 1.361 | 97.32 | Not … | 84.280 |
| 2007 | 5,919 | 3.085 | 2.685 | 3.789 | 0.565 | 147 | 9.6 | 9.7 | 0.01… | 1.435 | 99.32 | Not … | 87.711 |
| 2006 | 4,956 | 2.663 | 2.322 | Not … | 0.958 | 118 | 9.5 | >10.0 | Not … | Not … | 98.31 | Not … | 84.627 |
| 2005 | 4,375 | 2.103 | 1.943 | Not … | 0.476 | 82 | 9.1 | 9.7 | Not … | Not … | 93.90 | Not … | 82.448 |
| 2004 | 4,178 | 2.508 | 1.960 | Not … | 0.413 | 126 | 8.7 | 8.6 | Not … | Not … | 98.41 | Not … | 86.732 |
| 2003 | 4,085 | 2.555 | 2.335 | Not … | 0.290 | 69 | 8.5 | 8.4 | Not … | Not … | 100.00 | Not … | 86.992 |
| 2002 | 3,665 | 2.179 | 1.983 | Not … | 0.407 | 59 | 8.3 | 9.7 | Not … | Not … | 100.00 | Not … | 83.040 |

**Source Data**

- Rank
- Cited Journal Data
- Citing Journal Data
- Box Plot
- Journal Relationships

## Journal Source Data

| | Citable Items | | | Other (O) | Percentage (C/(C + O)) |
|---|---|---|---|---|---|
| | Articles | Reviews | Combined (C) | | |
| **Number in JCR Year 2017…** | 84 | 0 | **84** | 3 | 96% |
| **Number of References (B)** | 5,388 | 0 | 5,388 | 1 | 99% |
| **Ratio (B/A)** | 64.1 | 0.0 | 64.1 | 0.3 | |

*InCites Journal Citation Reports dataset updated Jun 06, 2018*

Tell us what you think.

Help us improve the Journal Citation Reports by providing your feedback! **Click Here >**

## JCR Impact Factor

| JCR Year | CHEMISTRY, MULTIDISCIPLINARY | | | OCEANOGRAPHY | | |
|---|---|---|---|---|---|---|
| | Rank | Quartile | JIF Percentile | Rank | Quartile | JIF Percentile |
| 2017 | 60/171 | Q2 | 65.205 | 5/64 | Q1 | 92.969 |
| 2016 | 69/166 | Q2 | 58.735 | 15/63 | Q1 | 76.984 |
| 2015 | 45/163 | Q2 | 72.699 | 7/61 | Q1 | 89.344 |
| 2014 | 48/157 | Q2 | 69.745 | 9/61 | Q1 | 86.066 |
| 2013 | 39/148 | Q2 | 73.986 | 7/59 | Q1 | 88.983 |
| 2012 | 43/152 | Q2 | 72.039 | 7/60 | Q1 | 89.167 |
| 2011 | 40/154 | Q2 | 74.351 | 5/59 | Q1 | 92.373 |
| 2010 | 38/147 | Q2 | 74.490 | 6/59 | Q1 | 90.678 |
| 2009 | 36/140 | Q2 | 74.643 | 5/56 | Q1 | 91.964 |
| 2008 | 29/127 | Q1 | 77.559 | 5/50 | Q1 | 91.000 |
| 2007 | 23/128 | Q1 | 82.422 | 4/50 | Q1 | 93.000 |
| 2006 | 27/124 | Q1 | 78.629 | 5/48 | Q1 | 90.625 |
| 2005 | 24/125 | Q1 | 81.200 | 8/46 | Q1 | 83.696 |
| 2004 | 23/125 | Q1 | 82.000 | 4/41 | Q1 | 91.463 |
| 2003 | 22/123 | Q1 | 82.520 | 4/41 | Q1 | 91.463 |
| 2002 | 22/119 | Q1 | 81.933 | 7/41 | Q1 | 84.146 |

## ESI Total Citations

| JCR Year | GEOSCIENCES |
|---|---|
| 2017 | 67/416-Q1 |
| 2016 | 65/417-Q1 |
| 2015 | 48/408-Q1 |
| 2014 | 47/393-Q1 |
| 2013 | 40/388-Q1 |

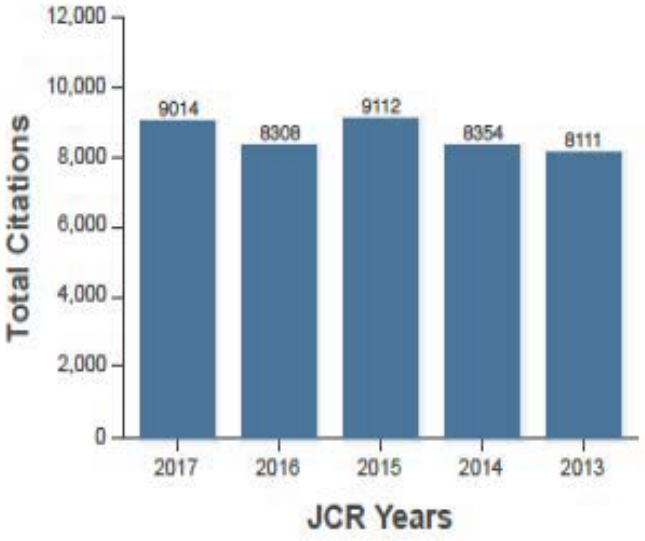

Marine Chemistry 203 (2018) 64–77

Contents lists available at ScienceDirect

Marine Chemistry

journal homepage: www.elsevier.com/locate/marchem

# Fe(II) oxidation kinetics in the North Atlantic along the 59.5° N during 2016

Carolina Santana-González[a], J. Magdalena Santana-Casiano[a,*], Melchor González-Dávila[a], Angelo Santana-del Pino[b], Sergey Gladyshev[c], Alexey Sokov[c]

[a] Instituto de Oceanografía y Cambio Global, IOCAG, Universidad de Las Palmas de Gran Canaria, 35017 Las Palmas de Gran Canaria, Spain
[b] Departamento de Matematicas, Universidad de Las Palmas de Gran Canaria, 35017 Las Palmas de Gran Canaria, Spain
[c] Shirshov Institute of Oceanology, Russian Academy of Science, Russia

ARTICLE INFO

*Keywords:*
Fe(II)
Oxidation
Atlantic subarctic

ABSTRACT

The Fe(II) oxidation rate was studied in different water masses present in the subarctic North Atlantic ocean along the 59.5° N transatlantic section. Temperature, pH, salinity and total organic carbon (TOC) in natural conditions, fixed temperature conditions and both fixed temperature and pH conditions, were considered in order to understand the combined effects of the variables that control the Fe(II) oxidation kinetics in the ocean. The study shows that in natural conditions, temperature was the master variable which controlled 75% of the pseudo-first order kinetics rate ($k'$). This value rose to 90% when $pH_F$ (free scale) and salinity were also considered. At a fixed temperature, 72% of $k'$ was controlled by pH and at both fixed temperature and pH, salinity controled 62% of the Fe(II) oxidation rate. Sources and characteristics of TOC are important factors influencing the oxidation of Fe(II). The organic matter had both positive and negative effects on Fe(II) oxidation. In surface and coastal waters, TOC accelerated $k'$, decreasing the Fe(II) half-life time ($t_{1/2}$). In Subpolar Mode Water, Labrador Sea Water (for the Irminger Basin) and Denmark Straight Overflow Water, TOC slowed down $k'$, increasing Fe(II) $t_{1/2}$. This shifting behaviour where TOC affects Fe(II) oxidation depending on its marine or terrestrial origin, depth and remineralization stage proves that TOC cannot be used as a variable in an equation describing $k'$. The temperature dependence study indicated that the energy requirement for Fe(II) oxidation in surface waters was 32% lower than the required for bottom waters at both pH 7.7 and 8.0. This variability confirmed the importance of the organic matter composition of the selected samples. The Fe(II) oxidation rate constants in the region can be obtained from an empirical equation considering the natural conditions of temperature, $pH_F$ and salinity for the area, producing an error of estimation of 0.0072 $min^{-1}$. This equation should be incorporated in global Fe models.

## 1. Introduction

Oceanic Fe distribution has been extensively studied in the Atlantic Ocean (Bergquist and Boyle, 2006; Bergquist et al., 2007; Bowie et al., 2003; Bowie et al., 2006; Bowie et al., 1998; Bowie et al., 2004; Bowie et al., 2002; Boye et al., 2006; Buck et al., 2016; Cullen et al., 2006; Fitzsimmons and Boyle, 2014; Fitzsimmons et al., 2013; Laës et al., 2005; Mills et al., 2004; Mohamed et al., 2011; Powell et al., 1995; Saito et al., 2013; Ussher et al., 2010; Wu et al., 2001), the Pacific Ocean (Chase et al., 2005; Coale, 1991; Hong and Kester, 1986; Mackey et al., 2002; Nishioka et al., 2001; Resing et al., 2015; Roy et al., 2008; Schmidt and Hutchins, 1999; Wu et al., 2001; Wu et al., 2011), the Indian Ocean (Nishioka et al., 2013; Statham et al., 2005), the Southern Ocean (Bowie et al., 2004; Bucciarelli et al., 2001; Chever et al., 2010; De Jong et al., 1998; Klunder et al., 2011; Tagliabue et al., 2012), the Arctic Ocean (Campbell and Yeats, 1982; Crusius et al., 2017; Klunder et al., 2012; Thuróczy et al., 2011; Wehrmann et al., 2014), the Arabian Sea (Measures and Vink, 1999) and the Mediterranean Sea (Sarthou and Jeandel, 2001).

In the past, global ocean Fe distribution models have been proposed (Tagliabue et al., 2014; Tagliabue et al., 2010; Tagliabue et al., 2017). However, there is a lack of knowledge in the processes that control the behaviour of the different iron species and the transference between them. Iron(III) is the thermodynamically stable form of iron in seawater (Millero and Izaguirre, 1989), but significant concentrations of Fe(II) can also be found in the ocean. This aspect is very important because Fe (II) is more bioavailable for marine phytoplankton than Fe(III) (Morel et al., 2008; Shaked et al., 2005; Shaked and Lis, 2012). The bioavailability of Fe in aquatic environments is strongly affected by redox reactions which recycle Fe between Fe(II) and Fe(III) oxidation states and

* Corresponding author.
*E-mail address:* magdalena.santana@ulpgc.es (J.M. Santana-Casiano).

https://doi.org/10.1016/j.marchem.2018.05.002
Received 20 December 2017; Received in revised form 7 May 2018; Accepted 8 May 2018
Available online 09 May 2018
0304-4203/ 

# Chapter V.

# Organic Matter effect on the Fe(II) oxidation kinetics in the Labrador Sea

Carolina Santana-González, J. Magdalena Santana-Casiano, Melchor González-Dávila, S. Gladyshev, A. Sokov

Chemical Geology (in revision)

## *Abstract*

The Fe(II) oxidation rate was studied in one latitudinal and one longitudinal transect crossing the Labrador Sea. The studies considered the temperature, pH, salinity and total organic carbon (TOC) content. The pseudo-first order kinetic rate, *k'* ($min^{-1}$), variability was controlled by temperature (77%) when recreating in situ conditions, by $pH_F$ (75%) at a fixed temperature of 15ºC and by salinity and TOC (80%) when samples were fixed in both temperature and $pH_F$ 8. Sources and characteristics of TOC affected the oxidation of Fe(II). Organic matter produced positive and negative effects on the Fe(II) oxidation rate. A theoretical approach that considers the temperature and inorganic interactions on the oxidation kinetics has been included to provide the organic ligand effects on the Fe(II) oxidation rate. An empirical equation for the calculation of Fe(II) oxidation rate constants was obtained considering the in situ conditions of temperature, $pH_F$ and salinity for the North Atlantic.

## *5.1. Introduction*

The Labrador Sea (LS) is the coldest and freshest basin of the North Atlantic Ocean. It is the source of the intermediate depth water mass Labrador Sea Water (LSW) (Lazier et al., 2002; Nielsen, 1928). The deep convection caused by the cold air blowing off the Canadian landmass during winter destabilizes the water column, extending as deep as two kilometers (Pickart et al., 2002). LSW is important because it contributes to the global meridional overturning circulation (McCartney, 1992) and to the oceanic flux of heat (Dickson et al., 2003; Talley and McCartney, 1982). It is characterized by low salinity and temperature. It is well ventilated providing a transport of atmospheric gases to intermediated depths of the North Atlantic Ocean (Azetsu-Scott et al., 2003) and a climate connection between the high-latitude atmosphere and mid depth ocean (Pickart et al., 2002). The LS contributes to the net poleward heat transport by the ocean–atmosphere system and experiences a net annual heat loss to the atmosphere of approximately 1 GJ $m^{-2}$. The LS is unique in distributing this heat loss over a depth of a kilometer or more (Straneo, 2006).

Other water masses are also present in the LS basin. Irminger Water (IW) is transported into the LS from the Irminger Sea in the East and West Greenland Currents. These saline waters lie over the continental shelf and slope (Yashayaev et al., 2003). Northeast Atlantic Deep Water (NEADW) is originated from the dense overflow entering the North Atlantic through the deep trenches in the Iceland-Faroe-Scotland Ridge. It is formed by a complex transformation in Iceland Surface Overflow Water (ISOW) properties in the Northern Iceland Basin. ISOW is mixed with fresher LSW along its spreading pathway during which its thickness tends to increase (Dickson et al., 2003; Yashayaev, 2007a; Yashayaev et al., 2003). NEADW is the oldest component in the water column of the LS (Azetsu-Scott et al., 2003). Denmark Strait Overflow Water (DSOW) descends from the cold and dense overflow from the Denmark Strait sill and fills the bottom layer of the LS (Yashayaev et al., 2007c), constituting the densest water in the Northern North Atlantic (Azetsu-Scott et al., 2003).

The LS is a productive region with elevated production rates near frontal boundaries and in Greenland coastal waters (Steemann Nielsen, 1958). This section of the LS is affected by the West Greenland Current (WGC). A current thought to bring bioavailable iron (Körtzinger et al., 2008), impacting the primary productivity both locally (Rysgaard et al., 2003) and regionally (Schofield et al., 2010; Statham et al., 2008). It presents phytoplankton which are often larger and acclimated to low temperature and light regimes (Cota et al., 2003).

Iron (Fe) is one of the most important trace metals in seawater (Bruland, 2001). It is an essential micronutrient for organisms, controlling primary production in the oceans (Martin et al., 1991). For the two Fe oxidation states, the ferrous iron (Fe(II)) is more bioavailable than ferric iron (Fe(III)) for the marine phytoplankton (Morel et al., 2008; Shaked et al., 2005; Shaked and Lis, 2012). Iron concentration have been studied in areas close to the LS as the Arctic Ocean with dissolved iron (dFe) concentrations in the Siberian shelf lower than 1 nM, except for the Laptev Sea where values higher than 10 nM were observed (Klunder et al., 2012). In the central Artic, dFe concentrations vary from 0.5 nM in the Nansen Basin to higher than 2 nM in the Amundsen and Makarov Basins (Klunder et al., 2012). The total dissolvable iron (TDFe) concentrations are higher than 3 nM on the shelves and lower than 2 nM in the Makarov Basin. Data has shown an enrichment of particulate Fe toward the bottom of the water column (Thuróczy et al., 2011). In the Baffin bay and Canadian Artic Archipelago, total dissolved iron (TdFe) concentrations were between 9.3-57.3 nM in the Davis strait, 12-41 nM in the central Baffin, 23-61.6 nM in Lancaster Sound, 19-47 nM in Jones Sound and 9-49 nM in Smith Sound (Campbell and Yeats, 1982). The Northern North of Alaska, is characterized by sediment resuspension during winter and spring storms generating high TDFe of up to 1000 nM along the entire continental shelf. The dFe concentrations in surface waters range from 4 nM near shore, to 0.6-1.5 nM seaward of the shelf break (Crusius et al., 2017). Campbell and Yeats (1982) showed elevated Fe levels, especially the particulate fraction, in Baffin Bay. They were attributed to the melting of glacier and sea ice coming from the Arctic Ocean through Lancaster and Jones Sounds. However, Fe concentrations are similar in the WGC and the Western North Atlantic Ocean (Campbell and Yeats, 1982), with dFe concentrations of 0.2-0.9 nM and 0.1-1.3 nM of particulate Fe (Wu and Luther III, 1994). The elevated Fe concentrations in the western channels of the Canadian Archipelago compared to water coming through Smith Sound have been interpreted as an input of nutrient-rich water from the Bering Sea and the surface circulation pattern in the Arctic Ocean (Campbell and Yeats, 1982).

The oxidation rate of Fe(II) affects the concentration of dFe(II) from the photic zone to deep waters. Iron cycles between Fe(II) and Fe(III) through oxidation-reduction processes (Burns et al., 2010; Rose and Waite, 2002; Rush and Bielski, 1985). The Fe(II) oxidation rate provides the half-life time ($t_{1/2}$) of Fe(II) in seawater as a measure of the time that Fe(II) would be available in the ocean. The Fe(II) is more bioavailable than Fe(III) for the marine phytoplankton (Morel et al., 2008; Shaked et al., 2005; Shaked and Lis, 2012). Nevertheless, Fe(II) is thermodynamically unstable, rapidly oxidizing in oxic water (seconds to minutes) by $O_2$ and $H_2O_2$ (González-Davila et al., 2005; González-Dávila et al., 2006; Santana-Casiano et al., 2006). It oxidizes as a function of the pH, ionic strength, temperature (Millero et al., 1987b; Santana-Casiano

et al., 2005; Trapp and Millero, 2007) and [$HCO_3^-$] (Santana-Casiano et al., 2005; Trapp and Millero, 2007). The presence of nutrients, specially silicate (González et al., 2010; Samperio-Ramos et al., 2016), and phosphate, which complexes the Fe(III) generated during the oxidation (Burns et al., 2011), Cu (González et al., 2016) and the organic matter composition (Santana-Casiano et al., 2000) also affect the oxidation rate.

Organic complexation often alters Fe(II) oxidation kinetics by either accelerating or retarding the oxidation rate. The effect depends on the source and characteristics of the Fe-binding organic ligands (Santana-Casiano et al., 2000; Theis and Singer, 1974). The effect of organic compounds in the Fe(II) oxidation kinetic has been studied in laboratory by using individual organic compounds (Kuma et al., 1995; Lee et al., 2017b; Rose and Waite, 2002; Santana-Casiano et al., 2014; Santana-Casiano et al., 2010; Santana-Casiano et al., 2000; Voelker and Sulzberger, 1996) and by exudates excreted by microorganisms (González et al., 2014; Lee et al., 2017b; Santana-Casiano et al., 2014). The effect of organic matter has also been studied in open ocean (Craig et al., 2009; Croot and Laan, 2002; Roy and Wells, 2011; Roy et al., 2008; Santana-González et al., 2018) and in coastal areas (Lee et al., 2017; Lee et al., 2016) suggesting that Fe(II) complexation by aliphatic components accelerate Fe(II) oxidation. Recent studies carried out by Daugherty et al. (2017) pointed out the Fe(II)-organic matter complexes as important forms of bioavailable Fe(II) for microorganisms, influencing Fe cycling and primary productivity.

This work aimed to study of the Fe(II) oxidation kinetic rate in two crossing transects in the Labrador Sea. The Fe(II) oxidation kinetic was studied in the different LS water masses considering temperature, $pH_F$, salinity and TOC values under in situ conditions and under fixed temperature and $pH_F$ conditions. One of the goals of this study was to better understand the combined effects of variables such as temperature, $pH_F$ and salinity controlling the Fe(II) oxidation rate in the ocean and at the same time, taking into account the organic matter effects. All these variables, which also affect the biogeochemical cycle of the Fe(II)-Fe(III) system in seawater, are changing under the ocean acidification and global warming processes.

A model approach to study the role played by the different organic ligands present in the region was carried out. It provides new insight into the Fe(II) oxidation kinetic and the effect of different physicochemical conditions on the Fe(II) oxidation processes from coastal to open ocean and from surface to bottom waters in the Labrador Sea.

## 5.2. Methods

### 5.2.1. Study location and characteristics of the water masses

The cruise took place from June 8th to July 11th 2016 on board of the Russian Oceanographic Research vessel AKADEMIK IOFFE in the Labrador Sea. The study area was separated in two transepts, East-West and North-South Labrador (Fig. 5.1). The water masses located in the studied area were delimited by their potential density limits, $\sigma_\theta$ (kg $m^{-3}$); were IW < 27.68; LSW ranges between 27.68-27.80; NEADW ranges between 27.80-27.88 and DSOW > 27.88 (Filippova et al., 2017; Stramma et al., 2004; Yashayaev, 2007a; Yashayaev et al., 2008; Yashayaev et al., 2003).

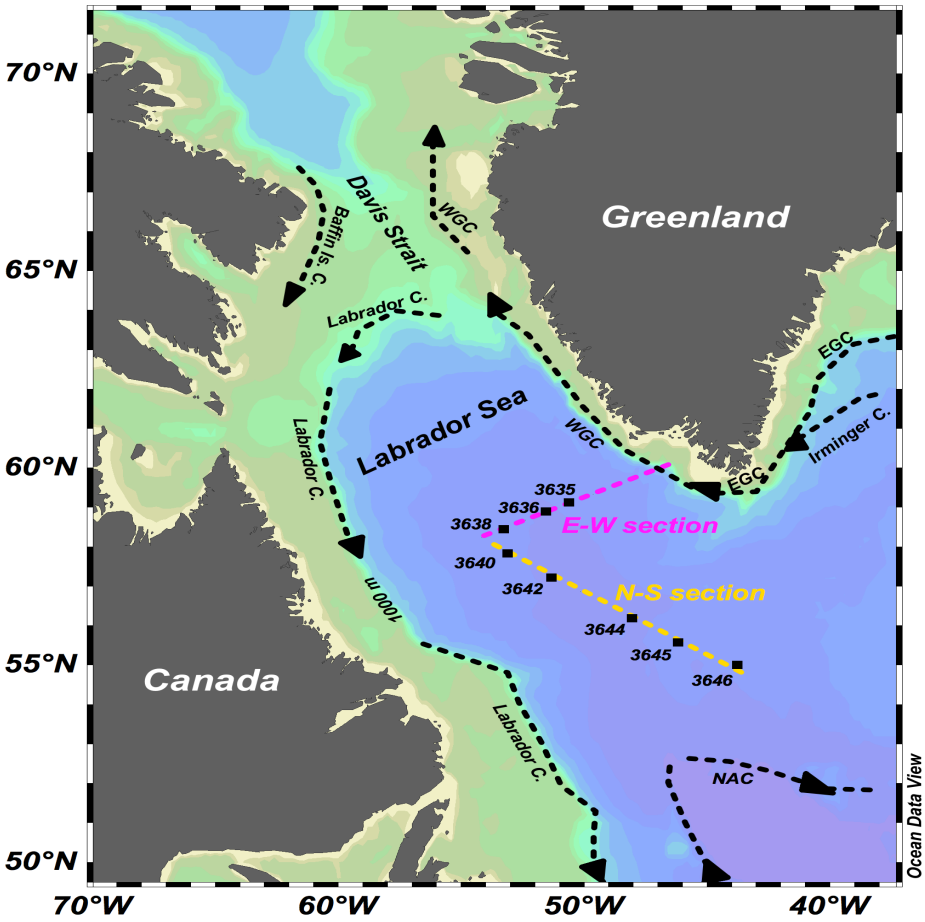


Fig. 5.1) General map of the Labrador Sea with the locations of the stations and the East-West (pink) and North-South (yellow) transects.

### *5.2.2. Reagents*

**Iron stock.** An iron stock of 6.21 x $10^{-4}$ M was prepared using ammonium iron(II) sulphate hexahydrate (Sigma-Aldrich). The stocks were prepared in 0.01 M HCl (Hiperpur-Plus- Panreac) to lower the pH to 2 and slow down any oxidation. The solution was stored in the dark until use. A diluted stock was prepared daily with a final concentration of 2.42 x $10^{-6}$ M.

**Luminol.** 5 L of luminol reagent was prepared using 2.71 x $10^{-4}$ M of 5-amino-2,3-dihydro-1,4-phthalazinedione (Sigma), 4.93 x $10^{-2}$ M of $Na_2CO_3$ (Sigma-Aldrich) and 0.4 M of previously distilled 25% $NH_3$ (Panreac). The final pH was adjusted to 10.4 by adding 0.06 M Q-HCl. At this pH, luminescence is optimal (Bowie et al., 1998). The luminol solution was stored in the dark due to its light sensitivity. To ensure complete dilution, it was prepared a few days prior to use. The solution became more stable 24 hours after preparation and remains usable for a month (King et al., 1995).

**HCl**. 0.01 M HCl (Hiperpur-Plus) was used to set the pH in the kinetic experiments.

**$NH_3$.** 4.28 x $10^{-2}$ M of 20% $NH_3$ (Hiperpur-Plus) was prepared in Milli-Q.

**Ammonium acetate buffer.** 0.04 M ammonium acetate was prepared and the pH was adjusted to 5.5 with acetic acid (glacial).

**FeLume cleaning**. The reaction vessel and the tubing for the peristaltic pump were rinsed three times with distilled water, three times with Milli-Q water and stored in 10% HCl solution. Immediately prior to use, it was re-rinsed three times with distilled water and three times with Milli-Q water. After the analysis, the material was cleaned and re-stored in the HCl solution.

### *5.2.3. Sampling and analysis*

Water column samples were collected using 12 L Niskin bottles mounted on a 24-position rosette frame fitted with a SeaBird SBE11 Plus CTD. Acid pre-cleaned

polyethylene containers were used to collect the unfiltered samples. 15 mL low density polyethylene (LDPE, Nalgene) containers were used for the samples of total dissolved Fe(II) (TdFe(II)). To keep the seawater solution at pH 6 and avoid any oxidation of Fe(II) until the analysis, 10 μL of 2 M HCl was added to the containers prior to sampling. 250 mL LDPE (Nalgene) containers were used for the kinetic studies with zero air headspace when sampling. TOC samples were collected in 50 mL polyethylene bottles and frozen until land-based laboratory analysis. All samples were kept in the dark until analysis.

#### *5.2.3.1. TdFe(II) samples*

Unfiltered and acidified to pH 6 were analysed on board on a period of less than 2 h. The concentration of TdFe(II) in seawater was determined using a FeLume system (Waterville Analytical). The Flow Injection Analysis by chemiluminescence (FIA-CL) technique uses the chemiluminescence strength produced by the reaction of luminol with Fe to determine concentrations (King et al., 1995). In the FIA system, four tygon tubes are placed in a peristaltic pump (Rainin Dynamax 15.8 V), transferring the sample and reagents to the mixing chamber and to the detector. The tubing pressure can be manipulated to allow a uniform flow. After adjusting the pressure in the tubing, the water-cleaning mode was enabled for 3 min. After this time, air was allowed to pass and then each line was introduced into the corresponding bottle: luminol, NaCl, Milli-Q water and sample. The software executed in the FeLume-chemiluminescence was provided by Waterville Analytical (WA control V105, photo counter control). An analysis time of 100 s was selected to allow full recording of the peak signal. To compute for the signal, the peak area mode was used. Triplicate measurements were carried out for each sample and the final result was obtained from the average. After each set of analyses, Milli-Q water was used to clean all the lines followed by air to empty the lines.

#### *5.2.3.2. Standards and calibration procedure*

The standard addition method was used to determinate TdFe(II) concentration at 15ºC, adding 3 standards to each sample. The required diluted iron stock was added after the sampling.

#### *5.2.3.3. Kinetic studies*

Samples were automatically mixed with the buffer just before being introduced into the detector by introducing a connector just before the detector. The sample plus luminol (1 mL $min^{-1}$ flux) and the ammonium acetate buffer (0.125 mL $min^{-1}$ flux) were introduced into the detector with a peristaltic pump. This modification provided a continuous registration of the measure.

The kinetic studies were carried out in a thermo-regulated cell connected to a thermostatic bath (Julabo) with a control to 0.01ºC. For each study, the seawater sample was acclimated to the desired temperature (in situ and 15ºC) as soon as they were sampled. When the temperature was stable, the $pH_F$ for the sample and a Tris buffer were measured (Millero, 1986). For each kinetic study, 50 mL of seawater from different seawater masses and depths was used. The initial addition of Fe(II) was 0.97 nM. All studies were performed in the dark to limit photo-transformation of Fe. The seawater was placed in the thermostated cell and the magnetic stirrer was switched on for 1 h to attain oxygen concentration equilibrium. When the solution stabilized at the desired temperature and pH, the sample line was introduced into the reaction cell. This was followed by the Fe stock addition, when the time would be noted.

#### *5.2.3.4. TOC samples*

Total organic carbon (TOC) was measured with a continuous flow analyzer (TOC V Shimadzu), previously calibrated with a hydrogen phthalate standard (Sigma-Aldrich) (Arístegui, 2014). 10 mL of sample, acidified with 10 μL 85% $H_3PO_4$ and purged with $CO_2$-free oxygen for at least 10 min to remove inorganic carbon, was transferred into a quartz combustion tube packed with Pt gauze (Aldrich), 7% Pt on alumina catalyst. The Pt gauze and Pt beads were heated to 800ºC in the upper zone while the remaining packing material was heated to 600ºC in the lower zone. The resulting $CO_2$ flowed through two water traps and a final copper halide trap leading into the $CO_2$ analyzer (Hansell, 2001).

#### *5.2.3.5. Statistical analysis*

The free R studio software (Team, 2016) was used. A correlation study between four independent variables (T, $pH_F$, S and TOC) was performed to avoid any correlated independent variables effects. A principal component analysis was performed to study the combined effect of independent variables on the measured *k'* for three sets of conditions of this study. Two components were selected for the principal component (PC) analysis; the first component (PC1) was a combination of T, $pH_F$ and TOC and the second component (PC2) a combination of TOC and S. The criteria to select two PC were that cumulative proportion and the proportion of variance could explain more than 70% of the variability. After the principal component study, a generalized additive model (GAM) (Hastie and Tibshirani, 1990) was used to determine the best fit between *k'* and each variable with empirical distribution functions to define the degree of the polynomial.

#### *5.2.3.6. Analysis of the contributions of organic ligands on the Fe(II) oxidation kinetics*

The organic effect on the Fe(II) oxidation rate was calculated as the difference between the *k'* measured at in situ conditions as a reference value and those for the theoretical *k'* in different situations.

In a first step, the theoretical *k'* ($k_T$') fixed at 15ºC was calculated by using the temperature dependence in Eq 5.1 of the inorganic kinetic model by Santana-Casiano et al. (2005) (T is in Kelvin and $k_0$ is the measured value at in situ conditions of temperature T).

$$\mathrm{Log}\left(\frac{k}{k_0}\right) = -5362\left(\frac{1}{T_0} - \frac{1}{T}\right) \quad (5.1)$$

After recalculating all the individual modelled rate constants for 15ºC, a second *k'* value was computed by applying the Santana-Casiano et al. (2005) model. Due to the lack of data correlating the temperature effect with the individual Fe(II) oxidation rate due to oxygen, the same temperature dependence as for $H_2O_2$ (González-Davila et al., 2005) was applied for the other oxygen reactive species. The temperature effect in the equilibrium constants was also considered following (González-Davila et al.,

2005). In this second step, the change in pH and the effect in the speciation due to the carbonate contribution (values for total dissolved inorganic carbon were provided by González-Dávila et al., unpublished data) were also considered to compute the theoretical oxidation rates at in situ conditions ($k_{T1}$') and those when the pH changed at 15ºC ($k_{T2}$'). In a third step the model was applied at a fixed temperature of 15ºC and pH 8 considering the changes in the carbonate speciation ($k_{T3}$'). The inorganic Fe(II) oxidation kinetics model (Santana-Casiano et al., 2005) was ran using the GEPASI software (Mendes, 1993). This model provided pair of data for Fe(II) and time in minutes for each conditions, and therefore, the theoretical *k'* values.

## *5.3. Results*

### *5.3.1. Kinetics of oxidation*

Fe(II) kinetic studies in the Labrador Sea were carried out under three different sets of conditions: 1st) recreating in situ temperature and $pH_F$ conditions, 2nd) at a fixed temperature of 15ºC (the $pH_F$ was allowed to change with temperature) and 3rd) at both fixed temperature (15ºC) and $pH_F$ (8). The three different sets of temperature and pH conditions were applied to improve the knowledge on the physicochemical processes affecting the Fe behavior in the marine environment.

The oxidation of Fe(II) in seawater follows the Haber-Weiss mechanism (Eq 5.2-5.5) and is also affected by ligand complexation equilibria (Eq 5.6-5.7).

$$Fe(II) + O_2 \rightarrow Fe(III) + O_2^{\cdot -} \quad (5.2)$$

$$Fe(II) + O_2^{\cdot -} + 2H^+ \rightarrow Fe(III) + H_2O_2 \quad (5.3)$$

$$Fe(II) + H_2O_2 \rightarrow Fe(III) + OH^- + OH^{\cdot} \quad (5.4)$$

$$Fe(II) + OH^{\cdot} \rightarrow Fe(III) + OH^- \quad (5.5)$$

$$Fe(II) + L \leftrightarrow Fe(II)L \quad (5.6)$$

$$Fe(III) + L \leftrightarrow Fe(III)L \quad (5.7)$$

The rate of oxidation of Fe(II) (Santana-Casiano et al., 2005) is expressed as an apparent oxidation rate, $k_{app}$ ($M^{-1}$ $min^{-1}$) (Eq 5.8), taking into account the inorganic and organic speciation of Fe(II) (Santana-Casiano et al. (2004) (Eq 5.9)

$$\frac{d[Fe(II)]}{dt} = -k_{app}[Fe(II)][O_2] \quad (5.8)$$

$$k_{app} = k_1\alpha_{Fe^{2+}} + k_2\alpha_{FeOH^+} + k_3\alpha_{Fe(OH)_2} + k_4\alpha_{FeHCO_3^+} + k_5\alpha_{Fe(CO_3)} + k_6\alpha_{Fe(CO_3)_2^{2-}} + k_7\alpha_{Fe(CO_3)OH^-} + k_8\alpha_{FeCl^+} + k_9\alpha_{FeSO_4} + \Sigma_i\, k_{L_i}\alpha_{FeL_i} \quad (5.9)$$

In aerate solutions, the Fe(II) oxidation kinetics follows a pseudo-first-order rate, $k'$ ($min^{-1}$) (Eq 5.10).

$$\frac{d[Fe(II)]}{dt} = -k'[Fe(II)] \quad (5.10)$$

$$\text{and } k' = k_{app}[O_2] \quad (5.11)$$

$$t_{1/2}\,(min) = \frac{\ln(2)}{k'} \quad (5.12)$$

Although the Fe(II) oxidation rate is independent of the initial Fe(II) concentration (Millero et al., 1987b; Roy and Wells, 2011; Santana-González et al., 2018) at nanomolar and subnanomolar concentrations, the TdFe(II) concentration present in the water samples used for the kinetic studies were measured (Table 5.1). Because of the samples were initially aerated, the in situ Fe(II) was oxidized and the initial Fe(II) in the samples for the kinetic studies was only the added 0.97 nM of Fe(II). The studies were carried out in saturated oxygen conditions and assuming that below the euphotic zone, the $H_2O_2$ concentrations were lower than 10 nM (Heller et al., 2013; Heller et al., 2016; Steigenberger and Croot, 2008) and in the upper 50–100 m an exponential

decrease with averaged values from 50 to 25 nM existed. Under these conditions, the pseudo-first order rate constant, *k'*, was obtained from plotting Ln Fe(II) versus time for the different samples selected to cover all the water masses found in the LS. The $t_{1/2}$ was calculated using Eq. 5.12. A description of *k'* is given in sections 5.3.1.1 to 5.3.1.3.

Table 5.1. TdFe(II) concentrations

| Station | Depth (m) | $\sigma_\theta$ (Kg/m$^3$) | TdFe(II) (nM) |
|---|---|---|---|
| 3635 | 1999 | 27.77 | 1.28 |
| Lat:59.113ºN | 958 | 27.73 | 1.67 |
| Lon:50.528ºW | 52 | 27.57 | 1.15 |
| | 18 | 27.14 | 1.54 |
| 3636 | 3485 | 27.92 | 0.88 |
| Lat:58.890ºN | | | |
| Lon:51.4633ºW | | | |
| 3638 | 3434 | 27.92 | 1.39 |
| Lat: 58.45896ºN | 2073 | 27.78 | 1.75 |
| Lon: 53.27622ºW | 792 | 27.73 | 0.43 |
| | 198 | 27.71 | 0.42 |
| | 10 | 27.03 | 0.20 |
| 3640 | 3468 | 27.92 | 1.09 |
| Lat: 57.83534ºN | 1971 | 27.77 | 0.61 |
| Lon: 53.18232ºW | 693 | 27.73 | 0.84 |
| | 169 | 27.70 | 0.64 |
| | 10 | 27.06 | 0.89 |
| 3642 | 3242 | 27.87 | 1.35 |
| Lat: 57.20896ºN | 2510 | 27.81 | 2.87 |
| Lon: 51.16765ºW | 1874 | 27.76 | 0.99 |
| | 992 | 27.73 | 1.21 |
| | 249 | 27.72 | 0.76 |
| 3644 | 3618 | 27.90 | 0.82 |
| Lat: 56.213ºN | 2218 | 27.78 | 0.88 |
| Lon: 48.11812ºW | 1282 | 27.73 | 0.93 |
| | 498 | 27.72 | 0.84 |
| | 159 | 27.68 | 0.84 |
| 3645 | 2834 | 27.86 | 0.93 |
| Lat: 55.57408ºN | 1775 | 27.79 | 1.43 |
| Lon: 46.22732ºW | 495 | 27.74 | 1.09 |
| | 64 | 27.49 | 1.30 |
| 3646 | 3346 | 27.87 | 1.47 |
| Lat: 55.00076ºN | 2464 | 27.82 | 0.65 |
| Lon: 43.7531ºW | 791 | 27.73 | 0.95 |
| | 184 | 27.69 | 1.33 |
| | 10 | 26.87 | 2.23 |

Table 5.2. Fe(II) oxidation rate in the study conditions.

| Section | Water mass | Latitude (N) | Longitude (W) | Depth (m) | Salinity | TOC (µM) | t (ºC) | $pH_F$ | $k'$ ($min^{-1}$) | Log $k_{app}$ ($M^{-1}$ $min^{-1}$) | $t_{1/2}$ (min) | $k'$ ($min^{-1}$) a | $k'$ ($min^{-1}$) b | $k'$ ($min^{-1}$) c | $k'$ ($min^{-1}$) c* | $k'$ ($min^{-1}$) d | $k'$ ($min^{-1}$) d* |
|---|---|---|---|---|---|---|---|---|---|---|---|---|---|---|---|---|---|
| **Natural conditions** | | | | | | | | | | | | | | | | | |
| E-W | IW | 59.113 | 50.529 | 18.4 | 34.622 | 77.5 | 7.6 | 8.12 | 0.025 ± 1E-03 | -4.068 | 27.73 | 0.029 | 0.029 | 0.022 | 0.053 | 0.037 | 0.037 |
| | | 58.459 | 53.276 | 10.5 | 34.615 | 71.7 | 7.6 | 8.14 | 0.038 ± 2E-03 | -3.886 | 18.24 | 0.031 | 0.030 | 0.024 | 0.056 | 0.039 | 0.039 |
| | LSW | 59.113 | 50.529 | 958.3 | 34.843 | 62 | 3.3 | 7.93 | 0.004 ± 2E-04 | -4.907 | 173.29 | 0.006 | 0.016 | 0.007 | 0.019 | 0.013 | 0.013 |
| | | 58.459 | 53.276 | 198.3 | 34.858 | 64.3 | 3.8 | 7.83 | 0.005 ± 3E-04 | -4.805 | 138.63 | 0.005 | 1.913 | 0.005 | 0.015 | 0.011 | 0.011 |
| | | 58.459 | 53.276 | 791.6 | 34.843 | 41.4 | 3.3 | 8.00 | 0.004 ± 2E-04 | -4.907 | 173.29 | 0.008 | 3.056 | 0.009 | 0.023 | 0.016 | 0.016 |
| | | 58.459 | 53.276 | 2073.5 | 34.916 | 48.8 | 3.3 | 7.96 | 0.006 ± 3E-04 | -4.731 | 115.52 | 0.007 | 3.561 | 0.008 | 0.020 | 0.014 | 0.014 |
| | DSOW | 58.89 | 51.463 | 3484.7 | 34.896 | 40.2 | 1.8 | 7.92 | 0.007 ± 4E-04 | -4.680 | 99.02 | 0.005 | 3.470 | 0.006 | 0.015 | 0.011 | 0.011 |
| N-S | IW | 57.835 | 53.182 | 10 | 34.673 | 76.2 | 7.6 | 8.12 | 0.046 ± 2E-03 | -3.803 | 15.07 | 0.029 | 9.372 | 0.022 | 0.053 | 0.037 | 0.037 |
| | | 56.213 | 48.118 | 159 | 34.798 | 55.6 | 3.5 | 7.97 | 0.009 ± 5E-04 | -4.553 | 77.02 | 0.008 | 6.009 | 0.008 | 0.021 | 0.015 | 0.015 |
| | | 55.574 | 46.227 | 64.2 | 34.735 | 73.6 | 4.7 | 8.02 | 0.005 ± 3E-04 | -4.796 | 138.63 | 0.012 | 7.730 | 0.011 | 0.028 | 0.020 | 0.020 |
| | | 55.001 | 43.753 | 9.9 | 34.589 | 78.9 | 8.5 | 8.13 | 0.070 ± 4E-03 | -3.612 | 9.90 | 0.034 | 13.205 | 0.026 | 0.060 | 0.042 | 0.042 |
| | LSW | 57.835 | 53.182 | 692.6 | 34.844 | 39.3 | 3.3 | 7.98 | 0.002 ± 1E-04 | -5.208 | 346.57 | 0.008 | 7.971 | 0.008 | 0.021 | 0.015 | 0.015 |
| | | 57.209 | 51.168 | 248.7 | 34.848 | 62.5 | 3.5 | 7.96 | 0.005 ± 3E-04 | -4.808 | 138.63 | 0.007 | 8.823 | 0.008 | 0.021 | 0.015 | 0.015 |
| | | 57.209 | 51.168 | 992.1 | 34.841 | 46.9 | 3.3 | 7.98 | 0.004 ± 2E-04 | -4.907 | 173.29 | 0.008 | 9.339 | 0.008 | 0.021 | 0.015 | 0.015 |
| | | 57.209 | 51.168 | 1874.3 | 34.913 | 64.1 | 3.7 | 8.03 | 0.005 ± 3E-04 | -4.805 | 138.63 | 0.010 | 10.770 | 0.010 | 0.026 | 0.018 | 0.018 |
| | | 56.213 | 48.118 | 497.9 | 34.841 | 53.6 | 3.4 | 7.95 | 0.007 ± 4E-04 | -4.663 | 99.02 | 0.007 | 9.911 | 0.007 | 0.020 | 0.014 | 0.014 |
| | | 56.213 | 48.118 | 1281.7 | 34.849 | 76.4 | 3.3 | 7.96 | 0.004 ± 2E-04 | -4.907 | 173.29 | 0.007 | 10.362 | 0.008 | 0.020 | 0.014 | 0.014 |
| | | 56.213 | 48.118 | 2218 | 34.915 | 75.2 | 3.4 | 8.03 | 0.022 ± 1E-03 | -4.165 | 31.51 | 0.010 | 11.850 | 0.010 | 0.025 | 0.018 | 0.017 |
| | | 55.574 | 46.227 | 495.3 | 34.848 | 103 | 3.3 | 7.89 | 0.003 ± 2E-04 | -5.032 | 231.05 | 0.005 | 10.187 | 0.006 | 0.017 | 0.012 | 0.012 |
| | | 55.574 | 46.227 | 1775.4 | 34.914 | 39.9 | 3.1 | 8.02 | 0.006 ± 3E-04 | -4.733 | 115.52 | 0.009 | 12.240 | 0.009 | 0.023 | 0.017 | 0.016 |
| | | 55.001 | 43.753 | 184.2 | 34.83 | 59.1 | 3.6 | 8.00 | 0.010 ± 5E-04 | -4.506 | 69.31 | 0.009 | 12.906 | 0.009 | 0.023 | 0.017 | 0.016 |
| | | 55.001 | 43.753 | 791.2 | 34.855 | 66.7 | 3.3 | 8.00 | 0.007 ± 4E-04 | -4.664 | 99.02 | 0.008 | 12.970 | 0.009 | 0.023 | 0.016 | 0.016 |
| | NEADW | 57.209 | 51.168 | 2509.5 | 34.915 | 91 | 3.0 | 8.02 | 0.004 ± 2E-04 | -4.910 | 173.29 | 0.009 | 13.339 | 0.009 | 0.023 | 0.016 | 0.016 |
| | | 57.209 | 51.168 | 3242.4 | 34.899 | 59 | 2.5 | 7.93 | 0.009 ± 5E-04 | -4.563 | 77.02 | 0.006 | 11.724 | 0.006 | 0.017 | 0.012 | 0.012 |
| | | 55.574 | 46.227 | 2833.8 | 34.908 | 53.2 | 2.7 | 7.95 | 0.006 ± 3E-04 | -4.737 | 115.52 | 0.006 | 12.592 | 0.007 | 0.018 | 0.013 | 0.013 |
| | | 55.001 | 43.753 | 2463.6 | 34.922 | 70.6 | 3.1 | 8.06 | 0.006 ± 3E-04 | -4.733 | 115.52 | 0.011 | 15.353 | 0.011 | 0.026 | 0.019 | 0.018 |

| | | | | | | | | | | | | | | | | | |
|---|---|---|---|---|---|---|---|---|---|---|---|---|---|---|---|---|---|
| | | 56.213 | 48.118 | 3618.5 | 34.894 | 69.8 | 1.7 | 7.91 | 0.006 ± 3E-04 | -4.748 | 115.52 | 0.005 | 12.109 | 0.005 | 0.015 | 0.011 | 0.010 |
| **15°C, $pH_F$ condition** | | | | | | | | | | | | | | | | | |
| E-W | IW | 59.113 | 50.529 | 18.4 | 34.622 | 77.5 | 15.0 | 8.06 | 0.018 ± 9E-04 | -4.144 | 38.51 | 0.068 | 48.376 | 0.039 | 0.098 | 0.071 | 0.076 |
| | | 59.113 | 50.529 | 52.2 | 34.725 | 78.1 | 15.0 | 7.86 | 0.020 ± 1E-03 | -4.098 | 34.66 | 0.030 | 38.252 | 0.020 | 0.056 | 0.042 | 0.047 |
| | | 58.459 | 53.276 | 10.5 | 34.615 | 71.7 | 15.0 | 8.07 | 0.062 ± 3E-03 | -3.607 | 11.18 | 0.071 | 51.108 | 0.041 | 0.101 | 0.073 | 0.078 |
| | LSW | 59.113 | 50.529 | 958.3 | 34.843 | 62 | 15.0 | 7.88 | 0.014 ± 7E-04 | -4.252 | 49.51 | 0.032 | 40.956 | 0.021 | 0.059 | 0.044 | 0.049 |
| | | 59.113 | 50.529 | 1999.3 | 34.918 | 56.1 | 15.0 | 7.91 | 0.010 ± 5E-04 | -4.398 | 69.31 | 0.036 | 43.478 | 0.023 | 0.064 | 0.047 | 0.052 |
| | | 58.459 | 53.276 | 198.3 | 34.858 | 64.3 | 15.0 | 7.89 | 0.016 ± 8E-04 | -4.194 | 43.32 | 0.033 | 43.179 | 0.021 | 0.060 | 0.045 | 0.050 |
| | | 58.459 | 53.276 | 791.6 | 34.843 | 41.4 | 15.0 | 7.91 | 0.016 ± 8E-04 | -4.194 | 43.32 | 0.036 | 45.200 | 0.023 | 0.064 | 0.047 | 0.052 |
| | | 58.459 | 53.276 | 2073.5 | 34.916 | 48.8 | 15.0 | 7.91 | 0.016 ± 8E-04 | -4.194 | 43.32 | 0.036 | 46.020 | 0.023 | 0.064 | 0.047 | 0.052 |
| | DSOW | 58.89 | 51.463 | 3484.7 | 34.896 | 40.2 | 15.0 | 7.84 | 0.015 ± 8E-04 | -4.222 | 46.21 | 0.027 | 42.610 | 0.018 | 0.053 | 0.040 | 0.044 |
| | | 58.459 | 53.276 | 3433.5 | 34.896 | 49.7 | 15.0 | 7.89 | 0.021 ± 1E-03 | -4.076 | 33.01 | 0.033 | 46.433 | 0.021 | 0.060 | 0.045 | 0.050 |
| N-S | IW | 57.835 | 53.182 | 10 | 34.673 | 76.2 | 15.0 | 8.05 | 0.062 ± 3E-03 | -3.606 | 11.18 | 0.065 | 57.965 | 0.038 | 0.095 | 0.069 | 0.074 |
| | | 56.213 | 48.118 | 159 | 34.798 | 55.6 | 15.0 | 7.87 | 0.016 ± 8E-04 | -4.194 | 43.32 | 0.031 | 46.774 | 0.020 | 0.057 | 0.043 | 0.047 |
| | | 55.574 | 46.227 | 64.2 | 34.735 | 73.6 | 15.0 | 7.91 | 0.023 ± 1E-03 | -4.037 | 30.14 | 0.036 | 50.191 | 0.023 | 0.064 | 0.047 | 0.052 |
| | | 55.001 | 43.753 | 9.9 | 34.589 | 78.9 | 15.0 | 8.04 | 0.091 ± 5E-03 | -3.440 | 7.62 | 0.062 | 60.178 | 0.037 | 0.093 | 0.067 | 0.073 |
| | LSW | 57.835 | 53.182 | 168.5 | 34.852 | 36.4 | 15.0 | 7.86 | 0.012 ± 6E-04 | -4.319 | 57.76 | 0.030 | 48.386 | 0.020 | 0.056 | 0.042 | 0.046 |
| | | 57.835 | 53.182 | 692.6 | 34.844 | 39.3 | 15.0 | 7.87 | 0.015 ± 8E-04 | -4.222 | 46.21 | 0.031 | 49.810 | 0.020 | 0.057 | 0.043 | 0.047 |
| | | 57.835 | 53.182 | 1971.1 | 34.917 | 50.2 | 15.0 | 7.84 | 0.014 ± 7E-04 | -4.252 | 49.51 | 0.027 | 48.492 | 0.018 | 0.053 | 0.040 | 0.044 |
| | | 57.209 | 51.168 | 248.7 | 34.848 | 62.5 | 15.0 | 7.77 | 0.012 ± 6E-04 | -4.319 | 57.76 | 0.021 | 44.561 | 0.015 | 0.044 | 0.034 | 0.038 |
| | | 57.209 | 51.168 | 992.1 | 34.841 | 46.9 | 15.0 | 7.90 | 0.018 ± 9E-04 | -4.143 | 38.51 | 0.035 | 54.197 | 0.022 | 0.062 | 0.046 | 0.051 |
| | | 57.209 | 51.168 | 1874.3 | 34.913 | 64.1 | 15.0 | 7.91 | 0.023 ± 1E-03 | -4.036 | 30.14 | 0.036 | 55.677 | 0.023 | 0.064 | 0.047 | 0.052 |
| | | 56.213 | 48.118 | 497.9 | 34.841 | 53.6 | 15.0 | 7.86 | 0.015 ± 8E-04 | -4.222 | 46.21 | 0.030 | 52.790 | 0.020 | 0.056 | 0.042 | 0.046 |
| | | 56.213 | 48.118 | 1281.7 | 34.849 | 76.4 | 15.0 | 7.90 | 0.017 ± 9E-04 | -4.168 | 40.77 | 0.035 | 56.484 | 0.022 | 0.062 | 0.046 | 0.051 |
| | | 55.574 | 46.227 | 495.3 | 34.848 | 103 | 15.0 | 7.90 | 0.006 ± 3E-04 | -4.620 | 115.52 | 0.035 | 57.989 | 0.022 | 0.062 | 0.046 | 0.051 |
| | | 55.574 | 46.227 | 1775.4 | 34.914 | 39.9 | 15.0 | 7.92 | 0.010 ± 5E-04 | -4.398 | 69.31 | 0.037 | 60.290 | 0.024 | 0.065 | 0.048 | 0.053 |
| | | 55.001 | 43.753 | 184.2 | 34.83 | 59.1 | 15.0 | 7.90 | 0.028 ± 1E-03 | -3.951 | 24.76 | 0.035 | 59.485 | 0.022 | 0.062 | 0.046 | 0.051 |
| | | 55.001 | 43.753 | 791.2 | 34.855 | 66.7 | 15.0 | 7.89 | 0.010 ± 5E-04 | -4.398 | 69.31 | 0.033 | 59.413 | 0.021 | 0.060 | 0.045 | 0.050 |
| | NEADW | 57.209 | 51.168 | 2509.5 | 34.915 | 91 | 15.0 | 7.91 | 0.013 ± 7E-04 | -4.284 | 53.32 | 0.036 | 61.744 | 0.023 | 0.064 | 0.047 | 0.052 |

| | | | | | | | | | | | | | | | | | |
|---|---|---|---|---|---|---|---|---|---|---|---|---|---|---|---|---|---|
| | | 57.209 | 51.168 | 3242.4 | 34.899 | 59 | 15.0 | 7.91 | 0.020 ± 1E-03 | -4.097 | 34.66 | 0.036 | 62.492 | 0.023 | 0.064 | 0.047 | 0.052 |
| | | 55.574 | 46.227 | 2833.8 | 34.908 | 53.2 | 15.0 | 7.87 | 0.010 ± 5E-04 | -4.398 | 69.31 | 0.031 | 59.915 | 0.020 | 0.057 | 0.043 | 0.047 |
| | | 55.001 | 43.753 | 2463.6 | 34.922 | 70.6 | 15.0 | 7.89 | 0.026 ± 1E-03 | -3.983 | 26.66 | 0.033 | 62.269 | 0.021 | 0.060 | 0.045 | 0.050 |
| | | 55.001 | 43.753 | 3346 | 34.899 | 61.8 | 15.0 | 7.89 | 0.019 ± 1E-03 | -4.119 | 36.48 | 0.033 | 62.989 | 0.021 | 0.060 | 0.045 | 0.050 |
| | DSOW | 57.835 | 53.182 | 3467.8 | 34.896 | 52.9 | 15.0 | 7.77 | 0.008 ± 4E-04 | -4.495 | 86.64 | 0.021 | 53.848 | 0.015 | 0.044 | 0.034 | 0.038 |
| | | 56.213 | 48.118 | 3618.5 | 34.894 | 69.8 | 15.0 | 7.87 | 0.012 ± 6E-04 | -4.319 | 57.76 | 0.031 | 62.684 | 0.020 | 0.057 | 0.043 | 0.047 |
| **15ºC, $pH_T$=8 condition** | | | | | | | | | | | | | | | | | |
| | | 59.113 | 50.529 | 18.4 | 34.622 | 77.5 | 15.0 | 8.00 | 0.024 ± 1E-03 | -4.019 | 28.88 | 0.052 | 75.998 | 0.032 | 0.083 | 0.060 | 0.065 |
| | IW | 59.113 | 50.529 | 52.2 | 34.725 | 78.1 | 15.0 | 8.00 | 0.026 ± 1E-03 | -3.984 | 26.66 | 0.052 | 76.753 | 0.031 | 0.082 | 0.060 | 0.065 |
| | | 58.459 | 53.276 | 10.5 | 34.615 | 71.7 | 15.0 | 8.00 | 0.025 ± 1E-03 | -4.001 | 27.73 | 0.052 | 77.605 | 0.032 | 0.083 | 0.060 | 0.066 |
| | | 59.113 | 50.529 | 1999.3 | 34.918 | 56.1 | 15.0 | 8.00 | 0.024 ± 1E-03 | -4.018 | 28.88 | 0.052 | 79.049 | 0.031 | 0.082 | 0.060 | 0.065 |
| E-W | LSW | 58.459 | 53.276 | 198.3 | 34.858 | 64.3 | 15.0 | 8.00 | 0.034 ± 2E-03 | -3.867 | 20.39 | 0.052 | 79.867 | 0.031 | 0.082 | 0.060 | 0.065 |
| | | 58.459 | 53.276 | 791.6 | 34.843 | 41.4 | 15.0 | 8.00 | 0.026 ± 1E-03 | -3.983 | 26.66 | 0.052 | 80.660 | 0.031 | 0.082 | 0.060 | 0.065 |
| | | 58.459 | 53.276 | 2073.5 | 34.916 | 48.8 | 15.0 | 8.00 | 0.028 ± 1E-03 | -3.951 | 24.76 | 0.052 | 81.407 | 0.031 | 0.082 | 0.060 | 0.065 |
| | DSOW | 58.89 | 51.463 | 3484.7 | 34.896 | 40.2 | 15.0 | 8.00 | 0.026 ± 1E-03 | -3.983 | 26.66 | 0.052 | 82.197 | 0.031 | 0.082 | 0.060 | 0.065 |
| | | 58.459 | 53.276 | 3433.5 | 34.896 | 49.7 | 15.0 | 8.00 | 0.040 ± 2E-03 | -3.796 | 17.33 | 0.052 | 82.973 | 0.031 | 0.082 | 0.060 | 0.065 |
| | | 57.835 | 53.182 | 10 | 34.673 | 76.2 | 15.0 | 8.00 | 0.058 ± 3E-03 | -3.635 | 11.95 | 0.052 | 83.861 | 0.031 | 0.083 | 0.060 | 0.065 |
| | IW | 56.213 | 48.118 | 159 | 34.798 | 55.6 | 15.0 | 8.00 | 0.018 ± 9E-04 | -4.143 | 38.51 | 0.052 | 84.568 | 0.031 | 0.082 | 0.060 | 0.065 |
| | | 55.574 | 46.227 | 64.2 | 34.735 | 73.6 | 15.0 | 8.00 | 0.043 ± 2E-03 | -3.765 | 16.12 | 0.052 | 85.369 | 0.031 | 0.082 | 0.060 | 0.065 |
| | | 55.001 | 43.753 | 9.9 | 34.589 | 78.9 | 15.0 | 8.00 | 0.077 ± 4E-03 | -3.513 | 9.00 | 0.052 | 86.212 | 0.032 | 0.083 | 0.060 | 0.066 |
| | | 57.835 | 53.182 | 168.5 | 34.852 | 36.4 | 15.0 | 8.00 | 0.023 ± 1E-03 | -4.037 | 30.14 | 0.052 | 86.836 | 0.031 | 0.082 | 0.060 | 0.065 |
| | | 57.835 | 53.182 | 692.6 | 34.844 | 39.3 | 15.0 | 8.00 | 0.026 ± 1E-03 | -3.983 | 26.66 | 0.052 | 87.600 | 0.031 | 0.082 | 0.060 | 0.065 |
| | | 57.835 | 53.182 | 1971.1 | 34.917 | 50.2 | 15.0 | 8.00 | 0.021 ± 1E-03 | -4.076 | 33.01 | 0.052 | 88.318 | 0.031 | 0.082 | 0.060 | 0.065 |
| N-S | | 57.209 | 51.168 | 248.7 | 34.848 | 62.5 | 15.0 | 8.00 | 0.012 ± 6E-04 | -4.319 | 57.76 | 0.052 | 89.110 | 0.031 | 0.082 | 0.060 | 0.065 |
| | | 57.209 | 51.168 | 992.1 | 34.841 | 46.9 | 15.0 | 8.00 | 0.028 ± 1E-03 | -3.951 | 24.76 | 0.052 | 89.865 | 0.031 | 0.082 | 0.060 | 0.065 |
| | LSW | 57.209 | 51.168 | 1874.3 | 34.913 | 64.1 | 15.0 | 8.00 | 0.028 ± 1E-03 | -3.951 | 24.76 | 0.052 | 90.575 | 0.031 | 0.082 | 0.060 | 0.065 |
| | | 56.213 | 48.118 | 497.9 | 34.841 | 53.6 | 15.0 | 8.00 | 0.018 ± 9E-04 | -4.143 | 38.51 | 0.052 | 91.362 | 0.031 | 0.082 | 0.060 | 0.065 |
| | | 56.213 | 48.118 | 1281.7 | 34.849 | 76.4 | 15.0 | 8.00 | 0.017 ± 9E-04 | -4.168 | 40.77 | 0.052 | 92.101 | 0.031 | 0.082 | 0.060 | 0.065 |
| | | 56.213 | 48.118 | 2218 | 34.915 | 75.2 | 15.0 | 8.00 | 0.027 ± 1E-03 | -3.967 | 25.67 | 0.052 | 92.806 | 0.031 | 0.082 | 0.060 | 0.065 |
| | | 55.574 | 46.227 | 495.3 | 34.848 | 103 | 15.0 | 8.00 | 0.019 ± 1E-03 | -4.120 | 36.48 | 0.052 | 93.583 | 0.031 | 0.082 | 0.060 | 0.065 |
| | | 55.574 | 46.227 | 1775.4 | 34.914 | 39.9 | 15.0 | 8.00 | 0.024 ± 1E-03 | -4.018 | 28.88 | 0.052 | 94.282 | 0.031 | 0.082 | 0.060 | 0.065 |

| | | | | | | | | | | | | | | | | |
|---|---|---|---|---|---|---|---|---|---|---|---|---|---|---|---|---|
| | 55.001 | 43.753 | 184.2 | 34.83 | 59.1 | 15.0 | 8.00 | 0.049 ± 2E-03 | -3.708 | 14.15 | 0.052 | 95.065 | 0.031 | 0.082 | 0.060 | 0.065 |
| | 55.001 | 43.753 | 791.2 | 34.855 | 66.7 | 15.0 | 8.00 | 0.029 ± 1E-03 | -3.936 | 23.90 | 0.052 | 95.783 | 0.031 | 0.082 | 0.060 | 0.065 |
| NEADW | 57.209 | 51.168 | 2509.5 | 34.915 | 91 | 15.0 | 8.00 | 0.032 ± 2E-03 | -3.893 | 21.66 | 0.052 | 96.478 | 0.031 | 0.082 | 0.060 | 0.065 |
| | 57.209 | 51.168 | 3242.4 | 34.899 | 59 | 15.0 | 8.00 | 0.031 ± 2E-03 | -3.907 | 22.36 | 0.052 | 97.215 | 0.031 | 0.082 | 0.060 | 0.065 |
| | 55.574 | 46.227 | 2833.8 | 34.908 | 53.2 | 15.0 | 8.00 | 0.019 ± 1E-03 | -4.119 | 36.48 | 0.052 | 97.935 | 0.031 | 0.082 | 0.060 | 0.065 |
| | 55.001 | 43.753 | 2463.6 | 34.922 | 70.6 | 15.0 | 8.00 | 0.044 ± 2E-03 | -3.755 | 15.75 | 0.052 | 98.650 | 0.031 | 0.082 | 0.060 | 0.065 |
| | 55.001 | 43.753 | 3346 | 34.899 | 61.8 | 15.0 | 8.00 | 0.045 ± 2E-03 | -3.745 | 15.40 | 0.052 | 99.385 | 0.031 | 0.082 | 0.060 | 0.065 |
| DSOW | 57.835 | 53.182 | 3467.8 | 34.896 | 52.9 | 15.0 | 8.00 | 0.023 ± 1E-03 | -4.036 | 30.14 | 0.052 | 100.106 | 0.031 | 0.082 | 0.060 | 0.065 |
| | 56.213 | 48.118 | 3618.5 | 34.894 | 69.8 | 15.0 | 8.00 | 0.017 ± 9E-04 | -4.168 | 40.77 | 0.052 | 100.824 | 0.031 | 0.082 | 0.060 | 0.065 |

The theoretical values of *k'* ($min^{-1}$) was calculated using: a) Santana-Casiano et al. (2005), b) Trapp and Millero (2007), c) González et al. (2010), d) Samperio-Ramos et al. (2016) . * Indicate equations high in nutrient concentrations.

### *5.3.1.1. Recreating in situ conditions*

Fe(II) oxidation kinetics was studied in situ temperature, $pH_F$, salinity and TOC. Pressure, dissolved oxygen and the content of total inorganic carbon ($C_T$) changed during the experimental design but they were considered in each new condition. In accordance, the total alkalinity ($A_T$) was assumed to be constant and the resulting $C_T$ value was computed from pH, in the new condition, and $A_T$, using the program $CO_2$sys (Pierrot et al., 2006). The bath temperature was fixed at the same value than that indicated in the CTD for each sample. Temperature equilibrium was reached before the addition of Fe(II). To keep a constant oxygen concentration, the samples were aerated for 1 h prior to the study. Under these conditions, a pseudo-first order behavior was kept at least until after the resulting $t_{1/2}$, and the oxidation rate constant, *k'*, was determined (Table. 5.2, Fig. 5.2).

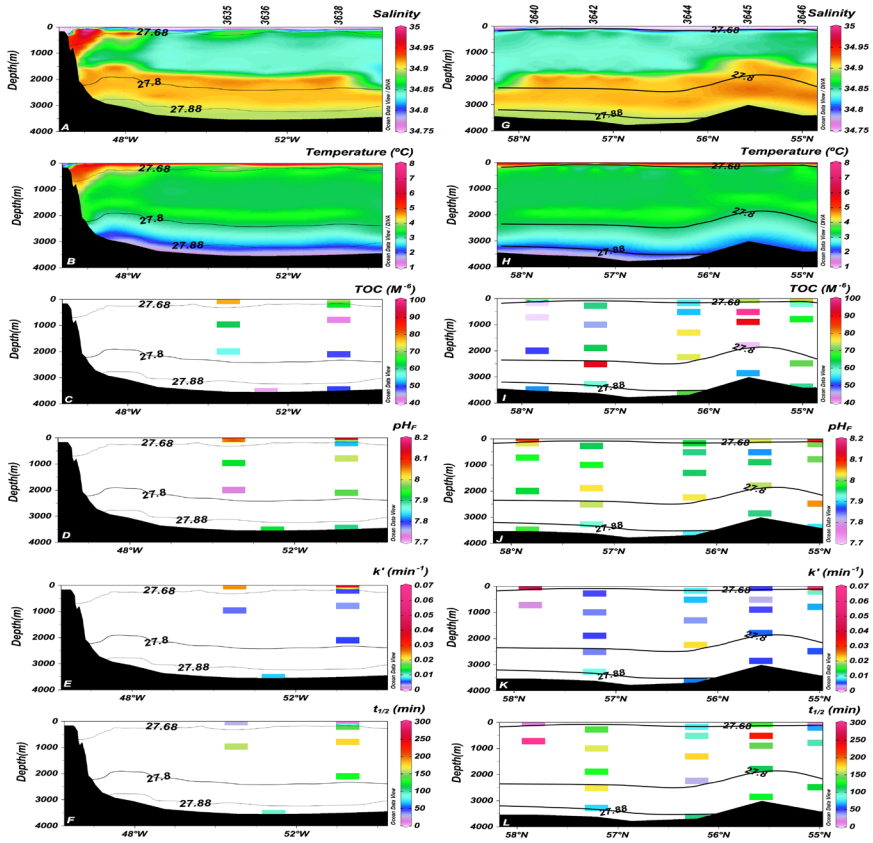


Fig. 5.2) East-West transect (A to F) and North–South transect (G to L) for salinity (A, G); temperature (B, H); Total Organic Carbon (C, I); $pH_F$ (D, J); *k'* ($min^{-1}$); for the Fe(II) oxidation in in situ conditions (E, K) and Half-life time ($t_{1/2}$) (F, L) of Fe(II).

In the East-West transect (Fig. 5.2A to F) the vertical distribution revealed that the IW samples presented the highest *k'* values (0.031±0.006 $min^{-1}$) coinciding with the highest temperature (7.2±0.31ºC), $pH_F$ (8.08±0.06), TOC (74.8±3.26 μM) and the lowest salinity (34.6±0.055). The LSW presented a lower *k'* (0.004±0.0007 $min^{-1}$), with lower temperatures (3.3±0.1ºC), $pH_F$ (7.92±0.06), TOC (54.53±7.12 μM) and higher salinity (34.86±0.05) than the IW. The DSOW samples showed *k'* of 0.007 $min^{-1}$ at 1.63ºC, however the $pH_F$ (7.92) and salinity (34.896) values were very close to LSW. The DSOW presented the lowest TOC values in the East-West transect (44.96±4.74 μM). The longitudinal distribution (Fig. 5.2A to F) showed IW samples presented *k'* values that increased with the temperature, $pH_F$ and salinity from East (0.0248 $min^{-1}$, 6.84ºC, 8.02, 34.620, respectively) to West (0.0376 $min^{-1}$, 7.61ºC, 8.14, 34.858) while TOC decreased from East (78.06 μM) to West (71.66 μM).

In the North-South transect (Fig. 5.2G to L), the vertical distribution showed the same pattern than the observed in the East-West transect. The IW presented the highest *k'* values (0.03±0.03$min^{-1}$) with the highest temperature (6.12±2.41ºC), $pH_F$ (8.06±0.007) and the lowest salinity (34.698±0.11) in the North-South transect. TOC values ranged from 55.63 to 78.90 μM. The LSW presented lower *k'* (0.0067±0.0154 $min^{-1}$) due to lower temperatures (3.37±0.12ºC) and $pH_F$ (7.98±0.05) and higher salinity (34.862±0.05) values than in the IW. However, TOC ranged from 39.32 to 102.99 $\mu$M in the LSW. The NEADW had lower *k'* (0.0061±0.0031 $min^{-1}$) with lower temperatures (2.71±0.3ºC) and $pH_F$ (7.96±0.09) values than LSW, while the salinity was the highest in the transect (34.910±0.01) and the TOC ranged from 68.46 to 22.5 $\mu$M. DSOW presented *k'* of 0.006 $min^{-1}$ with 1.81ºC, $pH_F$ 7.91, salinity 34.894 and 69.84 $\mu$M of TOC. The *k'* latitudinal distribution for IW followed the decrease in temperature and salinity while $pH_F$ and TOC increased from North (0.046 $min^{-1}$, 7.72ºC, 34.589, 7.97, 55.63 μM) to South (0.005 $min^{-1}$, 4.74ºC, 34.798, 8.13, 78.90 $\mu$M). In the LSW, *k'* increased with temperature from North (0.009±0.001 $min^{-1}$, 3.48±0.1ºC) to South (0.0022 $min^{-1}$, 3.3ºC). However, temperature, $pH_F$, salinity and TOC did not show any latitudinal variation. The TOC range increased from North (57.84±10.9 μM) to South (77.83±25.15 μM). In the NEADW, *k'* increased with $pH_F$ and salinity while TOC decreased from North (0.004 $min^{-1}$, 7.91, 34.915, 91.04 $\mu$M) to South (0.006 $min^{-1}$, 8.06, 34.926, 61.79 $\mu$M). Temperature did not show any latitudinal variation. DSOW was only analyzed in one station.

### *5.3.1.2. Temperature fixed at 15ºC*

Temperature controls the Fe(II) oxidation rate (Millero et al., 1987b; Santana-Casiano et al., 2005). In this study (2nd condition), in order to avoid the temperature effect on the Fe(II) oxidation rate, it was fixed at 15ºC, while pH was allowed to change (the pH is also temperature dependant). Deep waters, normally at 1-3ºC, presented the highest changes in pH, while surface waters with initial temperatures of around 8ºC showed the lowest variations. Temperature gradients in surface waters also had an important effect on $pH_F$. The $k'_{T2}$ values are presented in Table. 5.2 and in Fig. 5.3B and E.

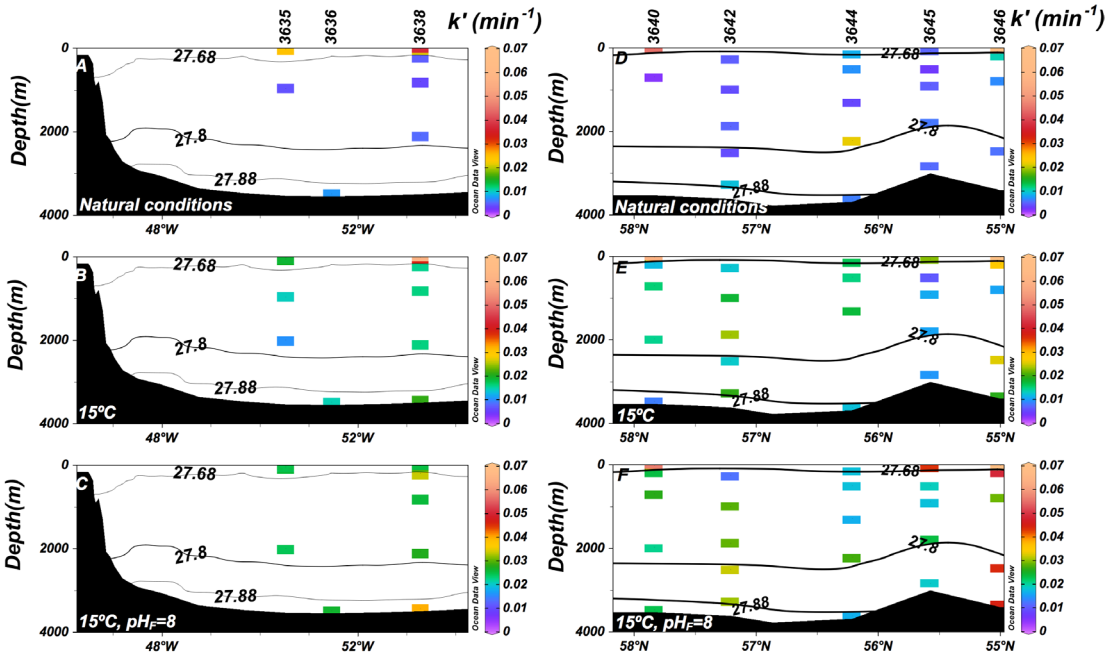


Fig. 5.3 East-West transect (A to C) and North–South transect (D to F) for the pseudo-first order constant $k'$ ($min^{-1}$) in natural conditions (A, D); at a fixed temperature of 15ºC (B, E); and at both fixed temperature of 15ºC and $pH_F$ of 8 (C, F).

In the vertical distribution of the East-West transect (Fig. 5.3B), the IW presented higher values of $k'$ and $pH_F$ (0.033±0.029 $min^{-1}$, 7.99±0.07) than the deeper LSW (0.014±0.0004 $min^{-1}$, 7.90±0.02) and DSOW (0.017±0.003 $min^{-1}$, 7.86±0.02). In the longitudinal distribution, $k'$ and $pH_F$ increased westward for IW (from 0.0189±0.0007 $min^{-1}$, 7.96±0.1 to 0.0624 $min^{-1}$, 8.07), LSW (from 0.012±0.001 $min^{-1}$, 7.89± 0.015 to 0.016±0.0001 $min^{-1}$, 7.9±0.01) and DSOW (from 0.0146 $min^{-1}$, 7.84 to 0.0213 $min^{-1}$, 7.89).

In the vertical distribution of the North-South transect (Fig. 5.3E), the IW had higher $pH_F$ (0.048±0.04 $min^{-1}$, 7.96±0.09) and *k'* than the deeper water masses, LSW (0.014±0.013 $min^{-1}$, 7.90±0.02), NEADW (0.015±0.005 $min^{-1}$, 7.89±0.02) and DSOW (0.010±0.001 $min^{-1}$, 7.82±0.05). The latitudinal distribution showed that *k'* followed pH, increasing from North to South in the IW (from 0.0162 $min^{-1}$, 7.87 to 0.091 $min^{-1}$, 8.04), LSW (from 0.015±0.007 $min^{-1}$, 7.86±0.02 to 0.013±0.01 $min^{-1}$, 7.9±0.01) and DSOW (from 0.0084 $min^{-1}$, 7.77 to 0.012 $min^{-1}$, 7.87). The NEADW followed the opposite pattern, decreasing from 0.016±0.003 $min^{-1}$, 7.91 to 0.022±0.003 $min^{-1}$, 7.89.

### *5.3.1.3. Fixed at 15ºC and $pH_F$ 8*

The Fe(II) oxidation rate is both temperature and pH dependent (González-Davila et al., 2005; Santana-Casiano et al., 2005). Fe(II) oxidation rates at a fixed temperature and $pH_F$ ($k'_{T3}$) are shown in Table. 5.2 and Fig. 5.3C and F. These results correspond to the third condition.

The East-West transect (Fig. 5.3C) showed $k'_{T3}$ ($min^{-1}$) values that slight increased with depth for IW (0.024±0.001), LSW (0.027±0.005) and DSOW (0.033±0.006). The longitudinal distribution revealed a small increase in *k'* values from East to West in IW (from 0.024±0.001 to 0.025), LSW (from 0.243 to 0.029) and DSOW (from 0.026 to 0.040).

In the North-South transect (Fig. 5.3F), IW had higher values of *k'* ($min^{-1}$) (0.048±0.02) than LSW (0.024±0.02), NEAWD (0.034±0.01) and DSOW (0.019±0.003). *k'* also increased from North to South in the IW (from 0.018 to 0.0766) and NEADW (from 0.031±0.0007 to 0.045±0.0002) but decreased in the LSW (from 0.023±0.01 to 0.0203±0.006) and DSOW (from 0.023 to 0.017).

Linear dependences were observed between $k'_{T3}$ and TOC in the East-West transect for LSW at 53.27ºW (+0.0004 $min^{-1}$ /µM, $r^2$=0.991) and in the North-South transect for IW from 9 to 65 m (+0.0063 $min^{-1}$/ µM, $r^2$=0.996) and for NEADW (+0.0015 $min^{-1}$/ µM, $r^2$=0.789, excluding the two samples of 91.03 and 69.83 µM which deviate from the linearity). Samples of DSOW (both transects) deeper than 3433 m, presented a negative dependence (-0.0003 $min^{-1}$/ µM, $r^2$=0.995).

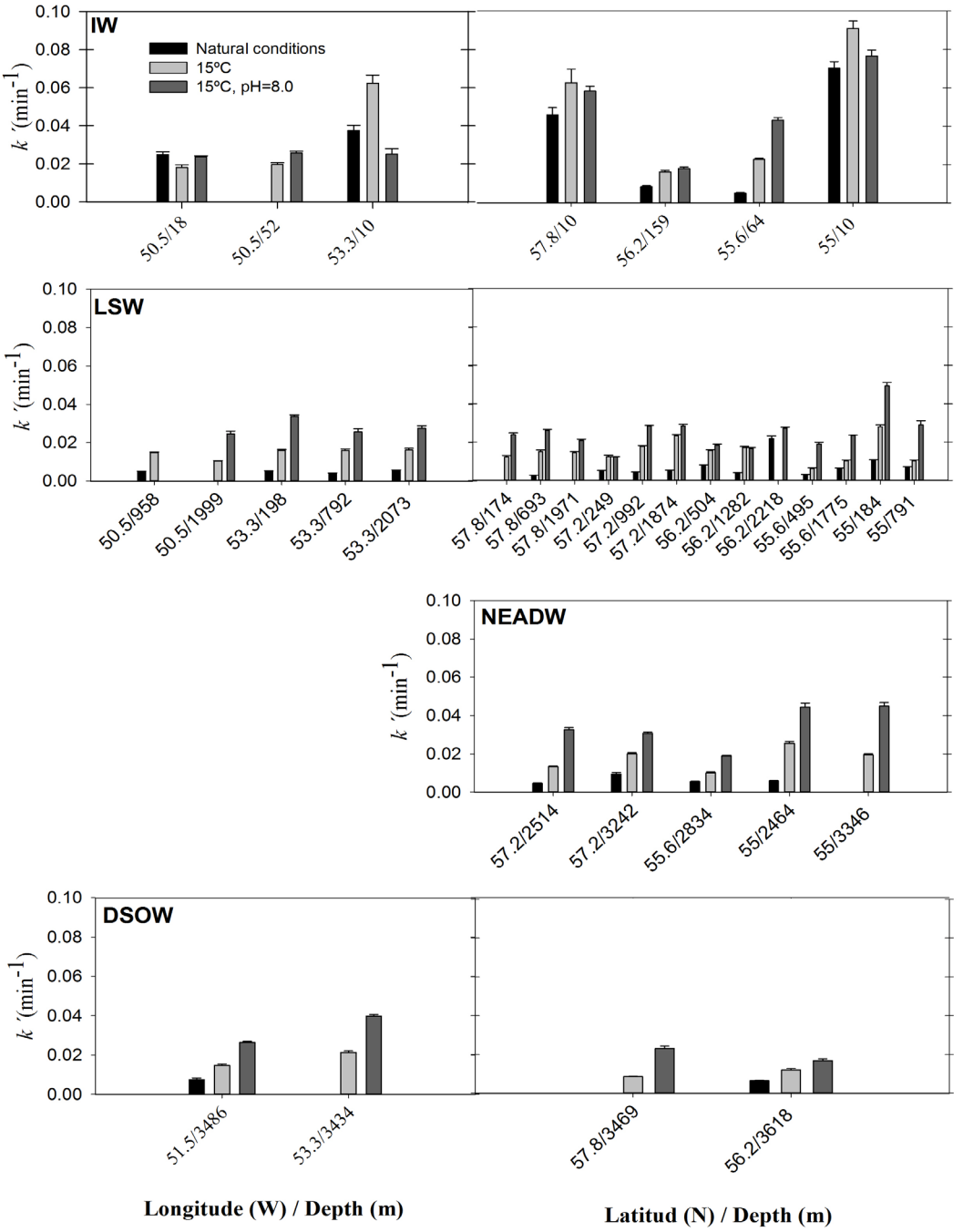


Fig. 5.4) Bar chart of *k'* ($min^{-1}$) for each transect, water mass and studied conditions.

The two transects presented higher *k'* values and variability inside the IW than the deeper water masses, with higher values in the North-South transect (Fig. 5.4), even when the temperature and pH were fixed. This indicated that TOC composition could be modulating *k'* distribution.

### *5.3.1.4. Statistical analysis*

The statistical analysis was carried out using the principal component analysis between *k'* ($min^{-1}$) and the four studied variables: temperature, $pH_F$, salinity and TOC (Table 5.3). The analysis was done for each individual variable and in subsets to understand their combined effects on the oxidation rate.

Table 5.3. Principal components analysis

| Conditions: | | Components: | | | | | | |
|---|---|---|---|---|---|---|---|---|
| Natural condition | Components: | T | pH | Sal | TOC | T+pH | T+pH+Sal | T+pH+Sal+TOC |
| | Standard Desviation | 1.243 | 1.244 | 1.217 | 1.083 | 1.502 | 1.731 | 1.772 |
| | Proportion of variance | 0.773 | 0.774 | 0.741 | 0.587 | 0.752 | 0.749 | 0.628 |
| | Cummulative proportion | 0.773 | 0.774 | 0.741 | 0.587 | 0.752 | 0.749 | 0.628 |
| 15ºC | Components: | pH | Sal | TOC | pH+Sal | pH+Sal+TOC | | |
| | Standard Desviation | 1.242 | 1.233 | 1.008 | 0.726 | 0.992 | | |
| | Proportion of variance | 0.771 | 0.760 | 0.508 | 0.176 | 0.246 | | |
| | Cummulative proportion | 0.771 | 0.760 | 0.508 | 0.906 | 0.837 | | |
| 15ºC and pH=8 | Components: | Sal | TOC | Sal+TOC | | | | |
| | Standard Desviation | 1.106 | 1.042 | 0.962 | | | | |
| | Proportion of variance | 0.611 | 0.543 | 0.308 | | | | |
| | Cummulative proportion | 0.611 | 0.543 | 0.800 | | | | |

Under in situ conditions, *k'* was strongly affected by each individual variable: temperature, $pH_F$, and salinity (between 74-77%) and by TOC (59%). When variables were coupled, it was observed that temperature and $pH_F$ could explain 75%, while the addition of salinity did not improve the fitting. However, when TOC was added, the fit was reduced to 63%. This suggests that TOC modulates the Fe(II) oxidation rate, accelerating or slowing down the process depending on its chemical characteristics. When the temperature was fixed at 15ºC, both $pH_F$ and salinity explained 73% of the *k'* variability, while TOC only the 59%. When combined, $pH_F$ and salinity explained 91% that was reduced to 84% when TOC was included, confirming again both positive and negative effects on the oxidation kinetics by the TOC. When the temperature was fixed at 15ºC and at $pH_F$ 8, salinity explained 61% of the *k'* variability, TOC a 54% whilst the combination explained 80% of the *k'* variability.

### *5.3.2. Empirical equation*

A general empirical equation (Eq. 5.13) was obtained for the Fe(II) oxidation rate in the Labrador Sea using the variables: temperature (ºC), $pH_F$ and salinity. The equation could explain 79% ($p<0.0001$) of the *k'* observed with a standard error of estimate of 0.0072 ($min^{-1}$). This same equation was also validated in the Irminger Sea (Santana-González et al., 2018), which confirms it can be used in North Atlantic model studies. The relation between measured and calculated *k'* ($min^{-1}$) is show in Fig. 5.5.

$$k'(min^{-1}) = 0.6930 - 0.0004T + 0.0003T^2 + 0.0389pH_F - 0.0287Sal \quad (5.13)$$

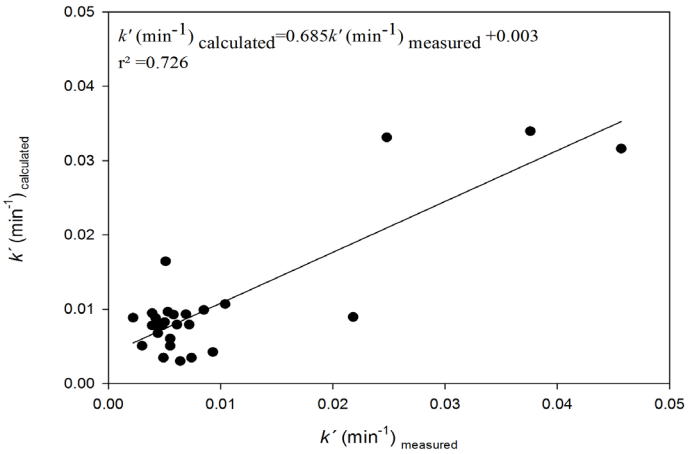


Fig. 5.5) Plot of *k'* ($min^{-1}$) measured in in situ conditions and *k'* ($min^{-1}$) calculated for the empirical equation.

### *5.3.3. Temperature dependence study*

To find out the minimum energy requirement to carry out the Fe(II) oxidative process, a temperature dependence study was carried out. Three different depths were selected (Table 5.4).

The surface sample was collected at 75 m in the IW water mass (50.354ºW, 56.865ºN, salinity of 34.759), the intermediate seawater was sampled at 1699 m in the LSW water mass (48.118ºW, 56.213ºN, salinity of 34.855) and the deepest seawater

was obtained at 3599 m in the DSOW water mass (50.354ºW, 56.865ºN, salinity of 34.895)

Table 5.4. Temperature dependece study on the Fe(II) kinetic of oxidation

.

| Sample | $pH_F = 7.7$ | $pH_F = 8.0$ |
|---|---|---|
| Surface | $\ln k' = -7178.17T^{-1}+19.85$<br>$r^2=0.991$<br>Ea= 60 kJ $mol^{-1}$ | $\ln k' = -10699.73T^{-1}+33.79$<br>$r^2=0.998$<br>Ea= 89 kJ $mol^{-1}$ |
| Intermediate | $\ln k' = -9910.14T^{-1}+30.24$<br>$r^2=0.998$<br>Ea= 82 kJ $mol^{-1}$ | $\ln k' = -9716.03T^{-1}+29.87$<br>$r^2=0.998$<br>Ea= 81 kJ $mol^{-1}$ |
| Deep | $\ln k' = -8582.20T^{-1}+25.83$<br>$r^2=0.999$<br>Ea= 71 kJ $mol^{-1}$ | $\ln k' = -9619.84T^{-1}+29.77$<br>$r^2=0.995$<br>Ea= 80 kJ $mol^{-1}$ |

The surface and deep samples were collected at the same station, but the intermediate sample was located 2 degrees eastern than the other two. All the kinetic studies were done at fixed $pH_F$ 7.7 and 8.0 and temperatures of 2, 5, 7.5, 10, 12.5 and 15ºC (Fig. 5.6).

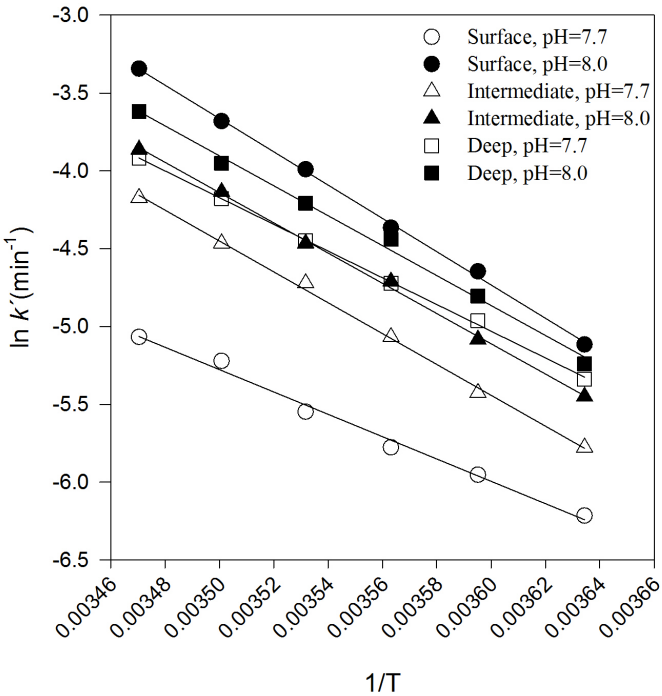


Fig. 5.6) Plot of ln *k'* ($min^{-1}$) and temperature (1/K $T^{1}$) for the kinetic studies in surface, intermediate and bottom water at $pH_F$ 7.7 and 8.0.

The Energy of activation was obtained by the Arrhenius equation (Arrhenius, 1889) (Eq. 5.14-5.15)

$$K = Ae^{\frac{-Ea}{RT}} \quad (5.14)$$

$$\text{and } LnK = LnA - \frac{Ea}{RT} \quad (5.15)$$

The Ea is an indicator of the mechanism that controls Fe(II) oxidation in seawater and indicates the minimum energy required to carry out the chemical oxidation process (Arrhenius, 1889). This study provides new knowledge on the oxidation processes of Fe(II) in the surface (IW), intermediate (LSW) and deep waters (DSOW) in the Labrador Sea. The Energy of activation (Ea) was 60, 82 and 71 kJ $mol^{-1}$ at $pH_F$=7.70 and 89, 81 and 80 kJ $mol^{-1}$ at $pH_F$ 8.00 for the surface, intermediate and deep water, respectively. The LSW sample presented similar Ea at both pH values. However, Ea for samples from the IW and DSOW fixed at pH 7.70 were 32% and 11% lower than those fixed at pH 8.00, respectively.

These results suggest that the mechanism controlling Fe(II) oxidation in surface, intermediate and deep seawater is not too different. The differences observed with pH could be related to changes in the Fe(II) species contribution to the kinetic process at pH between 7.7-7.8 (Santana-Casiano et al., 2006). $Fe^{2+}$ species predominate at pH lower than 7.7-7.8. At pH higher than 7.7-7.8, $Fe(OH)_2$ is the most important species controlling the Fe(II) oxidation rate (Santana-Casiano et al., 2006). Moreover, the differences in pH could affect the organic speciation and the corresponding complexation (Santana-Casiano et al., 2006).

### *5.3.4. Organic matter contribution to the Fe(II) oxidation kinetics*

The Fe(II) theoretical inorganic oxidation rate was computed by applying the Santana-Casiano et al. (2005) model at 15ºC. The values used in this study are presented in Table 5.5. The differences between measured *k'* and theoretical *k'* for each step were calculated. These differences quantify the organic effect on the Fe(II) oxidation after removing the effect of temperature (first step) and the effects of changes in pH and in the inorganic speciation due to the carbonate contribution (second and third steps). The difference between the measured *k'* and the theoretically calculated ($k'_{Ti}$) by the

Table 5.5. Stability constants (*K*) for the formation of Fe(II) and Fe(III) inorganic complexes and individual oxidation rate constants (*k*) considered in the kinetic model at 15ºC (after González-Davila et al. (2005) and Santana-Casiano et al. (2005)).

| Eq | Species | Log *K(k) (15ºC)* |
|---|---|---|
| 1 | $H_2O \leftrightarrow H^+ + OH^-$ | -13.98 |
| 2 | $CO_2 + H_2O \leftrightarrow HCO_3^- + H^+$ | -5.94 |
| 3 | $HCO_3^- \leftrightarrow CO_3^{2-} + H^+$ | -9.46 |
| 4 | $Na^+ + HCO_3^- \leftrightarrow NaHCO_3$ | -0.53 |
| 5 | $Na^+ + CO_3^{2-} \leftrightarrow NaCO_3^-$ | -0.42 |
| 6 | $Ca^{2+} + HCO_3^- \leftrightarrow CaHCO_3^+$ | 0.33 |
| 7 | $Ca^{2+} + CO_3^{2-} \leftrightarrow CaCO_3$ | 2.02 |
| 8 | $Mg^{2+} + HCO_3^- \leftrightarrow MgHCO_3^+$ | 0.28 |
| 9 | $Mg^{2+} + CO_3^{2-} \leftrightarrow MgCO_3$ | 1.88 |
| 10 | $2Mg^{2+} + CO_3^{2-} \leftrightarrow Mg_2(CO_3)^{2+}$ | 2.59 |
| 11 | $Mg^{2+} + OH^+ \leftrightarrow MgOH^+$ | 1.80 |
| 12 | $Fe^{2+} + HCO_3^- \leftrightarrow FeHCO_3^+$ | 0.97 |
| 13 | $Fe^{2+} + CO_3^{2-} \leftrightarrow FeCO_3$ | 4.21 |
| 14 | $Fe^{2+} + 2CO_3^{2-} \leftrightarrow Fe(CO_3)_2$ | 6.16 |
| 15 | $Fe^{2+} + CO_3^{2-} + OH^- \leftrightarrow Fe(CO_3)(OH)^-$ | 8.97 |
| 16 | $Fe^{2+} + H_2O \leftrightarrow Fe(OH)^+ + H^+$ | -9.99 |
| 17 | $Fe^{2+} + 2H_2O \leftrightarrow Fe(OH)_2 + 2H^+$ | -21.60 |
| 18 | $Fe^{2+} + Cl^- \leftrightarrow FeCl^+$ | -0.12 |
| 19 | $Fe^{2+} + SO_4^{2-} \leftrightarrow FeSO_4$ | 0.84 |
| 20 | $H^+ + SO_4^{2-} \leftrightarrow HSO_4^-$ | -0.92 |
| 21 | $Fe^{2+} + O_2 \rightarrow Fe(III) + O_2^{\cdot-}$ | 0.06 |
| 22 | $FeHCO_3^- + O_2 \rightarrow Fe(III) + O_2^{\cdot-}$ | -1.30 |
| 23 | $FeCO_3 + O_2 \rightarrow Fe(III) + O_2^{\cdot-}$ | 0.26 |
| 24 | $Fe(CO_3)_2^{2-} + O_2 \rightarrow Fe(III) + O_2^{\cdot-}$ | 2.96 |
| 25 | $FeCO_3OH^- + O_2 \rightarrow Fe(III) + O_2^{\cdot-}$ | 1.40 |
| 26 | $FeOH^+ + O_2 \rightarrow Fe(III) + O_2^{\cdot-}$ | 2.24 |
| 27 | $Fe(OH)_2 + O_2 \rightarrow Fe(III) + O_2^{\cdot-}$ | 4.72 |
| 28 | $FeCl^+ + O_2 \rightarrow Fe(III) + O_2^{\cdot-}$ | -2.70 |
| 29 | $FeSO_4 + O_2 \rightarrow Fe(III) + O_2^{\cdot-}$ | -2.70 |
| 30 | $Fe^{2+} + H_2O_2 \rightarrow Fe(III) + OH^{\cdot-}$ | 1.95 |
| 31 | $FeHCO_3^- + H_2O_2 \rightarrow Fe(III) + OH^{\cdot-}$ | 1.30 |
| 32 | $FeCO_3 + H_2O_2 \rightarrow Fe(III) + OH^{\cdot-}$ | 4.10 |
| 33 | $Fe(CO_3)_2^{2-} + H_2O_2 \rightarrow Fe(III) + OH^{\cdot-}$ | 6.55 |
| 34 | $FeCO_3OH^- + H_2O_2 \rightarrow Fe(III) + OH^{\cdot-}$ | 2.18 |
| 35 | $FeOH^+ + H_2O_2 \rightarrow Fe(III) + OH^{\cdot-}$ | 6.25 |
| 36 | $Fe(OH)_2 + H_2O_2 \rightarrow Fe(III) + OH^{\cdot-}$ | 9.10 |
| 37 | $FeCl^+ + H_2O_2 \rightarrow Fe(III) + OH^{\cdot-}$ | 1.25 |
| 38 | $FeSO_4 + H_2O_2 \rightarrow Fe(III) + OH^{\cdot-}$ | 0.78 |
| 39 | $Fe(III) + O_2^{\cdot-} \rightarrow Fe^{2+} + O_2$ | 7.95 |
| 40 | $Fe^{2+} + O_2^{\cdot-} \rightarrow Fe(III) + H_2O_2$ | 3.70 |
| 41 | $FeCO_3 + O_2^{\cdot-} \rightarrow Fe(III) + H_2O_2$ | 2.57 |
| 42 | $Fe(CO_3)_2^{2-} + O_2^{\cdot-} \rightarrow Fe(III) + H_2O_2$ | 9.00 |
| 43 | $FeOH^+ + O_2 \rightarrow Fe(III) + H_2O_2^-$ | 4.55 |
| 44 | $Fe(OH)_2 + O_2 \rightarrow Fe(III) + H_2O_2^-$ | 8.18 |
| 45 | $Cu(II) + O_2^{\cdot-} \rightarrow Cu(I) + O_2$ | 8.34 |
| 46 | $Cu(I) + O_2^{\cdot-} \rightarrow Cu(II) + H_2O_2$ | 9.00 |

Table 5.6. Effect of the organic matter on Fe(II) oxidation kinetics (*k'* in $min^{-1}$) calculated from the inorganic model after Santana-Casiano et al. (2005).

| | | *Experimental rates* | | | Calculated $C_T$ | | | *Theoretical model rates* | | | | Single effect | | | Theoretical expected values | | $k'_{T_{ox}}$ - $k'_{T_{ox}}$ | | |
|---|---|---|---|---|---|---|---|---|---|---|---|---|---|---|---|---|---|---|---|
| St | Depth (m) | $k_T'$ in situ | $k_T'$ T15ºC $pH_T$ | $k_T'$ T15ºC $pH_T$=8 | $C_T$ T15ºC, $pH_{ox}$ | $C_T$ T15ºC, $pH_{ESS}$ | $C_T$ T15ºC, $pH_T$=8 | $k_T'$ Eq 1 | $k_{T1}'$ T15ºC $pH_{ox}$ | $k_{T2}'$ T15ºC $pH_{ESS}$ | $k_{T3}'$ T15ºC $pH_T$=8 | T $k_T'$-$k_T'$ | Speciation 2ª step $k_{T2}'$-$k_{T1}'$ | Speciation 3ª step $k_{T3}'$-$k_{T2}'$ | $k'$ 2ª Cond $k_T'+(k_{T2}'-k_{T1}')= k'_{Tox}$ | $k'$ 3ª Cond $k_T'+(k_{T3}'-k_{T2}')= k'_{Tox}$ | 1ª step $k_T'$ - $k_T'$ | 2ª step $k_T'$ - $k'_{Tox}$ | 3ª step $k_T'$ - $k'_{Tox}$ |
| 3635 | 1999 | | 0.010 | 0.024 | 2287.2 | 2182.9 | 2146.5 | | 0.043 | 0.066 | 0.084 | | 0.023 | | | | | | |
| 3635 | 958 | 0.004 | 0.014 | | 2227.1 | 2191.0 | 2143.5 | 0.027 | 0.070 | 0.061 | 0.084 | 0.023 | -0.009 | 0.014 | 0.018 | 0.041 | -0.013 | -0.004 | |
| 3635 | 52 | | 0.020 | 0.026 | 2189.6 | 2199.1 | 2142.9 | | 0.091 | 0.057 | 0.083 | | -0.033 | | | | | | |
| 3635 | 18 | 0.025 | 0.018 | 0.024 | 2135.3 | 2116.6 | 2143.1 | 0.086 | 0.117 | 0.098 | 0.083 | 0.062 | -0.020 | -0.034 | 0.067 | 0.053 | -0.068 | -0.049 | -0.029 |
| 3636 | 3484 | 0.007 | 0.015 | 0.026 | 2239.3 | 2210.1 | 2147.5 | 0.062 | 0.070 | 0.055 | 0.084 | 0.055 | -0.015 | 0.014 | 0.047 | 0.076 | -0.048 | -0.033 | -0.050 |
| 3638 | 3433 | | 0.021 | 0.040 | 2241.1 | 2186.0 | 2141.5 | | 0.065 | 0.062 | 0.083 | | -0.003 | | | | | | |
| 3638 | 2073 | 0.006 | 0.016 | 0.028 | 2214.4 | 2180.6 | 2142.7 | 0.034 | 0.077 | 0.065 | 0.083 | 0.029 | -0.011 | 0.007 | 0.023 | 0.041 | -0.018 | -0.007 | -0.013 |
| 3638 | 791 | 0.004 | 0.016 | 0.026 | 2194.3 | 2171.3 | 2134.1 | 0.024 | 0.084 | 0.065 | 0.083 | 0.020 | -0.019 | -0.001 | 0.006 | 0.024 | -0.008 | 0.010 | 0.002 |
| 3638 | 198 | 0.005 | 0.016 | 0.034 | 2251.9 | 2183.3 | 2139.5 | 0.029 | 0.054 | 0.063 | 0.083 | 0.024 | 0.008 | 0.029 | 0.037 | 0.058 | -0.013 | -0.021 | -0.024 |
| 3638 | 10 | 0.038 | 0.062 | 0.025 | 2119.9 | 2106.3 | 2139.2 | 0.116 | 0.122 | 0.191 | 0.084 | 0.079 | 0.069 | -0.038 | 0.185 | 0.078 | -0.054 | -0.123 | -0.053 |
| 3640 | 3467 | | 0.008 | 0.023 | 2219.5 | 2236.4 | 2149.1 | | 0.083 | 0.046 | 0.084 | | -0.037 | | | | | | |
| 3640 | 1971 | | 0.014 | 0.021 | 2212.1 | 2206.9 | 2142.9 | | 0.078 | 0.054 | 0.083 | | -0.024 | | | | | | |
| 3640 | 692 | 0.002 | 0.015 | 0.026 | 2205.6 | 2191.6 | 2140.3 | 0.014 | 0.081 | 0.059 | 0.083 | 0.011 | -0.021 | 0.003 | -0.008 | 0.016 | 0.001 | 0.023 | 0.010 |
| 3640 | 168 | | 0.012 | 0.023 | 2187.7 | 2194.9 | 2139.8 | | 0.091 | 0.058 | 0.083 | | -0.033 | | | | | | |
| 3640 | 9 | 0.046 | 0.062 | 0.058 | 2136.7 | 2126.4 | 2149.1 | 0.139 | 0.117 | 0.096 | 0.084 | 0.093 | -0.021 | -0.033 | 0.118 | 0.106 | -0.076 | -0.055 | -0.048 |
| 3642 | 3242 | 0.009 | 0.020 | 0.031 | 2234.4 | 2185.5 | 2147.3 | 0.070 | 0.071 | 0.065 | 0.084 | 0.061 | -0.006 | 0.013 | 0.065 | 0.083 | -0.050 | -0.045 | -0.052 |
| 3642 | 2509 | 0.004 | 0.013 | 0.032 | 2197.1 | 2181.8 | 2143.9 | 0.027 | 0.090 | 0.065 | 0.084 | 0.023 | -0.024 | -0.006 | 0.003 | 0.021 | -0.014 | 0.010 | 0.011 |
| 3642 | 1874 | 0.005 | 0.023 | 0.028 | 2189.2 | 2179.4 | 2144.1 | 0.032 | 0.093 | 0.067 | 0.084 | 0.026 | -0.027 | -0.010 | 0.005 | 0.022 | -0.008 | 0.018 | 0.006 |
| 3642 | 992 | 0.004 | 0.018 | 0.028 | 2206.2 | 2179.4 | 2139.5 | 0.026 | 0.080 | 0.064 | 0.083 | 0.022 | -0.016 | 0.003 | 0.011 | 0.030 | -0.009 | 0.007 | -0.001 |
| 3642 | 248 | 0.005 | 0.012 | 0.012 | 2207.4 | 2221.6 | 2136.2 | 0.030 | 0.076 | 0.046 | 0.083 | 0.025 | -0.030 | 0.007 | 0.000 | 0.037 | -0.017 | 0.013 | -0.024 |
| 3644 | 3618 | 0.006 | 0.012 | 0.017 | 2235.0 | 2192.0 | 2140.7 | 0.052 | 0.068 | 0.059 | 0.083 | 0.046 | -0.008 | 0.016 | 0.044 | 0.068 | -0.040 | -0.032 | -0.051 |
| 3644 | 2218 | 0.022 | | 0.027 | 2184.6 | 2185.3 | 2137.3 | 0.136 | 0.092 | 0.061 | 0.083 | 0.114 | -0.032 | -0.009 | 0.104 | 0.127 | | | -0.100 |
| 3644 | 1281 | 0.004 | 0.017 | 0.017 | 2207.7 | 2175.2 | 2134.7 | 0.024 | 0.076 | 0.064 | 0.083 | 0.020 | -0.012 | 0.007 | 0.012 | 0.032 | -0.007 | 0.005 | -0.015 |
| 3644 | 497 | 0.007 | 0.015 | 0.018 | 2210.0 | 2190.0 | 2135.0 | 0.044 | 0.074 | 0.058 | 0.083 | 0.037 | -0.017 | 0.009 | 0.027 | 0.053 | -0.029 | -0.012 | -0.035 |
| 3644 | 158 | 0.009 | 0.016 | 0.018 | 2202.8 | 2186.2 | 2133.5 | 0.051 | 0.077 | 0.059 | 0.083 | 0.042 | -0.019 | 0.006 | 0.032 | 0.056 | -0.034 | -0.016 | -0.038 |
| 3645 | 2833 | 0.006 | 0.010 | 0.019 | 2224.8 | 2197.0 | 2145.9 | 0.040 | 0.075 | 0.060 | 0.084 | 0.034 | -0.016 | 0.008 | 0.024 | 0.048 | -0.030 | -0.014 | -0.029 |
| 3645 | 1775 | 0.006 | 0.010 | 0.024 | 2195.4 | 2174.9 | 2142.2 | 0.039 | 0.089 | 0.068 | 0.083 | 0.032 | -0.021 | -0.006 | 0.017 | 0.033 | -0.028 | -0.007 | -0.010 |
| 3645 | 495 | 0.003 | 0.006 | 0.019 | 2237.2 | 2181.7 | 2140.9 | 0.018 | 0.063 | 0.064 | 0.083 | 0.015 | 0.001 | 0.021 | 0.019 | 0.039 | -0.012 | -0.013 | -0.020 |
| 3645 | 64 | 0.005 | 0.023 | 0.043 | 2183.6 | 2178.2 | 2140.4 | 0.025 | 0.090 | 0.065 | 0.083 | 0.020 | -0.025 | -0.007 | 0.000 | 0.018 | -0.002 | 0.023 | 0.025 |
| 3646 | 3346 | | 0.019 | 0.045 | 2241.0 | 2188.4 | 2145.4 | | 0.066 | 0.063 | 0.084 | | -0.003 | | | | | | |
| 3646 | 2463 | 0.006 | 0.026 | 0.044 | 2185.3 | 2189.2 | 2145.3 | 0.039 | 0.099 | 0.063 | 0.084 | 0.033 | -0.036 | -0.016 | 0.002 | 0.023 | -0.013 | 0.023 | 0.021 |
| 3646 | 791 | 0.007 | 0.010 | 0.029 | 2197.6 | 2182.2 | 2139.6 | 0.042 | 0.085 | 0.063 | 0.083 | 0.035 | -0.022 | -0.002 | 0.020 | 0.040 | -0.032 | -0.010 | -0.011 |
| 3646 | 184 | 0.010 | 0.028 | 0.049 | 2193.7 | 2177.9 | 2138.1 | 0.061 | 0.086 | 0.064 | 0.083 | 0.051 | -0.022 | -0.003 | 0.039 | 0.058 | -0.033 | -0.011 | -0.009 |
| 3646 | 9 | 0.070 | 0.091 | 0.077 | 2115.6 | 2119.9 | 2168.9 | 0.188 | 0.119 | 0.092 | 0.084 | 0.118 | -0.027 | -0.034 | 0.161 | 0.154 | -0.097 | -0.070 | -0.077 |

inorganic model (Santana-Casiano et al., 2005) (see Table 5.6 and section 5.2.3.6) are represented in Fig 5.7. The differences obtained showed the average contribution of the organic ligands on the Fe(II) oxidation kinetics. A positive value indicates that the organic ligands accelerate the oxidation rate while a negative one, indicates that the organic ligands slowed down the oxidation of Fe(II). However, the obtained signal indicated the predominance of one type of ligands versus another at the selected sample.

In the first step, only the temperature was corrected, using Eq 5.1 ($k_T$'). All other parameters, such as pH and $C_T$ changed due to aerating the samples and modifies the $k$' values ($k_{T1}$') (Table 5.6). After the first step, differences between measured $k_2$´ (2nd condition) and $k'_T$ in Eq 5.1 produced negatives values in all samples and transects (from -0.002 to -0.097). Only the sample at St 3640 presented a positive value close to 0 (+0.001). This sample is located in the intersection between both transects and it also presented a positive value for the second and third steps (See Table 5.6).

In the second step, the temperature was corrected to 15ºC and the pH and $C_T$ were changed accordingly to the second conditions, but they were not fixed to a constant value. The $k_{T2}$' values presented different trends depending on the location of the samples (Table 5.6 and in Fig 5.7A and B). Samples collected close to Greenland (St 3635-3638 and 3644-3646), presented negatives differences (experimental minus $k'_{T2}$) from -0.004 to -0.123 (with the exception of the sample located at St 3645 (+0.023) in surface and in St 3646 (+0.023) in the NEADW). In the intersection between both transects (st 3638 to 3644) positive differences (from 0.007 to 0.023) indicated an acceleration in the Fe(II) oxidation rate. However, the values also included effects in pH and $C_T$ together with organic ligand content and composition, and cannot be compared among them.

After the third step, the temperature, pH and $C_T$ were corrected and fixed to a constant value, and the difference between theoretical and experimental values (third condition) removed the inorganic kinetics component in the Fe(II) oxidation. In Table 5.6 and Fig 5.7 C and D the predominance in negative values (blue colors) is observed in most of the studied area (from -0.001 to -0.100), indicating a reduction in the oxidation rates related to the presence of organic ligands. The resulting value informs about the balance between the synergetic and antagonistic effects of the organic ligands on the oxidation kinetics at each sample. Part of these computed values could be related to changes in salinity observed in the samples. To account for this salinity effect, (on average 0.3 units with a maximum of 0.5 units), Eq 5.16 by Santana-Casiano et al. (2005) was applied.

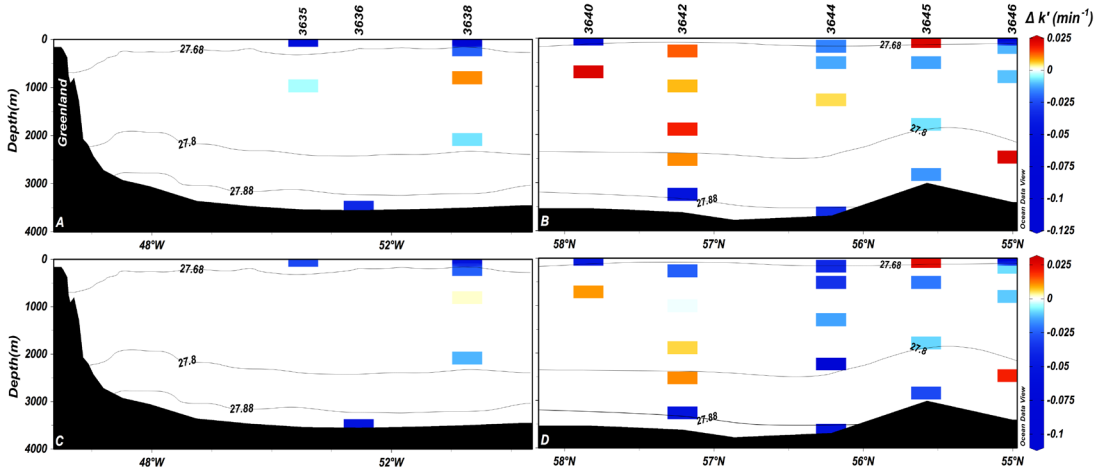


Fig 5.7) East-West transect (A and C) and North–South transect (B and D) for the difference between measured and theoretical Fe(II) oxidation rate after fixing the temperature to 15ºC (first step) and the corresponding $pH_F$ and $C_T$ in the 2nd condition (second step) (A and B) and after the normalization to a constant temperature of 15ºC and $pH_F$ 8 (third step) (C and D) obtained in the 3rd condition.

$$Log\ k' = \mathrm{Log}\, k_0^* - 1.54I^{1/2} + 0.59I \qquad (5.16)$$

Where the ionic strength (I) was calculated by $I=0.0199S/((1\text{-}10^{-3})\ S))$ and the $k_0^*$ is the log of $K_0$ in pure water, $k_0^* = 16.37$ at 15ºC.

The ionic strength effect contributed with a maximum of 0.007 $min^{-1}$ per salinity unit. Therefore, the difference between measured and theoretically calculated $k'_T$ were related to the organic ligands effect.

### *5.4. Discussion*

The studies of Fe(II) oxidation kinetic measured under three different sets of conditions allowed to determine *k'* and $t_{1/2}$ for Fe(II) in the Labrador Sea. For in situ conditions, the dependence of *k'* with the T, pH and salinity agreed with previous reported laboratory studies (Millero and Izaguirre, 1989; Millero et al., 1987b; Santana-Casiano et al., 2005), where the Fe(II) oxidation rate increased with temperature and $pH_F$, but decrease with salinity. An empirical equation to obtain a first estimation of *k'*

($min^{-1}$) from the in situ conditions that can be easily used by modelers to predict Fe distribution in the Labrador Sea was determined. This equation is also valid for the Irminger region (Santana-González et al., 2018) in the North Atlantic Ocean.

In this study, both positive and negative effects of TOC on the Fe(II) rate constant were observed. It suggests that the characteristics of the organic matter could be influencing the oxidation of Fe(II). Previous studies carried out by Lee et al. (2017); Lee et al. (2016) and Craig et al. (2009) reported that organic matter plays an important role in controlling the oxidation of Fe(II). Roy and Wells (2011) associated this effect to the differences in the chemical nature and origin of natural Fe(III)-complexing organic ligands. In the LS, the highest variations in *k'* values were observed for surface samples. This is similar to the reports from surface waters of the Eastern Subarctic Pacific by Roy and Wells (2011) and in the Irminger Sea (Santana-González et al., 2018), where strong Fe(III)-complexing organic ligands were more abundant than in the deep waters.

The chemical characteristics of each water mass and its position in a spatial distribution of the samples also affected theirs *k'*. In both East-West and North-South transects, the highest *k'* values were observed for IW and it decreased with depth. For the three studied conditions, *k'* increased from East to West and from North to South. Exceptions were noticed in in situ conditions for IW, temperature fixed for DSOW and fixed at both temperature and $pH_F$ for LSW and DSOW, in which *k'* increases from South to North. The studied area included oceanic samples through the whole water column, with different mixes of organic matter both in origin and chemical characteristics. The organic matter could provide a variety of interactions between Fe(II) with the multiple organic ligands present in the solution that affect both Fe(II)-L and Fe(III)-L species. This is in accordance with the observations made in a study of the complexation and redox buffering of Fe(II) by dissolved organic matter (Daugherty et al., 2017).

In the Labrador Sea, Ea values were inside a standard deviation of ±10 kJ $mol^{-1}$ at pH 7.7 and ±1 to pH 8 for surface, intermediate and deep waters. The obtained values are similar to those reported for the Northeast Atlantic of 88±2 kJ $mol^{-1}$ and 89.83±3.80 kJ $mol^{-1}$ (González et al., 2010; Samperio-Ramos et al., 2016). They differ from values from the Gulf Stream of 45 kJ $mol^{-1}$ (Santana-Casiano et al., 2005) and 29±2 kJ $mol^{-1}$ (Millero et al., 1987a; Millero et al., 1987b), and also from the Atlantic Subarctic Sea that ranged from 105 to 218 kJ $mol^{-1}$ (Santana-González et al., 2018). The small range in the values observed in the LS suggest that the oxidation could be affected by the composition of the organic ligands found in the area, but the resulting effects on the kinetic mechanism are compensated. The differences in Ea with pH are related to

changes in the inorganic speciation of Fe(II) around pH 7.7.

The developed method accounts for the organic matter contribution to the Fe(II) oxidation kinetics study in the LS providing a first quantitative estimation of the organic ligands effects in the ocean. The positive or negative effects observed should be interpreted as the predominance of the sum of the different organic ligands characteristics that bound Fe(II) and Fe(III) affecting the Fe(II) oxidation rate. A negative balance was observed in most of the LS, which indicated the predominance of ligands that slow down the Fe(II) oxidation rate (the opposite is observed when the balance is positive). The positive values obtained at St 3645 and 3646 for the NEADW and IW, respectively, are located in the last stations inside the LS and they could be related to the influence of Irminger Sea in the introduction of organic matter, because the current system in the LS could be spreading any organic matter from other part of the LS or even it could provide organic matter external to the LS. The contribution of organic ligands on Fe(II) oxidation rate is affected by their individual chemical characteristics, concentrations, the strength with which they can complex Fe(II) and Fe(III) but also the effect that those organic ligands that bond Fe(III) could favor the reduction of Fe(III) to Fe(II). The spatial distribution in the difference between measured vs. theoretical *k'* values indicated the organic matter effect is more effective in the surface waters and close to the coastal, while in the open LS the Fe(II) oxidation rate followed the expected values for the inorganic complexation models of Santana-Casiano et al. (2005) (Table 5.6). The application of the kinetic model appears as a very important tool in determining the global organic ligands contribution to the Fe(II) oxidation kinetics. However, the identity and type of organic ligands present in the different seawater masses that slow down the Fe(II) oxidation rate are still unknown.

## *5.5. Conclusion*

The Fe(II) oxidation kinetic studies carried out in 2016 in the Labrador Sea show that temperature, pH and salinity are the master variables controlling the Fe(II) oxidation kinetic under in situ conditions. The sources and characteristics of the organic matter are important factors influencing the oxidation of Fe(II), displaying both positive and negative effects on the Fe(II) oxidation rate. The Fe(II) oxidative process presented a similar pattern for surface, intermediate and deep waters. In this work, a general equation is obtained which allows computation of *k'* while considering the effect of temperature, pH and salinity under in situ conditions. It is valid for the North Atlantic and can be incorporated into global Fe models. A novel approach was applied in this work to account for the role played by the organic ligands on the Fe(II)

oxidation kinetics which needs values of both pH and total dissolved inorganic carbon. The comparison between experimental data with inorganic Fe(II) complexation models revealed an important contribution of organic matter retarding the oxidation of Fe(II) at surface and close to coastal areas. In the open ocean, below the photic zone, the values were similar to those controlled by the inorganic Fe(II) oxidation rates.

**Acknowledgements**

This work was supported by the Ministerio de Economía y Competitividad of the Spanish Government, through the EACFe (CTM2014-52342-P) and ATOPFe (CTM2017-83476-P) projects. CS-G was funded by the Spanish Grant BES-2015-071245. This work was completed while CS-G was a PhD student in the IOCAG Doctoral Program in Oceanography and Global Change. Special thanks go to David González-Santana for his comments and English revision and to the crew and captain of Akademik Ioffe. SG and AS were supported by RFBR grant No. 18-05-00194 and by RSF grant No. 14-17-00697.

## *References*

Arístegui, J.D., Carlos M.; Reche, Isabel; Gómez-Pinchetti, Juan L., 2014. Krill Excretion Boosts Microbial Activity in the Southern Ocean. PLOS ONE, 9(2).

Arrhenius, S., 1889. Über die Dissociationswärme und den Einfluss der Temperatur auf den Dissociationsgrad der Elektrolyte. Zeitschrift für physikalische Chemie, 4(1): 96-116.

Azetsu-Scott, K., Jones, E.P., Yashayaev, I., Gershey, R.M., 2003. Time series study of CFC concentrations in the Labrador Sea during deep and shallow convection regimes (1991–2000). Journal of Geophysical Research: Oceans, 108(C11): n/a-n/a.

Bowie, A.R., Achterberg, E.P., Mantoura, R.F.C., Worsfold, P.J., 1998. Determination of sub-nanomolar levels of iron in seawater using flow injection with chemiluminescence detection. Analytica Chimica Acta, 361(3): 189-200.

Bruland, K.W.R., E. L., 2001. Analytical methods for the determination of concentrations and speciation of iron. In: (Eds.), I.D.R.T.K.A.H. (Ed.), The biogeochemistry of iron in sea water (IUPAC Series on Analytical and Physical Chemistry of Environmental Systems). John Wiley & Sons Ltd., pp. 255.

Burns, J.M., Craig, P.S., Shaw, T.J., Ferry, J.L., 2010. Multivariate Examination of Fe(II)/Fe(III) Cycling and Consequent Hydroxyl Radical Generation. Environmental Science & Technology, 44(19): 7226-

7231.

Burns, J.M., Craig, P.S., Shaw, T.J., Ferry, J.L., 2011. Short-Term Fe Cycling during Fe(II) Oxidation: Exploring Joint Oxidation and Precipitation with a Combinatorial System. Environmental Science & Technology, 45(7): 2663-2669.

Campbell, J., Yeats, P., 1982. The distribution of manganese, iron, nickel, copper and cadmium in the waters of Baffin-Bay and the Canadian arctic archipelago. Oceanologica Acta, 5(2): 161-168.

Cota, G.F., Harrison, W.G., Platt, T., Sathyendranath, S., Stuart, V., 2003. Bio-optical properties of the Labrador Sea. Journal of Geophysical Research: Oceans, 108(C7).

Craig, P.S., Shaw, T.J., Miller, P.L., Pellechia, P.J., Ferry, J.L., 2009. Use of Multiparametric Techniques To Quantify the Effects of Naturally Occurring Ligands on the Kinetics of Fe(II) Oxidation. Environmental Science & Technology, 43(2): 337-342.

Croot, P.L., Laan, P., 2002. Continuous shipboard determination of Fe(II) in polar waters using flow injection analysis with chemiluminescence detection. Analytica Chimica Acta, 466(2): 261-273.

Crusius, J., Schroth, A.W., Resing, J.A., Cullen, J., Campbell, R.W., 2017. Seasonal and spatial variability in northern Gulf of Alaska surface-water iron concentrations driven by shelf sediment resuspension, glacial meltwater, a Yakutat eddy, and dust. Global Biogeochemical Cycles: n/a-n/a.

Daugherty, E.E., Gilbert, B., Nico, P.S., Borch, T., 2017. Complexation and Redox Buffering of Iron(II) by Dissolved Organic Matter. Environmental Science & Technology, 51(19): 11096-11104.

Dickson, R.R., Curry, R., Yashayaev, I., 2003. Recent changes in the North Atlantic. Philosophical Transactions: Mathematical, Physical and Engineering Sciences: 1917-1934.

Filippova, A. et al., 2017. Water mass circulation and weathering inputs in the Labrador Sea based on coupled Hf–Nd isotope compositions and rare earth element distributions. Geochimica et Cosmochimica Acta, 199: 164-184.

González, A.G., Pérez-Almeida, N., Santana-Casiano, J.M., Millero, F.J., González-Dávila, M., 2016. Redox interactions of Fe and Cu in seawater. Marine Chemistry, 179: 12-22.

Gonzalez, A.G., Santana-Casiano, J.M., González-Dávila, M., Pérez-Almeida, N., Suárez de Tangil, M., 2014. Effect of Dunaliella tertiolecta organic exudates on the Fe(II) oxidation kinetics in seawater. Environmental science & technology, 48(14): 7933-7941.

González, A.G., Santana-Casiano, J.M., Pérez, N., González-Dávila, M., 2010. Oxidation of Fe(II) in natural waters at high nutrient concentrations. Environmental science & technology, 44(21): 8095-8101.

González-Davila, M., Santana-Casiano, J.M., Millero, F.J., 2005. Oxidation of iron(II) nanomolar with $H_2O_2$ in seawater. Geochimica et Cosmochimica Acta, 69(1): 83-93.

González-Dávila, M., Santana-Casiano, J.M., Millero, F.J., 2006. Competition between $O_2$ and $H_2O_2$ in the oxidation of Fe(II) in natural waters. Journal of solution chemistry, 35(1): 95-111.

Hansell, D.A., Carlson, Craig A., 2001. Biogeochemistry of total organic carbon and nitrogen in the Sargasso Sea: control by convective overturn. Deep Sea Research Part II: Topical Studies in Oceanography, 48(8-9): 18.

Hastie, T.J., Tibshirani, R.J., 1990. Generalized additive models, volume 43 of Monographs on Statistics and Applied Probability. Chapman & Hall, London.

Heller, M.I., Gaiero, D.M., Croot, P.L., 2013. Basin scale survey of marine humic fluorescence in the Atlantic: Relationship to iron solubility and $H_2O_2$. Global Biogeochemical Cycles, 27(1): 88-100.

Heller, M.I., Wuttig, K., Croot, P.L., 2016. Identifying the sources and sinks of CDOM/FDOM across the Mauritanian Shelf and their potential role in the decomposition of superoxide ($O_2^-$). Frontiers in Marine Science, 3: 132.

King, D.W., Lounsbury, H.A., Millero, F.J., 1995. Rates and mechanism of Fe(II) oxidation at nanomolar total iron concentrations. Environmental science & technology, 29(3): 818-824.

Klunder, M.B. et al., 2012. Dissolved iron in the Arctic shelf seas and surface waters of the central Arctic Ocean: Impact of Arctic river water and ice-melt. Journal of Geophysical Research: Oceans, 117(C1).

Körtzinger, A., Send, U., Wallace, D.W., Karstensen, J., DeGrandpre, M., 2008. Seasonal cycle of $O_2$ and $pCO_2$ in the central Labrador Sea: Atmospheric, biological, and physical implications. Global Biogeochemical Cycles, 22(1).

Kuma, K., Nakabayashi, S., Matsunaga, K., 1995. Photoreduction of Fe(III) by hydroxycarboxylic acids in seawater. Water Research, 29(6): 1559-1569.

Lazier, J., Hendry, R., Clarke, A., Yashayaev, I., Rhines, P., 2002. Convection and restratification in the Labrador Sea, 1990–2000. Deep Sea Research Part I: Oceanographic Research Papers, 49(10): 1819-1835.

Lee, Y.P. et al., 2017. Importance of allochthonous and autochthonous dissolved organic matter in Fe(II) oxidation: A case study in Shizugawa Bay watershed, Japan. Chemosphere.

Lee, Y.P., Fujii, M., Kikuchi, T., Terao, K., Yoshimura, C., 2017b. Variation of iron redox kinetics and its relation with molecular composition of standard humic substances at circumneutral pH. PloS one, 12(4): e0176484.

Lee, Y.P., Fujii, M., Terao, K., Kikuchi, T., Yoshimura, C., 2016. Effect of dissolved organic matter on Fe(II) oxidation in natural and engineered waters. Water Research, 103: 160-169.

Martin, J.H., Gordon, M., Fitzwater, S.E., 1991. The case for iron. Limnology and Oceanography, 36(8): 1793-1802.

McCartney, M., 1992. Recirculating components to the deep boundary current of the northern North Atlantic. Progress in Oceanography, 29(4): 283-383.

Mendes, P., 1993. GEPASI: a software package for modelling the dynamics, steady states and control of biochemical and other systems. Bioinformatics, 9(5): 563-571.

Millero, F.J., 1986. The pH of estuarine waters. Limnology and Oceanography, 31(4): 839-847.

Millero, F.J., Izaguirre, M., 1989. Effect of ionic strength and ionic interactions on the oxidation of Fe(II). Journal of Solution Chemistry, 18(6): 585-599.

Millero, F.J., Izaguirre, M., Sharma, V.K., 1987a. The effect of ionic interaction on the rates of oxidation in natural waters. Marine Chemistry, 22(2-4): 179-191.

Millero, F.J., Sotolongo, S., Izaguirre, M., 1987b. The oxidation kinetics of Fe(II) in seawater. Geochimica et Cosmochimica Acta, 51(4): 793-801.

Morel, F.M., Kustka, A., Shaked, Y., 2008. The role of unchelated Fe in the iron nutrition of phytoplankton. Limnology and Oceanography, 53(1): 400-404.

Nielsen, J., 1928. The waters around Greenland. Greenland, The Discovery of Greenland, Exploration, and the Nature of the Country, 1: 185-230.

Pickart, R.S., Torres, D.J., Clarke, R.A., 2002. Hydrography of the Labrador Sea during active convection. Journal of Physical Oceanography, 32(2): 428-457.

Pierrot, D., Lewis, E., Wallace, D., 2006. MS Excel program developed for CO2 system calculations. ORNL/CDIAC-105a. Carbon Dioxide Information Analysis Center, Oak Ridge National Laboratory, US Department of Energy, Oak Ridge, Tennessee.

Rose, A.L., Waite, T.D., 2002. Kinetic Model for Fe(II) Oxidation in Seawater in the Absence and Presence of Natural Organic Matter. Environmental Science & Technology, 36(3): 433-444.

Roy, E.G., Wells, M.L., 2011. Evidence for regulation of Fe(II) oxidation by organic complexing ligands in the Eastern Subarctic Pacific. Marine Chemistry, 127(1): 115-122.

Roy, E.G., Wells, M.L., King, D.W., 2008. Persistence of iron(II) in surface waters of the western subarctic Pacific. Limnology and Oceanography, 53(1): 89-98.

Rush, J.D., Bielski, B.H.J., 1985. Pulse radiolytic studies of the reaction of perhydroxyl/superoxide O2- with iron(II)/iron(III) ions. The reactivity of HO2/O2- with ferric ions and its implication on the occurrence of the Haber-Weiss reaction. The Journal of Physical Chemistry, 89(23): 5062-5066.

Rysgaard, S. et al., 2003. Physical conditions, carbon transport, and climate change impacts in a Northeast Greenland fjord. Arctic, Antarctic, and Alpine Research, 35(3): 301-312.

Samperio-Ramos, G., Casiano, J.M.S., Dávila, M.G., 2016. Effect of ocean warming and acidification

on the Fe (II) oxidation rate in oligotrophic and eutrophic natural waters. Biogeochemistry, 128(1-2): 19-34.

Santana-Casiano, J. et al., 2014. Characterization of phenolic exudates from Phaeodactylum tricornutum and their effects on the chemistry of Fe(II)–Fe(III). Marine chemistry, 158: 10-16.

Santana-Casiano, J., Gonzalez-Davila, M., Millero, F., 2006. The role of Fe(II) species on the oxidation of Fe (II) in natural waters in the presence of O2 and H2O2. Marine chemistry, 99(1): 70-82.

Santana-Casiano, J.M., González-Dávila, M., González, A., Millero, F., 2010. Fe(III) reduction in the presence of catechol in seawater. Aquatic geochemistry, 16(3): 467-482.

Santana-Casiano, J.M., González-Dávila, M., Millero, F.J., 2004. The oxidation of Fe(II) in NaCl–$HCO_3^-$ and seawater solutions in the presence of phthalate and salicylate ions: a kinetic model. Marine chemistry, 85(1): 27-40.

Santana-Casiano, J.M., González-Dávila, M., Millero, F.J., 2005. Oxidation of nanomolar levels of Fe(II) with oxygen in natural waters. Environmental science & technology, 39(7): 2073-2079.

Santana-Casiano, J.M., González-Dávila, M., Rodrıguez, M.J., Millero, F.J., 2000. The effect of organic compounds in the oxidation kinetics of Fe(II). Marine Chemistry, 70(1): 211-222.

Santana-González, C. et al., 2018. Fe(II) oxidation kinetics in the North Atlantic along the 59.5° N during 2016. Marine Chemistry.

Schofield, O. et al., 2010. How do polar marine ecosystems respond to rapid climate change? Science, 328(5985): 1520-1523.

Shaked, Y., Kustka, A.B., Morel, F.M., 2005. A general kinetic model for iron acquisition by eukaryotic phytoplankton. Limnol. Oceanogr, 50(3): 872-882.

Shaked, Y., Lis, H., 2012. Disassembling Iron Availability to Phytoplankton. Frontiers in Microbiology, 3: 123.

Statham, P.J., Skidmore, M., Tranter, M., 2008. Inputs of glacially derived dissolved and colloidal iron to the coastal ocean and implications for primary productivity. Global Biogeochemical Cycles, 22(3).

Steemann Nielsen, E., 1958. A survey of recent Danish measurements of the organic productivity in the sea. Rapp. Cons. Explor. Mer, 144: 92-95.

Steigenberger, S., Croot, P.L., 2008. Identifying the processes controlling the distribution of $H_2O_2$ in surface waters along a meridional transect in the eastern Atlantic. Geophysical Research Letters, 35(3).

Stramma, L. et al., 2004. Deep water changes at the western boundary of the subpolar North Atlantic during 1996 to 2001. Deep Sea Research Part I: Oceanographic Research Papers, 51(8):

1033-1056.

Straneo, F., 2006. Heat and Freshwater Transport through the Central Labrador Sea. Journal of Physical Oceanography, 36(4): 606-628.

Talley, L., McCartney, M., 1982. Distribution and circulation of Labrador Sea water. Journal of Physical Oceanography, 12(11): 1189-1205.

Team, R.C., 2016. R: A language and environment for statistical computing. R Foundation for Statistical Computing, Viena, Austria.

Theis, T.L., Singer, P.C., 1974. Complexation of iron(II) by organic matter and its effect on iron(II) oxygenation. Environmental Science and Technology, 8(6): 569-573.

Thuróczy, C.E. et al., 2011. Distinct trends in the speciation of iron between the shallow shelf seas and the deep basins of the Arctic Ocean. Journal of Geophysical Research: Oceans, 116(C10).

Trapp, J.M., Millero, F.J., 2007. The oxidation of iron(II) with oxygen in NaCl brines. Journal of Solution Chemistry, 36(11-12): 1479-1493.

Voelker, B.M., Sulzberger, B., 1996. Effects of fulvic acid on Fe(II) oxidation by hydrogen peroxide. Environmental Science & Technology, 30(4): 1106-1114.

Wu, J., Luther III, G.W., 1994. Size-fractionated iron concentrations in the water column of the western North Atlantic Ocean. Limnology and Oceanography, 39(5): 1119-1129.

Yashayaev, I., 2007a. Hydrographic changes in the Labrador Sea, 1960–2005. Progress in Oceanography, 73(3–4): 242-276.

Yashayaev, I., Holliday, N.P., Bersch, M., van Aken, H.M., 2008. The history of the Labrador Sea Water: Production, spreading, transformation and loss, Arctic–Subarctic Ocean Fluxes. Springer, pp. 569-612.

Yashayaev, I., Lazier, J.R., Clarke, R.A., 2003. Temperature and salinity in the central Labrador Sea during the 1990s and in the context of the longer-term change, ICES Mar. Sci. Symp, pp. 32-39.

Yashayaev, I., van Aken, H.M., Holliday, N.P., Bersch, M., 2007c. Transformation of the Labrador Sea water in the subpolar North Atlantic. Geophysical Research Letters, 34(22).

# Chapter VI.

# General Conclusion

The main conclusions that arise from this Thesis are:

1. The hydrothermal emissions around Tagoro submarine volcano off El Hierro island emitted high amount of TdFe(II) which distribution was inversely correlated with a decrease in pH distribution of the surrounding waters in the water column.

2. The high-resolution study along the volcanic edifice following the temporal evolution from 2013 to 2015 revealed that the magnitude of TdFe(II) was not the same in all the sampling periods, with high variability over a short time scale. The emissions continue in the area four years after cessation of the molten eruptive phase, indicating changes in the emitted fluid composition with time.

3. The Fe(II) oxidation kinetics studies in the volcanic area revealed that Fe(II) oxidation rate constants were higher than those expected in oligotrophic seawater. These rates can be explained by the different nutrient concentrations of the seawater samples, in particular silicates.

4. The Fe(II) oxidation kinetics studies carried out in the Subarctic North Atlantic and in the Labrador Sea show that temperature, pH and salinity were the master variables controlling the Fe(II) oxidation kinetics under natural conditions.

5. The studied area in Subarctic North Atlantic and Labrador Sea included coastal and oceanic samples through the whole water column. The sources and characteristics of the organic matter present were important factors influencing the oxidation of Fe(II), displaying both positive and negative effects on the Fe(II) oxidation rate. The organic matter could provide a variety of interactions between Fe(II) with the multiple organic ligands present in the solution that affect both Fe(II)-L and Fe(III)-L species.

6. The spatial distribution of the samples affected *k'* due to the chemical characteristics of each water mass and their modification as the water mass moved from basin to basin and from the surface to the deep ocean. Faster Fe(II) oxidation rates were observed within the chlorophyll maximum, in surface and coastal samples than in deep waters.

7. The energy required for Fe(II) oxidation in the Subarctic North Atlantic differs from surface to bottom waters. However it presented similar values in Labrador Sea for surface, intermediate and bottom waters. Indicating that the Fe(II) oxidation kinetic could be affected by the composition of the organic ligands and the degradation of the organic matter, which is more degraded in deep waters than in surface water. The differences observed in the Subarctic North Atlantic are associated to different characteristics in organic matter composition and degradation. Nevertheless, the similar values obtained in the Labrador Sea reveal that the organic matter for these waters presented similar composition or even the net effect of the combination in organic matter has similar result for the Fe(II) kinetics oxidation found in the area.

8. A general equation for the oxidation rate was obtained which allows computation of $k'$ taking into account the effects of temperature, pH and salinity under natural conditions for the Subarctic North Atlantic and Labrador Sea. It was able to fix the observed values to an extent of the 79% with a standard error of estimate of 0.0072 $min^{-1}$, and can be incorporated into global Fe models.

9. A novel approach was applied to the oxidation kinetics of Fe(II) in the Labrador Sea, which allowed to determine the average contribution of the organic matter over the inorganic effect. When the inorganic effect is removed the organic matter slowed down the oxidation of Fe(II) at surface and close to coastal areas. The process is affected by their individual chemical characteristics, concentrations, the strength with which they can complex Fe(II) and Fe(III) but also can be affected by the reduction of those Fe(III) organic complexes to the corresponding Fe(II) ones.

# Chapter VII.

# Future Research

The present PhD Thesis has studied the Fe(II) oxidation kinetics in different areas in the North Atlantic Ocean and Labrador Sea. These studies revel the importance of temperature, pH and salinity controlling the Fe(II) oxidation kinetics under natural conditions. However the sources and characteristics of the organic matter present influencing the oxidation of Fe(II), displaying both positive and negative effects on the Fe(II) oxidation rate. This is because the organic matter could provide a variety of interactions between Fe(II) with the multiple organic ligands present in the solution that affect both Fe(II)-L and Fe(III)-L species. However the composition and behavior on Fe(II) oxidation kinetics of the organic matter in the ocean is unknown.

The results presented in this PhD Thesis have opened a number of doors in order to continue the investigation of Fe(II) oxidation in natural waters.

Fist of all the chemical interactions and competitive mechanism of iron with other trace metals present in seawater should be thoroughly studied.

Besides, it is very important to understand the composition of organic matter in seawater, attending to the chemical characteristics of the functional groups, specially the polyphenols, aminoacids and sugars acids, which are the main organic compounds in the phytoplankton growth. These steps must go hand to hand with isolate and identification the different organic compounds present in the seawater and mesocosms. Similar to the studies carried out in our lab with the identification of the different organic compounds present phytoplankton exudates obtained from monospecific, several species cultures. For the identification of polyphenols, aminoacids and sugars acids the High Performance Liquid Chromatography (HPLC) could be apply.

With the purpose of understanding the Fe(II)-Fe(III) redox process in the presence of different organic compounds presents in seawater, a complete set of studies of Fe(II) oxidation and Fe(III) reduction more studies with individuals organic compounds under different conditions of temperature, pH, salinity, oxygen, $H_2O_2$, nutrients and light should be done.

Finally, it is necessary to develop new methodology which let to study the complexation between Fe(II) and organic compounds.

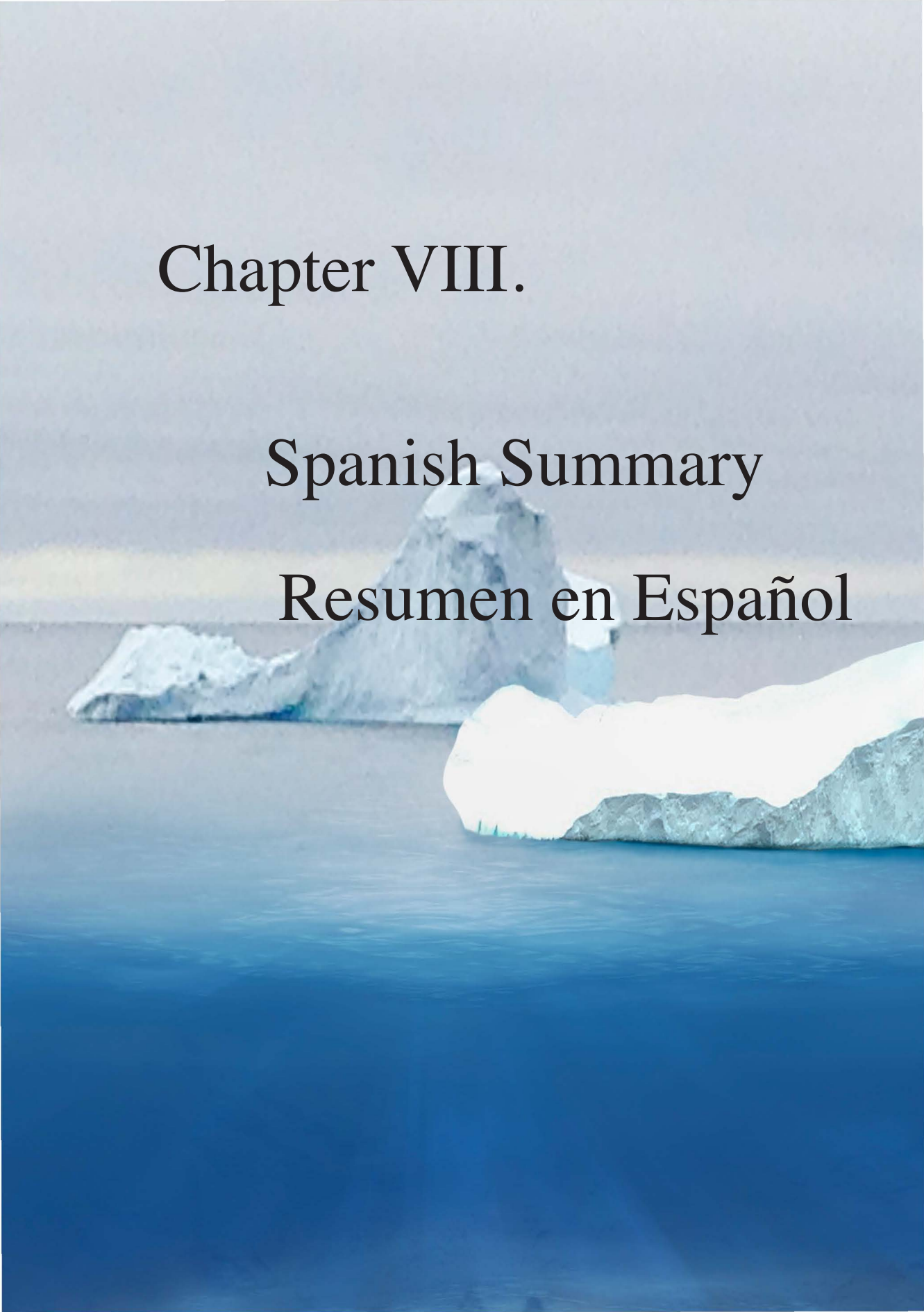

# Chapter VIII.

## Spanish Summary

## Resumen en Español

## 8.1. Introducción General

### 8.1.1. El hierro en los océanos

El hierro (Fe) es el cuarto elemento más abundante en la corteza terrestre (McDonough and Sun, 1995). Sin embargo sus concentraciones en océano abierto se encuentran en cantidades traza (< 1.0 nM) debido a su baja solubilidad en aguas óxicas (Millero, 1998).

Las mayores fuentes de hierro para el agua de mar son la deposición atmosférica, la regeneración de la plataforma continental (transporte fluvial, estuarios y sistemas costeros), resuspension de los márgenes costeros, las entradas hidrotermales y aguas subterráneas enriquecidas por afloramiento (Abadie et al., 2017; Bowie et al., 1998; Ye et al., 2009). Tagliabue et al. (2017) ha representado los principales procesos en el ciclo oceánico del hierro (figura 1.1.) que incluye las fuentes de hierro y sus procesos como absorción, degradación biológica, adsorción, desorción, precipitación y disolución.

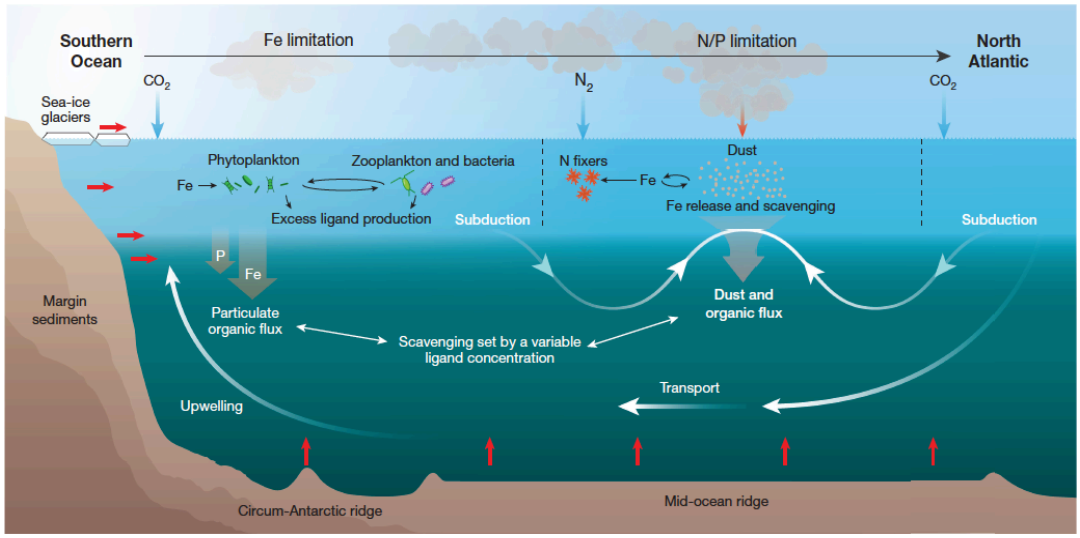


Figura 1.1. El ciclo del hierro en el océano (obtenido de Tagliabue et al. (2017))

El hierro es un micronutriente esencial para los organismos (Martin et al., 1991) y juega un papel clave en la bioquímica y fisiología del fitoplancton oceánico (Sunda et al., 1991). Tiene un papel importante como co-factor en enzimas celulares, relacionado con la fotosíntesis, transporte respiratorio de electrones (Chereskin and Castelfranco, 1982), asimilación de nitrato (Van Leeuwe et al., 1997), fijación de nitrógeno (Williams, 1981) y desintoxicación de especies reactivas de oxígeno (Sunda and Huntsman, 1995). Además, el hierro es reconocido como un micronutriente esencial que regula la magnitud y la dinámica de la productividad primaria en los océanos (Martin et al., 1991).

### *8.1.2. Fraccionamiento del hierro por tamaño*

El Fe en el agua de mar existe en una variedad de formas químicas y físicas, incluyendo complejos orgánicos disueltos, formas coloidales y unidas a partículas (Ye et al., 2009). El hierro se clasifica, de acuerdo al tamaño, en: particulado (pFe) (<0.2µm), disuelto (dFe) (<0.2µm), coloidal (cFe) (0.02-0.2µm) y soluble (sFe) (<0.02µm) (Ussher et al., 2010). El hierro total disuelto (TdFe) es la fracción de hierro excluida la particulada y el hierro total disoluble (TDFe) se corresponde con la fracción TdFe acidificada a pH 2 y analizada después de seis meses de su muestreo. La distribución de Fe se ha estudiado en diferentes océanos y mares, Atlántico, Pacífico y Mediterráneo entre otros y se incluyen en la Tabla 1.1. La concentración de hierro total disuelto para el Océano Atlántico se representa en la Figura 1.2.

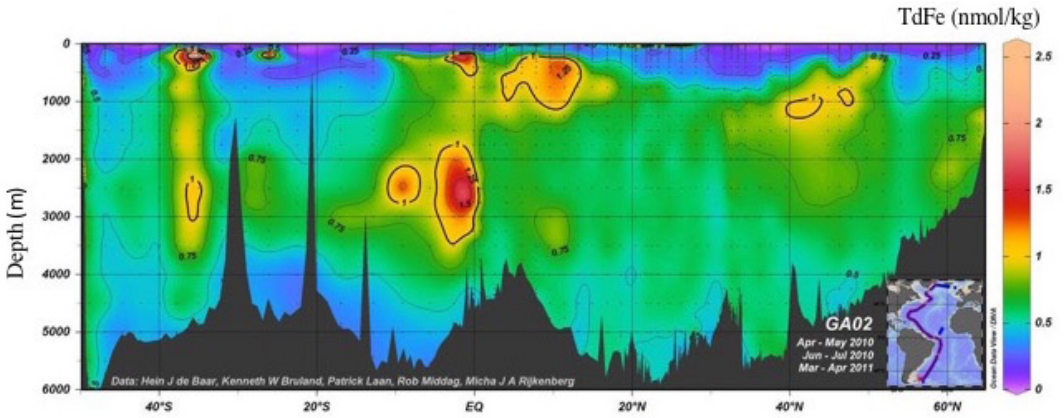


Figura 1.2. Distribución de Fe total disuelto en el Océano Atlántico (http://www.geotraces.org)

Tabla 1.1. Distribución de Fe en el océano

| | | dFe nM | sFe nM | cFe nM | pFe nM | TDFe nM | Ref. |
|---|---|---|---|---|---|---|---|
| Atlantic Ocean | Surface | 0.23–0.34 | 0.21-0.4 | 0.1-0.3 | | 0.28-1.67 | (Bergquist and Boyle, 2006; Bergquist et al., 2007; Bowie et al., 2003; Bowie et al., 2006; Bowie et al., 1998; Bowie et al., 2004; Bowie et al., 2002; Boye et al., 2006; Buck et al., 2016; Cullen et al., 2006; Fitzsimmons and Boyle, 2014; Fitzsimmons et al., 2013; Laës et al., 2003; Laës et al., 2005; Mills et al., 2004; Mohamed et al., 2011; Powell et al., 1995; Saito et al., 2013; Ussher et al., 2010; Wu et al., 2001) |
| | 1000 m | 0.62–0.86 | | | | | |
| | 2000 m | 1.19–1.12 | | | | | |
| | >2500 m | 0.71-0.79 | | | | | |
| Pacific Ocean | Surface | <1 nM | 0.05-0.4 | 0-0.8 | | | (Chase et al., 2005; Coale, 1991; Hong and Kester, 1986; Mackey et al., 2002; Nishioka et al., 2001; Resing et al., 2015; Schmidt and Hutchins, 1999; Wu et al., 2001; Wu et al., 2011). |
| | > 100 m | 5-7 up to 800 * | | | | | |
| Indian Ocean | Surface | 0.15-0.3 nM | | | | | (Nishioka et al., 2013) |
| Southern Ocean | Surface nearshore | 5.3-12.6 | | | | | (Bowie et al., 2004; Bucciarelli et al., 2001; Chever et al., 2010; De Jong et al., 1998; Klunder et al., 2011; Tagliabue et al., 2012); |
| | Mid Layer depth | 0.04-0.42 | | | | Mid Layer depth: 0.15-0.71 | |
| | Surface offshore | 0.1-0.3 | | | | | |
| | 2000-3000 | 0.6-0.7 | | | | | |
| | Deep water | 0.22-0.82 | | | | Deep water: 0.39-1.75 | |
| Artic Ocean | | 0.13-2.08[a] | | | | 0.6-63.08[b] | (Campbell and Yeats, 1982; Crusius et al., 2017; Klunder et al., 2012; Thuróczy et al., 2011; Wehrmann et al., 2014) |
| Arabian Sea | | 0.5-2.4 | | | | | (Measures and Vink, 1999) |
| Mediterranean Sea | | 0.13-4.8 | | | 0.8 - 14.5 | 0.7 -7.0 | |

* Hydrothermal, upwelling or riverine.
(a) Which increase from 4 nM in surface to >10 nM nearshore.
(b) With extreme values of 1000 nM in nearshore.

### *8.1.3. La especiación del hierro en agua de mar*

El hierro existe en dos estados de oxidación, ferroso (Fe(II)) y férrico Fe(III)) que exhiben características químicas diferentes. El Fe(II) es muy soluble, pero se oxida rápidamente en presencia de oxígeno. El Fe(III) es la especie termodinámicamente estable en aguas naturales, pero puede reducirse a Fe(II) bajo la influencia de la luz (Miller et al., 1995) y microorganismos generando una concentración significativa en estado estacionario de Fe(II) en aguas superficiales (Laglera and van den Berg, 2007).

La concentración de Fe(II) disuelto (dFe(II)) en el océano abierto es muy baja, 0.02-2 nM, debido a su rápida oxidación en alta concentración de oxígeno (González-Davila et al., 2005; Santana-Casiano et al., 2005). En las zonas de mínimos de oxígeno, las concentraciones de hierro en aguas subóxicas y anóxicas pueden ser de alrededor de 300-3000 nM. En aguas intersticiales de sedimentos marinos, las concentraciones son de aproximadamente 300 μM, mientras que los fluidos hidrotermales pueden contener hasta 3 mM de hierro disuelto (de Baar and de Jong, 2001). La presencia de sistemas de afloramiento aumenta el Fe(II) hasta 50 nM (Hong and Kester, 1986). En el Noreste del Océano Atlántico, el Fe (II) varía de <0.1 nM hasta 0.55 nM (Boye et al., 2006).

Los procesos que influyen en la especiación del hierro son la complejación orgánica, las reacciones fotoquímicas, las interacciones con los coloides y las superficies de las partículas (Weber et al., 2005). Por su parte, las diferentes entradas, reacciones químicas, asimilación biológica y procesos de remineralización modifican las concentraciones de Fe, estados redox y de agregación (Ye et al., 2009). Estos cambios en la especiación de Fe hacen que su concentración sea difícil de medir y, en muchos casos, determine, posiblemente, el tiempo de residencia del hierro en la superficie oceánica afectada por la luz, donde puede ser utilizado por el fitoplancton. A todo ello, debemos añadir que no todas las formas de hierro en el agua de mar están igualmente disponibles para su absorción por el fitoplancton (Hudson et al., 1990).

#### *8.1.3.1. Especiación inorgánica de Fe en agua de mar*

Las interacciones de Fe(II) y Fe(III) han sido examinadas con ligandos inorgánicos mayoritarios y minoritarios de las aguas naturales ($Na^+$, $Mg^{2+}$, $Ca^{2+}$, $K^+$, $Sr^{2+}$, $Cl^-$, $SO_4^{2-}$, $HCO_3^-$, $Br^-$, $CO_3^{2-}$, $B(OH)_4^-$, $B(OH)_3$, $CO_2$, $OH^-$ and $HS^-$) usando los modelos de interacción iónica específica y los modelos de par iónico (Millero et

al., 1995). La primera investigación cuantitativa de la oxidación del hierro en aguas naturales fue publicada por Stumm and Lee (1961). Posteriormente, se llevó a cabo un conjunto completo de estudios cinéticos más detallados sobre la oxidación de Fe(II), incluyendo toda la especiación inorgánica (González-Davila et al., 2005; Millero et al., 1987; Santana-Casiano et al., 2005) (Figura 1.3.). Esos trabajos cuantifican el papel de la fuerza iónica y la composición del medio en la oxidación de Fe(II) por oxígeno y peróxido de hidrógeno en un rango de temperatura, pH, salinidad, altas concentraciones de nutrientes e incluyen el efecto del cobre en su competencia con Fe para el ciclo redox.

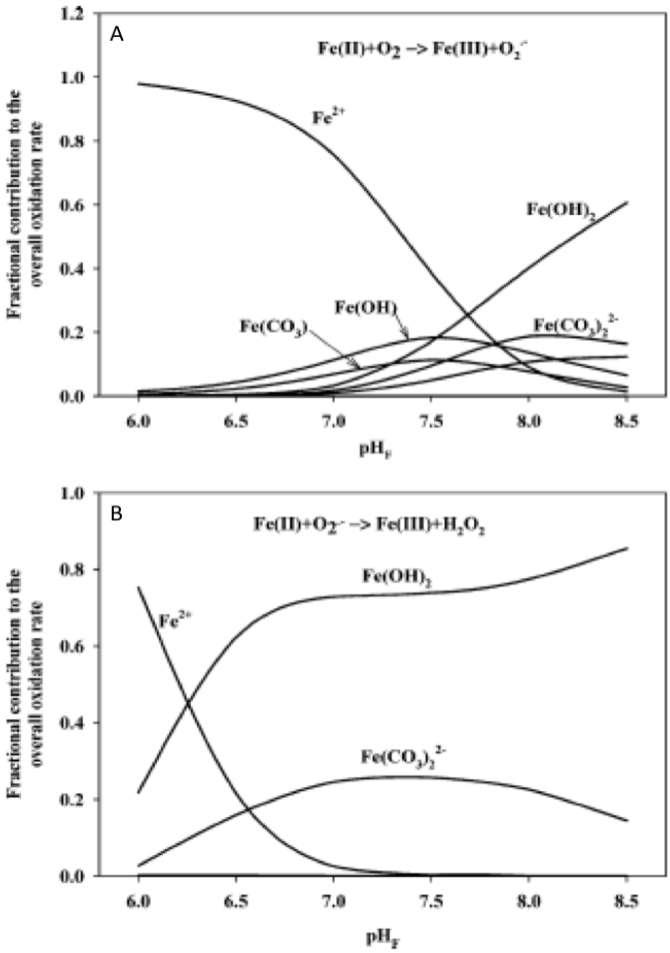


Figura 1.3. Diferentes contribuciones de especies específicas de Fe(II) en la oxidación total de Fe(II): A) por oxígeno y B) por oxígeno y superóxido (Santana-Casiano et al., 2005).

### *8.1.3.2. Especiación orgánica de hierro*

En el océano, el 90-99.9% de dFe aparece complejado por ligandos orgánicos que complejan a Fe(III) (Bruland et al., 2001). La complejación orgánica afecta la biodisponibilidad y la toxicidad de los metales (Sander and Koschinsky, 2011). Los compuestos orgánicos pueden formar complejos con Fe(II) y Fe(III) de acuerdo con el pH de la solución y, por lo tanto, tendrán la capacidad de estabilizar las formas inorgánicas del hierro (Santana-Casiano et al., 2000). Se han identificado cuatro clases distintas de ligandos complejantes de Fe, con diferentes afinidades para formar complejos de hierro, en función de la fuerza absoluta de los ligandos, su constante de complejación, $\log k^{cond}_{FeL,Fe'}$ (Bundy et al., 2015).

Tabla 1.2. Constantes de estabilidad condicional para ligandos complejantes de Fe en agua de mar, estuarios y aguas costeras (obtenidas por Bundy et al. (2015))

| Class of Fe-binding ligands | $\log k^{cond}_{FeL,Fe'}$ |
|---|---|
| $L_1$ | ≥12 |
| $L_2$ | 12-11 |
| $L_3$ | 11-10 |
| $L_4$ | <10 |

La clase de ligandos complejantes de hierro más fuerte ($L_1$) se encuentra en la columna de agua superficial hasta una profundidad de 200 m, pero las clases más débiles ($L_{2-4}$) se observan en toda la columna de agua y también en estuarios y aguas costeras (Bundy et al., 2015). Los ligandos más fuertes están asociados a la actividad biológica: descomposición de material particulado orgánico que se hunde; ligandos producidos por bacterias marinas tales como polisacáridos, porfirinas y sideróforos (Ibisanmi et al., 2011) y/o entradas terrestres (transportadas desde ríos y plataformas continentales) (Macrellis et al., 2001). Los sideróforos son ligandos que tienen diferentes estructuras moleculares como hidroxamatos y catecolatos (Wilhelm and Trick, 1994), restos funcionales mixtos como ligandos de β-hidroxiaspartato/catecolato con grupos funcionales que incluyen ácido carboxílico, aminas, tioles y grupos hidroxilo (Reid et al., 1993). Sin embargo, la composición de los ligandos aún se desconoce dada su complejidad, porque casi cualquier materia orgánica podría ser adecuada para generar ligandos complejantes de metales (Hunter and Boyd, 2007). Algunos estudios han considerado diferentes sustancias como ácidos húmicos (HA) y ácidos fúlvicos (FA) (Laglera and van den Berg, 2009), que consisten predominantemente en polifenoles y ácidos benzoicos/carboxílicos que se originan de la descomposición de organismos

muertos (Buffle et al., 1990). Otros estudios se han realizado en el medio marino, donde en el máximo de clorofila profundo, se encuentra un aumento de los niveles de hierro disuelto, como resultado de la excreción de ligandos y/o regeneración de hierro a través de la degradación de materia orgánica, la ingestión de partículas y la consecuente disolución y liberación de hierro biodisponible (Bowie et al., 2002). Esos mismos complejos también afectarán a la velocidad de oxidación de Fe(II) libre (Santana-Casiano et al., 2000).

### *8.1.4. Solubilidad/precipitación*

La química inorgánica del Fe(III) en el agua de mar, la forma termodinámica más estable del hierro, está controlada principalmente por su hidrólisis (Turner and Hunter, 2001). El hierro forma varias especies hidrolizadas en agua de mar a través de la pérdida secuencial de protones de las moléculas de agua coordinadas en la esfera interna, asociado a cambios en el pH del agua de mar. Este proceso da inicialmente como resultado la formación de oxihidróxido férrico hidratado simple amorfo que se convierte con el tiempo en sólidos termodinámicamente más estables que incluyen hematita, maghemita, goetita y lepidocrocita. Estas transformaciones se traducen en una disminución de su solubilidad (Kuma et al., 1993). Inicialmente la hidrólisis es rápida y el sólido precipitado es bastante lábil, pero rápidamente disminuye su solubilidad, con implicaciones importantes para la retención por ligandos orgánicos (Rich and Morel, 1990).

La concentración de hierro en las aguas oceánicas es típicamente de 0.1 a 0.8 nM, 100 veces mayor que su solubilidad (Laglera and van den Berg, 2009). En el agua de mar, el hierro soluble inorgánico está controlado por la temperatura, el pH (Liu and Millero, 2002), la fuerza iónica (Liu and Millero, 1999) y el tiempo de envejecimiento (Kuma et al., 1996). El efecto sobre la solubilidad debido a los cambios en el pH se ha atribuido a una transformación en estado sólido de $Fe(OH)_3$ a FeOOH (Liu and Millero, 1999). Sin embargo, la presencia de ligandos orgánicos en el agua de mar cambia la solubilidad del Fe(III), convirtiéndose en el principal control de su solubilidad en el agua de mar (Liu and Millero, 2002). La solubilidad de Fe(III) se las aguas costeras superficiales difiere de las aguas oceánicas abiertas, lo que se atribuye a concentraciones más altas de ligandos orgánicos en las aguas costeras (Kuma et al., 1996). El ciclo de Fe está finalmente limitado en los sistemas ambientales y biológicos por la pérdida de $Fe(III)_{aq}$ (Gunnars et al., 2002).

### *8.1.5. Cambios en el estado redox del hierro en el océano*

En las aguas superficiales, el hierro puede reducirse mediante procesos químicos o fotoquímicos que hacen posible determinar concentraciones detectables de Fe(II) (Bowie et al., 1998). Éste es termodinámicamente inestable y se oxida rápidamente a Fe(III) por $O_2$ y $H_2O_2$ siguiendo el proceso de Haber-Weiss (Ecuaciones. 1.1-1.4)

$$Fe(II) + O_2 \rightarrow Fe(III) + O_2^{\cdot -} \quad (1.1)$$

$$Fe(II) + O_2^{\cdot -} \xrightarrow{2H^+} Fe(III) + H_2O_2 \quad (1.2)$$

$$Fe(II) + H_2O_2 \rightarrow Fe(III) + OH^{\cdot} + OH^- \quad (1.3)$$

$$Fe(II) + OH^{\cdot} \rightarrow Fe(III) + OH^- \quad (1.4)$$

En adición, este mecanismo puede completarse al considerar la reducción de Fe(III) por el radical superóxido, y la hidrólisis y formación de Fe(III) coloidal. Además, se debe tener en cuenta la reacción competitiva entre las especies reactivas de oxígeno ($O_2^{\cdot -}$ y $H_2O_2$) con otras especies como el cobre (Santana-Casiano et al., 2005) (Ecuaciones. 1.5-1.8). Todo ello, es importante ya que a niveles nanomolares, la diferencia en el estado de oxidación afectará a la especiación y la biodisponibilidad del hierro (O'Sullivan et al., 1995).

$$Fe(III) + O_2^{\cdot -} \rightarrow Fe(II) + O_2 \quad 1.5$$

$$Fe(III) + 3OH^- \rightarrow Fe(OH)_{2(s)} \quad 1.6$$

$$Cu(II) + O_2^{\cdot -} \rightarrow Cu(I) + O_2 \quad 1.7$$

$$Cu(I) + O_2^{\cdot -} \xrightarrow{2H^+} Cu(II) + H_2O_2 \quad 1.8$$

### *8.1.6. Cinética de oxidación de Fe (II) en el océano*

La concentración de Fe(II) disuelto en la zona fótica y en aguas profundas depende de la velocidad de oxidación de Fe(II) (González-Davila et al., 2005; Santana-Casiano et al., 2005). La velocidad de oxidación de Fe(II) controlará, en parte, la concentración en estado estacionario de Fe(II) y, como consecuencia, el conjunto de hierro biodisponible. En las interfaces oxi-anóxicas, la oxidación de Fe(II) por oxígeno produce un conjunto de radicales libres oxidantes y peróxido de hidrógeno (King, 1998). Una comprensión mecanicista detallada de las reacciones de transferencia de electrones involucradas en Fe(III) es esencial para comprender estos complejos sistemas.

La velocidad global de oxidación de Fe(II) ($k_{app}$) podría explicarse en términos de la suma ponderada de las velocidades de oxidación de las especies individuales de Fe(II), que reaccionan a diferentes velocidades con oxígeno (González-Davila et al., 2005; González-Dávila et al., 2006; Millero et al., 1987; Santana-Casiano et al., 2006; Santana-Casiano et al., 2005). La velocidad de oxidación de Fe(II) se puede expresar como una velocidad de oxidación aparente, $k_{app}$ ($M^{-1}$ $min^{-1}$) teniendo en cuenta la especiación inorgánica y orgánica de Fe(II) (Ecuación 1.9).

$$k_{app} = k_{Fe^{2+}}\alpha_{Fe^{2+}} + k_{FeOH^{+}}\alpha_{FeOH^{+}} + k_{Fe(OH)_2}\alpha_{Fe(OH)_2} + k_{FeHCO_3^{+}}\alpha_{FeHCO_3^{+}} + k_{Fe(CO_3)}\alpha_{Fe(CO_3)} + k_{Fe(CO_3)_2^{2-}}\alpha_{Fe(CO_3)_2^{2-}} + k_{Fe(CO_3)OH^{-}}\alpha_{Fe(CO_3)OH^{-}} + k_{FeCl^{+}}\alpha_{FeCl^{+}} + k_{FeSO_4}\alpha_{FeSO_4} + k_{FeH_3SiO_4^{+}}\alpha_{FeH_3SiO_4^{+}} + \Sigma_i\, k_{L_i}\alpha_{FeL_i}$$

1.9

El Fe(II) termodinámicamente inestable se oxida rápidamente en aguas óxicas (segundos a minutos) por $O_2$ y $H_2O_2$ (González-Davila et al., 2005; Santana-Casiano et al., 2006) en función del pH, fuerza iónica, temperatura (Millero et al., 1987) y [$HCO_3^-$] (Santana-Casiano et al., 2005). Además, otros factores como la concentración de nutrientes, especialmente silicato (González et al., 2010; Samperio-Ramos et al., 2016), fosfato (Burns et al., 2011), Cu (González et al., 2016) y la composición de la materia orgánica (Santana-Casiano et al., 2000) afectan al proceso de oxidación. Al pH del agua de mar, el $O_2$ es el oxidante más importante cuando la concentración de $H_2O_2$ es inferior a 200 nM y la concentración de Fe(II) se encuentra a niveles nanomolares (Santana-Casiano et al., 2006).

La formación de complejos orgánicos, a menudo, altera la cinética de oxidación de Fe(II) al acelerar o retardar la velocidad de oxidación, dependiendo de las fuentes y características de los ligandos orgánicos que se unen a Fe (Emmenegger et al., 1998; Santana-Casiano et al., 2000; Theis and Singer, 1974). El efecto de compuestos orgánicos individuales sobre la cinética de oxidación de Fe(II) se ha estudiado en laboratorio (Kuma et al., 1995; Santana-Casiano et al., 2010; Santana-Casiano et al., 2000). Algunos estudios en océano abierto han propuesto la complejación de Fe(II) por ligandos orgánicos como un mecanismo subyacente para explicar los cambios en las velocidades de oxidación de Fe(II) (Roy and Wells, 2011; Roy et al., 2008; Sarthou et al., 2011). Una fracción significativa de estos ligandos están aparentemente unidos a coloides (Boyd and Ellwood, 2010). Sin embargo, aún no está claro cómo el origen y la composición molecular de la materia orgánica disuelta influye en los cambios de la oxidación de Fe(II) en aguas naturales (Lee et al., 2016). Tampoco, cómo los cambios en la composición de ligandos fuertes a través de diferentes regímenes de nutrientes (Boiteau et al., 2016) podría afectar a la velocidad de oxidación de Fe(II) y a la concentración en estado estacionario (Daugherty et al., 2017). Lo que si se ha comprobado es que los ligandos complejantes de Fe presentes en el agua de mar juegan un papel clave para mantener el Fe en disolución (Rijkenberg et al., 2008).

### *8.1.7. Comportamiento de Fe(II) dentro de un escenario de cambio global*

Como se ha indicado anteriormente, el Fe es un elemento muy reactivo en el agua de mar. Su concentración, distribución, especiación y cambios redox se ven afectados principalmente por las entradas, salidas, las reacciones redox en función de las condiciones del agua de mar y los posibles efectos de la complejación por la materia orgánica. Por ello, no es de extrañar que las características del agua de mar en temperatura, pH, salinidad, oxígeno, $H_2O_2$, [$HCO_3^-$], fuerza iónica, nutrientes, concentraciones de metales y composición de materia orgánica implican un cambio en el comportamiento del Fe. De acuerdo con las indicaciones del Panel Intergubernamental sobre Cambio Climático (IPCC) (página web: http://www.ipcc.ch) y con el enfoque sobre los cambios oceánicos pronosticados, presentamos a continuación los posibles efectos sobre la cinética de oxidación del Fe(II) dentro del pronóstico para el próximo siglo.

### *8.1.7.1. Temperatura*

La temperatura es uno de los factores clave más importantes que controlan la cinética de oxidación del Fe(II). Los diferentes escenarios de cambio climático propuestos por el panel intergubernamental de cambio climático (IPCC) muestran calentamiento de la superficie de los océanos entre 1ºC (RCP2.6) hasta más de 3ºC en (RCP8.5). En el océano global, el cambio de calentamiento entre 0.5°C (RCP2.6) y 1.5°C (RCP8.5), alcanzará una profundidad de aproximadamente 1 km (Collins et al., 2013). Los patrones se caracterizan por un ligero enfriamiento en las latitudes medias y altas por debajo de 1000 m y una absorción de calor pronunciada en las profundidades del Océano Austral a fines del siglo XXI (Collins et al., 2013). El calor se transporta dentro del océano por su circulación general a gran escala y por procesos de mezcla a menor escala. Esos cambios en los transportes conducen a la redistribución del contenido de calor existente y pueden causar enfriamiento local a pesar de que el contenido de calor promedio global esté aumentando (Banks and Gregory, 2006). Los modelos climáticos revelan un aumento de la temperatura y precipitación en latitudes altas. Ambos efectos tienden a hacer que las aguas superficiales de altas latitudes sean más ligeras y por lo tanto aumenten su estabilidad (Meehl et al., 2007). Por lo tanto, un aumento en la temperatura acelerará la velocidad de oxidación de Fe(II) (Millero et al., 1987; Santana-Casiano et al., 2005) en función del incremento observado.

### *8.1.7.2. Acidificación*

El término de acidificación implica una disminución en el pH del agua de mar. El pH es un factor clave en la cinética de oxidación de Fe(II). Un aumento en el pH acelera la velocidad de oxidación de Fe(II) (Millero et al., 1987; Santana-Casiano et al., 2005). Las concentraciones atmosféricas de $CO_2$ han aumentado de 280 μatm en tiempos preindustriales a aproximadamente 400 μatm (Le Quéré et al., 2017) y se prevé que alcancen hasta 1000 μatm a fines de este siglo (escenario RPC6.0 del IPCC) (Collins et al., 2013). Alrededor del 30% del $CO_2$ emitido a la atmósfera es absorbido por los océanos (Sabine et al., 2004), afectando al sistema de carbonato en los océanos y llevando a una disminución en el pH de aproximadamente de 0.3 unidades para el final del siglo XXI (Ciais et al., 2014). Durante las últimas tres décadas el contenido de carbono inorgánico total disuelto (DIC) y la presión parcial del dióxido de carbono ($pCO_2$) de las aguas superficiales ha aumentado, al tiempo que el pH y los estados de saturación de los minerales de $CaCO_3$ han disminuido y la capacidad del océano para absorber $CO_2$ de la atmósfera ha disminuido (Bates et al., 2014). La reducción en la capacidad de amortiguación del sistema de $CO_2$ en el océano es una respuesta

crítica del sistema con importante potencial retroalimentación (Riebesell et al., 2009). Se prevé que este efecto afecte a diferentes procesos biogeoquímicos y biológicos marinos, lo que podría tener como resultado efectos adversos no solo a nivel de especie sino también a nivel de comunidad y ecosistemas (Riebesell et al., 2007) que, a su vez, afectará, indirectamente a la velocidad de oxidación del Fe(II).

El pH del agua de mar afecta a la fisiología del fitoplancton. Esto incluye a los exudados que pueden complejar al hierro, alterando la solubilidad y el ciclo del hierro (Riebesell, 2004). La dependencia del pH en la complejación del hierro y la precipitación de hidróxidos de hierro pueden ser responsables de mantener niveles elevados de dFe en medios con altos niveles de $CO_2$ (Kuma et al., 1996). Una disminución del pH puede afectar a la estabilidad de los complejos hierro-ligando, dando como resultado una alteración en la foto-labilidad de los complejos de Fe(III) (Lewis et al., 1995). La re-oxidación de Fe(II) a Fe(III) posiblemente aumentará la formación de coloides de Fe, lo que puede reflejarse en concentraciones más altas de dFe en los ambientes con niveles altos de $CO_2$.

La acidificación del océano puede conducir a una mayor biodisponibilidad de Fe debido a una mayor fracción de dFe y concentraciones elevadas de Fe(II) en los sistemas costeros (Breitbarth et al., 2010).

### *8.1.7.3. Desoxigenación*

El oxígeno es el principal oxidante del Fe(II). El calentamiento oceánico y el aumento en la estratificación del océano superficial conducirá a disminuciones en el contenido de $O_2$ disuelto (Keeling et al., 2010). Las concentraciones de oxígeno en los márgenes continentales están disminuyendo en muchas regiones debido al aumento de las cargas de nutrientes antropogénicas (Rabalais et al., 2002). Sin embargo, el contenido de oxígeno del interior del océano está determinado por el intercambio del gas a través de la superficie océano-atmósfera y el consumo debido principalmente a la respiración microbiana (Falkowski et al., 2011). Los modelos oceánicos predicen descensos del 1 al 7% en el registro global de $O_2$ en el océano durante el próximo siglo (Keeling et al., 2010). La desoxigenación será mucho más importante en las zonas con mínimos de oxígeno donde los niveles de $O_2$ son demasiado bajos para soportar la macrofauna y dónde se producen grandes cambios en los ciclos biogeoquímicos (Keeling et al., 2010). El oxígeno está disminuyendo tanto en el Océano Pacífico Norte central como en los océanos tropicales en todo el mundo (Falkowski et al., 2011;

Keeling et al., 2010).

#### *8.1.7.4. Cambios en la salinidad*

La salinidad es otro de los factores clave que controlan la cinética de oxidación del Fe(II) en el agua de mar. Un aumento en la salinidad ralentiza la oxidación de Fe(II) (Millero et al., 1987). Las proyecciones del modelo climático Quinta Fase del Proyecto de Intercomparación de Modelos Acoplados (CMIP5) disponibles sugieren que las regiones subtropicales donde la salinidad superficial del océano es alta y están dominadas por la evaporación neta, serán típicamente más salinas. Por su parte, las regiones de salinidad superficial del océano más bajas en latitudes altas serán cada vez más menos salinas (Durack and Wijffels, 2010).

### *8.1.8. Modelos de distribución oceánica global de Fe*

Se han propuesto modelos de especiación oceánica global y de distribución de Fe que buscan representar el ciclo biogeoquímico del hierro en los océanos e incluyen los parámetros que están relacionados con los efectos del cambio climático.

Los modelos numéricos se utilizan para describir el ciclo del hierro entre las formas físicas y químicas en la capa de mezcla superficial (Weber et al., 2005), la especiación y biogeoquímica de Fe (Ye et al., 2009) e incluyen la velocidad de oxidación de Fe(II) (Tagliabue and Voelker, 2011), la complejación orgánica del hierro (Völker and Wolf-Gladrow, 1999) y la absorción de hierro por el fitoplancton (Völker and Wolf-Gladrow, 2000). Estos modelos consideran las diferentes entradas de Fe: polvo atmosférico, ríos, fuentes hidrotermales, sedimentos y se han mejorado incluyendo variables como la especiación de hierro y concentración de ligandos, reacciones químicas, complejación y adsorción. Incluyen fitoplancton, zooplancton, distintas clases de tamaño de partículas, nutrientes limitantes ($NO_3$, $PO_4$, DFe, $NH_4$, and $Si(OH)_4$), oxígeno, carbono inorgánico disuelto, carbono orgánico disuelto, alcalinidad, calcita, sílice biogénico y, además se simula el sistema de carbono (ver apéndice D).

## *8.2. Objetivos Generales*

Los objetivos generales de esta Tesis son:

1. Estudiar y caracterizar la cinética de oxidación de Fe(II) en el área del volcán submarino Tagoro (El Hierro, Islas Canarias) y en el Océano Atlántico Norte (Atlántico Subártico y el Mar del Labrador).

2. Entender el efecto de la temperatura, el pH, la salinidad, la concentración de oxígeno y la materia orgánica en el control de la velocidad de oxidación del hierro y determinar la contribución de cada variable al proceso de oxidación en condiciones naturales.

De una manera más pormenorizada, los objetivos específicos para cada uno de los capítulos son:

***Objetivos del capítulo III: "Emisiones de Fe(II) y su cinética de oxidación en el volcán submarino Tagoro, El Hierro"***

1º Objetivo: Detectar cualquier variación en las concentraciones de TdFe(II) debido a las emisiones hidrotermales en la fase post-eruptiva del volcán submarino Tagoro.

2º Objetivo: Estudiar los cambios en la concentración de TdFe(II) de las aguas circundantes del volcán submarino y la correlación con los cambios de pH.

3º Objetivo: Estudiar la variabilidad temporal de la concentración de TdFe(II) en períodos que van de horas a días sobre el cono principal y conos secundarios en el edificio volcánico del volcán submarino Tagoro.

4º Objetivo: Estudiar la cinética de oxidación del Fe(II) analizando los efectos de las propiedades del agua de mar en las proximidades del volcán sobre las constantes de

velocidad de oxidación y $t_{1/2}$ (tiempo de vida media) del hierro ferroso.

***Objetivos del capítulo IV: "Cinética de oxidación de Fe(II) en el Atlántico Norte a lo largo de 59.5ºN durante 2016"***

1º Objetivo: Estudiar la velocidad de oxidación de Fe(II) en diferentes masas de agua presentes en el Océano Atlántico Norte Subártico, que es una de las áreas más sensibles para la acidificación de los océanos, con el fin de conocer el tiempo que estaría disponible el Fe(II) en el agua de mar.

2º Objetivo: Estudiar las variables que controlan la velocidad de oxidación de Fe(II) en el océano: temperatura, pH, salinidad y carbono orgánico total (COT), bajo diferentes condiciones de temperatura y pH.

3º Objetivo: Estudiar los efectos combinados de las variables que controlan la cinética de oxidación de Fe(II) en el océano.

4º Objetivo: Comprender el efecto de la materia orgánica en la cinética de oxidación del Fe(II).

5º Objetivo: Comprender el requerimiento de energía para la oxidación de Fe(II) en las aguas superficiales y profundas.

6º Objetivo: Obtener una ecuación empírica para las constantes de velocidad de oxidación de Fe(II) en la región considerando las condiciones naturales de temperatura, $pH_F$ y salinidad del área.

***Objetivos del Capítulo V: "Efecto de la materia orgánica sobre la cinética de oxidación de Fe(II) en el mar de Labrador"***

1º Objetivo: Estudiar la velocidad de oxidación de Fe(II) en diferentes masas de agua presentes en el Mar de Labrador desde la costa hasta el océano abierto y desde la

superficie hasta las aguas de fondo.

2º Objetivo: Estudiar las variables que controlan la velocidad de oxidación de Fe(II) en el océano: temperatura, pH, salinidad y carbono orgánico total (COT), bajo diferentes condiciones.

3º Objetivo: Estudiar los efectos combinados de las variables que controlan la cinética de oxidación de Fe(II) en el océano.

4º Objetivo: Comprender el efecto de la materia orgánica en la cinética de oxidación del Fe(II).

5º Objetivo: Comprender el requerimiento de energía para la oxidación de Fe(II) en aguas superficiales, intermedias y profundas.

6º Objetivo: Obtener una ecuación empírica para las constantes de velocidad de oxidación de Fe(II) en el mar de Labrador teniendo en cuenta las condiciones naturales de temperatura, $pH_F$ y salinidad del área, que también sea válida para el Atlántico Norte y se pueda incorporar en modelos globales.

7º Objetivo: Obtener un enfoque teórico que considere la temperatura y las interacciones inorgánicas en la cinética de oxidación para determinar la contribución de los ligandos orgánicos sobre la velocidad de oxidación de Fe(II).

## *8.3. Conclusiones Generales*

Las principales conclusiones que surgen de esta Tesis son:

1. Las emisiones hidrotermales alrededor del volcán submarino Tagoro en la isla de El Hierro emitieron grandes cantidades de TdFe(II) cuya distribución está inversamente correlacionada con una disminución en la distribución del pH de las aguas circundantes en la columna de agua.

2. El estudio de alta resolución en el edificio volcánico desde 2013 a 2015 reveló que la magnitud de TdFe(II) no era la misma en todos los períodos de muestreo, con una alta variabilidad en una escala temporal corta. Las emisiones continúan en el área cuatro años después del cese de la fase eruptiva.

3. Los estudios de cinética de oxidación de Fe(II) en el área volcánica revelaron que las constantes de velocidad de oxidación de Fe(II) eran más altas que las esperadas en el agua de mar oligotrófica. Estas velocidades pueden explicarse por las diferentes concentraciones de nutrientes de las muestras, en particular los silicatos.

4. Los estudios de cinética de oxidación de Fe(II) llevados a cabo en el Atlántico Subártico y en el Mar del Labrador muestran que la temperatura, el pH y la salinidad fueron las principales variables que controlaron la cinética de oxidación de Fe(II) en condiciones naturales.

5. El área estudiada en el Atlántico Subártico y el Mar de Labrador incluyó muestras costeras y oceánicas a través de toda la columna de agua. Las fuentes y características de la materia orgánica presente fueron factores importantes que influyen en la oxidación de Fe(II), y muestran efectos tanto positivos como negativos sobre la velocidad de oxidación del Fe(II). La materia orgánica podría proporcionar una variedad de interacciones entre Fe(II) con los múltiples ligandos orgánicos presentes en la disolución que afectan tanto a las especies Fe(II)-L como Fe(III)-L.

6. La distribución espacial de las muestras afectó a la constante de velocidad *k'* debido a las características químicas de cada masa de agua y su modificación a medida que la masa de agua se desplazó de una cuenca a otra y de la superficie al océano profundo. Se observaron velocidades de oxidación más altas de Fe(II) en el máximo de clorofila, en muestras superficiales y costeras que en aguas profundas.

7. La energía requerida para la oxidación de Fe(II) en el Atlántico Subártico difiere de las aguas superficiales a las profundas. Sin embargo, presentó valores similares en el Mar del Labrador para aguas superficiales, intermedias y profundas. Ello indica que la cinética de oxidación de Fe(II) podría verse afectada por la composición de los ligandos orgánicos y la degradación de la materia orgánica, que está más degradada en aguas profundas que en aguas superficiales. Las diferencias observadas en el Atlántico Subártico se asocian a diferentes características en la composición y degradación de la materia orgánica. Sin embargo, los valores similares obtenidos en el mar de Labrador revelan que la materia orgánica para estas aguas presentaba una composición similar o, que el efecto neto obtenido por la combinación de distinta materia orgánica tiene un resultado similar para la cinética de oxidación de Fe(II) encontrada en el Mar del Labrador.

8. Se obtuvo una ecuación general para la velocidad de oxidación que permite calcular la constante de velocidad *k'* teniendo en cuenta los efectos de la temperatura, el pH y la salinidad en condiciones naturales para el Atlántico Subártico y el Mar del Labrador. Los valores observados se pueden ajustar en un 79% con un error estándar de estimación de 0.0072 $min^{-1}$, y puede ser incorporado a los modelos globales de Fe.

9. Se aplicó un enfoque novedoso a la cinética de oxidación de Fe(II) en el mar de Labrador, que permitió determinar la contribución promedio de la materia orgánica sobre el efecto inorgánico. Cuando se elimina el efecto inorgánico, la materia orgánica ralentiza la oxidación del Fe(II) en la superficie y cerca de las áreas costeras. El proceso se ve afectado por las características químicas individuales, concentraciones, la fuerza con la que pueden formar complejos de Fe(II) y Fe(III), pero también pueden verse afectados por la reducción de esos complejos orgánicos de Fe(III) a Fe(II).

# Appendices

The pH was measured potentiometrically by calibrating the electrode system with Tris-(hydroximethyl) aminomethane (Tris)-artificial seawater buffers (TRIS buffer) (Millero, 1986). The buffer was prepared in 0.005 mol $kg^{-1}$ Tris and 0.005 mol $kg^{-1}$ Tris-HCl, in artificial seawater. The electrode used in the experiment was a combination electrode, RossTM Combination, glass body.

The pH can be calculated using the Eq (1).

$$pH = pH_{(s)} + \frac{(Es-Ex)F}{2.303RT} = pH_{(s)} + \frac{(Es-Ex)}{1.984x10^{-4}T} \quad (1)$$

where the subscript s corresponds to Tris and x to the sample with unknown pH.

Es and Ex, are the potential (mV) for Tris and sample respectively. F is the Faraday constant (96485.3 C $mol^{-1}$), R is the universal gases constant (8.314 J $mol^{-1}$ $K^{-1}$) and T is temperature (K).

The pH(s) for the Tris was calculated using the Eq (2) (Dickson et al., 2007)

$$\begin{aligned} pH_S = {} & (11911.08 - 18.2499S - 0.039336S^2)\frac{1}{T} - 366.27059 \\ & + 0.053993607S + 0.00016329S^2 \\ & + (64.52243 - 0.084041S)\ln(T) - 0.11149858(T) \end{aligned} \quad (2)$$

T is the temperature (K). The studies in this Thesis have been done using the free-ion scale ($pH_F$) in order to facilitate the comparison of data with previous studies. However in oceanography different scales of pH can be used (Millero et al., 1993) as total pH ($pH_T$) and seawater pH ($pH_{SWS}$) Eqs (3-5)

$$pH_F = -\log[H^+] \quad (3)$$

$$pH_T = -\log([H^+] + [SO_4^-]) \quad (4)$$

$$pH_{SWS} = -\log([H^+] + [SO_4^-] + [HF]) \quad (5)$$

The TRIS-seawater solution was prepared following the Table 1 (Millero, 1986). The effect of temperature and salinity on the pK* of the Tris-buffer were considered in this thesis

Table 1. Composition of TRIS-seawater buffer solution (Millero, 1986).

| **Reagent** | **m** | **mol $kg^{-1}$** | **g $kg^{-1}$** | **g $dm^{-3}$ (25ºC)** |
|---|---|---|---|---|
| | | **m=0.06 TRIS buffer** | | |
| NaCl | 0.36664 | 0.34933 | 20.416 | 20.946 |
| $Na_2SO_4$ | 0.02926 | 0.02788 | 3.960 | 4.063 |
| KCl | 0.01058 | 0.01008 | 0.752 | 0.772 |
| $CaCl_2$ | 0.01077 | 0.01026 | 1.139 | 1.169 |
| $MgCl_2$ | 0.05518 | 0.05258 | 5.006 | 5.136 |
| TRIS | 0.06 | 0.05717 | 6.926 | 7.106 |
| TRIS-HCl | 0.06 | 0.05717 | 9.01 | 9.244 |
| | | g salt | 47.209 | |
| | | g H2O | 952.791 | |

The studies carried out in this Thesis were done in air equilibrated with atmosphere, during 1 hour equilibrium time.

The oxygen equilibrium concentration was calculated using the Benson and Krause (1984) expression Eq (6).

$$\ln[O_2] = -135.29996 - \frac{1.572288x10^5}{T} - \frac{6.637146x10^7}{T^2} + \frac{1.243678x10^{10}}{T^3} - \frac{8.62106x10^{11}}{T^4} - S(0.020573 - \frac{12.142}{T} + \frac{2363.1}{T^2} + \ln(1 + 10^{-3}s)$$

(6)

T is temperature (K) and S is salinity.

The distillation of HCl and $NH_3$ used to prepare the Luminol reagent was carried out by the sub-boiling distillation. Because the HCl or $NH_3$ are never heated to boiling point, no bubbling, spitting or splashing occurs. High purity vapor is produced, while metallic impurities remain in the liquid phase.

For the HCl distillation the DST-1000 model (Savillex) was used. This distillation consists in the purification via the process of sub-boiling. The Operation consists in the addition of acid and switch on the power to start generating high purity acid. A controller maintains the required temperature used for heating the acid. The DST-1000 has a basic temperature controller with three temperature settings; the temperature settings only affect the production rate and not the purity of the acid. The maximum acid temperature that can be generated by the heating element is below the boiling point of any of the acids that can be purified, preventing metal contaminants from being carried over to the distillate. The lower part of the vessel (reservoir) is surrounded by an electrically heated mantle, sealed inside a polymer bowl. Acid (trace metal grade) to be purified is added to the vessel via the fill tube, which fills the reservoir from the bottom. The liquid level gauge on the fill tube displays the acid level in the reservoir. Power is supplied to the heater, and the acid in the reservoir is gently heated and high purity acid vapor is generated. The acid vapor condenses on the walls of the upper part of the vessel (condenser), collects in a channel running along the lower part of the vessel, and exits the system via a PFA tube into a Purillex™ PFA collection bottle (a 1 L bottle). The size and shape of the vessel promotes efficient condensation of acid, which eliminates the need for water-cooling.

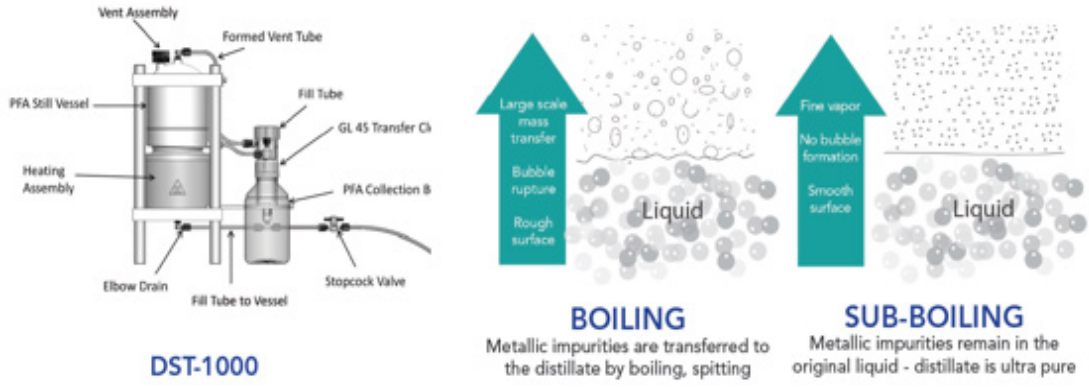


Fig 1. HCl Distiller

For the $NH_3$ distillation two separately PFA tubes with are joined thought a connection which separate 90º both tubes. In the operational we clean the tubes before with Milli-Q for three times. The first tube is filled with ammonia and the second tube with Milli-Q water; both tubes should be filled with the same volume. Then, they are connected with a specific key that closes completely the tubes forming a close system in "L" form. We should avoid mixing the content of each tube. The "system" is placed in vertical and the tube containing the $NH_3$ is heated with an IR lamp (Philips, IR-100R-PAR, 230V, 100W, Poland), which evaporate the $NH_3$. The clean vapor is transferred into the second tube, which contains Milli-Q, by the condensation process. By the end of the distillation, we separate carefully both tubes, and place the clean $NH_3$ (now in the second tube) in a trace metal clean bottle. The fist tube that initially has the $NH_3$, now contains the impurities.

Fig 2. $NH_3$ Distiller

| Model | Characteristics | References |
|---|---|---|
| BEC | Dust source of Fe, river input of Fe, hydrothermal Fe input, second-order scavenging rate, constant ligand concentration (1 nM), variable Fe/C ratios, fixed rate of recycling by zooplankton, represent sinking implicitly and run for a few decades or centuries. | Moore et al. (2013) |
| BFM | Dust source of Fe, river input of Fe, free Fe concentration, constant ligand concentration (0.6 nM), variable Fe/C ratios, assumed zooplankton Fe quota, include one particulate Fe pool and run for a few decades or centuries. | Vichi et al. (2007) |
| BLING | Dust source of Fe, free Fe concentration, second-order scavenging rate, constant ligand concentration (1 nM), switches off Fe scavenging when oxygen drops below 1 mmol $m^{-3}$, reduce the stability of Fe-ligand complexes in the presence of light, variable Fe/C ratios, fixed rate of recycling by zooplankton and it include one particulate Fe pool. | Galbraith et al. (2010) |
| COBALT | Dust source of Fe, free Fe concentration, a constant ligand concentration (1 nM), reduce the stability of Fe-ligand complexes in the presence of light, variable Fe/C ratios, assumed zooplankton Fe quota, reduced regeneration efficiency relative to organic material that elongates the regeneration depth scale beyond that for sinking organic material and it run for a few decades or centuries. | Stock et al. (2014) |
| GENIE | Dust source of Fe, free Fe concentration, second-order scavenging rate, constant ligand concentration (1 nM), assumed zooplankton Fe quota and include one particulate Fe pool. | Matsumoto et al. (2013) |
| MEDUSA1 | Dust source of Fe, free Fe concentration, retaining fixed Fe/C ratios, constant ligand concentration (1 nM), fixed rate of recycling by zooplankton, it include one particulate Fe pool and it run for a few decades or centuries. | Yool and Popova (2011) |
| MEDUSA2 | Dust source of Fe, free Fe concentration, constant ligand concentration (1 nM), retaining fixed Fe/C ratios, fixed rate of recycling by zooplankton, include one particulate Fe pool and it run for a few decades or centuries. | Yool et al. (2013) |
| MITecco | Dust source of Fe, free Fe concentration, have a second-order scavenging rate, constant ligand concentration (1 nM), limit Dfe to a dissolve value of 1.3 nM with any excess Fe being numerically deleted. Due to the noted flexibility in planktonic demands for Fe, retaining fixed Fe/C ratios, assumed zooplankton Fe quota, include one particulate Fe pool and run for a few decades or centuries. | Dutkiewicz et al. (2015) |
| MITigsm | Dust source of Fe, Free Fe concentration, have a second-order scavenging rate, constant ligand concentration (1 nM), limit Dfe to a 1dissolve value of 1.3 nM with any excess Fe being numerically deleted. Due to the noted flexibility in planktonic demands for Fe, retaining fixed Fe/C ratios, assumed zooplankton Fe quota, include one particulate Fe pool, run for a few decades or centuries. | Dutkiewicz et al. (2014) |

| | | |
|---|---|---|
| PISCES1 | Dust source of Fe, Include river input of Fe, represent hydrothermal Fe input, free Fe concentration, have a second-order, scavenging rate, representation of dissolved losses of Dfe, dissolved aggregation of dissolved organic material, constant ligand concentration (0.6 nM), variable Fe/C ratios, assumed zooplankton Fe quota and consider two particulate Fe pool. | Tagliabue et al. (2009) |
| PISCES2 | Dust source of Fe, Include river input of Fe, represent hydrothermal Fe input, free Fe concentration, have a second-order scavenging rate, representation of 1 dissolved losses of Dfe, dissolved aggregation of dissolved organic material, constant ligand concentration (1 nM), represent a dynamic ligand pool with explicit sources and sink, a variable computation of the dissolved Fe fraction, modified to account for hydrothermal ligand supply, variable Fe/C ratios, assumed zooplankton Fe quota and consider two particulate Fe pool. | Resing et al. (2015) |
| RecoM | Dust source of Fe, free Fe concentration, have a second-order scavenging rate, constant ligand concentration (1 nM), variable Fe/C ratios and fixed rate of recycling by zooplankton. | Hauck et al. (2013) |
| TOPAZ | Dust source of Fe, free Fe concentration, have a second-order scavenging rate, constant ligand concentration (1 nM), applies an empirical relationship to Dissolved Organic Carbon (DOC) to derive ligand concentrations ($5x10^{-5}$ mol ligand per mol DOC), variable Fe/C ratios, assumed zooplankton Fe quota and include one particulate Fe pool. | Tagliabue et al. (2016) |
| CIAO | Coupled ice-atmosphere-ocean ecosystem includes air-sea $CO_2$ exchange and non-Redfield C/N/P uptake ratios of the dominant phytoplankton taxa, iron speciation on phytoplankton dynamics, processes governing the supply of iron to phytoplankton. | Tagliabue and Arrigo (2005) |
| MET | Eleven compartments: small phytoplankton, diatoms, diazotrophs, zooplankton, sinking and non-sinking detrital pools, and the nutrients ammonium, nitrate, phosphate, silicate, and iron; multiple elements for the biota and detrital pools (N, C, P, Fe, Si, CaCO3, and Chl), is used to study iron cycling and nutrient-limitation patterns in surface waters of the world ocean. The ecosystem model has a small phytoplankton size class whose growth can be limited by N, P, Fe, and/or light, a diatom class which can also be Si-limited, and a diazotrophs phytoplankton class whose growth rates can be limited by P, Fe, and/or light levels. Primary production, community structure, and the sinking carbon flux are quite sensitive to large variations in the atmospheric iron source, particularly in the HNLC regions, supporting the Iron Hypothesis. | Moore et al. (2001) |

| | | |
|---|---|---|
| INCA-PISCES and NCAR-PISCES | Includes two phytoplankton functional types, two zooplankton, two particle size classes, five limiting nutrients ($NO_3$, $PO_4$, DFe, $NH_4$, and $Si(OH)_4$), oxygen, dissolved inorganic carbon, dissolved organic carbon, alkalinity, calcite, and biogenic silica. The full carbon system is simulated Fe is explicitly simulated in the dissolved pool, two particle fractions, and the biological compartments. DFe is removed by scavenging, with free Fe explicitly calculated using a fixed ligand concentration (0.6 nM) and conditional stability ($10^{12}M^{-1}$), alongside additional colloidal pumping DFe losses. Scavenging rates depend on particle concentrations and scavenged Fe is returned to DFe via dissolution. It accounts for the external DFe supply from dust, continental margin sediments, hydrothermal vents, and rivers, with sea ice incorporation/release of dissolved Fe. The total DFe flux is 26.9 and 13.5 Gmol DFe from sediments and hydrothermalism, in INCA-PISCES dust providing 32.7 Gmol DFe and in NCAR-PISCES 37.5 Gmol Dfe. | Tagliabue et al. (2014) |
| NEMO-PISCES | The biogeochemical component PISCES includes two phytoplankton functional types, two zooplankton, two particle size classes, five limiting nutrients ($NO_3$, $PO_4$, DFe, $NH_4$, and $Si(OH)_4$), oxygen, dissolved inorganic carbon, dissolved organic carbon, alkalinity, calcite, and biogenic silica, the full carbon system is simulated, Fe is explicitly simulated in the dissolved pool, two particle fractions, and the biological compartments, DFe is removed by scavenging, with free, Fe explicitly calculated using a fixed ligand concentration (0.6 nM) and conditional stability ($10^{12}$ $M^{-1}$), alongside additional colloidal pumping DFe losses, the scavenging rates depend on particle concentrations and scavenged Fe is returned to DFe via dissolution. | Tagliabue et al. (2010) |

# References

Abadie, C., Lacan, F., Radic, A., Pradoux, C. and Poitrasson, F., 2017. Iron isotopes reveal distinct dissolved iron sources and pathways in the intermediate versus deep Southern Ocean. Proceedings of the National Academy of Sciences, 114(5): 858-863.

Arístegui, J.D., Carlos M.; Reche, Isabel; Gómez-Pinchetti, Juan L., 2014. Krill Excretion Boosts Microbial Activity in the Southern Ocean. PLOS ONE, 9(2).

Arrhenius, S., 1889. Über die Dissociationswärme und den Einfluss der Temperatur auf den Dissociationsgrad der Elektrolyte. Zeitschrift für physikalische Chemie, 4(1): 96-116.

Azetsu-Scott, K., Jones, E.P., Yashayaev, I., Gershey, R.M., 2003. Time series study of CFC concentrations in the Labrador Sea during deep and shallow convection regimes (1991–2000). Journal of Geophysical Research: Oceans, 108(C11): n/a-n/a.

Banks, H.T. and Gregory, J.M., 2006. Mechanisms of ocean heat uptake in a coupled climate model and the implications for tracer based predictions of ocean heat uptake. Geophysical Research Letters, 33(7).

Bates, N. et al., 2014. A time-series view of changing ocean chemistry due to ocean uptake of anthropogenic $CO_2$ and ocean acidification. Oceanography, 27(1): 126-141.

Bennett, S.A., et al., 2008. The distribution and stabilisation of dissolved Fe in deep-sea hydrothermal plumes. Earth Planet. Sci. Lett. 270 (3), 157–167.

Benson, B.B. and Krause, D., 1984. The concentration and isotopic fractionation of oxygen dissolved in freshwater and seawater in equilibrium with the atmosphere. Limnology and oceanography, 29(3): 620-632.

Bergquist, B. and Boyle, E., 2006. Dissolved iron in the tropical and subtropical Atlantic Ocean. Global Biogeochemical Cycles, 20(1).

Bergquist, B., Wu, J. and Boyle, E., 2007. Variability in oceanic dissolved iron is dominated by the colloidal fraction. Geochimica et Cosmochimica Acta, 71(12): 2960-2974.

Bersch, M., Meincke, J. and Sy, A., 1999. Interannual thermohaline changes in the northern North Atlantic 1991–1996. Deep Sea Research Part II: Topical Studies in Oceanography, 46(1): 55-75.

Bhatia, M.P. et al., 2013. Greenland meltwater as a significant and potentially bioavailable source of iron to the ocean. Nature Geoscience, 6(4): 274-278.

Boiteau, R.M. et al., 2016. Siderophore-based microbial adaptations to iron scarcity across the eastern Pacific Ocean. Proceedings of the National Academy of Sciences, 113(50): 14237-14242.

Bowie, A.R., Achterberg, E.P., Mantoura, R.F.C. and Worsfold, P.J., 1998. Determination of sub-nanomolar levels of iron in seawater using flow injection with chemiluminescence detection. Analytica Chimica Acta, 361(3): 189-200.

Bowie, A.R., Whitworth, D.J., Achterberg, E.P., Mantoura, R.F.C. and Worsfold, P.J., 2002. Biogeochemistry of Fe and other trace elements (Al, Co, Ni) in the upper Atlantic Ocean. Deep Sea Research Part I: Oceanographic Research Papers, 49(4): 605-636.

Bowie, A.R. et al., 2003. Shipboard analytical intercomparison of dissolved iron in surface waters along a north–south transect of the Atlantic Ocean. Marine Chemistry, 84(1): 19-34.

Bowie, A.R., Sedwick, P.N. and Worsfold, P.J., 2004. Analytical intercomparison between flow injection chemiluminescence and flow injection spectrophotometry for the determination of picomolar concentrations of iron in seawater. Limnology and Oceanography: methods, 2(2): 42-54.

Bowie, A.R. et al., 2006. A community-wide intercomparison exercise for the determination of dissolved iron in seawater. Marine Chemistry, 98(1): 81-99.

Boyd, P. and Ellwood, M., 2010. The biogeochemical cycle of iron in the ocean. Nature Geoscience, 3(10): 675.

Boye, M. et al., 2006. The chemical speciation of iron in the north-east Atlantic Ocean. Deep Sea Research Part I: Oceanographic Research Papers, 53(4): 667-683.

Brambilla, E. and Talley, L.D., 2008. Subpolar Mode Water in the northeastern Atlantic: 1. Averaged properties and mean circulation. Journal of Geophysical Research: Oceans, 113(C4).

Brand, L.E., 1991. Minimum iron requirements of marine phytoplankton and the implications for the biogeochemical control of new production. Limnol. Oceanogr. 36 (8), 1756–1771.

Breitbarth, E., et al., 2010. Ocean acidification affects iron speciation during a coastal seawater mesocosm experiment. Biogeosciences 7 (3), 1065–1073.

Bruland, K.W.R., E. L., 2001. Analytical methods for the determination of concentrations and speciation of iron. In: (Eds.), I.D.R.T.K.A.H. (Ed.), The biogeochemistry of iron in sea water (IUPAC Series on Analytical and Physical Chemistry of Environmental Systems). John Wiley & Sons Ltd., pp. 255.

Bucciarelli, E., Blain, S. and Tréguer, P., 2001. Iron and manganese in the wake of the Kerguelen Islands (Southern Ocean). Marine Chemistry, 73(1): 21-36.

Buck, K.N., Gerringa, L.J.A. and Rijkenberg, M.J.A., 2016. An Intercomparison of Dissolved Iron Speciation at the Bermuda Atlantic Time-series Study (BATS) Site: Results from GEOTRACES Crossover Station A. Frontiers in Marine Science, 3(262).

Buffle, J., Altmann, R.S., Filella, M. and Tessier, A., 1990. Complexation by natural heterogeneous compounds: site occupation distribution functions, a normalized description of metal complexation. Geochimica et Cosmochimica Acta, 54(6): 1535-1553.

Bundy, R.M. et al., 2015. Iron-binding ligands and humic substances in the San Francisco Bay estuary and estuarine-influenced shelf regions of coastal California. Marine Chemistry, 173: 183-194.

Burns, J.M., Craig, P.S., Shaw, T.J., Ferry, J.L., 2010. Multivariate Examination of Fe(II)/Fe(III) Cycling and Consequent Hydroxyl Radical Generation. Environmental Science & Technology, 44(19): 7226-7231.

Burns, J.M., Craig, P.S., Shaw, T.J., Ferry, J.L., 2011. Short-Term Fe Cycling during Fe(II) Oxidation: Exploring Joint Oxidation and Precipitation with a Combinatorial System. Environmental Science & Technology, 45(7): 2663-2669.

Campbell, J. and Yeats, P., 1982. The distribution of manganese, iron, nickel, copper and cadmium in the waters of Baffin-Bay and the Canadian arctic archipelago. Oceanologica Acta, 5(2): 161-168.

Carlson, C.A., 2002. Production and removal processes. Biogeochemistry of marine dissolved organic matter: 91-151.

Chase, Z. et al., 2005. Manganese and iron distributions off central California influenced by upwelling and shelf width. Marine Chemistry, 95(3): 235-254.

Chereskin, B.M. and Castelfranco, P.A., 1982. Effects of iron and oxygen on chlorophyll biosynthesis II. Observations on the biosynthetic pathway in isolated etiochloroplasts. Plant physiology, 69(1): 112-116.

Chever, F. et al., 2010. Physical speciation of iron in the Atlantic sector of the Southern Ocean along a transect from the subtropical domain to the Weddell Sea Gyre.

Journal of Geophysical Research: Oceans, 115(C10).

Ciais, P. et al., 2014. Carbon and other biogeochemical cycles, Climate change 2013: the physical science basis. Contribution of Working Group I to the Fifth Assessment Report of the Intergovernmental Panel on Climate Change. Cambridge University Press, pp. 465-570.

Clayton, T.D., Byrne, R.H., 1993. Spectrophotometric seawater pH measurements: total hydrogen ion concentration scale calibration of m-cresol purple and at-sea results. Deep-Sea Res. I Oceanogr. Res. Pap. 40 (10), 2115–2129.

Coale, K.H., 1991. Effects of iron, manganese, copper, and zinc enrichments on productivity and biomass in the subarctic Pacific. Limnology and Oceanography, 36(8): 1851-1864.

Collins, M. et al., 2013. Long-term climate change: projections, commitments and irreversibility.

Cota, G.F., Harrison, W.G., Platt, T., Sathyendranath, S., Stuart, V., 2003. Bio-optical properties of the Labrador Sea. Journal of Geophysical Research: Oceans, 108(C7).

Craig, P.S., Shaw, T.J., Miller, P.L., Pellechia, P.J. and Ferry, J.L., 2009. Use of Multiparametric Techniques To Quantify the Effects of Naturally Occurring Ligands on the Kinetics of Fe(II) Oxidation. Environmental Science & Technology, 43(2): 337-342.

Croot, P.L., Laan, P., 2002. Continuous shipboard determination of Fe(II) in polar waters using flow injection analysis with chemiluminescence detection. Analytica Chimica Acta, 466(2): 261-273.

Crusius, J., Schroth, A.W., Resing, J.A., Cullen, J. and Campbell, R.W., 2017. Seasonal and spatial variability in northern Gulf of Alaska surface-water iron

concentrations driven by shelf sediment resuspension, glacial meltwater, a Yakutat eddy, and dust. Global Biogeochemical Cycles: n/a-n/a.

Cullen, J.T., Bergquist, B.A. and Moffett, J.W., 2006. Thermodynamic characterization of the partitioning of iron between soluble and colloidal species in the Atlantic Ocean. Marine Chemistry, 98(2): 295-303.

Daugherty, E.E., Gilbert, B., Nico, P.S. and Borch, T., 2017. Complexation and Redox Buffering of Iron(II) by Dissolved Organic Matter. Environmental Science & Technology, 51(19): 11096-11104.

de Baar, H.J.W., de Jong, J.T.M., 2001. Distributions, sources and sinks of iron in seawater. In: Turner, D.R., Hunter, K.A. (Eds.), The Biogeochemistry of Iron in Sea Water. John Wiley & Sons Ltd, p. 123.

De Jong, J. et al., 1998. Dissolved iron at subnanomolar levels in the Southern Ocean as determined by ship-board analysis. Analytica Chimica Acta, 377(2): 113-124.

Dickson, A., Millero, F.J., 1987. A comparison of the equilibrium constants for the dissociation of carbonic acid in seawater media. Deep Sea Res. Part A 34 (10), 1733–1743.

Dickson, R.R., Curry, R., Yashayaev, I., 2003. Recent changes in the North Atlantic. Philosophical Transactions: Mathematical, Physical and Engineering Sciences: 1917-1934.

Dickson, A.G., Sabine, C.L. and Christian, J.R., 2007. Guide to best practices for ocean CO2 measurements. North Pacific Marine Science Organization.

Dittmar, T. and Kattner, G., 2003. The biogeochemistry of the river and shelf ecosystem of the Arctic Ocean: a review. Marine Chemistry, 83(3): 103-120.

Durack, P.J. and Wijffels, S.E., 2010. Fifty-year trends in global ocean salinities and their relationship to broad-scale warming. Journal of Climate, 23(16): 4342-4362.

Dutkiewicz, S. et al., 2015. Capturing optically important constituents and properties in a marine biogeochemical and ecosystem model.

Dutkiewicz, S., Ward, B., Scott, J. and Follows, M., 2014. Understanding predicted shifts in diazotroph biogeography using resource competition theory.

Emmenegger, L., King, D.W., Sigg, L. and Sulzberger, B., 1998. Oxidation kinetics of Fe(II) in a eutrophic Swiss lake. Environmental science & technology, 32(19): 2990-2996.

Falkowski, P.G. et al., 2011. Ocean deoxygenation: past, present, and future. Eos, Transactions American Geophysical Union, 92(46): 409-410.

Field, M.P., Sherrell, R.M., 2000. Dissolved and particulate Fe in a hydrothermal plume at 9°45'N, East Pacific rise: slow Fe(II) oxidation kinetics in Pacific plumes. Geochim.Cosmochim. Acta 64 (4), 619–628.

Filippova, A. et al., 2017. Water mass circulation and weathering inputs in the Labrador Sea based on coupled Hf–Nd isotope compositions and rare earth element distributions. Geochimica et Cosmochimica Acta, 199: 164-184.

Fitzsimmons, J.N., Zhang, R. and Boyle, E.A., 2013. Dissolved iron in the tropical North Atlantic Ocean. Marine Chemistry, 154: 87-99.

Fitzsimmons, J.N. and Boyle, E.A., 2014. Both soluble and colloidal iron phases control dissolved iron variability in the tropical North Atlantic Ocean. Geochimica et Cosmochimica Acta, 125: 539-550.

Fitzwater, S.E., Coale, K.H., Gordon, R.M., Johnson, K.S., Ondrusek, M.E.,

1996. Iron deficiency and phytoplankton growth in the equatorial Pacific. Deep-Sea Res. II Top. Stud. Oceanogr. 43 (4), 995–1015.

Fraile-Nuez, E., et al., 2012. The submarine volcano eruption at the island of El Hierro: physical-chemical perturbation and biological response. Sci. Rep. 2, 1–6.

Fu, F.-X., et al., 2008. Interactions between changing $pCO_2$, $N_2$ fixation, and Fe limitation in the marine unicellular cyanobacterium Crocosphaera. Limnol. Oceanogr. 53 (6), 2472–2484.

Galbraith, E.D., Gnanadesikan, A., Dunne, J.P. and Hiscock, M.R., 2010. Regional impacts of iron-light colimitation in a global biogeochemical model. Biogeosciences, 7(3).

García-Ibáñez, M.I., 2015. Acidification and transports of water masses and $CO_2$ in the North Atlantic.

García-Ibáñez, M.I., Carracedo, L.I., Ríos, A.F. and Pérez, F.F., 2016. Ocean acidification in the subpolar North Atlantic: rates and mechanisms controlling pH changes. Biogeosciences, 13(12): 3701.

German, C., et al., 2015. Hydrothermal Fe cycling and deep ocean organic carbon scavenging: model-based evidence for significant POC supply to seafloor sediments. Earth Planet. Sci. Lett. 419, 143–153.

Gladyshev, S., Gladyshev, V., Gulev, S. and Sokov, A., 2017. Subpolar mode water classes in the northeast Atlantic: Interannual and long-term variability, Doklady Earth Sciences. Springer, pp. 1203-1206.

González-Dávila, M., Santana-Casiano, J.M., Rueda, M.J., Llinás, O., González-Dávila, E.F., 2003. Seasonal and interannual variability of sea-surface carbon dioxide species at the European station for time series in the ocean at the Canary Islands (ESTOC) between 1996 and 2000. Glob. Biogeochem. Cycles 17 (3), 1–5.

González-Davila, M., Santana-Casiano, J.M. and Millero, F.J., 2005. Oxidation of iron(II) nanomolar with $H_2O_2$ in seawater. Geochimica et Cosmochimica Acta, 69(1): 83-93.

González-Dávila, M., Santana-Casiano, J.M. and Millero, F.J., 2006. Competition between $O_2$ and $H_2O_2$ in the oxidation of Fe(II) in natural waters. Journal of solution chemistry, 35(1): 95-111.

González, A.G., Santana-Casiano, J.M., Pérez, N., González-Dávila,M., 2010. Oxidation of Fe(II) in natural waters at high nutrient concentrations. Environ. Sci. Technol. 44 (21), 8095–8101.

Gonzalez, A.G., Santana-Casiano, J.M., González-Dávila, M., Pérez-Almeida, N., Suárez de Tangil, M., 2014. Effect of Dunaliella tertiolecta organic exudates on the Fe(II) oxidation kinetics in seawater. Environmental science & technology, 48(14): 7933-7941.

González, A.G. et al., 2014. Iron adsorption onto soil and aquatic bacteria: XAS structural study. Chemical Geology, 372: 32-45.

González, A.G., Pérez-Almeida, N., Santana-Casiano, J.M., Millero, F.J., González-Dávila, M., 2016. Redox interactions of Fe and Cu in seawater. Marine Chemistry, 179: 12-22.

Gunnars, A., Blomqvist, S., Johansson, P. and Andersson, C., 2002. Formation of Fe(III) oxyhydroxide colloids in freshwater and brackish seawater, with incorporation of phosphate and calcium. Geochimica et Cosmochimica Acta, 66(5): 745-758.

Haber, F. and Weiss, J., 1934. The catalytic decomposition of hydrogen peroxide by iron salts. Proc. R. Soc. Lond. A, 147(861): 332-351.

Hansard, S.P., Landing, W.M., 2009. Determination of iron(II) in acidified seawater samples by luminol chemiluminescence. Limnol. Oceanogr. Methods 7 (3),

222–234.

Hansell, D.A. and Carlson, C.A., 1998. Net community production of dissolved organic carbon. Global Biogeochemical Cycles, 12(3): 443-453.

Hansell, D.A., Carlson, Craig A., 2001. Biogeochemistry of total organic carbon and nitrogen in the Sargasso Sea: control by convective overturn. Deep Sea Research Part II: Topical Studies in Oceanography, 48(8-9): 18.

Hansell, D., 2002. DOC in the global ocean carbon cycle. Biogeochemistry of marine dissolved organic matter: 685-715.

Hansell, D.A., Carlson, C.A., Repeta, D.J. and Schlitzer, R., 2009. Dissolved organic matter in the ocean: A controversy stimulates new insights.

Hauck, J. et al., 2013. Seasonally different carbon flux changes in the Southern Ocean in response to the southern annular mode. Global Biogeochemical Cycles, 27(4): 1236-1245.

Hastie, T.J. and Tibshirani, R.J., 1990. Generalized additive models, volume 43 of Monographs on Statistics and Applied Probability. Chapman & Hall, London.

Hay, M.B. and Myneni, S.C.B., 2007. Structural environments of carboxyl groups in natural organic molecules from terrestrial systems. Part 1: Infrared spectroscopy. Geochimica et Cosmochimica Acta, 71(14): 3518-3532.

Heller, M.I., Gaiero, D.M. and Croot, P.L., 2013. Basin scale survey of marine humic fluorescence in the Atlantic: Relationship to iron solubility and $H_2O_2$. Global Biogeochemical Cycles, 27(1): 88-100.

Heller, M.I., Wuttig, K. and Croot, P.L., 2016. Identifying the sources and sinks of CDOM/FDOM across the Mauritanian Shelf and their potential role in the

decomposition of superoxide ($O_2^-$). Frontiers in Marine Science, 3: 132.

Hong, H. and Kester, D.R., 1986. Redox state of iron in the offshore waters of Peru. Limnology and Oceanography, 31(3): 612-626.

Hudson, R.J., Morel, F.M. and Morel, F., 1990. Iron transport in marine phytoplankton: Kinetics of cellular and medium coordination reactions. Limnol. Oceanogr, 35(5): 1002-1020.

Hunter, K.A. and Boyd, P.W., 2007. Iron-binding ligands and their role in the ocean biogeochemistry of iron. Environmental Chemistry, 4(4): 221-232.

Hutchins, D.A., DiTullio, G.R., Burland, K.W., 1993. Iron and regenerated production: evidence for biological iron recycling in two marine environments. Limnol. Oceanogr. 38 (6), 1242–1255.

Ibisanmi, E., Sander, S.G., Boyd, P.W., Bowie, A.R. and Hunter, K.A., 2011. Vertical distributions of iron-(III) complexing ligands in the Southern Ocean. Deep Sea Research Part II: Topical Studies in Oceanography, 58(21-22): 2113-2125.

Keeling, R.F., Körtzinger, A. and Gruber, N., 2010. Ocean deoxygenation in a warming world. Marine Science, 2.

King, D.W., Lounsbury, H.A. and Millero, F.J., 1995. Rates and mechanism of Fe(II) oxidation at nanomolar total iron concentrations. Environmental science & technology, 29(3): 818-824.

King, D.W., 1998. Role of carbonate speciation on the oxidation rate of Fe(II) in aquatic systems. Environmental science & technology, 32(19): 2997-3003.

King, D. and Farlow, R., 2000. Role of carbonate speciation on the oxidation of Fe(II) by $H_2O_2$. Marine Chemistry, 70(1): 201-209.

Klunder, M., Laan, P., Middag, R., De Baar, H. and Van Ooijen, J., 2011. Dissolved iron in the Southern Ocean (Atlantic sector). Deep Sea Research Part II: Topical Studies in Oceanography, 58(25): 2678-2694.

Klunder, M.B. et al., 2012. Dissolved iron in the Arctic shelf seas and surface waters of the central Arctic Ocean: Impact of Arctic river water and ice-melt. Journal of Geophysical Research: Oceans, 117(C1).

Körtzinger, A., Send, U., Wallace, D.W., Karstensen, J., DeGrandpre, M., 2008. Seasonal cycle of $O_2$ and $pCO_2$ in the central Labrador Sea: Atmospheric, biological, and physical implications. Global Biogeochemical Cycles, 22(1).

Kuma, K., Suzuki, Y. and Matsunaga, K., 1993. Solubility and dissolution rate of colloidal γ-FeOOH in seawater. Water research, 27(4): 651-657.

Kuma, K., Nakabayashi, S. and Matsunaga, K., 1995. Photoreduction of Fe(III) by hydroxycarboxylic acids in seawater. Water Research, 29(6): 1559-1569.

Kuma, K., Nishioka, J. and Matsunaga, K., 1996. Controls on iron(III) hydroxide solubility in seawater: the influence of pH and natural organic chelators. Limnology and Oceanography, 41(3): 396-407.

Kustka, A.B., Shaked, Y., Milligan, A.J., King, D.W. and Morel, F.M., 2005. Extracellular production of superoxide by marine diatoms: Contrasting effects on iron redox chemistry and bioavailability. Limnology and Oceanography, 50(4): 1172-1180.

Laës, A. et al., 2003. Deep dissolved iron profiles in the eastern North Atlantic in relation to water masses. Geophysical Research Letters, 30(17): n/a-n/a

Laës, A. et al., 2005. Impact of environmental factors on in situ determination of iron in seawater by flow injection analysis. Marine Chemistry, 97(3): 347-356.

Laglera, L.M. and van den Berg, C.M., 2009. Evidence for geochemical control of iron by humic substances in seawater. Limnology and Oceanography, 54(2): 610-619.

Laglera, L.M. and van den Berg, C.M.G., 2007. Wavelength Dependence of the Photochemical Reduction of Iron in Arctic Seawater. Environmental Science & Technology, 41(7): 2296-2302.

Lazier, J., Hendry, R., Clarke, A., Yashayaev, I., Rhines, P., 2002. Convection and restratification in the Labrador Sea, 1990–2000. Deep Sea Research Part I: Oceanographic Research Papers, 49(10): 1819-1835.

Le Quéré, C. et al., 2017. Global carbon budget 2017. Earth System Science Data Discussions: 1-79.

Lee, Y.P., Fujii, M., Terao, K., Kikuchi, T. and Yoshimura, C., 2016. Effect of dissolved organic matter on Fe(II) oxidation in natural and engineered waters. Water Research, 103: 160-169.

Lee, Y.P. et al., 2017. Importance of allochthonous and autochthonous dissolved organic matter in Fe(II) oxidation: A case study in Shizugawa Bay watershed, Japan. Chemosphere.

Lee, Y.P., Fujii, M., Kikuchi, T., Terao, K., Yoshimura, C., 2017b. Variation of iron redox kinetics and its relation with molecular composition of standard humic substances at circumneutral pH. PloS one, 12(4): e0176484.

Leenheer, J.A., Brown, G.K., MacCarthy, P. and Cabaniss, S.E., 1998. Models of Metal Binding Structures in Fulvic Acid from the Suwannee River, Georgia. Environmental Science & Technology, 32(16): 2410-2416.

Lewis, B.L. et al., 1995. Voltammetric estimation of iron(III) thermodynamic stability constants for catecholate siderophores isolated from marine bacteria and

cyanobacteria. Marine Chemistry, 50(1-4): 179-188.

Lewis, E., Wallace, D., Allison, L.J., 1998. Program Developed for $CO_2$ System Calculations. Carbon Dioxide Information Analysis Center, Managed by Lockheed Martin Energy Research Corporation for the US Department of Energy Tennessee.

Liu, X. and Millero, F.J., 1999. The solubility of iron hydroxide in sodium chloride solutions. Geochimica et Cosmochimica Acta, 63(19): 3487-3497.

Liu, X., Millero, F.J., 2002. The solubility of iron in seawater. Mar. Chem. 77 (1), 43–54.

Luther, G.W., et al., 2001. Chemical speciation drives hydrothermal vent ecology. Nature 410 (6830), 813–816.

Mackey, D., O'Sullivan, J.O. and Watson, R., 2002. Iron in the western Pacific: a riverine or hydrothermal source for iron in the Equatorial Undercurrent? Deep Sea Research Part I: Oceanographic Research Papers, 49(5): 877-893.

Macrellis, H.M., Trick, C.G., Rue, E.L., Smith, G. and Bruland, K.W., 2001. Collection and detection of natural iron-binding ligands from seawater. Marine Chemistry, 76(3): 175-187.

Manceau, A. and Matynia, A., 2010. The nature of Cu bonding to natural organic matter. Geochimica et Cosmochimica Acta, 74(9): 2556-2580.

Mantas, V.M., Pereira, A., Morais, P.V., 2011. Plumes of discolored water of volcanic origin and possible implications for algal communities. The case of the home reef eruption of 2006 (Tonga, Southwest Pacific Ocean). Remote Sens. Environ. 115 (6), 1341–1352.

Martin, J.H., Gordon, M., Fitzwater, S.E., 1991. The case for iron. Limnology

and Oceanography, 36(8): 1793-1802.

Martin, J.H., et al., 1994. Testing the iron hypothesis in ecosystems of the equatorial Pacific Ocean. Nature 371, 123.

Matsumoto, K., Tokos, K., Huston, A. and Joy-Warren, H., 2013. MESMO 2: A mechanistic marine silica cycle and coupling to a simple terrestrial scheme. Geoscientific Model Development, 6(2): 477.

McCartney, M., 1992. Recirculating components to the deep boundary current of the northern North Atlantic. Progress in Oceanography, 29(4): 283-383.

McDonough, W.F. and Sun, S.-S., 1995. The composition of the Earth. Chemical geology, 120(3-4): 223-253.

Measures, C. and Vink, S., 1999. Seasonal variations in the distribution of Fe and Al in the surface waters of the Arabian Sea. Deep Sea Research Part II: Topical Studies in Oceanography, 46(8): 1597-1622.

Meehl, G.A. et al., 2007. Global climate projections.

Mehrbach, C.C.C.H., Hawley, J.E., Pytkowicx, R.M., 1973. Measurement of the apparent dissociation constants of carbonic acid in seawater at atmospheric pressure. Limnol. Oceanogr. 18 (6), 10.

Mendes, P., 1993. GEPASI: a software package for modelling the dynamics, steady states and control of biochemical and other systems. Bioinformatics, 9(5): 563-571.

Miller, W.L., King, D.W., Lin, J. and Kester, D.R., 1995. Photochemical redox cycling of iron in coastal seawater. Marine Chemistry, 50(1): 63-77.

Millero, F.J., 1986. The pH of estuarine waters. Limnology and Oceanography, 31(4): 839-847.

Millero, F.J., Izaguirre, M., Sharma, V.K., 1987a. The effect of ionic interaction on the rates of oxidation in natural waters. Marine Chemistry, 22(2-4): 179-191.

Millero, F.J., Sotolongo, S., Izaguirre, M., 1987b. The oxidation kinetics of Fe(II) in seawater. Geochimica et Cosmochimica Acta, 51(4): 793-801.

Millero, F.J. and Izaguirre, M., 1989. Effect of ionic strength and ionic interactions on the oxidation of Fe(II). Journal of Solution Chemistry, 18(6): 585-599.

Millero, F.J. et al., 1993. The use of buffers to measure the pH of seawater. Marine Chemistry, 44(2-4): 143-152.

Millero, F.J., Yao, W. and Aicher, J., 1995. The speciation of Fe(II) and Fe(III) in natural waters. Marine Chemistry, 50(1): 21-39.

Millero, F.J., 1998. Solubility of Fe(III) in seawater. Earth and Planetary Science Letters, 154(1): 323-329.

Mills, M.M., Ridame, C., Davey, M., La Roche, J. and Geider, R.J., 2004. Iron and phosphorus co-limit nitrogen fixation in the eastern tropical North Atlantic. Nature, 429(6989): 292-294.

Mohamed, K.N., Steigenberger, S., Nielsdottir, M.C., Gledhill, M. and Achterberg, E.P., 2011. Dissolved iron(III) speciation in the high latitude North Atlantic Ocean. Deep Sea Research Part I: Oceanographic Research Papers, 58(11): 1049-1059.

Moore, J.K., Doney, S.C., Glover, D.M. and Fung, I.Y., 2001. Iron cycling and nutrient-limitation patterns in surface waters of the World Ocean. Deep Sea Research Part II: Topical Studies in Oceanography, 49(1-3): 463-507.

Moore, J.K., Lindsay, K., Doney, S.C., Long, M.C. and Misumi, K., 2013. Marine ecosystem dynamics and biogeochemical cycling in the Community Earth System Model [CESM1 (BGC)]: Comparison of the 1990s with the 2090s under the RCP4. 5 and RCP8. 5 scenarios. Journal of Climate, 26(23): 9291-9312.

Morel, F.M., Kustka, A. and Shaked, Y., 2008. The role of unchelated Fe in the iron nutrition of phytoplankton. Limnology and Oceanography, 53(1): 400-404.

Nielsen, J., 1928. The waters around Greenland. Greenland, The Discovery of Greenland, Exploration, and the Nature of the Country, 1: 185-230.

Nishioka, J., Takeda, S., Wong, C. and Johnson, W., 2001. Size-fractionated iron concentrations in the northeast Pacific Ocean: distribution of soluble and small colloidal iron. Marine Chemistry, 74(2): 157-179.

Nishioka, J., Obata, H. and Tsumune, D., 2013. Evidence of an extensive spread of hydrothermal dissolved iron in the Indian Ocean. Earth and Planetary Science Letters, 361: 26-33.

O'Sullivan, D.W., Hanson, A.K. and Kester, D.R., 1995. Stopped flow luminol chemiluminescence determination of Fe(II) and reducible iron in seawater at subnanomolar levels. Marine Chemistry, 49(1): 65-77.

Pham, A.N. and Waite, T.D., 2008. Oxygenation of Fe(II) in natural waters revisited: Kinetic modeling approaches, rate constant estimation and the importance of various reaction pathways. Geochimica et Cosmochimica Acta, 72(15): 3616-3630.

Pickart, R.S., Torres, D.J., Clarke, R.A., 2002. Hydrography of the Labrador Sea during active convection. Journal of Physical Oceanography, 32(2): 428-457.

Pickart, R.S., Spall, M.A., Ribergaard, M.H., Moore, G.W.K. and Milliff, R.F., 2003. Deep convection in the Irminger Sea forced by the Greenland tip jet. Nature, 424(6945): 152-156.

Pierrot, D., Lewis, E., Wallace, D., 2006. MS Excel program developed for $CO_2$ system calculations. ORNL/CDIAC-105a. Carbon Dioxide Information Analysis Center, Oak Ridge National Laboratory, US Department of Energy, Oak Ridge, Tennessee.

Powell, R.T., King, D.W. and Landing, W.M., 1995. Iron distributions in surface waters of the south Atlantic. Marine Chemistry, 50(1): 13-20.

Rabalais, N.N., Turner, R.E. and Wiseman Jr, W.J., 2002. Gulf of Mexico hypoxia, aka "The dead zone". Annual Review of ecology and Systematics, 33(1): 235-263.

Reid, R.T., Livet, D.H., Faulkner, D.J. and Butler, A., 1993. A siderophore from a marine bacterium with an exceptional ferric ion affinity constant. Nature, 366(6454): 455.

Resing, J.A. et al., 2015. Basin-scale transport of hydrothermal dissolved metals across the South Pacific Ocean. Nature, 523(7559): 200-203.

Rich, H.W. and Morel, F.M., 1990. Availability of well-defined iron colloids to the marine diatom Thalassiosira weissflogii. Limnology and Oceanography, 35(3): 652-662.

Riebesell, U., 2004. Effects of $CO_2$ Enrichment on Marine Phytoplankton. Journal of Oceanography, 60(4): 719-729.

Riebesell, U. et al., 2007. Enhanced biological carbon consumption in a high $CO_2$ ocean. Nature, 450(7169): 545.

Riebesell, U., Körtzinger, A. and Oschlies, A., 2009. Sensitivities of marine carbon fluxes to ocean change. Proceedings of the National Academy of Sciences, 106(49): 20602-20609.

Rijkenberg, M.J. et al., 2008. Changes in iron speciation following a Saharan dust event in the tropical North Atlantic Ocean. Marine Chemistry, 110(1): 56-67.

Rose, A.L. and Waite, T.D., 2002. Kinetic Model for Fe(II) Oxidation in Seawater in the Absence and Presence of Natural Organic Matter. Environmental Science & Technology, 36(3): 433-444.

Rose, A.L. and Waite, T.D., 2003. Kinetics of iron complexation by dissolved natural organic matter in coastal waters. Marine Chemistry, 84(1–2): 85-103.

Roy, E.G., Wells, M.L. and King, D.W., 2008. Persistence of iron(II) in surface waters of the western subarctic Pacific. Limnology and Oceanography, 53(1): 89-98.

Roy, E.G. and Wells, M.L., 2011. Evidence for regulation of Fe(II) oxidation by organic complexing ligands in the Eastern Subarctic Pacific. Marine Chemistry, 127(1): 115-122.

Rush, J.D., Bielski, B.H.J., 1985. Pulse radiolytic studies of the reaction of perhydroxyl/superoxide $O_2^-$ with iron(II)/iron(III) ions. The reactivity of $HO_2/O_2^-$ with ferric ions and its implication on the occurrence of the Haber-Weiss reaction. The Journal of Physical Chemistry, 89(23): 5062-5066.

Rysgaard, S. et al., 2003. Physical conditions, carbon transport, and climate change impacts in a Northeast Greenland fjord. Arctic, Antarctic, and Alpine Research, 35(3): 301-312.

Sabine, C.L. et al., 2004. The oceanic sink for anthropogenic $CO_2$. science, 305(5682): 367-371.

Saito, M.A. et al., 2013. Slow-spreading submarine ridges in the South Atlantic as a significant oceanic iron source. Nature Geoscience, 6(9): 775-779.

Samperio-Ramos, G., Santana Casiano, J.M., González Dávila, M., 2016. Effect of ocean warming and acidification on the Fe(II) oxidation rate in oligotrophic and eutrophic natural waters. Biogeochemistry 128 (1), 19–34.

Sander, S.G., Koschinsky, A., 2011. Metal flux from hydrothermal vents increased by organic complexation. Nat. Geosci. 4 (3), 145–150.

Santana-Casiano, J.M., González-Dávila, M., Rodrıguez, M.J. and Millero, F.J., 2000. The effect of organic compounds in the oxidation kinetics of Fe(II). Marine Chemistry, 70(1): 211-222.

Santana-Casiano, J.M., González-Dávila, M. and Millero, F.J., 2004. The oxidation of Fe(II) in NaCl–$HCO_3^-$ and seawater solutions in the presence of phthalate and salicylate ions: a kinetic model. Marine chemistry, 85(1): 27-40.

Santana-Casiano, J.M., González-Dávila, M. and Millero, F.J., 2005. Oxidation of nanomolar levels of Fe(II) with oxygen in natural waters. Environmental science & technology, 39(7): 2073-2079.

Santana-Casiano, J., Gonzalez-Davila, M. and Millero, F., 2006. The role of Fe(II) species on the oxidation of Fe(II) in natural waters in the presence of $O_2$ and $H_2O_2$. Marine chemistry, 99(1): 70-82.

Santana-Casiano, J.M., González-Dávila, M., González, A. and Millero, F., 2010. Fe(III) reduction in the presence of catechol in seawater. Aquatic geochemistry, 16(3): 467-482.

Santana-Casiano, J., González-Dávila, M., 2011. pH decrease and effects on the chemistry of seawater. In: Duarte, P., Santana-Casiano, J.M. (Eds.), Oceans and the Atmospheric Carbon Content. Springer Netherlands, pp. 95–114.

Santana-Casiano, J.M., et al., 2013. The natural ocean acidification and fertilization event caused by the submarine eruption of El Hierro. Sci. Rep. 3, 1–8.

Santana-Casiano, J. et al., 2014. Characterization of phenolic exudates from Phaeodactylum tricornutum and their effects on the chemistry of Fe(II)–Fe(III). Marine chemistry, 158: 10-16.

Santana-Casiano, J., et al., 2016. Significant discharge of $CO_2$ from hydrothermalism associated with the submarine volcano of El Hierro Island. Sci. Rep. 6.

Santana-González, C. et al., 2018. Fe(II) oxidation kinetics in the North Atlantic along the 59.5° N during 2016. Marine Chemistry.

Sarafanov, A., Falina, A., Mercier, H., Lherminier, P. and Sokov, A., 2009. Recent changes in the Greenland–Scotland overflow-derived water transport inferred from hydrographic observations in the southern Irminger Sea. Geophysical Research Letters, 36(13).

Sarthou, G. and Jeandel, C., 2001. Seasonal variations of iron concentrations in the Ligurian Sea and iron budget in the Western Mediterranean Sea. Marine Chemistry, 74(2): 115-129.

Schmidt, M.A. and Hutchins, D.A., 1999. Size-fractionated biological iron and carbon uptake along a coastal to offshore transect in the NE Pacific. Deep Sea Research Part II: Topical Studies in Oceanography, 46(11–12): 2487-2503.

Schofield, O. et al., 2010. How do polar marine ecosystems respond to rapid climate change? Science, 328(5985): 1520-1523.

Shaked, Y., Kustka, A.B. and Morel, F.M., 2005. A general kinetic model for iron acquisition by eukaryotic phytoplankton. Limnol. Oceanogr, 50(3): 872-882.

Shaked, Y. and Lis, H., 2012. Disassembling Iron Availability to Phytoplankton. Frontiers in Microbiology, 3: 123.

Shi, D., Xu, Y., Hopkinson, B.M., Morel, F.M., 2010. Effect of ocean acidification on iron availability to marine phytoplankton. Science 327 (5966), 676–679.

Shi, D.K., Sven A.; Kim, Ja-Myung; Morel, François M. M., 2012 Ocean acidification slows nitrogen fixation and growth in the dominant diazotroph Trichodesmium under low-iron conditions. Proceedings of the National Academy of Sciences 109 (45): 6.

Spokes, L., Jickells, T. and Jarvis, K., 2001. Atmospheric inputs of trace metals to the northeast Atlantic Ocean: the importance of southeasterly flow. Marine Chemistry, 76(4): 319-330.

Statham, P., German, C. and Connelly, D., 2005. Iron(II) distribution and oxidation kinetics in hydrothermal plumes at the Kairei and Edmond vent sites, Indian Ocean. Earth and Planetary Science Letters, 236(3): 588-596.

Statham, P.J., Skidmore, M., Tranter, M., 2008. Inputs of glacially derived dissolved and colloidal iron to the coastal ocean and implications for primary productivity. Global Biogeochemical Cycles, 22(3).

Steemann Nielsen, E., 1958. A survey of recent Danish measurements of the organic productivity in the sea. Rapp. Cons. Explor. Mer, 144: 92-95.

Steigenberger, S. and Croot, P.L., 2008. Identifying the processes controlling the distribution of $H_2O_2$ in surface waters along a meridional transect in the eastern Atlantic. Geophysical Research Letters, 35(3).

Stramma, L. et al., 2004. Deep water changes at the western boundary of the subpolar North Atlantic during 1996 to 2001. Deep Sea Research Part I: Oceanographic Research Papers, 51(8): 1033-1056.

Straneo, F., 2006. Heat and Freshwater Transport through the Central Labrador Sea. Journal of Physical Oceanography, 36(4): 606-628.

Stock, C.A., Dunne, J.P. and John, J.G., 2014. Global-scale carbon and energy flows through the marine planktonic food web: An analysis with a coupled physical–biological model. Progress in Oceanography, 120: 1-28.

Stumm, W. and Lee, G.F., 1961. Oxygenation of ferrous iron. Industrial & Engineering Chemistry, 53(2): 143-146.

Sunda, W.G., Swift, D.G. and Huntsman, S.A., 1991. Low iron requirement for growth in oceanic phytoplankton. Nature, 351(6321): 55.

Sunda, W.G. and Huntsman, S.A., 1995. Iron uptake and growth limitation in oceanic and coastal phytoplankton. Marine Chemistry, 50(1-4): 189-206.

Tagliabue, A. and Arrigo, K.R., 2005. Iron in the Ross Sea: 1. Impact on $CO_2$ fluxes via variation in phytoplankton functional group and non-Redfield stoichiometry. Journal of Geophysical Research: Oceans, 110(C3).

Tagliabue, A., Bopp, L., Aumont, O. and Arrigo, K.R., 2009. Influence of light and temperature on the marine iron cycle: From theoretical to global modeling. Global Biogeochemical Cycles, 23(2).

Tagliabue, A. et al., 2010. Hydrothermal contribution to the oceanic dissolved iron inventory. Nature Geoscience, 3(4): 252-256.

Tagliabue, A. and Voelker, C., 2011. Towards accounting for dissolved iron speciation in global ocean models. Biogeosciences, 8(10): 3025.

Tagliabue, A. et al., 2012. A global compilation of dissolved iron measurements: focus on distributions and processes in the Southern Ocean. Biogeosciences, 9(6): 2333-2349.

Tagliabue, A., Aumont, O. and Bopp, L., 2014. The impact of different external

sources of iron on the global carbon cycle. Geophysical Research Letters, 41(3): 920-926.

Tagliabue, A. et al., 2016. How well do global ocean biogeochemistry models simulate dissolved iron distributions? Global Biogeochemical Cycles, 30(2): 149-174.

Tagliabue, A. et al., 2017. The integral role of iron in ocean biogeochemistry. Nature, 543(7643): 51-59.

Talley, L., McCartney, M., 1982. Distribution and circulation of Labrador Sea water. Journal of Physical Oceanography, 12(11): 1189-1205.

Team, R.C., 2016. R: A language and envirnment for statistical computing. R Foundation for Statistical Computing, Viena, Austria.

Theis, T.L. and Singer, P.C., 1974. Complexation of iron(II) by organic matter and its effect on iron(II) oxygenation. Environmental Science and Technology, 8(6): 569-573.

Thuróczy, C.E. et al., 2011. Distinct trends in the speciation of iron between the shallow shelf seas and the deep basins of the Arctic Ocean. Journal of Geophysical Research: Oceans, 116(C10).

Trapp, J.M. and Millero, F.J., 2007. The oxidation of iron(II) with oxygen in NaCl brines. Journal of Solution Chemistry, 36(11-12): 1479-1493.

Turner, D.R. and Hunter, K.A., 2001. The biogeochemistry of iron in seawater, 6. Wiley Chichester.

Ussher, S.J. et al., 2010. Distribution of size fractionated dissolved iron in the Canary Basin. Marine environmental research, 70(1): 46-55.

Våge, K. et al., 2011. The Irminger Gyre: Circulation, convection, and interannual variability. Deep Sea Research Part I: Oceanographic Research Papers, 58(5): 590-614.

Van Leeuwe, M., Scharek, R., De Baar, H., De Jong, J. and Goeyens, L., 1997. Iron enrichment experiments in the Southern Ocean: physiological responses of plankton communities. Deep Sea Research Part II: Topical Studies in Oceanography, 44(1): 189-207.

Vichi, M., Pinardi, N. and Masina, S., 2007. A generalized model of pelagic biogeochemistry for the global ocean ecosystem. Part I: Theory. Journal of Marine Systems, 64(1-4): 89-109.

Voelker, B.M. and Sedlak, D.L., 1995. Iron reduction by photoproduced superoxide in seawater. Marine Chemistry, 50(1): 93-102.

Voelker, B.M., Sulzberger, B., 1996. Effects of fulvic acid on Fe(II) oxidation by hydrogen peroxide. Environmental Science & Technology, 30(4): 1106-1114.

Völker, C. and Wolf-Gladrow, D.A., 1999. Physical limits on iron uptake mediated by siderophores or surface reductases. Marine Chemistry, 65(3): 227-244.

Völker, C. and Wolf-Gladrow, D.A., 2000. Numerical models of iron uptake by phytoplankton cells. Journal of plant nutrition, 23(11-12): 1657-1665.

Weber, L., Völker, C., Schartau, M. and Wolf-Gladrow, D., 2005. Modeling the speciation and biogeochemistry of iron at the Bermuda Atlantic Time-series Study site. Global Biogeochemical Cycles, 19(1).

Wehrmann, L.M. et al., 2014. Iron and manganese speciation and cycling in glacially influenced high-latitude fjord sediments (West Spitsbergen, Svalbard): Evidence for a benthic recycling-transport mechanism. Geochimica et Cosmochimica Acta, 141: 628-655.

Wilhelm, S.W. and Trick, C.G., 1994. Iron-limited growth of cyanobacteria: Multiple siderophore production is a common response. Limnology and Oceanography, 39(8): 1979-1984.

Williams, R.J.P., 1981. The Bakerian Lecture, 1981 Natural Selection of the Chemical elements. Proc. R. Soc. Lond. B, 213(1193): 361-397.

Wu, J., Luther III, G.W., 1994. Size-fractionated iron concentrations in the water column of the western North Atlantic Ocean. Limnology and Oceanography, 39(5): 1119-1129.

Wu, J., Boyle, E., Sunda, W. and Wen, L.-S., 2001. Soluble and colloidal iron in the oligotrophic North Atlantic and North Pacific. Science, 293(5531): 847-849.

Wu, J., Wells, M.L. and Rember, R., 2011. Dissolved iron anomaly in the deep tropical–subtropical Pacific: Evidence for long-range transport of hydrothermal iron. Geochimica et Cosmochimica Acta, 75(2): 460-468.

Yashayaev, I., 2007a. Hydrographic changes in the Labrador Sea, 1960–2005. Progress in Oceanography, 73(3–4): 242-276.

Yashayaev, I., Holliday, N.P., Bersch, M., van Aken, H.M., 2008. The history of the Labrador Sea Water: Production, spreading, transformation and loss, Arctic–Subarctic Ocean Fluxes. Springer, pp. 569-612.

Yashayaev, I., Lazier, J.R., Clarke, R.A., 2003. Temperature and salinity in the central Labrador Sea during the 1990s and in the context of the longer-term change, ICES Mar. Sci. Symp, pp. 32-39.

Yashayaev, I., van Aken, H.M., Holliday, N.P., Bersch, M., 2007c. Transformation of the Labrador Sea water in the subpolar North Atlantic. Geophysical Research Letters, 34(22).

Ye, Y., Völker, C. and Wolf-Gladrow, D.A., 2009. A model of Fe speciation and biogeochemistry at the Tropical Eastern North Atlantic Time-Series Observatory site. Biogeosciences, 6(10): 2041-2061.

Yool, A. and Popova, E., 2011. Medusa-1.0: a new intermediate complexity plankton ecosystem model for the global domain. Geoscientific Model Development, 4(2): 381.

Yool, A., Popova, E. and Anderson, T., 2013. MEDUSA-2.0: an intermediate complexity biogeochemical model of the marine carbon cycle for climate change and ocean acidification studies. Geoscientific Model Development, 6(5): 1767-1811.

Yücel, M., Gartman, A., Chan, C.S., Luther, G.W., 2011. Hydrothermal vents as a kinetically stable source of iron-sulphide-bearing nanoparticles to the ocean. Nat. Geosci. 4 (6), 367–371.

***"For every dark night there's a brighter day"***

– Tupac Amaru Shakur (1971-1996, New York) Singer and actor. His lyrics spoke of freedom, equality and criticism of the government and the police.